

Copyright is owned by the Author of the thesis. Permission is given for a copy to be downloaded by an individual for the purpose of research and private study only. The thesis may not be reproduced elsewhere without the permission of the Author.

Appendix D

MASSEY UNIVERSITY
Application for Approval of Request to Embargo a Thesis
(Pursuant to AC98/168 (Revised 2), Approved by Academic Board 17/02/99)

Name of Candidate..... Daniel Rexin ID Number:..... 11140289

Degree:..... PhD Dept/Institute/School:..... IFS

Thesis title:.. A molecular analysis of the requirement of TOR kinase signalling for plant growth


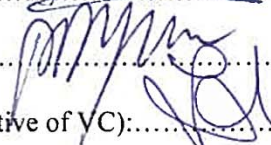
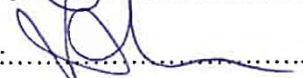
Name of Chief Supervisor:.. Paul Dijkwel Telephone Ext:.. 84731

As author of the above named thesis, I request that my thesis be embargoed from public access until (date) 1/6/2017 for the following reasons:

- Thesis contains commercially sensitive information.
- Thesis contains information which is personal or private and/or which was given on the basis that it not be disclosed.
- Immediate disclosure of thesis contents would not allow the author a reasonable opportunity to publish all or part of the thesis.
- Other (specify):... Contractual agreement with AgResearch

Please explain here why you think this request is justified:

- The data presented in the thesis has not yet been published and extra time is required to submit a manuscript
- The stipend was given with the agreement of AgResearch that the thesis will be submitted and held in confidence

Signed (Candidate):  Date: 2/11/15
Endorsed (Chief Supervisor):  Date: 4/11/15
Approved/Not Approved (Representative of VC):  Date: 11.12.15

Note: Copies of this form, once approved by the representative of the Vice-Chancellor, must be bound into every copy of the thesis.

**A molecular genetic analysis of the requirement of TOR kinase
signalling for plant growth**

A thesis presented in partial fulfilment of the requirements for the degree

Doctor of Philosophy

in

Plant Biology

at Massey University, Palmerston North, New Zealand.

Daniel Rexin

2015

Abstract

Eukaryotes have developed a highly complex mechanism to incorporate signals from nutrient, energy, stress, developmental, and environmental cues to modulate their growth. To promote this growth, eukaryotes have to coordinate the expansion in cellular mass and size through macromolecular synthesis with the increase in cell number through division. This demands a complex orchestration of a plethora of cellular processes such as transcription, protein synthesis, metabolism and cell wall synthesis. The TARGET OF RAPAMYCIN (TOR) pathway was identified as a central integrator of this growth-regulating mechanism. Components of this pathway, including the TOR kinase and its interaction partners REGULATORY-ASSOCIATED PROTEIN OF TOR (RAPTOR) and LETHAL WITH SEC 13 PROTEIN 8 (LST8), are highly conserved among eukaryotes. This includes plants, for which the adaptation to changing environmental conditions is particularly important given their sessile lifestyle and highly plastic development.

This work sought to further expand the knowledge of how TOR function was adapted to suit the requirements of plants. Therefore, I analysed genetic knock-out mutants of *raptor* in *Arabidopsis thaliana*, which resulted in a severe reduction of growth but did not cause an early developmental arrest as reported by previous studies. Detailed analysis of these mutants further revealed defects in the development of trichomes, gametophytes, and the polar extension of root hairs and pollen tubes. Potential causes for these defects were indicated by lower DNA content and limited ROS accumulation in *raptor* mutants. High similarities between *raptor* and *lst8* mutants indicated that the formation of TOR complexes as found in other eukaryotes might not be functionally conserved in plants.

Further, I adapted a CRE//ox system for the induction of mosaic deletions of RAPTOR, which indicated no tissue-specific requirement for RAPTOR functions within the root of *A. thaliana*, but demonstrated a role in the regulation of meristem size.

To conclude, this data presents further evidence for an altered requirement of RAPTOR and LST8 function for TOR signalling in plants compared to fungi and animals. This thesis revealed novel functions of TOR in plant development, ROS homeostasis and endoreduplication. It further draws attention to the connection with other signalling pathways to regulate growth and development in plants.

Acknowledgments

I would like to express my deep appreciation to everyone who has supported me during my PhD study. I would like to thank my supervisors Bruce Veit and Paul Dijkwel for giving me the opportunity to do my PhD project under their guidance. In particular, I would express my appreciation to Bruce Veit for his intellectual support and for giving me the freedom to explore science in my own way. I am particularly grateful for the tremendous efforts of Paul Dijkwel in mentoring and advising me during this time. I would also like to thank Mei Lin Tay and Anna Larking, whose support and company was indispensable for this project and made the time spent in the lab enjoyable. In particular, I would like to recognize Mei Lin Tay's contribution to the cloning of LST8.1 and Anna Larking's immense efforts in genotyping, crossing, and the propagation and caretaking of plants.

I would like to thank Michael McManus and the members of the Dijkwel & McManus group, especially Matt, Jay, Jibrán, Rubina and Srishti, for their vital discussions and jokes during the lab meetings.

I am thankful for the financial support I received from the Royal Society of New Zealand and AgResearch, and I would also like to thank Massey University for supporting my travel to overseas conferences.

I am sincerely grateful to my parents, who have supported me throughout the years of my study as they have done my whole life. Anne and Elaine: words cannot express how grateful I am to know you are by my side. This thesis would not have been possible without your support and love. I would also like to thank you for your efforts in proof reading my writing and Mitsui for her constant attempts to distract me during the writing process. Last but not least, I would like to thank my friends and flatties who made the time in Palmerston North an unforgettable and most enjoyable experience.

Table of contents

Abstract	iii
Acknowledgments	v
Abbreviations	xi
List of figures	xvii
List of tables	xix
Chapter 1 General introduction	1
1.1 Target of rapamycin	2
1.2 Discovery	2
1.3 TOR protein features.....	3
1.4 TOR complex formation	4
1.4.1 The TOR complex 1	5
1.4.2 RAPTOR	5
1.4.3 LST8.....	6
1.4.4 Additional interaction partners of TOR in TORC1.....	7
1.5 TORC1 substrates and functions	8
1.5.1 Protein synthesis	8
1.5.2 Ribosome biogenesis.....	10
1.5.3 Cell cycle	10
1.5.4 Metabolism and mitochondrial activity	11
1.5.5 Autophagy	11
1.5.6 Lifespan.....	12
1.6 The TOR complex 2	13
1.6.1 TORC2 substrates and functions	14
1.7 Regulation of TORC1	16
1.7.1 Nutrients	17
1.7.2 Growth factors	18
1.7.3 Energy	19
1.7.4 Stress	19
1.8 Regulation of TORC2.....	19
1.9 TOR signalling in plants	20

1.9.1 TOR	21
1.9.2 Raptor	23
1.9.3 LST8	23
1.10 Functions and downstream targets of TOR in plants	25
1.10.1 Protein synthesis	25
1.10.2 Cell cycle	26
1.10.3 Transcription	27
1.10.4 Development.....	27
1.10.5 Metabolism	28
1.10.6 Stress.....	28
1.10.7 Autophagy.....	29
1.11 Regulation of TOR activity in plants	30
1.11.1 Glucose.....	30
1.11.2 Energy	31
1.11.3 Hormones	31
1.11.4 Nutrients	33
1.11.5 Conclusion and Outlook.....	33
1.12 Aim of this research.....	34
Chapter 2 Material & Methods.....	37
2.1 Cloning.....	37
2.1.1 Overview of the cloning strategy	37
2.1.2 Colony PCR	43
2.2 Creation of transcriptional fusions	44
2.3 Plant methods.....	45
2.3.1 Plant lines	45
2.3.2 Growth conditions	45
2.3.3 Genotyping PCR.....	46
2.3.4 Plant transformation.....	47
2.3.5 Extraction of genomic DNA of <i>A. thaliana</i>	49
2.3.6 Genomic mapping of T-DNA insertions using high-efficiency thermal asymmetric interlaced PCR (hiTAIL-PCR).....	50
2.3.7 H ₂ O ₂ assay	51
2.4 Transcriptomic analysis	52
2.4.1 RNA extraction.....	52
2.4.2 Bioinformatic analysis of transcriptomic data	52
2.5 Flow Cytometry.....	53

2.6 Microscopy	54
2.6.1 β -glucuronidase (GUS) staining	54
2.6.2 Differential interference contrast microscopy	54
2.6.3 Aniline blue staining	54
2.6.4 Alexander staining	55
2.6.5 Propidium iodide staining	55
2.6.6 Electron microscopy	55
2.6.7 ROS staining using H ₂ DCF-DA	56
2.6.8 S-phase cell detection using ethynyl deoxyuridine (EdU)	56
Chapter 3 Characterization of <i>raptor3g raptor5g</i> mutants in <i>A. thaliana</i>	57
Introduction	57
Results	58
3.1 Isolation of <i>raptor</i> mutants	58
3.2 <i>Raptor</i> mutants show limited growth	61
3.3 <i>A. thaliana raptor3g raptor5g</i> mutants show RAPTOR-independent TOR activity	64
3.4 Expression of RAPTOR3G and RAPTOR5G in <i>A. thaliana</i>	65
3.5 Transcriptomic profile of <i>raptor</i> mutants	68
3.6 Root hairs of <i>raptor3g raptor5g</i> mutants show altered development and ROS accumulation	73
3.7 RAPTOR is involved in regulating growth and development through controlling meristem size	76
3.8 <i>Raptor</i> mutants show reduced endoreduplication accompanied with altered trichome development and reduced organ size	78
Discussion	84
Chapter 4 Flower development and transmission of <i>raptor</i> mutants	93
Introduction	93
Results	93
4.1 Flower development of <i>A. thaliana raptor</i> mutants	93
4.2 Arrest of female gametophyte in <i>raptor3g raptor5g</i> mutants causes sterility	96
4.3 RAPTOR is involved in pollen maturation and pollen tube growth	98
Discussion	102
Chapter 5 Analysis of mosaic <i>raptor</i> knock-outs	107
Introduction	107
Results	109
5.1 Generation of <i>A. thaliana</i> lines with <i>lox</i> -flanked <i>RAPTOR</i>	109
5.2 Introduction of an inducible CRE recombinase to <i>A. thaliana</i>	112
5.3 Generation of the CRE/ <i>RAPTOR3G^{lox}</i> system in <i>A. thaliana</i>	115

5.4 Functional testing of the CRE/lox system through the induction of HSp::CRE RAPTOR3G ^{lox} and control lines	116
5.5 <i>RAPTOR</i> is not required to maintain growth and development in small <i>RAPTOR</i> ^{lox} deletion sectors within the root meristem	119
5.6 <i>Raptor</i> deletion sectors in the root show reduced meristem size	123
Discussion	125
Chapter 6 Comparison of <i>raptor</i> and <i>Ist8</i> knock-out mutants in <i>A. thaliana</i> and its implications on the presence of a TORC2 in plants	129
Introduction	129
Results	130
6.1 Generation of <i>A. thaliana</i> lines with lox-flanked <i>LST8</i>	130
6.2 Generation of the CRE/ <i>LST8.1</i> ^{lox} system in <i>A. thaliana</i>	132
6.3 Functional testing of the CRE/lox system in HSp::CRE <i>LST8.1</i> ^{lox} and control lines	133
6.4 Deletion of <i>LST8</i> mimics the phenotype of <i>raptor</i> null sectors	134
6.5 <i>Raptor3g raptor5g</i> and <i>Ist8.1</i> mutants show differences in the response to changes of the light period	137
6.6 <i>Raptor3g raptor5g</i> and <i>Ist8.1</i> mutants show differences in DNA content under long day condition.	139
6.7 <i>Raptor3g raptor5g</i> and <i>Ist8.1</i> mutants show a similar but not identical transcriptomic profile	142
6.8 <i>RAPTOR</i> and <i>LST8</i> are not essential for TOR activity in plants	145
Discussion	146
Chapter 7 Final discussion, outlook and concluding remarks	151
Appendices	157
Bibliography.....	175

Abbreviations

°C	Degrees Celsius
μE	Micro-Einstein
μm	Micro-meter
μM	micro-molar
4E-BP	4E-BINDING PROTEIN
ABA	Abscisic acid
ABRC	Arabidopsis Biological Resource Center
Akt	s. PKB
amiRNA	artificial microRNA
AML1	ARABIDOPSIS MEI2-LIKE 1
AMPK	AMP-ACTIVATED PROTEIN KINASE
APC/C	Anaphase promoting complex/cyclosome (APC/C)
APR2	ADENOSINE 5'-PHOSPHOSULFATE REDUCTASE
ATG	AUTOPHAGY-RELATED
ATP	Adenosine triphosphate
AVO	ADHERES VORACIOUSLY TO TOR2
bp	Nucleotide base pairs
Ca ²⁺	Calcium
CDC	CELL DIVISION CYCLE
CDK	CYCLIN-DEPENDENT KINASE

cm	Centi-meter
Col-0	Columbia-0
CTAB	Cetyltrimethyl ammonium bromide
DAG	Days after germination
DAI	Days after induction
ddH ₂ O	Double-distilled water
DEPTOR	DEP DOMAIN-CONTAINING MTOR-INTERACTING PROTEIN
DEX	Dexamethasone
DNA	Deoxyribonucleic acid
EdU	Ethynyl deoxyuridine
eIF2	EUKARYOTIC INITIATION FACTOR 2
eIF3h	EUKARYOTIC TRANSLATION INITIATION FACTOR 3h
eIF4E	EUKARYOTIC TRANSLATION INITIATION FACTOR 4E
FAT	FRAP, ATM, TRAPP2
FATC	FAT, C-terminal
FKBP12	FK506 BINDING PROTEIN
FLC	FLOWERING LOCUS C
FRB	FKBP12-rapmycin binding
FT	FLOWERING LOCUS T
g	Gram
GAP	GTPase activating protein
GEF	GUANINE NUCLEOTIDE EXCHANGE FACTOR
GFP	GREEN FLUORESCENCE PROTEIN
GL	GLABRA

GOI	Gene of interest
GUS	β -glucuronidase
h	Hour(s)
H ₂ O ₂	Hydrogen peroxide
HEAT	Huntingtin, Elongation factor 3, A subunit of protein phosphatase 2a, and TOR1
hiTAIL-PCR	High-efficiency thermal asymmetric interlaced PCR
HM	Hydrophobic motif
HSp	Heat shock promoter
kbp	1000bp
KOG1	KONTROLER OF GROWTH
LD	Long day
LD	Long day (16h light 8h dark)
LRX1	LEUCINE-RICH REPEAT/EXTENSIN 1
LST8	Lethal with SEC 13 protein 8
LTP1	LIPID TRANSFER PROTEIN 1
MEI2	MEIOSIS REGULATOR-2
mg	Milli-gram
MIPS1	MYO-INOSITOL-1 PHOSPHATE SYNTHASE 1
mL	Milli-liter
mm	Milli-meter
mRNA	Messenger ribonucleic acid
MS	Murashige and Skoog
mTOR	Mechanistic/Mammalian TOR
n	Sample size

NiR	NITRITE REDUCTASE
nm	nano-meter
NR	NITROGEN REDUCTASE
PA	Phosphatidic acid
PCG1 α	PEROXISOME PROLIFERATOR-ACTIVATED RECEPTOR (PPAR)- γ coactivator
PDK1	PHOSPHOINOSITIDE-DEPENDENT KINASE 1
PI	Phosphatidylinositol
PI(3,4,5)P ₃	Phosphatidylinositol 3,4,5-triphosphate
PI3K	PHOSPHATITYLINOSITOL-30-KINASE
PI-3P	Phosphatidylinositol 3-phosphate
PIKK	Phosphatidylinositol 3-kinase-related kinase
PIN	PIN-FORMED
PKC	PROTEIN KINASE C
PLD	PHOSPHOLIPASE D
PP2A	PROTEIN PHOSPHATASE 2A
PRAS40	PROLINE-RICH AKT SUBSTRATE OF 40KDA
PTEN	PHOSPHATASE AND TENSIN HOMOLOG
RAG	RAS-RELATED GTPASE
RAM	Root apical meristem
RAPTOR	REGULATORY-ASSOCIATED PROTEIN OF TOR
RBR1	RETINOBLASTOMA-RELATED 1
RD	Regulatory domain
RHEB	RAS HOMOLOG ENRICHED IN BRAIN

RHO1	RAS HOMOLOG 1
RiBi	Ribosome biogenesis
RICTOR	RAPAMYCIN-INSENSITIVE COMPANION OF MTOR
RNA	Ribonucleic acid
RNC	RAPTOR N-terminal conserved
RNC/C	RAPTOR N-terminal Conserved / putative Caspase
ROM2	RHO1 MULTICOPY SUPPRESSOR 2
ROS	Reactive oxygen species
RRM	RNA-recognition motifs
RT	Room temperature
RTG	Retrograde response pathway
S6K	40S RIBOSOMAL PROTEIN S6 KINASE
SD	Short day
SD	Short day (10h light 12h dark)
SEM	Scanning electron microscope
SFP1	SPLIT FUNGER PROTEIN 1
SNRK1	SNF1-RELATED KINASE-1
STAT3	SIGNAL TRANSDUCER AND ACTIVATOR OF TRANSCRIPTION 3
TAG	Triacylglyceride
TAP	TWO A PHOSPHATASE ASSOCIATED PROTEIN
TCA	Tricarboxylic acid cycle
TCO89	89-KDA SUBUNIT OF TOR COMPLEX ONE
TM	Turn motif
TOR	TARGET OF RAPAMYCIN

TORC	TOR complex
TOS	MTOR signalling motif
TPR	Tetratricopeptide repeat
TSC	TUBEROUS SCLEROSIS
U2AF	U2 AUXILIARY FACTOR
ULK1	UNC51-LIKE KINASE 1
uORF	Upstream open reading frame
VPS34	VACUOLAR PROTEIN-SORTING DEFECTIVE 34
Wat1p	WD repeat-containing protein
WOX5	WUSCHEL-RELATED HOMEODOMAIN 5
Wt	Wild type

List of figures

Figure 1.1 Protein domain structures of TOR, RAPTOR and LST8 in representative species.	4
Figure 1.2 The mammalian TOR pathway.....	13
Figure 1.3 Overview of the TOR pathway in plants.	30
Figure 3.1 Genomic locations of T-DNA insertions within <i>RAPTOR</i> genes.	60
Figure 3.2 Agarose gel of genotyping-PCR with <i>RAPTOR3G</i> lines.....	60
Figure 3.3 Agarose gel of genotyping PCR with <i>RAPTOR5G</i> lines.	61
Figure 3.4 Phenotypes of <i>A. thaliana raptor</i> mutants.	63
Figure 3.5 Root growth of <i>raptor</i> mutants.....	63
Figure 3.6 Dose-response curve of <i>A. thaliana</i> to the TOR inhibitor AZD8055.....	65
Figure 3.7 Genomic sequences of <i>RAPTOR3G</i> and <i>RAPTOR5G</i>	66
Figure 3.8 Expression profile of GUS reporter lines.	67
Figure 3.9 GUS activity in floral organs and gametophytes of GUS reporter lines.....	68
Figure 3.10 Significantly activated and repressed gene clusters in <i>raptor3g raptor5g</i> mutants.....	70
Figure 3.11 Representation of differentially expressed genes between <i>raptor3g raptor5g</i> mutants and wt plants.....	71
Figure 3.12 Expression profile of cell cycle-related genes in wt and <i>raptor3g raptor5g</i> mutants.....	72
Figure 3.13 Length of root hairs in wt and <i>raptor3g raptor5g</i> mutants.	74
Figure 3.14 Root hairs of mature primary roots.....	74
Figure 3.15 ROS accumulation in root hairs.....	75
Figure 3.16 Quantitative measurements of H ₂ O ₂ levels.	75
Figure 3.17 S-phase staining of cell with EdU.....	77
Figure 3.18 Longitudinal length of cortex cells in wt and <i>raptor3g raptor5g</i> mutants. ...	78
Figure 3.19: Leaf development of wt and <i>raptor3g raptor5g</i> mutants.	80
Figure 3.20 Leaf epidermis of wt and <i>raptor3g raptor5g</i> mutants.	81
Figure 3.21 Quantitative measurements of the surface area of pavement cells.	81
Figure 3.22 Trichomes of wt and <i>raptor3g raptor5g</i> mutants.....	82
Figure 3.23 DNA content analysis using flow cytometry.....	83
Figure 4.1 Flower initiation of wt and <i>raptor3g raptor5g</i> mutants.....	95
Figure 4.2 Phenotypes of wt and <i>raptor3g raptor5g</i> mutants at time of flowering	95

Figure 4.3 Inflorescences of <i>A. thaliana raptor</i> mutants.....	96
Figure 4.4 Female gametophytes of wt and <i>raptor3g raptor5g</i> mutants.....	98
Figure 4.5 Pollen viability test using Alexander staining.	100
Figure 4.6 Measurement of pollen tube growth.	101
Figure 4.7 Quantitative measurement of pollen tube growth.	101
Figure 5.1 T-DNA sequence of pCBI- <i>RAPTOR3G</i> ^{lox} vector.....	111
Figure 5.2 Scheme for the creation of <i>RAPTOR3G</i> ^{lox} lines.....	112
Figure 5.3 T-DNA sequences of pCRE vectors.	114
Figure 5.4 Scheme for the creation of <i>A. thaliana CRE</i> lines.....	114
Figure 5.5 Overview of the generation of <i>RAPTOR</i> ^{lox} CRE lines.	116
Figure 5.6 Induction of HSp::CRE <i>RAPTOR3G</i> ^{lox} and control lines.	119
Figure 5.7 Induction of <i>raptor</i> deletion sectors in various tissue of the RAM.....	122
Figure 5.8 Induction of large <i>raptor</i> deletion sectors in the root.....	124
Figure 6.1 Control series of HSp::CRE <i>LST8.1</i> ^{lox} and control lines.....	134
Figure 6.2 Induction of large <i>lst8.1</i> deletion sectors in the root.....	136
Figure 6.3 Induction of <i>lst8.1</i> deletion sectors in various tissue of the RAM.	137
Figure 6.4 Phenotypes of wt, <i>raptor3g raptor5g</i> and <i>lst8.1</i> mutants in response to light period changes.	139
Figure 6.5 DNA content analysis of <i>raptor3g raptor5g</i> and <i>lst8.1</i> mutants using flow cytometry.	141
Figure 6.6 Phenotypes of <i>raptor3g raptor5g</i> and <i>lst8.1</i> with reduced TOR gene dosage.	146

List of tables

Table 1.1 Components of TORC1 and TORC2.....	16
Table 2.1 LST8 PCR-reaction mixture.....	38
Table 2.2 RAPTOR-PCR reaction mixture.....	39
Table 2.3 Cloning-PCR setup.....	39
Table 2.4 Sequencing reaction mixture.....	40
Table 2.5 Sequencing reaction setup.....	41
Table 2.6 Colony-PCR mixture.....	44
Table 2.7 Colony-PCR setup.....	44
Table 2.8 Promoter-PCR mixture.....	45
Table 2.9 Promoter-PCR setup.....	45
Table 2.10 Genotyping-PCR mixture.....	47
Table 2.11 Genotyping-PCR setup.....	47
Table 2.12 Agrobacterium strains and selective antibiotics.....	48
Table 2.13 Thermocycling conditions of hiTAIL-PCR reactions.....	51
Table 3.1 Relative representation of trichome phenotypes of wt and <i>raptor3g raptor5g</i> mutants.....	82
Table 4.1 Transmission ratio of <i>raptor</i> alleles through the male and female gametophyte.....	100
Table 5.1 List of RAPTOR3G ^{lox} lines.....	112
Table 5.2 List of <i>CRE</i> lines.....	115
Table 6.1 List of LST8.1 ^{lox} lines.....	132
Table 6.2 Transcriptomic comparison of <i>raptor3g raptor5g</i> and <i>lst8.1</i> mutants.....	143

Chapter 1

General introduction

The ability to grow is an essential aspect of life. Since the formulation of the cell theory and the discovery of cell division in the middle of the 19th century, growth has been defined by the increase of cell size and mass, which is often accompanied by an increased cell number. With the discovery of *CELL DIVISION CYCLE (CDC)* genes in the early 1970s, a relatively detailed model of how cells regulate and organize division has emerged (Hartwell et al., 1973; Nurse, 1975). By contrast, our knowledge of the mechanisms that lead to an increase in cell mass and size is less advanced. However, molecular genetic studies in more recent years provided evidence that this growth is also an actively regulated process. For example, in *Drosophila melanogaster*, down-regulation of insulin signalling mimics a starvation phenotype (Bohni et al., 1999). Conversely, activation of the pathway leads to overgrowth (Brogiolo et al., 2001). These studies illustrated that growth is not simply a function of available nutrients, but also reflects the activity of intermediate signalling pathways that orchestrate growth with respect to prevailing developmental, physiological and environmental conditions. A dramatic example of the importance of this harmonized regulation is seen in various forms of cancer where the coupling between limiting signalling inputs and growth is impaired.

In order to adapt the physiology to the environment, organisms must link their growth outputs to several factors such as nutrients, energy and stress. Therefore, strategies have been developed to modulate the balance between storage and anabolic metabolism. In eukaryotes, which include unicellular as well as more complex multicellular organisms, some of the basic mechanisms are expected to be retained, given the conservative nature of evolution, and the ongoing need to maintain environmentally sensitive growth strategies. Here, the TARGET OF RAPAMYCIN

(TOR) was identified as a conserved regulator to integrate signals from nutrients, energy, stress and environmental cues to coordinate the proliferation and cell division.

1.1 Target of rapamycin

Originally discovered in yeast, homologues of TOR proteins (earlier also referred to as FRAP, RAFT1, and RAPT1) were found subsequently in other eukaryotes, including insects, mammals and plants. The human TOR homologue, often referred to as mTOR (for mechanistic or mammalian TOR), shares ~44% and 46% amino acid sequence identity with the TOR1 and TOR2 proteins of *Saccharomyces cerevisiae* (Brown, 1994). The importance of TOR is demonstrated by its conservation in most eukaryotes, with the exception of intracellular parasites (van Dam et al., 2011).

1.2 Discovery

The discovery of the TOR pathway goes back to the 1970s, when the macrolide rapamycin was isolated from soil samples collected on Easter Island (in the native language *Rapa nui*). It was found to be produced by the bacteria *Streptomyces hygroscopicus* and to cause a strong inhibition of growth in yeast (Vezina et al., 1975). A screen of resistant *S. cerevisiae* strains mapped rapamycin resistance to recessive mutations in three genes, *FPR1*, *TOR1* and *TOR2*. Together, the combined activity of these three genes could be held responsible for the toxic effect of rapamycin (Kunz and Hall, 1993; Helliwell et al., 1994). The most frequent mutations were observed in the *FPR1* gene encoding for the peptidyl-prolyl cis-trans isomerase FKBP12 (FK506 BINDING PROTEIN), which was demonstrated to be required for the action of rapamycin (Heitman et al., 1991). However, this binding did not account for the toxicity of rapamycin, because *fpr1*-mutants were not affected in their growth (Heitman et al., 1991; Koltin et al., 1991). By contrast, both *TOR1* and *TOR2* genes are essential for normal growth, but TOR proteins do not bind rapamycin directly. Instead, rapamycin was shown to bind to a hydrophobic pocket of FKBP12, forming a heterodimer, which

subsequently was able to interact with TOR and block its kinase activity (Brown, 1994). This indirect action of rapamycin through a ternary complex formation with FKBP12 was confirmed in studies using rapamycin-insensitive *TOR* mutations, in which the FKBP12-rapamycin binding (FRB) domain was disrupted (Chen et al., 1994; Stan et al., 1994; Choi et al., 1996).

1.3 TOR protein features

With a size of about 280kDa, TOR proteins are relatively large. Their complex but well conserved domain organization groups them into the family of Phosphatidylinositol 3-kinase-related kinases (PIKKs). The typical domain pattern of TOR proteins is illustrated in Figure 1.1. The N-terminal region of TOR proteins is characterized by 20 HEAT (for Huntingtin, Elongation factor 3, A subunit of protein phosphatase 2a, and TOR1) repeats, which feature a ~40 amino acid sequence, that forms two anti-parallel α -helices (Groves and Barford, 1999). These HEAT repeats were demonstrated to mediate protein-protein interactions and membrane associations (Andrade and Bork, 1995; Kunz et al., 2000). Downstream of the HEAT domain, a FRAP, ATM, TRAPP2 (FAT) domain is located, which is conserved within the PIKK family and potentially contributes to protein interactions and the kinase activity of TOR (Knutson, 2010; Hardt et al., 2011). The FAT domain is followed by the FRB domain, which mediates formation of the inhibitory ternary complex with FKBP12 and rapamycin. Adjacent to the FRB domain is the catalytic kinase domain, which shares high similarity to those of PHOSPHATIDYLINOSITOL-3 KINASE (PI3K). Despite this similarity, TOR, together with the five other members of the PIKK family, represents a Ser/Thr-protein kinase. (Brunn et al., 1997; Burnett et al., 1998). Another FAT domain, named FATC (for FAT, C-terminal) is located at the C-terminal end. In yeast and mammals, mutations in the very C-terminal region indicated a crucial role in TOR functionality (Takahashi et al., 2000; Dames, 2010). Further studies in yeast indicated that the FATC domain

mediates protein interactions, and also promotes correct folding of the kinase domain through interacting with the FAT domain (Alarcon et al., 1999).

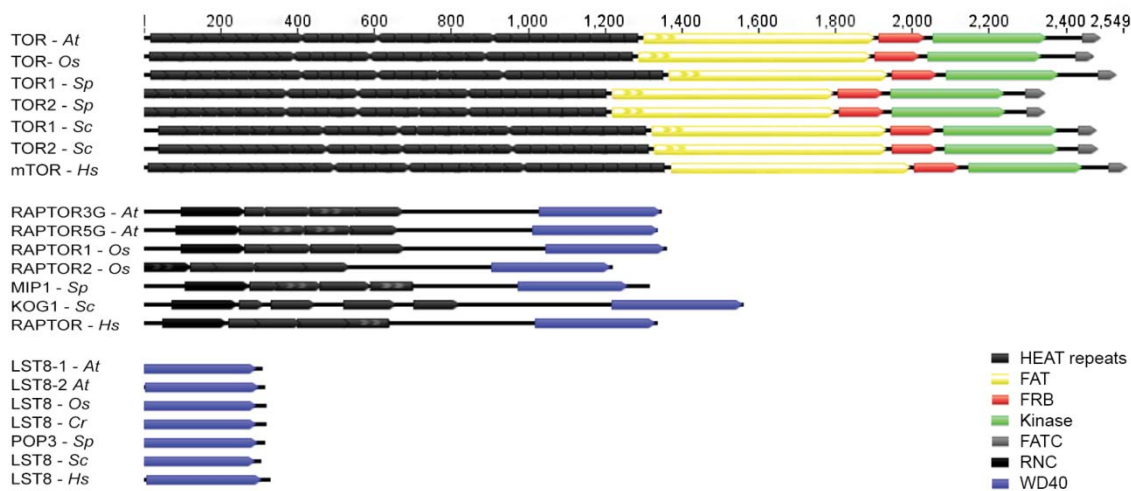


Figure 1.1 Protein domain structures of TOR, RAPTOR and LST8 in representative species. Numbers above figure indicate length of primary protein structure in amino acids. At, *Arabidopsis thaliana*; Os, *Oryza sativa*; Sp, *Saccharomyces pombe*; Sc, *Saccharomyces cerevisiae*; Hs, *Homo sapiens*; Cr, *Chlamydomonas reinhardtii*.

1.4 TOR complex formation

The FKBP12-rapamycin complex was demonstrated to be highly specific for binding the FRB domain within TOR, which resulted in an efficient inhibition of the kinase activity (Heitman et al., 1991). This has proven to be an excellent tool for the analysis of TOR functions. The additional use of genetics revealed functional differences between TOR1 and TOR2. Knock-out mutants of *TOR1* in *S. cerevisiae* showed reduced cell growth, which is also seen after rapamycin treatment. However, the deletion of *TOR2* led to a more severe phenotype, in which cells are arrested during the cell cycle (Cafferkey et al., 1993; Kunz and Hall, 1993). Similar observations were made in double knock-outs of both *TOR* genes (Cafferkey et al., 1993; Kunz et al., 1993; Helliwell et al., 1994). These findings indicated a redundant function of both TOR

proteins, which was affected by rapamycin and required for cell growth. Later, Zheng et al. (1995) demonstrated that the treatment of *tor2* mutants with rapamycin caused a lethal arrest, which could not be rescued by introducing a rapamycin-resistant TOR1. This implied that TOR2 has additional functions, which are rapamycin-insensitive. The occurrence of two TOR genes in yeast helped to discover these two different branches of TOR function, which anticipated the discovery of two different TOR complexes, TOR complex 1 and 2 (TORC1 and TORC2), which were later revealed in biochemical studies in yeast and animals (Loewith et al., 2002).

1.4.1 The TOR complex 1

TOR1 or TOR2 were found incorporated with KONTROLER OF GROWTH (KOG1) and LETHAL WITH SEC 13 PROTEIN 8 (LST8) in the TORC1 of budding yeast (Loewith et al., 2002). In contrast, only TOR2 was found incorporated in TORC2, which additionally contained the subunits AVO1, 2, 3 (for ADHERES VORACIOUSLY TO TOR1, -2, -3) (Loewith et al., 2002). It was later confirmed that TOR, KOG1 (outside of yeast also known as RAPTOR (for REGULATORY-ASSOCIATED PROTEIN OF TOR)), and LST8 (also known as G β L (for G protein β -subunit-like protein)) are highly conserved across diverse eukaryotic taxa (van Dam et al., 2011). Protein components of the TOR complexes in yeast and their homologs in other species are listed in Table 1.1.

1.4.2 RAPTOR

The first description of RAPTOR was carried out in *Saccharomyces pombe*, where it was shown to interact with the meiotic regulator Mei2p (Shinozaki-Yabana et al., 2000). Shortly after, co-precipitation assays in human cell lines and budding yeast identified RAPTOR as an interaction partner of TOR (Kim et al., 2002; Loewith et al., 2002). Subsequently, RAPTOR was found to be as conserved across eukaryotes as TOR (van Dam et al., 2011). The protein structure of RAPTOR does not provide any indication of a catalytic function. However, several highly conserved regions were

identified that were shown to mediate protein-protein interactions. The RNC (RAPTOR N-terminal conserved) domain was identified to be required for substrate recognition of mTOR (Dunlop et al., 2009). Similar to TOR, the protein sequence contains multiple HEAT repeats (Figure 1.1), which therefore are believed to contribute to the interaction of both proteins (Kim et al., 2002; Kim et al., 2003). This was later confirmed with *in vivo* studies in several species (Mahfouz et al., 2006; Adami et al., 2007). The interaction with other proteins is also mediated by seven WD40 repeats at the C-terminal region of RAPTOR. These were demonstrated to provide a platform for protein interactions with various types of proteins (reviewed by Smith et al., 1999). Coinciding with observations of *tor* mutants, deletion of *RAPTOR* was shown to cause lethality in several species. In *S. pombe*, where RAPTOR/Mip1p was found to interact with Mei2p, a disruption of *RAPTOR* caused a lethal arrest. As this was not observed in *mei2p* mutants, the essential function of RAPTOR was not linked to its Mei2p-related role in meiosis (Shinozaki-Yabana et al., 2000). Later, RAPTOR was also found to be essential in *S. cerevisiae* and animals (Loewith et al., 2002; Guertin et al., 2006). In animals, *raptor* knock-outs were shown to lead to an early embryonic arrest in mice, similar to *mtor* mutants (Guertin et al., 2006). Knock-out experiments in *Caenorhabditis elegans* and *D. melanogaster* also confirmed its essential role for growth and development in insects (Jia et al., 2004; Lee and Chung, 2007).

1.4.3 LST8

In contrast to RAPTOR, LST8 is incorporated in both TOR complexes. In budding yeast, a screen found it to cause lethality in *sec13* mutants, defective in membrane trafficking (Roberg et al., 1997). In the same year, the homologue in fission yeast, Wat1p, was found in interaction with a subunit of the splicing factor U2AF (Kemp, 1997). Homologues were also discovered throughout eukaryotes including mammals, in which the homologue GβL was initially described by Rodgers et al. (2001) in 2001 before it was linked to TOR activity (Kim et al., 2003). The primary protein sequence of

LST8 resembles heterotrimeric G protein β -subunits and contains seven well-conserved WD40 repeats, which is one of the most abundant protein domains found in eukaryotes (Rodgers et al., 2001; Loewith et al., 2002). These form a stable propeller-like structure that is well-characterized in its ability to mediate protein and DNA binding (Smith et al., 1999; Stirnimann et al., 2010). Similar to RAPTOR, no catalytic function has yet been detected in LST8 and therefore it is thought to act as a scaffolding protein (Kim et al., 2003). This is further supported by functional characterizations of other WD40 domain-proteins, which have been shown to recruit target proteins to catalytic domains (Nash et al., 2001; Yaffe and Elia, 2001). Functional studies revealed that the disruption of *LST8* caused lethality in budding yeast and mice, probably due to its essential function in TORC2 (Kim et al., 2003; Wullschleger et al., 2005; Guertin et al., 2006). Yet the impact of LST8 on TORC1 function is still controversial. Earlier results in yeast, nematodes, and human cell lines indicated that LST8 mediated interaction between RAPTOR and the kinase domain of TOR through its WD40 domain, which was essential for the catalytic activity of TOR (Chen, 2003; Kim et al., 2003). This rationale was supported by recent co-crystallization studies that showed the association of LST8 close to the active site of the kinase domain of TOR (Yip et al., 2010; Yang et al., 2013). However, knock-out studies in flies and fibroblasts of mice indicate that LST8 is dispensable for TORC1 and only required for TORC2 activity (Guertin et al., 2006; Wang et al., 2012).

1.4.4 Additional interaction partners of TOR in TORC1

In addition to TOR, LST8 and RAPTOR, further components of the TORC1 were described but these are generally less conserved (van Dam et al., 2011). In budding yeast, subsequent co-immunoprecipitation studies identified TCO89 (for 89-KDA SUBUNIT OF TOR COMPLEX ONE), Bit61 (for 61-kDa Binding partner of Tor2) and Bit2 as additional components in both TOR complexes (Reinke, 2004). Additional components of the mammalian TORC1 include PROLINE-RICH AKT SUBSTRATE OF

40KDA (PRAS40) and DEP DOMAIN-CONTAINING MTOR-INTERACTING PROTEIN (DEPTOR). These are thought to act as negative regulators of TORC1 through binding to the kinase domain. Phosphorylation of PRAS40 and DEPTOR by TORC1 itself weakens their association with TOR, which subsequently promotes further activation of TOR activity (Oshiro et al., 2007; Sancak, 2007; Thedieck, 2007; Vander Haar et al., 2007). The lower evolutionary conservation of these factors might reflect the specific adaptation of TOR signalling in these species.

1.5 TORC1 substrates and functions

Since its discovery in the early 1990s, the use of rapamycin has helped to characterize the function of TOR mediated growth control. Several substrates were identified, which linked TOR activity to a broad spectrum of cellular processes including different aspects of proliferation, cell cycle regulation and modulation of various metabolic pathways. An overview of the mammalian TOR signalling pathway is given in Figure 1.2.

1.5.1 Protein synthesis

The most well-known targets of TORC1 affecting protein synthesis are 4E-BINDING PROTEIN 1 and -2 (4E-BP1 and -2) and the 40S RIBOSOMAL PROTEIN S6 KINASE (S6K). Through the activation by TOR, both promote the activation of translation, either through direct or indirect phosphorylation of ribosomal proteins and translation factors (Gingras, 2001; Miron et al., 2003). In its dephosphorylated state, 4E-BP1 suppresses initiation of translation by binding to EUKARYOTIC TRANSLATION INITIATION FACTOR 4E (eIF4E), which prevents the assembly of the pre-initiation complex. Upon phosphorylation by TORC1, 4E-BP1 dissociates from eIF4E and allows for mRNA translation (Beretta et al., 1996).

The first discovered rapamycin-sensitive target of TOR was S6K, which is well conserved in eukaryotes (Burnett et al., 1998). Like 4EBP, S6K contains a mTOR

signalling motif (TOS), that was shown to mediate direct interaction with RAPTOR and subsequent phosphorylation by TOR (Nojima et al., 2003; Schalm et al., 2003). S6K groups into the family of AGC kinases, which is well represented in the TOR pathway and also includes PHOSPHOINOSITIDE-DEPENDENT KINASE 1 (PDK1), PROTEIN KINASE B (PKB or Akt) and PROTEIN KINASE C (PKC) (reviewed by Pearce et al., 2010). The general domain structure of AGC kinases consists of a lipid binding PH domain, kinase domain and two conserved regions near the C-terminus, the turn motif (TM) and hydrophobic motif (HM) (reviewed by Su and Jacinto, 2011). mTORC1 was found to phosphorylate Thr389 within the HM of S6K in several species (Stocker, 2003; Urban et al., 2007; Polak et al., 2008). Phosphorylation at this site promotes binding and subsequent phosphorylation by PDK1 at the T-loop site within the kinase domain of S6K (Pullen et al., 1998; Biondi et al., 2001). This results in an up-regulation of translation through activation of transcription factors as well as ribosomal proteins. An example would be the phosphorylation of eIF4B by S6K, which leads to an increased activity of the helicase eIF-4A (Raught et al., 2004). Subsequently, this promotes the binding of eIF-4A to the eIF4F complex and thereby increases its affinity to the 5' UTR of mRNAs (Shahbazian et al., 2006).

TORC1 has also been linked to the activation of translation initiation factor EUKARYOTIC INITIATION FACTOR 2 (eIF2) in multiple ways via S6K and PROTEIN PHOSPHATASE 2A (PP2A) phosphorylation (Cherkasova and Hinnebusch, 2003). Other studies have provided further indications of TORC1-mediated regulation of protein synthesis via phosphorylation of translation factors and related proteins, i.e. eIF4E (Berset et al., 1998; Cosentino et al., 2000; Soulard et al., 2010).

1.5.2 Ribosome biogenesis

A key requirement in activating mRNA translation and protein synthesis is the synthesis, processing, and assembly of ribosome proteins and rRNA, which is also referred to as ribosome biogenesis (RiBi). In yeast, TORC1 impinges on RiBi in multiple ways via Sch9, the homologue of S6K. For example, Sch9-mediated phosphorylation causes Maf1 to disassociate from RNA Polymerase III, which activates rRNA transcription (Michels, 2011). In mammals, a similar mechanism was found by which Maf1 is directly phosphorylated by TORC1 (Wei et al., 2009). Another Sch9-mediated response includes the transcriptional up-regulation of polymerase genes through phosphorylation of myb-family transcription factors (Lippman and Broach, 2009; Liko et al., 2010; Huber et al., 2011). In yeast and animals, TORC1 phosphorylates the conserved zinc finger transcription factor SPLIT FINGER PROTEIN 1 (SFP1), which regulates RiBi expression (Jorgensen et al., 2004; Lempiäinen et al., 2009). The impact of TOR on RiBi was recently demonstrated by a transcriptional analysis of *s6k* mutants in mice, which found 75% of all RiBi genes differentially expressed (Chauvin et al., 2014).

1.5.3 Cell cycle

Regulation of cell size and pre-mitotic cell expansion are key functions of TOR. Mutants of *sch9* and *sfp1* in *S. cerevisiae* displayed a reduced cell size (Jorgensen et al., 2004; Lempiäinen et al., 2009). This might reflect the specific characteristic of unicellular yeast, in which the initiation of the cell cycle is blocked until cells have reached a certain size (Cook and Tyers, 2007). Other, more direct impacts on cell cycle regulation include roles in DNA replication through controlling DNA synthesis, and G2 to M phase transition (Nakashima et al., 2008). In mammals, TORC1 has been shown to enhance the expression of genes involved in protein synthesis through phosphorylating SIGNAL TRANSDUCER AND ACTIVATOR OF TRANSCRIPTION 3 (STAT3), a key regulator of cell cycle and apoptosis (Yokogami et al., 2000; Kim,

2009). These studies indicate that cell cycle regulation is a major branch of TOR function.

1.5.4 Metabolism and mitochondrial activity

Transcriptional studies in yeast demonstrated that TORC1 is involved in regulating metabolic activity *via* the retrograde response pathway (RTG), which communicates feedback responses from mitochondria to the nucleus (Komeili et al., 2000; Shamji et al., 2000; Chen, 2003). However, the RTG signalling found in yeast is not well-conserved across eukaryotes. Yet the importance of adjusted metabolic activity to growth conditions suggest a close relation with TOR signalling (reviewed by Wei et al., 2014). In mammalian cell lines, TORC1 activity has been shown to increase copy number of mitochondrial DNA and up-regulate the expression of genes involved in the regulation of mitochondrial enzymes. This included PEROXISOME PROLIFERATOR-ACTIVATED RECEPTOR (PPAR)- γ coactivator (PCG1 α), a transcription factor involved in regulation of mitochondrial biogenesis and metabolism (Lin et al., 2005; Cunningham et al., 2007; Koyanagi et al., 2011). Further, phospho-proteomic studies indicated that TOR is likely to impinge directly on primary metabolism by phosphorylating enzymes of glycolysis (Loewith, 2011).

1.5.5 Autophagy

Autophagy describes the degradation and recycling of macromolecules and organelles to generate energy and building blocks for new synthesis. This process is generally antagonistic to growth. Autophagy is functionally well-conserved in eukaryotes and is mediated through the complex formation of AUTOPHAGY-RELATED (ATG) proteins. In *S. cerevisiae*, TORC1 phosphorylates ATG13, which prevents formation of the pre-autophagosome initiation complex (Yorimitsu et al., 2009; Kamada et al., 2010). In mammals, several studies confirmed an analogous mechanism, in which phosphorylation altered the kinase activity of UNC51-LIKE KINASE 1 (ULK1), the

homologue of ATG1 (Ganley et al., 2009; Hosokawa et al., 2009; Jung et al., 2009). Recent studies confirmed direct phosphorylation of ULK1 by TOR at Ser758 *in vivo* (Kim et al., 2011; Shang et al., 2011). Apart from preventing autophagosome formation, this was also reported to affect the interaction of ULK1 with AMPK, the energy sensing kinase. These studies prove a close and complex interplay between AMPK mediated energy sensing, ULK1 driven autophagy and TOR regulated growth response (reviewed by Dunlop and Tee, 2013). Further clues were provided by studies in *D. melanogaster*, which showed that ATG1 negatively regulates S6K. This indicated a bidirectional signalling between growth and autophagy (Lee et al., 2007; Scott et al., 2007). Furthermore, recent studies in mammalian cell lines showed a feedback response between ULK1 and TORC1 via ULK1-mediated phosphorylation of RAPTOR (Dunlop et al., 2011; Jung et al., 2011).

1.5.6 Lifespan

The inhibition of TORC1 leads to an extension of lifespan in yeast, nematodes, flies, and mice (Vellai et al., 2003; Kapahi et al., 2004; Wanke et al., 2008; Harrison et al., 2009). In *C. elegans*, reduced translation of Daf-15, the homolog of RAPTOR, increased the lifespan by 30%, and a dominant TOR mutation in *D. melanogaster* increased lifespan by 15% (Jia et al., 2004; Kapahi et al., 2004). In yeast and animals, lifespan elongation is also observed under dietary restriction. Interestingly, studies in yeast and insects showed no additive effect of dietary restriction and rapamycin treatment, indicating an overlap between both effects (Grandison et al., 2009). Recent studies in *D. melanogaster* and mice however highlighted some differences in metabolomic changes after dietary restriction and rapamycin treatment (Bjedov et al., 2010; Miller et al., 2014). Therefore, the relation between TOR activity and lifespan extension still demands further clarification.

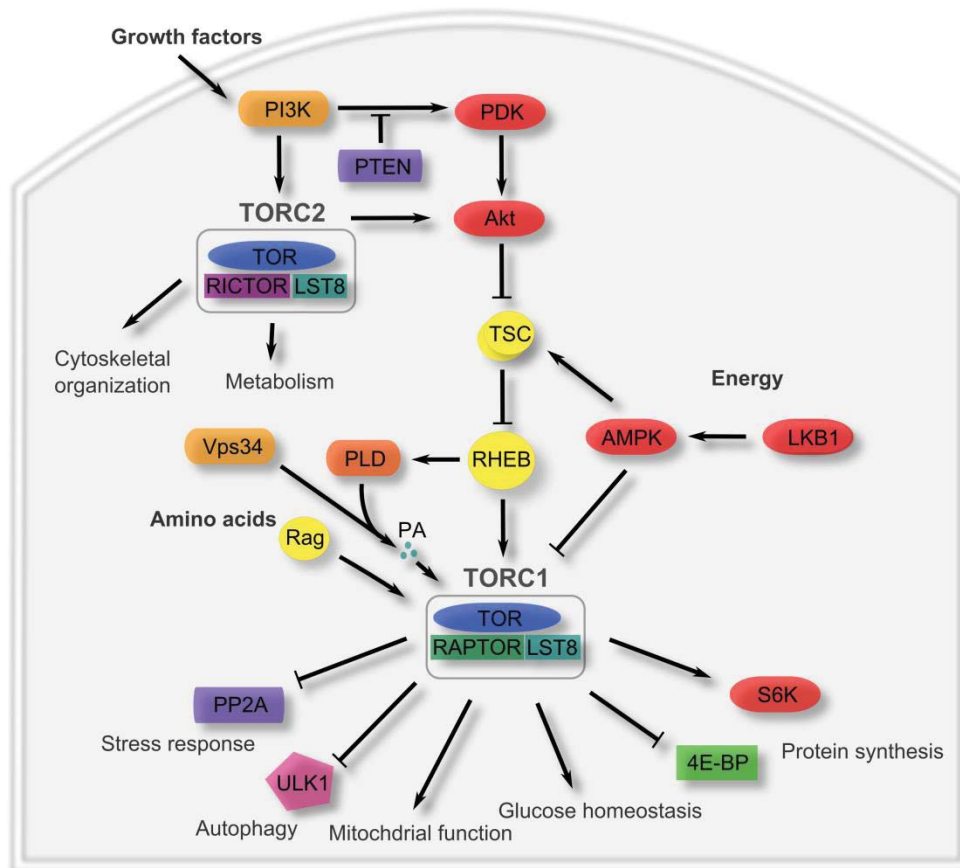


Figure 1.2 The mammalian TOR pathway.

1.6 The TOR complex 2

The early genetic studies in *S. cerevisiae* were able to uncover a second functional branch of TOR, which consisted exclusively of TOR2 and showed no sensitivity to rapamycin (Cafferkey et al., 1993; Kunz and Hall, 1993). Later, biochemical studies confirmed this function also in species containing only a single TOR gene through the discovery of the TOR complex formations (Loewith et al., 2002). The conserved components of TORC2 consist of a TOR2, LST8, AVO1, and AVO3 (Loewith et al., 2002; van Dam et al., 2011). A list of TORC2 components in different *taxa* is given in Table 1.1. Studies of knock-out mutants in mice showed that a deletion of any TORC2 component caused a lethal arrest during embryonic development (Gangloff et al., 2004; Guertin et al., 2006; Jacinto et al., 2006; Shiota et al., 2006; Yang et al., 2006). Some

evidence suggested that TORC2 function could be tissue specific, as knock-out mutants of RAPAMYCIN-INSENSITIVE COMPANION OF MTOR (*RICTOR*), the homologue of AVO3, displayed only minor effects in mice (Bentzinger et al., 2008; Kumar et al., 2008; Cybulski et al., 2009). However, the requirement for TORC2 seems to be less consistent across species than TORC1. For instance, the depletion of *RICT-1*, the homologue of RICTOR in *C. elegans*, caused slow growth, delayed development and shortened lifespan but was not lethal (Webster et al., 2013). Similar observations were also made in *D. melanogaster*, in which *lst8* and *rictor* knock-out mutants caused a similar viable phenotype. Studies in yeast also suggested differential roles of TORC2 in *S. pombe* and *S. cerevisiae*. While *tor2* knock-out mutants in *S. pombe* showed arrests only under stress conditions, deletion of *tor2* in *S. cerevisiae* caused an arrest in the G2/M phase within a few generations (Kuru et al., 1993; Helliwell et al., 1994; Schmidt et al., 1996; Kawai, 2001; Weisman and Choder, 2001). The divergent observations of TORC2 mutants in different species emphasize the adaptation of TOR activity and function to the specific physiology of one organism.

1.6.1 TORC2 substrates and functions

The first functional characterization of TORC2 in yeast hinted at a role in spatially directing growth through actin cytoskeleton polarization, which directs the secretory pathway to guide lipids and proteins towards growing regions of the cell. Here, TOR2 has been shown to signal to ROM2, the GUANINE NUCLEOTIDE EXCHANGE FACTOR (GEF) of the GTPase RHO1, which is involved in actin cytoskeleton polarization (Schmidt et al., 1997; Bickle et al., 1998). In yeast, the membrane bound Slm proteins, involved in sphingolipid synthesis, were linked to PI(4,5)P₂ and TORC2 signalling. Upon plasma membrane stress, TORC2 affects membrane composition by relocating Slm proteins to the plasma membrane (Audhya et al., 2004; Fadri et al., 2005; Berchtold et al., 2012).

As described above, the most prominent target of TORC1, S6K, falls into the family of AGC kinases. Members of this family have also been identified as targets of TORC2. Studies in mammalian cell lines and *D. melanogaster* demonstrated a TORC2-dependent phosphorylation of PKB and PKC, although further studies have yet to confirm a direct interaction with the latter (Sarbasov et al., 2005; Yang et al., 2006; Ikenoue et al., 2008). These interactions link TORC2 to the wide spectrum of cellular functions associated with PKB, which include metabolic regulation and G1/S cell cycle progression, and PKC, which is linked to cell cycle regulation, proliferation and apoptosis (reviewed by Poli et al., 2014; Toker and Marmiroli, 2014). As described in the next section, PKB is also a central regulator of TORC1 activity (Inoki et al., 2002; Potter et al., 2002). This highlights the well-integrated regulation of both TOR complexes.

Table 1.1 Components of TORC1 and TORC2. List of TORC1 and TORC2 proteins in *S. cerevisiae*, *S. pombe*, *C. elegans*, *D. melanogaster*, and *H. sapiens*. Table adapted from Wullschleger et al. (2006).

	<i>S. cerevisiae</i>	<i>S. pombe</i>	<i>C. elegans</i>	<i>D. melanogaster</i>	<i>H. sapiens</i>
TORC1	TOR1 or TOR2	TOR2p or TOR1p	TOR	TOR	Tor
	KOG1	Mip1p	Daf-15	RAPTOR	RAPTOR
	LST8	Wat1p	LST8	LST8	LST8
	TCO89	-	-	-	-
	-	-	-	-	DEPTOR
TORC2	TOR2	TOR1p	TOR	TOR	TOR
	AVO1	Sin1p	-	-	hSin1
	AVO2	-	-	-	-
	AVO3	Ste20p	-	-RICTOR	RICTOR
	LST8	Wat1p	LST8	LST8	LST8
	BIT61	-	-	-	-
	-	-	-	-	DEPTOR

1.7 Regulation of TORC1

As a central regulator of various pathways that contribute to growth outputs, TOR activity itself has to be adjusted to reflect the current physiological status and environmental conditions of the organism. Sufficient nutrients to enable the build-up of

new cell components and energy for synthesis are two essential factors to support growth. In multi-cellular organisms, signalling reflecting the overall physiological state must somehow be coupled to processes that occur on a cellular level. These cellular responses may also be confined to specific tissues. Stimuli by growth factors and hormones provide one means to achieve this coupling. Similarly, unfavourable conditions (i.e. DNA damage or hypoxia) must also be communicated to cells in a coordinated manner to limit their growth. The emerging view holds that these disparate inputs are integrated in part at the level of TOR to modulate its growth controlling kinase activity.

1.7.1 Nutrients

Amino acids are an essential requirement for anabolism, and also TOR activity. The availability of amino acids is sensed by the GTPase Gtr1p in *S. cerevisiae* or RAS-RELATED GTPASE (RAG) in animals. In mammals, different Rag proteins were shown to form the so-called Ragulator complex, which interacts with RAPTOR (Kim et al., 2002; Sancak et al., 2008). This interaction is thought to guide TORC1 towards endosomal and lysosomal membranes to allow further activation of TOR (Sancak et al., 2010).

Although Rag proteins and the Ragulator complex are functionally well-conserved it remains unclear how amino acids are sensed by these proteins. Despite these open questions, recent discoveries have provided significant progress in our understanding of how TORC1 is regulated, which has elucidated the impact of amino acid availability and also the importance of subcellular localisation for TORC1 activity.

A parallel nutrient-dependent regulation of TOR activity is mediated by VACUOLAR PROTEIN-SORTING DEFECTIVE 34 (VPS34) and PHOSPHOLIPASE D (PLD). VPS34 represents a class III PI3K, which phosphorylates phosphatidylinositol (PI) to phosphatidylinositol 3-phosphate (PI-3P) and has been linked to regulation of TOR

activity in mammalian cell lines in response to nutrients (Byfield et al., 2005; Nobukuni et al., 2005). A recent study by Yoon et al. proposed a model, by which PI-3P generated by VPS34 generates a membrane associated anchor to bind proteins containing cognate FVYE or PX domains, including PLD. PLD has been proposed to activate TOR through localised production of phosphatidic acid (PA) (Sun et al., 2008; Yoon et al., 2011). PA was also shown to activate TORC1 via and RAS HOMOLOG ENRICHED IN BRAIN (RHEB) and was required for TOR complex formation (Fang et al., 2001; Toschi et al., 2009). Yet it remains unclear how conserved this form of TOR regulation is, as data from *D. melanogaster* and mammalian cell lines contradict a function of Vps34 in TOR regulation (Kim et al., 2008; Jaber et al., 2012).

1.7.2 Growth factors

With the development of multi-cellularity came the need to relay information relevant to the physiology of the whole organism to enable focused growth in specific organs and tissues. To this end, *metazoa* have developed a strong dependence on growth factors, whose absence may limit growth of specific cells even when sufficient energy and nutrients are available. A well-studied link through which the TOR pathway is connected to a growth factor is the insulin pathway. A simplified model of this signalling pathway is shown in Figure 1.2. Central steps in this signalling cascade are the heterodimeric complex of TUBEROUS SCLEROSIS1 and -2 (TSC1 and -2) and RHEB. TSC2, in complex with TSC1, acts as a GTPase activating protein (GAP) for RHEB and effectively inhibits TORC1 (Manning et al., 2002; Inoki et al., 2003). Insulin-triggered phosphorylation of TSC2 via the PI3K-PDK1-Akt pathway inhibits the GAP activity and prevents inhibition of TORC1 (Manning et al., 2002; Potter et al., 2002; Inoki et al., 2003).

1.7.3 Energy

Growth requires energy to maintain metabolic and cellular processes. The energy status is sensed via adenosine triphosphate (ATP) levels within the cell. The AMP-ACTIVATED PROTEIN KINASE (AMPK) plays a central role in sensing and signalling the cellular energy level (reviewed by Xu et al., 2011). Low energy, signalled by low ATP/high AMP ratios, activates AMPK and inhibits TORC1 activity indirectly through phosphorylation of TSC2 (Inoki et al., 2006). Further, activated AMPK was shown to directly alter TORC1 activity by phosphorylating RAPTOR, which decreased its binding affinity towards TOR (Gwinn et al., 2008).

1.7.4 Stress

Cellular stress, such as lack of oxygen or damaged DNA, has been linked to the TOR pathway by acting through AMPK and TSC2 to inhibit TOR growth stimulation (Brugarolas et al., 2004; Reiling and Hafen, 2004; DeYoung et al., 2008). In mammals and flies, hypoxia activates TSC1/2 to inhibit TORC1 (Brugarolas et al., 2004; Reiling and Hafen, 2004). DNA damage was shown to inhibit TORC1 activity through an activation of TSC1/2 and PTEN in mammalian cell lines (Stambolic et al., 2001; Ellisen et al., 2002; Feng et al., 2005).

1.8 Regulation of TORC2

The regulation of the TORC2 activity is far less explored than that of the TORC1 and is dominantly based on studies in mammals. Here, binding to ribosomes was found to be required to activate TORC2, which was thought to limit its activity to growing cells (Zinzalla et al., 2011). *In vitro* studies showed a response of TORC2 to growth factors but it remains unclear how these affect TORC2 directly (Sarbasov et al., 2005; Frias et al., 2006). Initial studies identified a phosphorylation of RICTOR in response to growth factors and PI3K activity (Boulbes et al., 2010). Additionally, RICTOR has been shown to be phosphorylated by S6K, the target of TORC1 (Dibble et al., 2009; Julien et

al., 2010; Treins et al., 2010). Together with the TORC2-mediated control of TORC1 activity *via* PKB, this underscores the immediate connection between the regulations of both complexes. A shared regulator of both TOR complexes was found in the TSC1/2 complex, which has been shown to be required for full TORC2 activity (Huang et al., 2008). In contrast to TORC1, the signalling between TSC and TORC2 seems to be independent of RHEB (Huang and Manning, 2008, 2009).

1.9 TOR signalling in plants

Although plants have proteins with homology to many elements that have been shown to regulate growth in other eukaryotes, the significance of their function remains unclear. This knowledge gap is potentially significant given the unique aspects of nutrient acquisition and multicellular development in plants. Their ability to utilize light as a direct energy source and to fix atmospheric carbon dioxide to build hydrocarbons creates a unique physiological condition that differs significantly from heterotrophic fungi and animals. Being immobile, plants are wholly dependent on the surrounding environment. These features demand elaborate mechanisms to sense and enable physiological adjustment to the environment. Moreover, the development and general *bauplan* of plants is fundamentally different. For example, the general body plan of animals is typically established during embryogenesis. In contrast, plants have a more plastic pattern of development and retain the ability to grow and to adapt their morphology throughout their lifespan. In some cases, such as *Pinus longaeva*, this growth continues over several thousand years (Schulman, 1958). Despite these fundamental differences, homologues of proteins from the TOR pathway have been retained in plants where they may play important roles in the regulation of growth.

In contrast to animals and yeast, very little has been published about the TOR pathway in plants. Part of this disparity can be attributed to the relevance of TOR to cancer biology, which has driven much of the animal-focused studies. Another factor is the relative insensitivity of plants to rapamycin, which has limited the use of a powerful tool

for TOR analysis. Only a recent study was able to show a noticeable response from *Arabidopsis thaliana* treated with far higher concentrations of rapamycin than applied to other species (Xiong and Sheen, 2012). Despite these shortcomings, orthologues of TOR itself, as well as RAPTOR, and LST8 were identified in *A. thaliana* by DNA sequence analysis (Deprost et al., 2005; Moreau et al., 2012). Other members of the pathway, such as RICTOR and Rheb remain undefined, possibly because of a lower level of conservation that complicates their identification or alternatively, because these are simply not present in plants (van Dam et al., 2011). Nevertheless, recent functional analyses of elements of the TOR pathway in plants support the general conservation of TOR mediated regulation of growth, which is summarised below.

1.9.1 TOR

As in animals, plants appear to maintain TOR exclusively as a single copy gene. For example, despite the whole-genome duplication and common local duplications in *A. thaliana* (Blanc et al., 2000), only one *TOR* gene (*AT1G50030*) is maintained. The protein sequence of TOR in *A. thaliana* shares 40% overall identity with mTOR, while certain domains such as FATC and the kinase domain show a much higher identity of around 75%. Generally, the protein structure of TOR in yeast and animals is well conserved in *A. thaliana*, which hints at a similar function (Figure 1.1). This is underlined by the same phenotype of *TOR* knock-out mutants, which arrested during early embryonic development (Menand et al., 2002). The first functional studies of post-embryonic functions of TOR utilized the yeast *FKBP12* gene or inducible RNAi silencing to overcome the rapamycin resistance (Deprost et al., 2007; Sormani et al., 2007). These studies showed that reduced TOR activity led to an early arrest in growth and development, reduced translational activity, and early senescence. Overall, these findings echoed the observations made by TOR inhibition in yeast and animals (Deprost et al., 2007; Sormani et al., 2007). A study using knock-out lines of *A. thaliana* revealed that the kinase domain alone was capable of compensating for the loss of

TOR in knock-out mutants (Ren et al., 2011). In contrast, over-expression of *TOR* led to an increase in growth rate, size, and seed yield, suggesting that in some conditions, *TOR* activity is limiting for growth (Deprost et al., 2007).

The stable yeast *FKBP12*-containing mutant was characterised by Ren et al. (2012) in great detail. When these were treated with rapamycin they resembled wild type plants which were grown under nutrient and energy limited conditions by showing reduced growth and decrease in cell size. Metabolic and transcriptomic analysis revealed a reduced activity of primary metabolic pathways and an increase of intermediate compounds. Reduced expression of genes involved in RiBi and lower ROS accumulation reconciled with these findings. Further, anabolic pathways, including cell wall synthesis and photosynthesis, were found to be down-regulated (Ren et al., 2012). Interestingly, these plants displayed a greatly delayed flowering and senescence, which conflicted with earlier reports from *tor* RNAi lines (Deprost et al., 2007). The conflicting data might reflect differences in the degree of translational inhibition and experimental design, which highlights the importance of the spatial and temporal regulation of *TOR* function (Xiong and Sheen, 2014).

The transcription of *TOR* was detected throughout plant tissues, but its translation was found concentrated in meristematic tissue, which indicates a focussing of *TOR* function to the growing regions of the plant (Menand et al., 2002). More recent studies, which utilized tissue-specific expression of artificial microRNA (amiRNA) against *TOR*, suggested that the requirement for *TOR* might differ between various tissues (unpublished dataset, B.Veit). For instance, an epidermal limited amiRNA line showed a profound reduction in growth, whereas expression of the same amiRNA within central regions of meristems had relatively little effect. This disparity may reflect in part the limiting character of epidermal growth during normal plant development and also suggests that the growth of certain tissues is less dependent on *TOR* activity (reviewed in Savaldi-Goldstein et al., 2007).

1.9.2 Raptor

In *A. thaliana*, two genes were identified to encode *RAPTOR*, *RAPTOR3G* (*AT3G08850*) and *RAPTOR5G* (*AT5G1770*) (Deprost et al., 2005). These share 41 and 38% identity with the human RAPTOR protein and display the typical organisation found in RAPTOR proteins of other species, including HEAT repeats, seven WD40 and a RNC/C domain (for RAPTOR N-terminal Conserved / putative Caspase) (Figure 1.1). This suggests that RAPTOR retains a similar scaffold-related function in plants as postulated in fungi and animals. In contrast to the high similarity of both *RAPTOR* genes in *A. thaliana*, large discrepancies were found in the expression levels. While *RAPTOR3G* was found ubiquitously expressed, *RAPTOR5G* was expressed at a lower level (Anderson and Hanson, 2005; Deprost et al., 2005).

Two loss-of-function studies of both *A. thaliana* *RAPTOR* genes have been published to date, which have supported a growth promoting role. However, these reports reach conflicting conclusions on the degree to which growth is affected in individual knock-out mutants (Anderson et al., 2005; Deprost et al., 2005). While both groups saw no phenotypic abnormalities in *raptor5g* knock-out mutants, the role of *RAPTOR3G* remained controversial. While Deprost et al. (2005) described *raptor3g* mutant lines as embryonically lethal, Anderson et al. observed a slow growing phenotype, with increased branching and delayed flowering. In the latter study, the disruption of both genes in *raptor3g raptor5g* mutants led to an arrest at an early seedling stage (Anderson et al., 2005). The severely retarded growth of these plants suggested that RAPTOR is required for TOR activity in a similar fashion described in yeast and animals.

1.9.3 LST8

LST8 is well-conserved throughout plants and, like TOR and RAPTOR, generally found as a single copy. As with *RAPTOR*, *A. thaliana* contains two *LST8* genes, *LST8.1*

(*AT3G18140*) and *LST8.2* (*AT2G22020*), which share 75% sequence identity (Moreau et al., 2012). However, sequence conservation and expression data has suggested that *LST8.1* is the only functional homologue (Moreau et al., 2012). In the first characterization of LST8 in plants, the *LST8* of the single-celled algae *Chlamydomonas reinhardtii* was able to complement for loss of *LST8* in yeast, which indicated a generally conserved function (Diaz-Troya et al., 2008). This was recently confirmed with the *A. thaliana* homologue *LST8.1* (Moreau et al., 2012). While knock-out lines of *LST8.2* did not indicate any phenotypic differences from wild type plants, *lst8.1* mutants showed a slow growing and sterile phenotype (Moreau et al., 2012). This stands in contrast to observations in yeast and mammals, in which depleted LST8 is lethal, probably due to its essential contribution to TORC2 function (Kim et al., 2003; Wullschleger et al., 2005; Guertin et al., 2006). Metabolic and transcriptomic analysis of *lst8.1* mutants reflected similar observations as in TOR-inhibited experiments, which included the increase of amino acids and intermediates of primary metabolism and the decrease in expression levels of genes involved in cell wall synthesis (Moreau et al., 2012; Ren et al., 2012; Xiong and Sheen, 2012; Caldana et al., 2013). Fluorescence-tagged *LST8.1* protein was localized to endosomes, which replicated observations in other species including yeast and algae (Chen, 2003; Diaz-Troya et al., 2008; Moreau et al., 2012). Coinciding with phenotypic description of *raptor3g* mutants, *LST8.1* deficient plants showed an increase in branching, which is likely a result of impaired auxin regulation (Anderson et al., 2005; Moreau et al., 2012). Interestingly, Moreau et al. (2012) discovered a strong sensitivity to changes in the light period, which caused a more severe phenotype with dramatically altered expression levels of genes involved in RiBi, mitochondrial electron chain, and cell wall synthesis (Moreau et al., 2012).

Like other eukaryotes, the absence of TOR is lethal in plants but in contrast to animals and fungi, plants do not seem to entirely rely on the presence of LST8 and RAPTOR for their survival. These findings indicate a differential function of TOR signalling

compared to fungi and animals. Moreover, the absence of any obvious homologue of RICTOR suggests that TORC2 might not be implemented in plants. The poor conservation of RICTOR may be one explanation for this apparent missing link. Additionally, the partially functional redundancy of TOR complexes that was observed in yeast and mammals might also support the idea that TOR function could be maintained by a single TOR complex, which may be the case in plants.

1.10 Functions and downstream targets of TOR in plants

1.10.1 Protein synthesis

The TOR-mediated regulation of protein synthesis via the translational regulation of capped mRNA through phosphorylation of 4E-BP is a well-described mechanism in animals (see above). It is unclear if this mechanism is specific to animals due to the lack of clear homologues in other *taxa*. Proteins with potential eIF4E-binding domains were identified in plants but these lacked a TOS motif, which has been identified as a characteristic feature of TOR interaction in animals (Freire et al., 2000; Schalm et al., 2003). However, recent data supported a phosphorylation of 4E-BP proteins in plants, as *A. thaliana* TOR was able to phosphorylate human 4E-BP *in vitro* (Xiong et al., 2013).

S6K, which is a well-established target of TOR to regulate translational activation in fungi and animals, is represented by two closely related homologues in *A. thaliana* (Mizoguchi et al., 1995). Recently, these were shown to be phosphorylated in a rapamycin-responsive manner (Xiong and Sheen, 2012). Both S6K proteins were also shown to phosphorylate S6, which confirmed that they functionally represent the human p70S6K (Zhang et al., 1994; Turck et al., 1998; Mahfouz et al., 2006). Like *metazoa*, differences in cellular localization of both proteins suggest a potentially distinct function (Mahfouz et al., 2006). Studies on s6 knock-out mutants by Ren et al.

showed a similar phenotype to that seen with TOR-inhibited plants, which supported the conclusion that the regulation of S6K and S6 is also a central function of TOR signalling in plants (Ren et al., 2012).

A new angle of translational regulation was recently presented by Schepetilnikov et al. (2013), who linked TOR activity to translation of genes containing upstream open reading frames (uORF). uORFs are small coding regions within the 5' untranslated region of the mRNA, which represent a recently discovered mechanism that allows for complex regulation of gene expression in eukaryotes (reviewed by von Arnim et al., 2014). In *A. thaliana*, about 35% of genes contain uORFs and therefore cover a wide range of functions in development and metabolism (von Arnim et al., 2014). TOR activity via S6K is thought to phosphorylate ribosomal factors like EUKARYOTIC TRANSLATION INITIATION FACTOR 3H (eIF3h), which stabilizes the ribosome after passage through the uORF to enable re-initiation of translation of the main downstream ORF (Roy et al., 2010). Interestingly, re-initiation occurred in an auxin-responsive manner, which provided the first evidence of hormonal regulation of TOR activity in *A. thaliana* (Schepetilnikov et al., 2013).

1.10.2 Cell cycle

TOR-activated S6K has been shown to interact with RETINOBLASTOMA-RELATED 1 (RBR1) in plants (Henriques et al., 2010). Similar to its animal counterparts, RBR1 function represses the transcription of genes that contribute to cell proliferation. In plants, S6K-mediated phosphorylation of RBR1 triggers its nuclear localization, where it inhibits the activity of E2F transcription factors and thus represses expression of cell cycle promoting genes. Although evidence of any direct regulation by TOR contributing to the nuclear localisation of RBR1 is still missing, this hints at a mechanism to explain changes in cell sizes of plants grown in nutrient-limited conditions and in various TOR-inhibited mutants. This inhibition of cell cycle progression via RBR1 seemingly stands in conflict to a more recent finding by Xiong et al. (2013), who found E2Fa to be directly

phosphorylated by TOR *in vitro*. The complex regulation of S6K by other kinases besides TOR might provide some explanation of this contradiction, but further investigation is needed to elucidate the role of TOR in regulating cell cycle progression.

1.10.3 Transcription

Several transcriptomic analyses using various strategies to inhibit or promote TOR activity concur that TOR signalling promotes expression of genes of anabolic pathways including cell wall synthesis, cell cycle progression, and carbohydrate and nitrogen metabolism and transport. Conversely, TOR signalling was found to repress catabolic processes like autophagy and senescence (Moreau et al., 2012; Ren et al., 2012; Caldana et al., 2013). Despite these findings, little is known how TOR impinges on these functions directly. Recently, Ren et al. were able to present a new mechanism by which TOR activates translation through enhancing the transcription of rRNA. This also demonstrated a novel aspect of TOR function through direct binding of DNA (Ren et al., 2011).

1.10.4 Development

A putative downstream target that was identified in *S. pombe* and plants, is the RNA binding protein MEIOSIS REGULATOR-2 (MEI2). In an early study, Mei2p triggered pre-meiotic DNA synthesis and was shown to interact with Mip1, the homologue of RAPTOR in *S. pombe* (Shinozaki-Yabana et al., 2000). Mei2-like proteins are represented by nine genes in plants, sharing a pair of weakly conserved N-terminal RNA-recognition motifs (RRM) and a single highly conserved C-terminal RRM domain (Anderson and Hanson, 2005). Supporting a conserved function between yeast and plants, the *ARABIDOPSIS MEI2-LIKE 1* (*AML1*) complements depletion of *mei2* in fission yeast (Hirayama et al., 1997). A study utilizing an RNAi approach to decrease *AML1* expression confirmed a role in meiosis, vegetative growth, and chromosome organization also *in planta* (Kaur et al., 2006). In a yeast two-hybrid assay, *AML1* was

further found to interact with RAPTOR3G (Anderson and Hanson, 2005). These results support the conclusion that TOR-mediated regulation of MEI2-like proteins is conserved in plants. However, the knowledge of their function in vegetative growth, meiosis and development is still very limited (Kaur et al., 2006).

1.10.5 Metabolism

In fungi and animals, TOR activity was identified to promote the production of metabolites for immediate growth, while it suppresses the synthesis of the storage forms for longer term growth and reproductive strategies (reviewed by De Virgilio and Loewith, 2006). This is supported by several metabolic and transcriptomic studies in *A. thaliana*, in which genetic or pharmacological methods were used to inhibit TOR activity. These resulted in an accumulation of starch, tricarboxylic acid cycle (TCA) intermediates and triacylglycerides (TAG), together with associated changes in gene expression profiles (Deprost et al., 2007; Moreau et al., 2012; Ren et al., 2012; Caldana et al., 2013). Similar responses were also seen *C. reinhardtii* following application of rapamycin (Lee, 2013). The accumulation of storage metabolites mimicked growth arrest responses triggered by nitrogen limitation. Altered levels of glutamine and genes associated with its metabolism further supported a role for TOR activity in regulating nitrogen metabolism (Moreau et al., 2012; Caldana et al., 2013).

1.10.6 Stress

The PP2A phosphatase is a well-described target of TOR in fungi and animals (see above). In *A. thaliana*, TWO A PHOSPHATASE ASSOCIATED PROTEIN (TAP) 46 was identified as the homologue of TAP42, the catalytic subunit of PP2A in *S. cerevisiae* (Ahn et al., 2011). In plants, PP2A is associated with a wide spectrum of functions, which include stress response, auxin and brassinosteroid signalling, and defence responses (He et al., 2002; Kwak et al., 2002; He et al., 2004; Xu et al., 2007). An *in vitro* kinase assay demonstrated that the TOR kinase domain of *Nicotiana*

tabacum was able to phosphorylate TAP46 (Ahn et al., 2011). In the same study, it was also shown that down regulation of TAP46 with RNAi mimics cellular effects of a TOR knock down, which supported that TAP46 is an important mediator between TOR activity and growth. Further, a recent study confirmed that TAP46 itself is also a positive effector of TOR activity, which has been previously discovered in *S. cerevisiae* (Di Como and Arndt, 1996; Ahn et al., 2014).

1.10.7 Autophagy

Genomic and functional analysis suggests that ATG genes are functionally conserved in plants (Diaz-Troya et al., 2008; Liu and Bassham, 2010; Perez-Perez and Crespo, 2010). Recent results indicate that autophagosome formation is controlled in a similar manner via TOR and AMPK as described in fungi and animals (Li and Vierstra, 2012; Xiong et al., 2013).

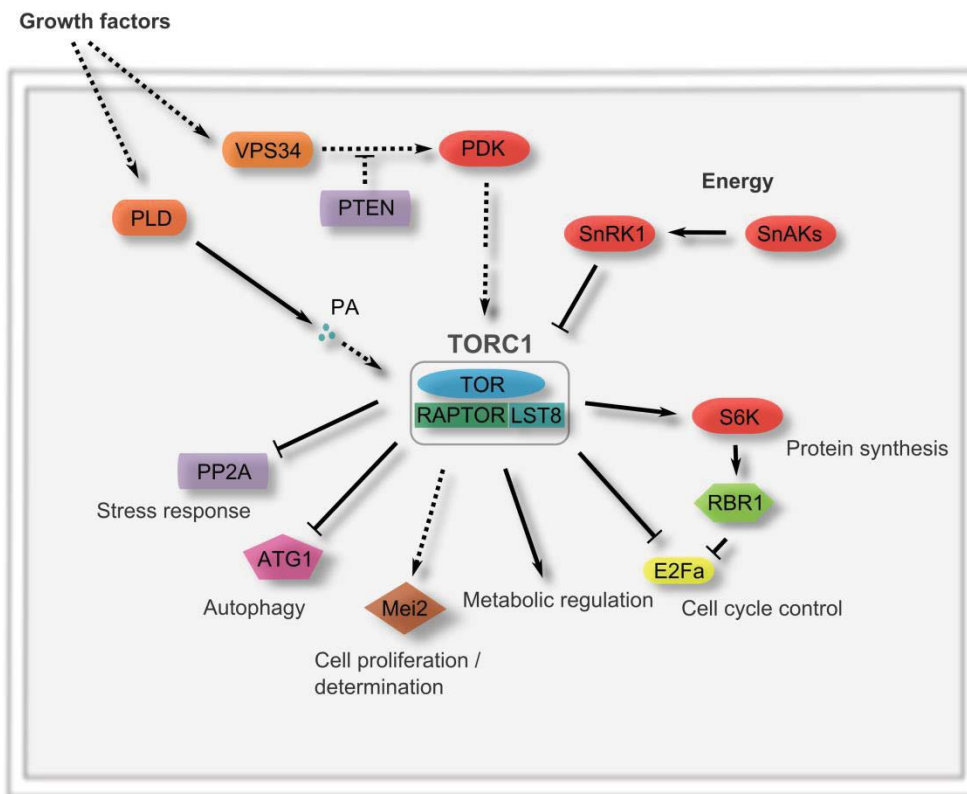


Figure 1.3 Overview of the TOR pathway in plants. Hypothetical connections are indicated with dotted lines.

1.11 Regulation of TOR activity in plants

The conservation of core components of the TOR complex might indicate some degree of similarity in factors that impinge on TOR activity in plants. Despite the fundamental differences in metabolism and development compared to yeast and animals, plants may have maintained a set of basic cues. Conversely, because of these differences it is expected that plants have developed specific mechanisms to adjust TOR-mediated growth outputs to their unique photoautotroph and sessile lifestyle.

1.11.1 Glucose

Recent studies have highlighted the importance of glucose signalling in relation to TOR signalling. Aside from its role as a central energy and carbon source, or probably

because of this role, glucose is an important signalling molecule (Smeekens et al., 2010; Sheen, 2014). Its mechanism as a signalling molecule is as yet poorly understood but it may relate to functions of HEXOKINASE-1, which catalyses the initial step in glycolysis and is additionally linked to mediating activation of growth-related genes, i.e. genes involved in photosynthesis (Xiao et al., 2000). However, recent studies by Sheen et al. found that glucose was required for TOR activity in a HEXOKINASE-1-independent manner (Xiong and Sheen, 2012; Xiong et al., 2013).

1.11.2 Energy

As described above, the inhibition of TOR activity due to low energy status or stress is mediated via AMPK in animals and yeast. A reliance on an AMPK-like activity for energy sensing is also supported in plants, as SNF1-RELATED KINASE-1 (SNRK1) represents a functional homologue in *A. thaliana* (Hardie et al., 1998; Bhalerao et al., 1999). Further, one of the two confirmed AMPK-dependent phosphorylation sites detected in yeast and animals was found conserved in RAPTOR proteins, which supports an AMPK-mediated regulation of TOR in plants (Jossier et al., 2009). However, the establishment of the second branch of AMPK-TOR signalling as found in animals and *S. cerevisiae* via TSC and RHEB remains uncertain since the TSC1/2 complex has not yet been identified in plants (Figure 1.2).

1.11.3 Hormones

In contrast to the well-characterized insulin signalling in animals, a direct link between hormone signalling and TOR activity is yet to be identified in plants. The stress signalling molecule abscisic acid (ABA) has been shown to influence AMPK activity, and thereby inhibits TOR indirectly (Jossier et al., 2009). The fact that phenotypes of *raptor3g* and *s6* null mutants in *A. thaliana* show an increase in branching and limited meristematic growth suggest an imbalance of the auxin:cytokinin ratio (Morimoto et al., 2002; Anderson et al., 2005). A recent study, which found auxin-responsive

phosphorylation of S6K, further strengthened this view (Schepetilnikov et al., 2013). However, it remains to be elucidated how these hormones affect TOR signalling. Although only supported by weak evidence from a study in *Z. mays*, an insulin-like growth factor might regulate TOR in a similar fashion to that described in animals (Garrocho-Villegas and de Jimenez, 2012). However, G protein-coupled receptors and receptor tyrosine kinases, which mediate the membrane transduction of growth factors like insulin in animals, are poorly conserved in plants (reviewed by De Smet et al., 2009). Further homologues of the mammalian insulin-TOR signalling cascade that have been identified in plants include the inhibitory PHOSPHATASE AND TENSIN HOMOLOG (PTEN) and PDK (Deak et al., 1999; Gupta, 2002). Overexpression of the PTEN homologues in *A. thaliana* increased accumulation of autophagic bodies, which generally aligns with TOR down-regulation (Welters et al., 1994). PDK was also identified in plants and was shown to directly phosphorylate the kinase domain of S6K (Long et al., 2004; Mahfouz et al., 2006). This generally indicates an at least partly conserved function of this pathway in plants, although any evidence of a direct link to TOR activity is still missing. It remains also speculative how the signalling is transduced from a membrane receptor to downstream kinases, since neither the second messenger phosphatidylinositol 3,4,5-triphosphate (PI(3,4,5)P₃) nor the class I PI3K required for its synthesis within the mammalian pathway have been detected in plants (Munnik and Vermeer, 2010). Interestingly, *in vitro* studies of homologues of PTEN in *A. thaliana* indicated a wide spectrum of affinities to several PIs and PA (Pribat et al., 2012). This suggests that plants may have evolved a signalling mechanism utilizing a different second messenger in place of PI(3,4,5)P₃. A potential candidate is PA, which is already linked to nutrient-dependent TOR regulation in other taxa (see below). In *A. thaliana*, functions that were related to PA included root growth, root hair and pollen tube development through regulating cytoskeleton and vesicle trafficking, and stress response (Monteiro et al., 2005; Li and Xue, 2007; McLoughlin et al., 2013). However, further investigation is needed to confirm any role of PA in regulating TOR in plants.

1.11.4 Nutrients

The mechanism of nutrient-mediated TOR regulation in yeast and animals *via* the RAG and the Ragulator complex is unlikely to be conserved in plants, since no functional homologues have been identified yet (see above). Instead, signalling of amino acid availability may be relayed *via* the well-conserved VPS34 and PLD. *Vps34* mutant lines in *A. thaliana* showed a severe reduction of growth and development (Welters et al., 1994). More recent studies revealed functions in ROS accumulation, which caused reduction of root hairs and pollen tube growth (Lee et al., 2008a; Lee et al., 2008b). However, further investigation is needed to confirm a link to TOR signalling. The same applies to PA signalling and PLD, which have been linked to growth regulation through knock-out and overexpression experiments of PLD α 3 and PLD ϵ (Hong et al., 2008). However the PLD superfamily is more diverse in plants compared to other *taxa*, and further exploration is required to confirm a similar role to that described for fungi and yeast (reviewed by Selvy et al., 2011).

1.11.5 Conclusion and Outlook

In summary, the knowledge of TOR signalling and function in plants is still very limited. Advancements have been made in areas where homologues of described TOR components of other species could be identified. This includes TOR itself, RAPTOR, LST8 and the downstream target S6K. Initial studies confirmed the growth-promoting function of TOR activity in plants. However, some prominent components of the TOR pathway in yeast and animals are missing or as yet undiscovered in plants. For instance, the absence of homologues of RICTOR or any other characteristic members of TORC2 raises the question of whether this complex is represented in plants at all. Additionally, studies of the conserved homologues LST8 and RAPTOR have suggested an altered function compared to their counterparts in fungi and animals. This indicates

that the TOR pathway is an important key regulator of growth, as found in yeast and animals, though central aspects of its regulation and function have been modulated in plants.

1.12 Aim of this research

The primary hypothesis addressed by this thesis can be formulated as follows: RAPTOR is required for TOR-mediated growth regulation to maintain vegetative growth in plants. By using comparative genomic and functional genetic approaches, I will test this hypothesis and address conflicting reports in the literature (Anderson et al., 2005; Deprost et al., 2005). I will further exploit *raptor* mutant lines in *A. thaliana* to gain further insight into specific RAPTOR-related functions in the development of plants.

In parallel, I will address results of an early study that suggested that TOR activity may differ between tissues (unpublished dataset, B. Veit). The following hypothesis can be eventuated from this finding: Plants depend on tissue-specific TOR-activity to maintain their growth and development. I will address this by creating and analysing genetic mosaics, in which genes encoding for TOR components are deleted in specific tissues of the root meristem. Utilizing confocal microscopy, I will analyse and compare morphological changes in these induced sectorial deletions within various cell types and developmental stages to that of unaffected cells.

In contrast to reports from studies in fungi and animals, mutants of LST8 were reported to be viable in *A. thaliana* (Moreau et al., 2012). Since LST8 represents the only known interaction partner of TOR characterizing TORC2 in plants, I formulate the hypothesis, that TORC2 is not functionally conserved in plants. I will test this hypothesis by comparing the phenotypes of knock-out lines of *raptor* and *lst8* in *A. thaliana*. Since RAPTOR was exclusively found within TORC1, whereas LST8 was found to be

incorporated in both TOR complexes, differences in the phenotypes between these mutants will highlight potential evidence for an establishment of TORC2 in plants.

The use of these different genetic tools will help to refine the knowledge on how TOR signalling is implemented in plants and how its activity contributes to growth and development.

Chapter 2

Material & Methods

2.1 Cloning

2.1.1 Overview of the cloning strategy

The genes of *LST8.1* (*AT3G18140*) and *RAPTOR3G* (*AT3G08850*) were amplified by PCR from BAC library clones using flanking primers, which included promoter and terminator regions (Chapter 2.1.1.1.1; Chapter 2.1.1.1.2). The blunt-ended PCR products were afterwards purified and integrated into the pCR4[®] cloning vector (Invitrogen[™], USA) using the topoisomerase enzyme (Chapter 2.1.1.2). Subsequently, gene inserts were confirmed by sequencing (Chapter 2.1.1.3). The *LST8.1* clone carried a single mutation within the fourth intron (Appendix 11), while the *RAPTOR3G* insert was entirely identical to the reference sequence (obtained from NCBI database at www.ncbi.nlm.nih.gov). Both genes were cut out of the confirmed pCR4 clones using specific restriction enzymes (RE) and ligated into the binary pCBI vector (provided by B. Scheres; Chapter 2.1.1.2; Appendix 2). Correct integration of the genes within the pCBI vector was subsequently confirmed by sequencing.

2.1.1.1 PCR for cloning genomic sequences

Particular DNA sequences were amplified *in vitro* by PCR. The specific reaction conditions and thermal cycling programs are listed below. For the reaction, the PrimeSTAR polymerase (Clontech, Japan) was used. DNA fragments generated by PCR were separated on a 0.8% or 1% (w/v) agarose gel and stained with ethidium bromide for detection under UV light.

2.1.1.1.1 Amplification of the genomic *LST8.1* sequence

The *LST8.1* gene was amplified from the BAC library clone PAD10SACBII (Arabidopsis Biological Resource Center, USA) using the primers LST8.1 gen and Lst8 gen as (Appendix 14). The reaction mixture is shown in Table 2.1 and the thermocycling conditions of the PCR reaction is given in Table 2.3. Primers are given in details.

Table 2.1 LST8 PCR-reaction mixture.

Component	Volume
PrimeSTAR buffer (5x)	10 μ L
dNTP mixture (2.5mM each)	4 μ L
PAD10SACBII vector DNA (21ng/ μ L)	2 μ L
Primer (10 μ M)	1 μ L each
PrimeSTAR polymerase (2.5U/ μ L)	0.5 μ L
Sterilized and distilled water	31.5 μ L

The reaction mix was applied to following thermocycling program for 30 cycles: 95°C for 10s, 60°C for 5s, 72°C for 3.5min.

2.1.1.1.2 Amplification of the genomic *RAPTOR3G* sequence

The *RAPTOR3G* gene was amplified from the BAC library clone T16011 (Arabidopsis Biological Resource Center, USA) using the primers Rap gen and Rap gen as (Appendix 14). The composition of the reaction mixture is given in Table 2.2 and the thermocycling setup shown in Table 2.3.

Table 2.2 RAPTOR-PCR reaction mixture.

Component	Volume
PrimeSTAR buffer (5x)	2.5µL
dNTP mixture (2.5mM each)	2µL
T16011 vector DNA (67ng/ µL)	1µL
Primer (10µM)	0.5µL each
PrimeSTAR polymerase (2.5U/µL)	0.5µL
Sterilized and distilled water	18µL

Table 2.3 Cloning-PCR setup.

Temperature	Time	Repeats
98°C	30s	
55°C	10s	14x
72°C	6min	
98°C	30s	
55°C	10s	16x
72°C	6min+15s/cycle	
72°C	15min	

2.1.1.2 Restriction enzyme digestion and ligation

For the evaluation of the correct sequence length and for the specific excision of a fragment, DNA samples were digested with restriction enzymes (NEB[®], USA and Invitrogen[™], USA) according to the manufactures' manual. Sequences of *LST8.1* and *RAPTOR3G* were sequentially cut from the corresponding pCR4[®] vector constructs (1 µg/20µL reaction volume) using NotI and XbaI (Invitrogen[™]). DNA fragments were separated by gel electrophoresis and extracted with QIAEX[®] II Gel Extraction Kit (Qiagen, Germany). Fragments of both genes were ligated in the likewise cut pCBI

vector by T4 DNA ligase (Invitrogen™, USA) at 4°C for 12h. The ligation mix was then transformed into chemical competent *E. coli* DH5α cells (Chapter 2.1.1.5).

2.1.1.3 Sequencing of DNA

Sequencing of DNA vector inserts was carried using a Genetic Analyzer 3130xl (Applied Biosystems™). The sequencing reaction was combined as shown in Table 2.4 including a sample specific primer (Appendix 14). The temperature cycling conditions were based on the protocol by Platt et al. as listed in Table 2.5 (Platt et al., 2007). Afterwards, the products were purified on microplate containing swelled Sephadex G-50 (Sigma-Aldrich, USA). Therefore, Sephadex G-50 was swelled up in a microplate with 300µl ddH₂O for two hours. Samples are washed with 150µl ddH₂O by centrifuging at 910 x g for 5min at 4 °C. Then, ddH₂O was added to the sequencing reaction mix to a total volume of 20µl. This was loaded onto the microplate on top of the swelled Sephadex G-50 and centrifuged at 910 x g for 3 min at 4°C. The flow through was collected and applied to the sequencer.

Table 2.4 Sequencing reaction mixture.

Component	Volume
Big Dye®	0,85µL
Big Dye® Buffer (5x)	3.85µL
Primer [50 µM]	1,2µL
Template (200 ng/ µL)	1,0µL
Sterilized and distilled water	13.1µL

Table 2.5 Sequencing reaction setup.

Temperature	Time	Repeats
96°C	1min	
96°C	10s	
50°C	5s	15x
60°C	1min 15s	
96°C	10s	
50°C	5s	5x
60°C	1min 30s	
96°C	10s	
96°C	5s	10x
96°C	2min	

2.1.1.4 Plasmid DNA isolation

Plasmid DNA of *E. coli* was isolated by boiling lysis (Maniatis et al., 1982). 2 mL of an overnight culture were centrifuged down for 5 min at 5,000 x g. The pelleted cells were re-suspended in 350µL STET buffer (Appendix 10) and treated with 25µL lysoszyme solution (10 mg/mL). The mixture was incubated for 5min at RT before being placed in boiling water for 1min. After 10 min centrifugation at 12,000 x g, the supernatant was carefully taken off. DNA was precipitated using 0.75 volumes of isopropanol and 0.1 volumes 3M sodium acetate (pH 5.5). The sample was incubated for 1 min and centrifuged afterwards for 10min at 12,000 x g. The precipitate was washed with 70% ethanol and then resuspended in 20µL TE buffer containing RNase (20µg/µL). The concentration and purity grade of isolated DNA was measured by Nanodrop™ 1000 spectrometer (Thermo Fisher Scientific, USA) afterwards.

For high quality plasmid DNA isolation of *E. coli* the NucleoBond® PC 100 Kit (Macherey-Nagel, USA) was used following the manufacturers' manual.

2.1.1.5 Bacterial transformation

2.1.1.5.1 Transformation by electroporation

To introduce DNA into bacterial cells, the electroporation technique was used. An aliquot (40 μL) of electro-competent cells was thawed on ice for 5min. 2 μL of the DNA (1 to 30 ng of DNA) was added and then transferred to an electroporation cuvette. The cells were pulsed (voltage 2.5 kV, field strength 25 kV/ cm, time 4-5ms) using a MicroPulser[™] (BioRad, USA) and mixed with 1mL of SOC media immediately. Cells of *E.coli* were incubated at 37 °C for 90min under continuous agitation, while *A. tumefaciens* cells were grown at 28°C for 3h. An aliquot (~75 μL) was spread on a LB agarose plate (Appendix 10) containing the corresponding antibiotic concentrations for negative selection of transformed clones.

2.1.1.5.2 Transformation using heat-shock method

An 150 μL aliquot of chemical competent *E. coli* cells (stored at -80°C) was mixed with 10 μL of DNA (5 to 50ng), and thawed on ice for 10min. After incubation at 41°C for 90s, cells were immediately cooled on ice for 2min. The cells were supplied with 1mL of pre-warmed SOC media before cultivated at 37°C for 45min. Transformants were selected by spreading out an aliquot of ~75 μL on LB media plates containing an appropriate antibiotic.

2.1.1.6 Preparation of competent cells

2.1.1.6.1 Chemical competent cells

E. coli DH5 α (GIBCO BRL, USA) were prepared following the method of Inoue et al. (Inoue et al., 1990). A 5mL culture was grown at 37°C overnight from a single colony. 200 μL of this culture were used to inoculate 100mL LB medium and incubated at 16°C for ~32h until cells reached a optical density at 600nm (OD600) of 0.6. Cells were chilled on ice for 20min before pelleted and re-suspended in 10mL ice cold SEM buffer

for 20min. Afterwards, cells were centrifuged again and re-suspended in 3mL SEM supplied with 230 μ L DMSO. Aliquots of approximately 100 μ L were prepared and stored at -80°C.

2.1.1.6.2 Electro competent cells

As described above, a 5mL culture of *E. coli* DH5 α (GIBCO BRL, USA) was grown from a single colony and used to inoculate 500mL SOC medium (Appendix 10). The culture was incubated at 37°C until cells reached a density of OD600 0.6. The culture was chilled on ice for 20min before centrifuged. Cells were washed twice with ice cold sterile ddH₂O (400mL, 200mL). Afterwards, cells were resuspended in 4mL of 10% (v/v) glycerol and aliquots of ~50 μ L stored at -80°C.

The electro competent cells of *A. tumefaciens* were equally prepared as described above, but grown at 28°C in SOC medium which included selective antibiotics. For the strain GV3101 rifampicin (10 μ g/mL) and gentamycin (50 μ g/mL), and for AGL1 rifampicin (10 μ g/mL) and carbenicillin (60 μ g/mL) were applied.

2.1.2 Colony PCR

Subsequently to transformation (Chapter 2.1.1.5), colonies were checked for the transgene by colony PCR. The colonies from the selective plate were picked and mixed in 10 μ l of LB media. 1 μ l of this suspension was added to the PCR mixture (Table 2.1). Specific primers for the corresponding transgene were used to identify candidates. Temperature cycling conditions were implemented as mentioned below (Table 2.7).

Table 2.6 Colony-PCR mixture.

Component	Volume
ExTaq buffer (10x)	2 μ L
dNTP mixture (2.5mM each)	2 μ L
Cell suspension	1 μ L
Primer (10 μ M)	0.5 μ L each
ExTaq polymerase (5U/ μ L)	0.1 μ L
Sterilized and distilled water	13.9 μ L

Table 2.7 Colony-PCR setup.

Temperature	Time	Repeats
98°C	2min	
98°C	30s	
55°C	30s	34x
72°C	2min	
72°C	5min	

2.2 Creation of transcriptional fusions

The promoter regions of *RAPTOR3G* and *RAPTOR5G* were amplified from genomic DNA of *Arabidopsis* Col-0 by PCR with PrimeSTAR polymerase (Clontech, Japan). DNA was extracted from plant as described in Chapter 2.3.5.2. PCR mixture and thermocycling conditions are shown in Table 2.8 and Table 2.9, respectively. Extracted PCR products were ligated into the pCRTM-Blunt vector (InvitrogenTM, USA) and subsequently cloned into the pB121 vector (created by Jefferson (1987)) using *Xba*I and *Hind*III restriction sites. Correct insertion of constructs was confirmed by EcoRI RE digestion and subsequent sequencing (Chapter 2.1.1.3). Constructs were subsequently transformed into wt plants of *A. thaliana* (Chapter 2.3.4)

Table 2.8 Promoter-PCR mixture.

Component	Volume
PrimeSTAR buffer (5x)	10 μ L
dNTP mixture (2.5mM each)	4 μ L
BSA (10mg/mL)	0.8 μ L
Extracted genomic DNA	1 μ L
Primer (10 μ M)	1.5 μ L each
PrimeSTAR polymerase (2.5U/ μ L)	0.5 μ L
Sterilized and distilled water	30.7 μ L

Table 2.9 Promoter-PCR setup.

Temperature	Time	Repeats
98°C	5s	
55°C	5s	34x
72°C	1min	

2.3 Plant methods

2.3.1 Plant lines

The Col-0 accession of *A. thaliana* was used as wild-type reference for this study. Seeds of Col-0 and T-DNA insertion lines used in this study were received from the Arabidopsis Biological Resource Center (ABRC) and are listed in Appendix 12.

2.3.2 Growth conditions

2.3.2.1 Soil growth conditions

Seeds were stratified at 4 °C in the dark for 3 days and afterwards sown on soil (potting mix topped up with a 2 cm layer of seeding mix). Pots were placed in a growth chamber and covered with a hood (Perspex[®] (Lucite, Japan)) for the first two weeks.

Light periods were adjusted to long day conditions (16 h light and 8 h dark) with an average light intensity of $350\mu\text{mol m}^{-2} \text{s}^{-1}$ PAR and a controlled temperature of 23°C.

2.3.2.2 *In vitro* growth conditions

Seeds were surface sterilized in 50% ethanol containing 0.01% Triton-X for 5 min and seeded onto plates with half-strength Murashige and Skoog (MS) medium containing 1% sucrose and 0.9% agarose. Plates were kept at 4 °C in the dark for 3 days before being placed in growth chambers with fluorescent light tubes providing a light intensity of $20\mu\text{mol m}^{-2} \text{s}^{-1}$ PAR. Light conditions were adjusted to either long day (17h light) or short day (10h light) with a controlled temperature of 23°C.

2.3.3 Genotyping PCR

Genotypes of various *A. thaliana* T-DNA insertion lines (received from Arabidopsis Biological Resource Center, USA) were confirmed by PCR. A list of *A. thaliana* lines and corresponding primers is shown in Appendix 14. These primers were used in a multiplex PCR reaction together with a T-DNA specific primer LB1 (for SAIL lines) or pROC-737 (for SALK lines). The use of three primers allows the simultaneous amplification of two possible products representing the allele states, wild-type and mutant. The composition of the reaction mixture is shown in Table 2.10 and the cycling program is listed in Table 2.11.

Table 2.10 Genotyping-PCR mixture.

Component	Volume
ExTaq buffer (10x)	2 μ L
dNTP mixture (2.5mM each)	2 μ L
Genomic DNA	2 μ L
Primer (10 μ M)	0.5 μ L each
ExTaq HS polymerase (5U/ μ L)	0.1 μ L
BSA (10mg/mL)	0.8 μ L
Sterilized and distilled water	11.6 μ L

Table 2.11 Genotyping-PCR setup.

Temperature	Time	Repeats
95°C	2min	
95°C	30s	
55°C	30s	34x
72°C	90s	

2.3.4 Plant transformation

The transformation by the floral dip method was carried out as described in Weigel and Glazebrook (2002). Plants were grown for five to six weeks until first inflorescences were formed. These were removed to allow more vigorous growth of secondary inflorescences which are transformed in the following week. For transformation of *A. thaliana*, the *Agrobacterium* strains GV3101 MP90 and AGL1 were used (Koncz and Schell, 1986; Lazo et al., 1991). A cell line carrying the desired binary vector was spread out on selective LB media plates including antibiotics for selection of the used strain (Table 2.12) and kanamycin (50 μ g/mL) to select for the corresponding binary vector. The plate was incubated at 28°C for 2 days and transformants were verified by

colony PCR (Chapter 2.1.2). An overnight culture of a positive clone (1 mL) was used to inoculate 100mL LB medium with corresponding antibiotics for 36 h at 28 °C under vigorous agitation. This culture was used then to inoculate 400 mL YEBS and grown for 6 h at 28 °C. Directly before applying the solution to the plants, 150µl of Silwett L77 (Sigma-Aldrich, USA) were added. Inflorescences were then dipped into the bacterial suspension for 30s. Then plants were tilted on their sides and kept in the dark for 24h at room temperature. They were returned to normal growing conditions for about 3 weeks before seeds were collected.

Table 2.12 Agrobacterium strains and selective antibiotics.

Strain	Antibiotics (applied concentration)	
AGL1	Rifampicin (10 µg/mL)	Carbenicillin (60 µg/mL)
GV3101 MP90	Rifampicin (10 µg/mL)	Gentamycin (100 µg/mL)

2.3.4.1 Selection

2.3.4.1.1 Hygromycin selection

The seeds of plants which were transformed with a pCRE vector constructs were selected on agarose plates applying the protocol of Harrison et al., 2006. Seeds were sterilized in 50% ethanol with 0.5% Triton X-100 (Sigma-Aldrich, USA) for 5min, followed by a 100% ethanol wash. Seeds were dried and sprinkled on 0.5 x MS media plates with 0.9% agarose and stratified for 48h at 4°C. After 6h incubation in light at 22°C, plates were wrapped with aluminum foil and kept at 22°C for 3 days. Then the foil was removed and plates were incubated in long day light conditions with 13h light at 22°C for 3 days. Positive transformants were identified by an etiolated phenotype, which was identified by a hypocotyl length of 0.8 to 1cm. In contrast, hygromycin sensitive seedlings showed very reduced growth of roots and hypocotyls (less than 0.2cm). Resistant plants were then moved to standard growth conditions and genotyped by PCR (Chapter 2.3.3).

2.3.4.1.2 Phosphinothricin selection

Plants transformed with a pCBI vector construct were selected using phosphinothricin (also known as glufosinate ammonium). Seeds were sown on soil as described in 2.3.2.1. After the development of the first true leaves, plants were sprayed with Buster® (Sanofi-Aventis, France) using a concentration of 470µl/L. In intervals of 3 days, spraying was repeated three times and surviving plants were subsequently genotyped.

2.3.5 Extraction of genomic DNA of *A. thaliana*

2.3.5.1 Quick DNA Prep for PCR analysis

To confirm transgenes and genotyping of *A. thaliana* by PCR, genomic DNA was isolated according to the “Quick DNA Prep for PCR” protocol Weigel and Glazebrook (2002). Therefore, a small tissue sample of a leaf was grinded and meshed by a micro pestle in 400µl Plant DNA extraction buffer. After 5 min centrifugation at maximum speed in a microcentrifuge, the supernatant was taken and mixed with 300µl isopropanol. After another centrifugation at same conditions, the pellet was washed with 70% ethanol and finally dissolved in 100µl TE buffer.

2.3.5.2 Cetyltrimethyl ammonium bromide (CTAB) DNA extraction

DNA of *A. thaliana* leaves was extracted using the CTAP DNA Miniprep protocol described in Weigel and Glazebrook (2002). 300mg of plant tissue was snap frozen and grinded to fine powder. CTAB DNA extraction buffer (100mM Tris-Cl (pH 8), 20mM EDTA (pH 8), 1.4M NaCl, 2% w/v CTAB, 1% PVP 40,000) was preheated to 65°C and 1mL added to each sample. Samples were incubated at 65°C for 30min before adding 1mL phenol/chloroform/isoamyl alcohol (48:48:4). Samples were vortexed and centrifuged at maximum speed for 2 minutes. The aqueous phase was transferred to a new tube with 1mL of chloroform/isoamyl alcohol (96:4). Samples were centrifuged again and 0.7 volumes of isopropanol were added to the aqueous layer. Samples were mixed by inversion and pelleted by centrifuging for 10min at maximum speed. The

resulting supernatant was removed and the pellet washed with cold 70% ethanol. The pellet was re-suspended in 50 μ L TE buffer (10mM Tris-Cl (pH 8), 1mM EDTA).

2.3.6 Genomic mapping of T-DNA insertions using high-efficiency thermal asymmetric interlaced PCR (hiTAIL-PCR)

The unknown flanking region of the T-DNA insertion was identified using the hiTAIL method described by Liu and Chen (2007). Initially, the flanking sequence is amplified linearly using a T-DNA border region specific primer. Through the use of a long arbitrary degenerate (LAD) primer, which included a 16-mer adapter sequence and six or seven degenerate nucleotides (Appendix 14), a known adapter sequence is added to the unknown flanking region. In two subsequent TAIL-PCR reactions, the adapter binding primer together with nested primers, which are specific for the T-DNA, are then used to amplify the product. Amplified sequences were then isolated from agarose electrophoresis and sequenced. The initial pre-amplification mix contained 2 μ L 10x reaction buffer, 0.2mM dNTP mixture, 0.5U Ex Taq polymerase (Clontech, Japan), 0.3 μ M T-DNA border specific primer (i.e. RB1 for the right border), 1 μ M LAD primer, and water to a total volume of 20 μ L. For the subsequent first TAIL-PCR, 1 μ L of 40-fold diluted product of the pre-amplification reaction was used as template. The reaction mix of the first TAIL-PCR reaction contained 2.5 μ L 10x reaction buffer, 0.2mM dNTP mixture, 0.5U Ex Taq polymerase, 0.3 μ M nested T-DNA specific primer (i.e. RB-2 for right border), 0.3 μ M adapter sequence containing AC primer, and water to a total volume of 25 μ L. For the subsequent secondary TAIL-PCR, 1 μ L of 10-fold diluted product of the first TAIL-PCR reaction was used as template. The reaction mix of the secondary TAIL-PCR reaction contained 2.5 μ L 10x reaction buffer, 0.2mM dNTP mixture, 0.5U Ex Taq polymerase, 0.3 μ M nested T-DNA specific primer (i.e. RB-3), 0.3 μ M AC primer, and water to a total volume of 25 μ L. The thermocycling conditions of all reactions is shown in Table 2.13.

Table 2.13 Thermocycling conditions of hiTAIL-PCR reactions. This table is adapted from Liu and Chen (2007).

Pre-amplification			Primary TAIL-PCR			Secondary TAIL-PCR		
Step	Temperature (°C)	Time (min:s)	Step	Temperature (°C)	Time (min:s)	Step	Temperature (°C)	Time (min:s)
1	93	2:00	1	94	0:20	1	94	0:20
2	95	1:00	2	65	1:00	2	65	1:00
3	94	0:30	3	72	3:00	3	72	3:00
4	60	1:00	4	Go to Step 1	1 Time	4	94	0:20
5	72	3:00	5	94	0:20	5	68	1:00
6	Go to Step 3	10x	6	68	1:00	6	72	3:00
7	94	0:30	7	72	3:00	7	94	0:20
8	25	2:00	8	94	0:20	50	94	1:00
9	Ramp to 72	0.5°C/s	9	68	1:00	9	72	3:00
10	72	3:00	10	72	3:00	10	Go to Step 1	7x
11	94	0:20	11	94	0:20	11	72	5:00
12	58	1:00	12	50	1:00			
13	72	3:00	13	72	3:00			
14	Go to Step 11	25xs	14	Go to Step 5	13x			
15	72	5:00	15	72	5:00			

2.3.7 H₂O₂ assay

Plants grown *in vitro* under short day conditions were harvested at 8-10 leaf stage. Shoot or root tissue of 3-4 plants was pooled and weighted before being snap frozen in liquid nitrogen. For each genotype and tissue, three pooled samples were collected. Tissue was grinded to fine powder before H₂O₂ concentration and peroxidase activity were detected using the Amplex[®] Red Hydrogen Peroxide/Peroxidase Assay Kit

(Invitrogen™, USA). Samples were mixed with 200µL reaction buffer and further processed following the manufacturer's manual. Standard curves were created using a dilution series of H₂O₂. The background absorbance within samples was corrected by subtracting the value of a control without H₂O₂.

Samples and H₂O₂ standards were split into three technical replicas with 50µL volume each. The reaction was started by adding 50µL of Amplex® Red reagent solution with 0.2U/mL HRP to each sample, control, and standard. After an incubation time of 30min in the dark, the absorbance was measured at 560nm for 30min in 1min intervals.

2.4 Transcriptomic analysis

2.4.1 RNA extraction

Three pooled samples, each containing 2-4 individual wt plants (3 weeks old; 10-12 leaves) or *raptor3g raptor5g* mutants (5 weeks old; 10-12 leaves) to make up ~100mg of fresh weight tissue, were snap frozen in liquid nitrogen and grinded to fine powder. The RNeasy Mini Kit (Qiagen, Germany) was used to extract RNA according to the manufacturers' instructions. Grinded material was immediately mixed with 450µL Buffer RLT and incubated at 56°C for 1min. Samples were filtered through a QIAshredder spin column for 2min at full speed. The supernatant of the flow-through was mixed with 0.5 volume of ethanol. Samples were applied to an RNeasy spin column and centrifuged for 15s at 8.000xg. The flow-through was discarded and 700µL Buffer RW1 was added to the column before centrifuging again. Samples were then washed twice with 500µL RPE before RNA was eluted in RNase-free water. RNA samples were sent to Macrogen Inc., Korea for sequencing.

2.4.2 Bioinformatic analysis of transcriptomic data

The transcriptomic data was processed using the Galaxy platform (Giardine et al., 2005). Quality of read data was assessed initially with the FastQC profile. The mean inner distance between paired-end reads was determined using the Picard tool

InsertSize Metrics (<http://picard.sourceforge.net>). Further steps followed the “tuxedo” pipeline described by Trapnell et al. (2014). Paired-end reads were mapped with TOPHAT (v0.6) to the *A. thaliana* reference genome (build AtTAIR10.22; provided by EMBL-EBI) using the previously calculated mean inner distance of 58bp. Mapped reads were then assembled using Cufflinks (v0.0.7) with default settings (Max Intron Length: 300000; Min Isoform Fraction: 0.1; Pre mRNA Fraction: 0.15). The assembled transcripts were merged with Cuffmerge using the reference transcriptome (build AtTAIR10.22; provided by EMBL-EBI). Transcript expression level and differential expression testing was calculated with Cuffdiff applying the default settings (geometric library normalization; pooled dispersion estimation; False Discovery Rate: 0.05; Min Alignment Count: 10) and including multi-read and bias corrections. Transcript levels were visualized with the cummeRbund package in R using RStudio (Team, 2008; RStudio, 2012; Goff, 2013). For the classification of differentially expressed genes into functional clusters, genes were categorized using DAVID (<http://david.abcc.ncifcrf.gov/>). Expression levels of these genes were subsequently displayed using MAPMAN and Excel (Microsoft, USA)(Thimm et al., 2004; Huang da et al., 2009b, a).

2.5 Flow Cytometry

Analysis of DNA content by flow cytometry was achieved by following the protocol of Jing et al. (2009). Selected tissue material (~50 – 100mg) was chopped with a razor blade in a glass petri dish containing 500µL chopping buffer (45mM magnesium chloride, 30mM sodium citrate, 20mM 4-morpholinepropane sulfonate, and 0.1% Triton X-100, pH 7.0). The finely minced material was filtered through a 70µm cell strainer (BD Biosciences, USA) and 1mL of chopping buffer containing 20µg/mL propidium iodide was added and incubated for 2h. The fluorescence of the extract was analysed with a FACScalibur cytometer (BD Biosciences, USA). The fluorescence of nuclei was detected with the FL2 laser set as primary DDM parameter, and voltage and gain of the

FL2-H and FL2-A detectors were adjusted so that the G2 peak equalled a value of 200. The FLS-W gain was adjusted for values of nuclei populations being between 200 and 600. 15k events were recorded per sample and data was analysed afterwards using FlowJo software (Tree Star Inc., USA). Histograms were created based on the FL2-H fluorescence values. The histogram data was subsequently used to estimate the populations with certain DNA content to calculate the endoreduplication index (EI), which describes the number of endocycles per nuclei (Bourdon et al., 2011).

2.6 Microscopy

2.6.1 β -glucuronidase (GUS) staining

Expression of GUS in transcriptional fusion lines was detected as described by Weigel and Glazebrook (2002). Whole plants or dissected tissues were fixed in 90% acetone for at least 20min on ice. Samples were washed once with staining buffer (50mM sodium phosphate buffer pH7.2, 0.2% Triton-X100, 2mM potassium ferrocyanide, 2mM potassium ferricyanide) before incubated in staining buffer supplemented with 2mM X-Gluc for at least 16h at 37°C. Samples were analysed either directly or after fixation in FAA (50% ethanol, 10% glacial acetic acid, 5% formaldehyde). Images were taken using a SZX12 dissecting or BX50 bright field microscope (both Olympus, Japan).

2.6.2 Differential interference contrast microscopy

Samples were dissected and fixed in 10% acetic acid overnight. Specimen were cleared for at least 2h in Hoyer`s solution (30g gum arabic, 200g chloral hydrate, 20g glycerol, and 50mL water) before imaging were taken using a BX50 microscope with Nomarski prisms (Olympus, Japan).

2.6.3 Aniline blue staining

Unopened inflorescences were emasculated one day before pollination. Pollen was applied manually and carpels harvested after 3h or 24h. Sample preparation was done

as described by Mori et al. (2006). Pistils were fixed in acetic acid:ethanol mix (3:1) for at least 2h. Samples were then rehydrated by successive washes in 70%, 50% 30% ethanol, and water before incubating in 8M NaOH overnight. Samples were washed with water and stained with decolorized aniline blue solution (0.1% (w/v) aniline blue. 108mM K_3PO_4 , pH 11) for 2h. Imaging was done using a BX50 microscope (Olympus, Japan) under UV light.

2.6.4 Alexander staining

Pollen were stained according to the method established by Alexander (1969). Anthers of dissected inflorescences were fixed in 10% acetic acid for at least 2h and then incubated in Alexander's stain solution (10mL ethanol, 1mL Malachite green (1% in ethanol), 5mL Fuchsin acid (1% in water), 0.5mL Orange G (1% in water), 5g phenol, 5g chloral hydrate, 2mL glacial acetic acid, 25mL glycerol, 50mL water) over night. (Alexander 1969) Bright field images of samples were taken through a BX50 microscope (Olympus, Japan).

2.6.5 Propidium iodide staining

Samples were stained with 10 μ g/mL propidium iodide and analysed with a FV10i confocal microscope (Olympus). Using the ImageJ software, images were analysed and coloration was adjusted using a reference lookup table (Schneider et al., 2012).

2.6.6 Electron microscopy

Seedlings were grown on 0.5x MS media agarose (0.9%) plates supplied with 1% sucrose. Whole seedlings or partially dissected larger plants were fixed overnight in 2% formaldehyde, 2% glutaraldehyde, 20mM $NaPO_4$ (pH 7) at 4°C. Samples were washed twice with 20mM phosphate buffer at RT for 10min, and then dehydrated through an ethanol series of 10, 20, 40, 60, 80, 95, and 100% ethanol for 1 h each under gentle shaking at RT. The samples were incubated with 100% ethanol for >1 h twice before applied to critical point drying. The critical point drying and further handling of samples

and the scanning electron microscope (SEM) was done at the Manawatu Microscopy Imaging Centre, New Zealand.

2.6.7 ROS staining using H₂DCF-DA

Plants were grown *in vitro* under short day conditions for 4d (wt) and 10d (mutant). Samples were prepared according to Tyburski et al. (2012). Roots were incubated with 50mM phosphate buffer (pH 7.5) containing 50µM H₂DCF-DA (Sigma-Aldrich, USA) for 15min. Additionally, roots of wt plants were incubated in CDF-DA (Sigma-Aldrich, USA) or phosphate buffer with H₂DCF-DA and 500µM ascorbate for positive and negative controls respectively. Roots were then rinsed in phosphate buffer and subsequently analysed with a FV10i confocal microscope (Olympus, Japan).

2.6.8 S-phase cell detection using ethynyl deoxyuridine (EdU)

Staining of S-phase cells in *A. thaliana* roots was performed using the EdU Click-iT[®] Imaging Kit (Invitrogen[™], USA) as described by Kotogány et al. (2010). Conditions were adjusted following the descriptions in Xiong et al. (2013). Roots were submerged in 10µM EdU solution for 30min. Subsequently, roots were immediately fixed by submerging them in 3.7% (w/v) formaldehyde in PBS solution (137mM NaCl, 10mM PO₄³⁻, 2,7mM KCl, pH 7.4) containing 0.1% Triton X-100 for 30min. Samples were washed three times with PBS for 10min each and then incubated in EdU Click-iT[®] reaction cocktail with Alexa Fluor[®] 488 for 30min in the dark. Samples were washed again three times with PBS and fluorescence was detected using a FV10i confocal microscope (Olympus, Japan).

Chapter 3

Characterization of *raptor3g raptor5g* mutants in *A. thaliana*

Introduction

Initial studies on TOR function in *A. thaliana* by Menand et al. reported TOR deficient plants to be embryonically lethal (Menand et al., 2002). This confirmed observations of *tor* knock-outs in other systems, including yeast and animals (Chapter 1.4.1). Menand et al. described *tor* mutants to arrest at the early embryonic dermatogen stage (Menand et al., 2002). Similarly as discovered in *D. melanogaster*, it was postulated that arrest occurred due to lack of cell mass synthesis (Galloni and Edgar, 1999). In later studies, knock-down lines of *tor* were reported to display a strong reduction of growth, which also matched observations of similar experiments in other systems (Sormani et al., 2007). A first indication of plant-specific characteristics of the TOR pathway was reported with the description of *RAPTOR* in *A. thaliana*. In contrast to studies in fungi and animals in which only single *RAPTOR* genes were found, two gene loci, *RAPTOR3G* (AT3G08850) and *RAPTOR5G* (AT5G01770), were identified in *A. thaliana* (Deprost et al., 2007). The two *RAPTOR* genes in *A. thaliana* were reported to share a high protein identity of 76%. Compared to orthologues in fungi and animals, *RAPTOR3G* and *RAPTOR5G* were reported to share 43% and 41% identity with the yeast KOG1, and 41% and 38% to the human *RAPTOR* protein, respectively (Deprost et al., 2005). Analysis of microarray data indicated a divergent expression profile of both genes with *RAPTOR3G* being generally four-fold higher expressed than the very low expressed *RAPTOR5G* (Deprost et al., 2007). While no distinct phenotype was detected in *raptor5g* mutants, analysis of five *raptor3g* T-DNA lines showed an early embryonic arrest at the pre-globular stage. In the same year of the first study on *RAPTOR* in *A. thaliana* by Deprost et al., a second characterization of the two

RAPTOR genes by Anderson et al. followed (Anderson et al., 2005). Contrastingly, herein the *raptor3g* mutant was described to overcome the embryonic arrest, giving rise to slow-growing and sterile plants. Both studies feature the same T-DNA insertion lines of *A. thaliana*, however, these were grown under long day conditions by Anderson et al., while Deprost et al. applied short day conditions. These differences in light conditions are likely to contribute to the contradicting observations described in these studies.

The growth limitation of *raptor3g* mutants was less prominent when grown in the dark, indicating that cell expansion and cell wall synthesis *per se* was not affected. This response was also reported in *tor* knock-down mutants later (Deprost et al., 2007). Further phenotypic description of *raptor3g* mutants by Anderson et al. described a defect in maintenance of the shoot apical meristem (SAM), which led to a loss of apical dominance and a bushy phenotype, with sterile flowers. These findings were attributed to an impaired auxin:cytokinin ratio, yet addition of auxin and other phytohormones to the growth medium did not complement the phenotype (Anderson et al., 2005). Plants disrupted in both *RAPTOR* genes were found to arrest at an early seedling stage. It was postulated that TOR function consisted of a RAPTOR-independent role in embryo development and a RAPTOR-dependent function in meristem activity and maintenance (Anderson et al., 2005). Here, I further characterise the function of RAPTOR in *A. thaliana* in order to extend the knowledge of TOR signalling in plants by identifying novel functions and to clarify the conflicting reports in the literature on *raptor* mutants.

Results

3.1 Isolation of *raptor* mutants

The use of T-DNA insertion lines is a widely used reverse genetics approach in plant research to study gene functions. I applied this method to investigate the role of RAPTOR function in *A. thaliana*. Several T-DNA insertion lines for both *RAPTOR*

genes in *A. thaliana* were characterized. The locations of the T-DNA insertion within the genomic sequence of the different lines are given in Figure 3.1. For the analysis of *RAPTOR3G*, seeds of the T-DNA insertion lines SALK_078159 and SAIL_400_D05 were received from the ABRC and grown in the glasshouse. In case of *RAPTOR5G*, SALK_043920 and SAIL_558_H11 were obtained. Plants were genotyped by multiplex PCR reactions to identify wt and mutant alleles of individual plants. Figure 3.2 and Figure 3.3 show examples of genotyping PCRs from plants of the previously mentioned T-DNA lines including wt, heterozygous and homozygous mutant genotypes. Based on their genotype, heterozygous plants were selected for further progression. To reduce the possibility of additional insertions in regions outside of the respective genes, the selected plants were crossed to wild type plants (Col-0) at least three times subsequently before homozygous lines were selected for analysis. From here on I will refer to SALK_078159 as *raptor3g* and SALK_043920 as *raptor5g*.

To generate plants disrupted in both *RAPTOR* genes, T-DNA lines for *RAPTOR3G* and *RAPTOR5G* were crossed. Combinations of SALK_078159 with SALK_043920, and SAIL_400_D05 with SAIL_558_H11 were made. Initially, plants heterozygous for both lines were selected and self-pollinated. The progeny was then screened for plants, which were homozygous for one, and heterozygous for the other T-DNA line. Seeds of these plants were then used to yield *raptor3g raptor5g* double mutants for further analysis. Experiments were primarily carried out with the SALK_078159/SALK_043920 cross, which I will refer to as *raptor3g raptor5g* mutants from now on. SAIL_400_D05/SAIL_558_H11 plants were used in parallel to confirm observations.

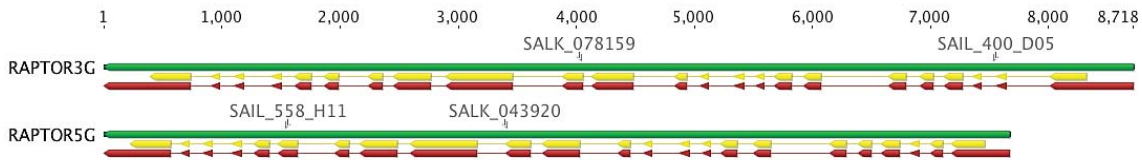


Figure 3.1 Genomic locations of T-DNA insertions within *RAPTOR* genes. The coding (yellow) and transcribed sequences (red) are shown underneath the gene (green) with the locations of T-DNA insertions indicated above. Numbers above figure represent sequence length in bp.

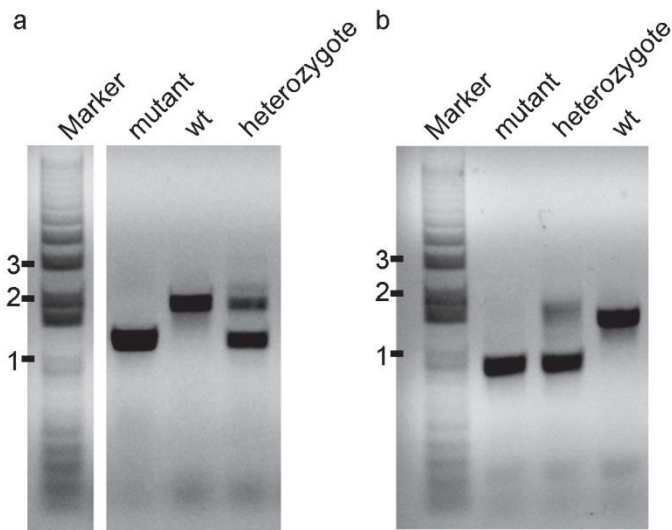


Figure 3.2 Agarose gel of genotyping-PCR with *RAPTOR3G* lines. (a) Genotyping-PCR with genomic DNA of wt, heterozygous, and mutant plants of SALK_078159 using MLTF1, MLTR1, and pROK-737 primers. (b) Genotyping-PCR with genomic DNA of wt, heterozygous, and mutant plants of SAIL_400_D05 using SAIL_400LP, SAIL_400RP2, and LB1 primers. Sequences of primers are given in Appendix 14. Lengths of marker bands are indicated in kbp.

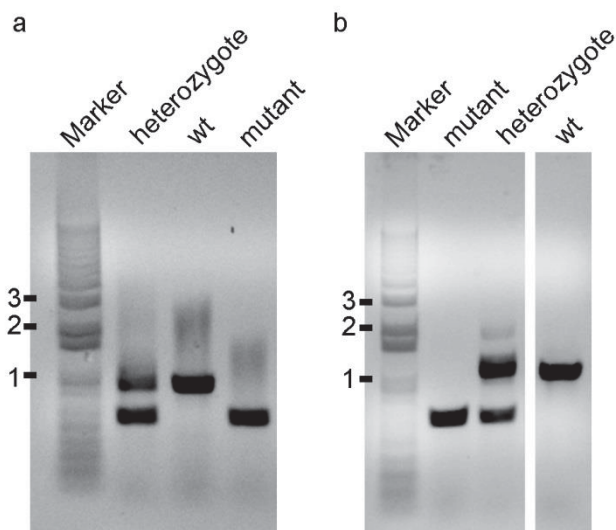


Figure 3.3 Agarose gel of genotyping PCR with RAPTOR5G lines. (a) Genotyping-PCR with genomic DNA of wt, heterozygous, and mutant plants of SALK_043920 using SALK_043920LP1, SALK_043920RP1, and pROK-737 primers. (b) Genotyping-PCR with genomic DNA of wt, heterozygous, and mutant plants of SAIL_558_H11 using SAIL_558_H11 LP, SAIL_558_H11 RP2, and LB1 primers. Sequences of primers are given in Appendix 14. Lengths of marker bands are indicated in kbp.

Thus, homozygous lines of individual and combinations of *raptor3g* and *raptor5g* T-DNA lines were created to provide a powerful tool to investigate gene function of RAPTOR in *A. thaliana*.

3.2 Raptor mutants show limited growth

Given the conflicting descriptions of *raptor* phenotypes presented in the previous reports, I grew several different T-DNA lines of *raptor3g* and *raptor5g* as described above, to clarify the role of *RAPTOR* in growth and development in plants.

Plants disrupted in the *RAPTOR5G* gene showed no obvious phenotype compared to the wild type, but *RAPTOR3G* were reduced in growth rate. I identified mutants disrupted in both *RAPTOR* genes, which completed embryonic development and showed relatively normal vegetative growth (Figure 3.4). This stands in contrast to findings described in the previous publication on *RAPTOR* deletions (Anderson et al., 2005). Compared to the *raptor3g* mutant phenotype, the combination of both gene disruptions added a further decrease in growth and intensified the phenotype observed

in *raptor3g* mutants (Figure 3.4). To quantify differences in growth rates, I measured the root growth rate of seedlings grown vertically on MS plates. While *raptor5g* roots showed an identical growth rate compared to wt, the rate of *raptor3g* roots was ~80%, and that of *raptor3g raptor5g* showed 30% of the growth compared to wt roots (Figure 3.5).

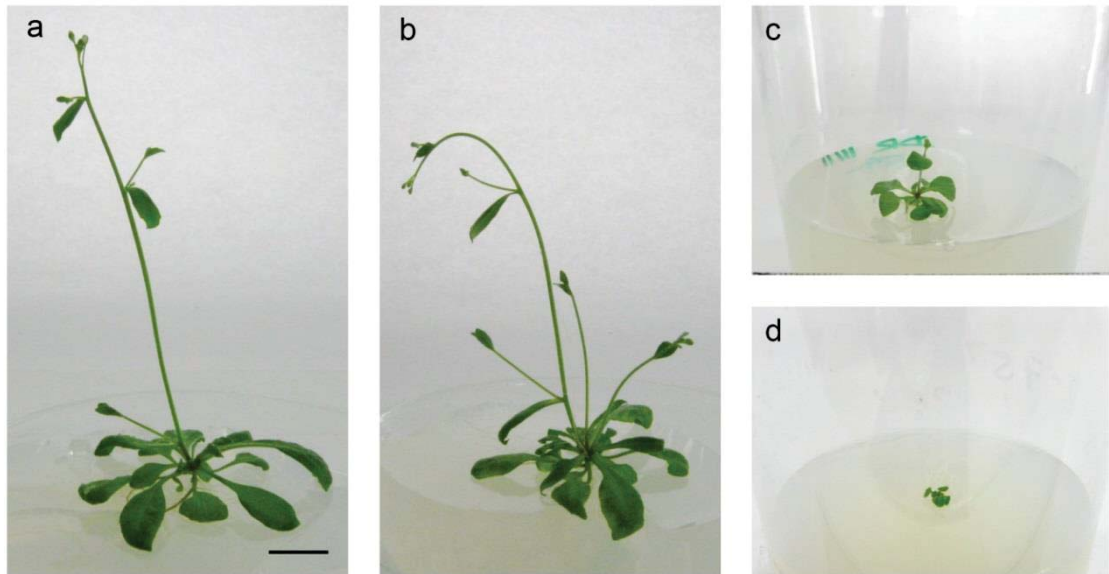


Figure 3.4 Phenotypes of *A. thaliana* *raptor* mutants. (a) wt;(b) *raptor5g*;(c) *raptor3g*;(d) *raptor3g raptor5g*. Plants were grown on MS media for four weeks under long day conditions. Scale bar = 1cm.

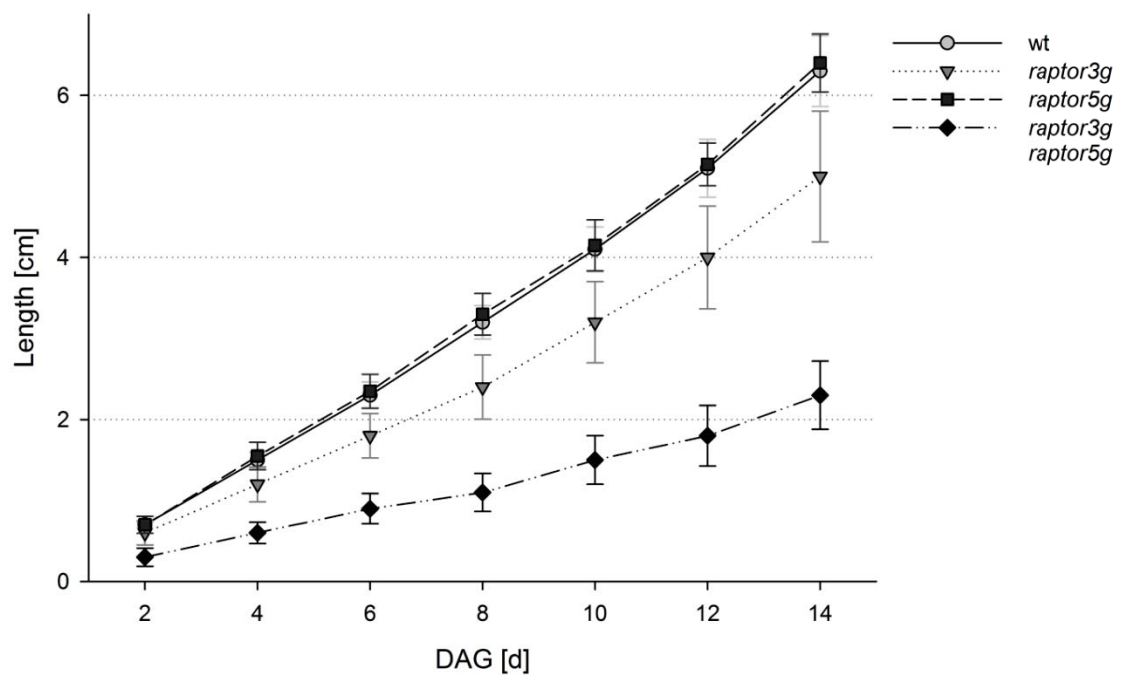


Figure 3.5 Root growth of *raptor* mutants. Wt plants, *raptor3g*, *raptor5g*, and *raptor3g raptor5g* mutants were grown vertically on MS media under short day conditions for 14 days after germination (DAG); (n≥10).

The observed phenotypes of *raptor* T-DNA insertion lines confirm *RAPTORs* function in promoting growth. The analysis showed that only the disruption of *RAPTOR3G*

resulted in a noticeable phenotype compared to wt plants, which is limited in its growth rate. Furthermore, the severe decrease in growth between *raptor3g* and *raptor3g raptor5g* mutants indicates an at least partial redundancy in the function of both RAPTOR alleles.

3.3 *A. thaliana* *raptor3g raptor5g* mutants show RAPTOR-independent TOR activity

RAPTOR is thought to act as an important scaffolding protein, which facilitates interactions between the kinase domain of TOR and its target proteins (Hara et al., 2002). To determine if TOR remains active despite the disruption of *RAPTOR*, I applied the specific kinase inhibitor AZD8055 to *raptor3g raptor5g* mutants (Montane and Menand, 2013). Two days after germination under long day conditions, seedlings of wt and *raptor3g raptor5g* mutants were transferred to MS medium containing different concentrations of the AZD8055. Plants were grown for six days under the same light conditions, while the root growth was measured every 48 hours. Based on these measurements, the growth rate *per day* was calculated for each concentration of AZD8055 (Figure 3.6). The growth curve of *raptor3g raptor5g* with different concentrations of AZD8055 indicated that these mutants responded to further TOR inhibition (Figure 3.6). While *raptor3g raptor5g* mutants showed a complete growth arrest at concentrations higher than 0.1 μ M AZD8055, wt plants only started to respond to ten-fold higher concentrations. This hypersensitivity indicated a reduced TOR activity in *raptor3g raptor5g* mutants. However, the observation that *raptor3g raptor5g* mutants respond to AZD8055 suggested that TOR maintained some activity in these plants despite disruption of RAPTOR.

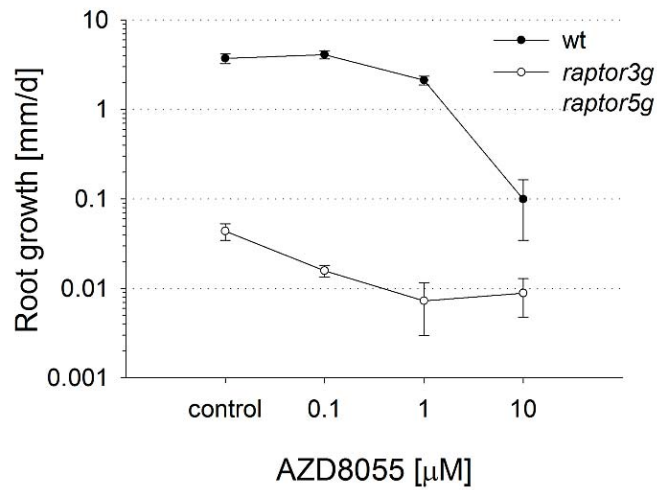


Figure 3.6 Dose-response curve of *A. thaliana* to the TOR inhibitor AZD8055. Seedlings of wt and *raptor3g raptor5g* mutants were grown under long day conditions on MS media containing a series of AZD8055 concentrations; (n \geq 4 per concentration).

3.4 Expression of RAPTOR3G and RAPTOR5G in *A. thaliana*

Previously published data of *RAPTOR* expression in *A. thaliana* was based on collective microarray data and *in vitro* analysis (Anderson et al., 2005). To allow for an *in vivo* confirmation and a more detailed resolution of transcription levels, I created transcriptional fusions of *RAPTOR3G* and *RAPTOR5G* promoter regions to the GUS reporter gene. The promoter sequences of *RAPTOR3G* and *RAPTOR5G*, which ranged between the translational start codon of *RAPTOR* and the start of the neighbouring gene sequence upstream of the *RAPTOR* genes, were cloned into the GUS-expression vector pB121 (Figure 3.7). Vector sequences of pB121-ProRAPTOR3G::GUS and pB121-ProRAPTOR5G::GUS are given in Appendix 8 and Appendix 9, respectively. The constructs were transformed and analysed in *A. thaliana* Col-0 plants.

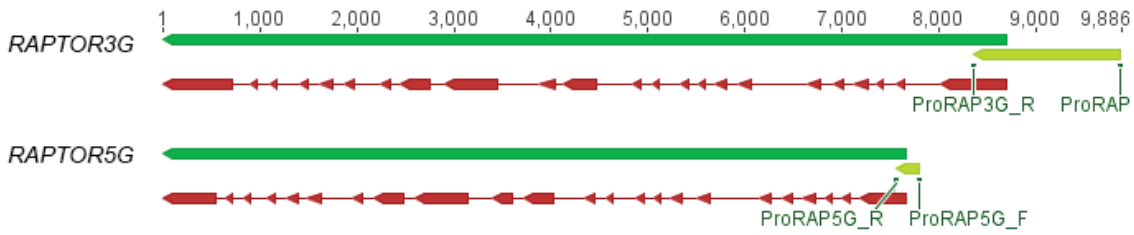


Figure 3.7 Genomic sequences of *RAPTOR3G* and *RAPTOR5G* on chromosome 3 and 5, respectively. Gene sequence (green), mRNA (red), and cloned promoter regions (yellow) are indicated. DNA sequence length is indicated above in bp.

The GUS expression profile showed *RAPTOR3G* as the dominantly expressed gene, while *RAPTOR5G* expression was only detectable in very specific tissues in the gametophyte and embryo (Figure 3.8). *RAPTOR3G* showed a broad expression pattern in vegetative organs, which was particularly pronounced in vascular tissues. In contrast, no visible *RAPTOR5G* promoter activity was detectable in vegetative tissue (Figure 3.8). In reproductive organs, *RAPTOR3G* expression was highest around the shoot apical meristem. A similar pattern was found in the root, with *RAPTOR3G* strongly expressed in the meristematic and vascular tissues and no detectable *RAPTOR5G* promoter activity. *RAPTOR* expression was also detected in gametophytes of flowering plants (Figure 3.9). Here, *RAPTOR3G* promoter activity was detected in carpels and in mature pollen. *RAPTOR5G::GUS* expression was observed in developing anthers, which peaked at stage 7 of flower development (according to Smyth et al., 1990). In developing seeds, *RAPTOR3G* promoter activity was found in the developing embryo and surrounding tissues, while *RAPTOR5G::GUS* expression was only detected in the funiculus (Figure 3.9).

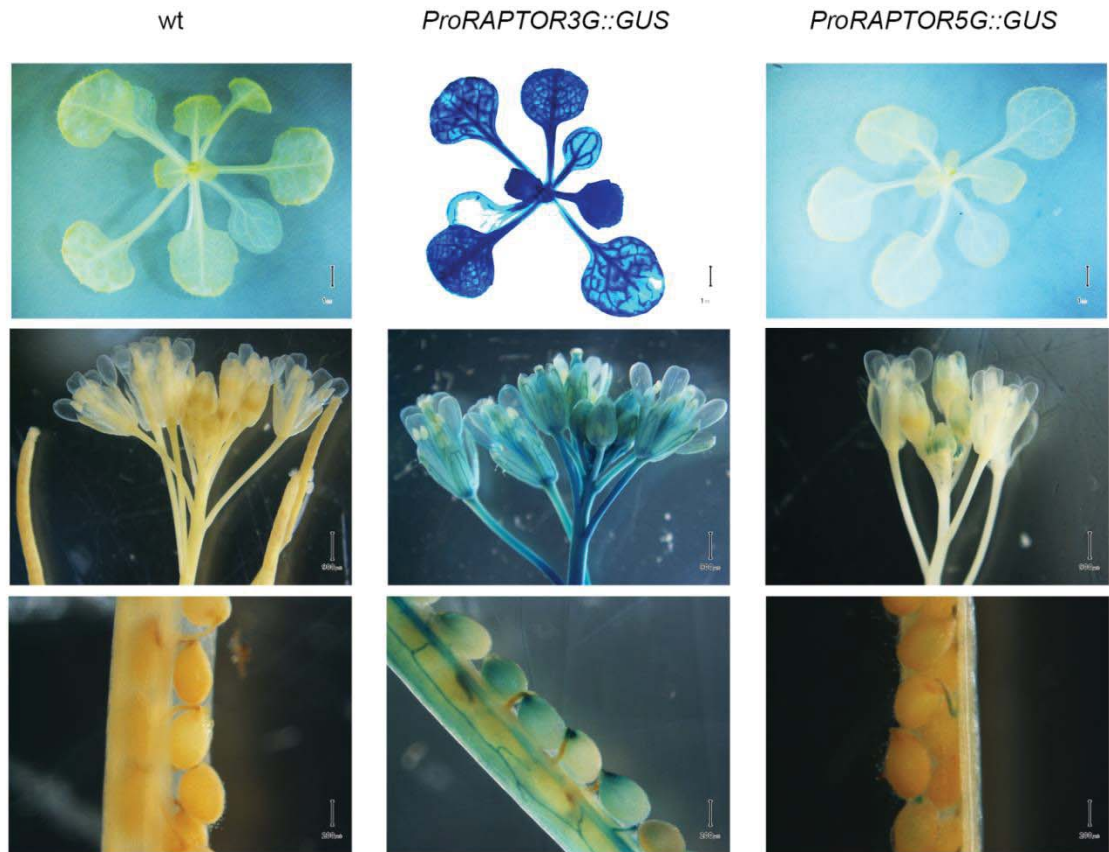


Figure 3.8 Expression profile of GUS reporter lines. GUS activity in wt (control), *ProRAPTOR5g::GUS*, and *ProRAPTOR3g::GUS* lines in 7-days old seedlings (top row), flower bud (middle row) and immature seed pods (bottom row) of mature plants. Scale bars indicates 1mm (upper row), 900 μ m(middle row), and 300 μ m(bottom row).

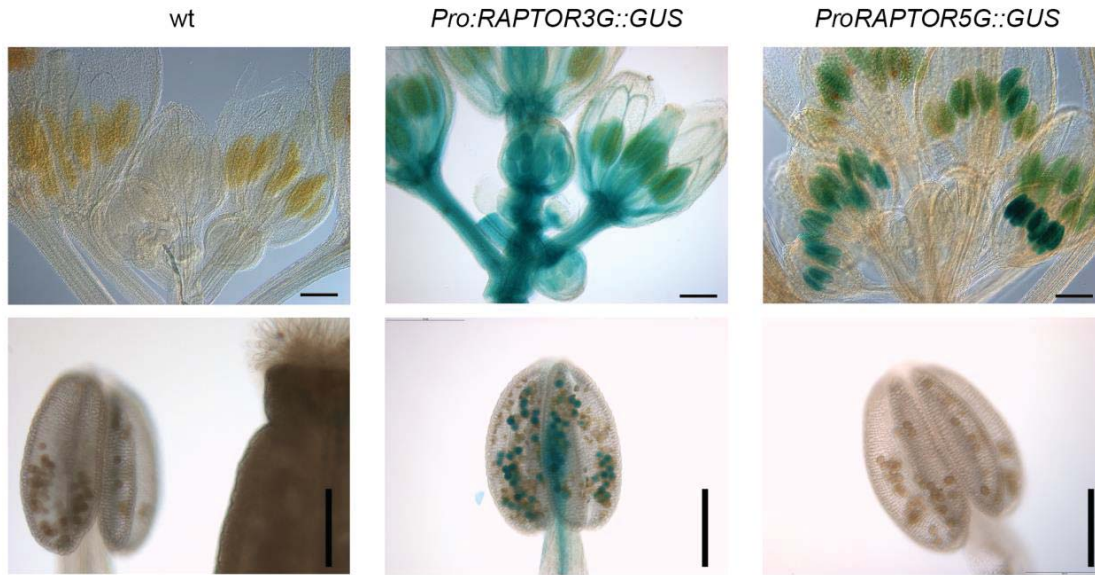


Figure 3.9 GUS activity in floral organs and gametophytes of GUS reporter lines. Developing inflorescences (upper row) and mature anthers (bottom row) of wt (control), *ProRAPTOR5g::GUS*, and *ProRAPTOR3g::GUS* plants. Scale bar = 200 μ m.

The GUS expression data confirmed *RAPTOR3G* as the dominantly expressed *RAPTOR* gene in *A. thaliana*, with particularly high expression in vascular tissues and developing tissues like meristematic regions and young pollen. In contrast, *RAPTOR5G* expression was only detectable in very limited areas during anther and seed development.

3.5 Transcriptomic profile of *raptor* mutants

To identify *RAPTOR*-dependent functions I isolated and compared the whole seedling transcriptomes of *raptor3g raptor5g* mutants with wild type plants. Through the comparison of this data to previously published transcriptomes from TOR-inhibited plants, I further hoped to detect *RAPTOR*-dependent and independent aspects of TOR activity (Ren et al., 2012; Xiong et al., 2013). For the transcriptomic analysis, RNA was isolated from *raptor3g raptor5g* mutants and wt plants, which were grown to the same developmental stage of ten to twelve leaves on MS medium. Equal amounts of shoot tissue from two to four seedlings were pooled per sample. For each genotype, three

biological replicas were included. RNA was handed over to MacroGen Inc. for library construction and sequencing using the Illumina HiSeq2000 platform.

The analysis of the transcriptome of *raptor3g raptor5g*, as described in Chapter 2.4, showed 8,437 (with P value ≤ 0.05) differentially expressed genes compared to the wild type. Differentially expressed genes involved in RNA and protein synthesis, protein modification and degradation, but also hormone and stress signalling are highly represented in the fraction of up-regulated genes (Figure 3.10). Widely repressed gene clusters include auxin regulation, cell degradation and vesicle transport. Further, the comparison of functional clusters indicated a down-regulation of synthesis and degradation of starch, nucleotides, and amino acid synthesis in *raptor3g raptor5g* mutants (Figure 3.11a). In contrast, the data indicates only minor changes in transcript levels of genes involved in glycolysis and TCA (Figure 3.11a). Oxidoreductases and ATP synthases of the mitochondrial electron chain were significantly repressed in their expression (Figure 3.11b). The transcriptomic profile also indicated a differential expression of several cell cycle regulating genes including CDKBs, FZR2 and TCP15 (Figure 3.12a), as well as genes particularly associated with endoreduplication (Figure 3.12c). However, not all E2Fa-target genes were affected equally (Figure 3.12b).

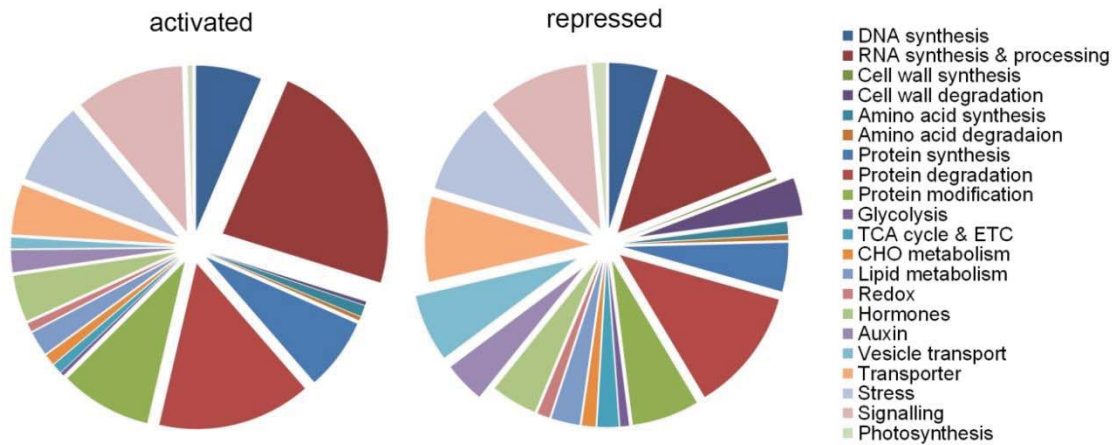


Figure 3.10 Significantly activated and repressed gene clusters in *raptor3g raptor5g* mutants. Differentially expressed genes between wt and *raptor3g raptor5g* mutants with a P value ≤ 0.05 were grouped in functional clusters using MAPMAN. Highly represented clusters of activated and repressed clusters are accentuated.

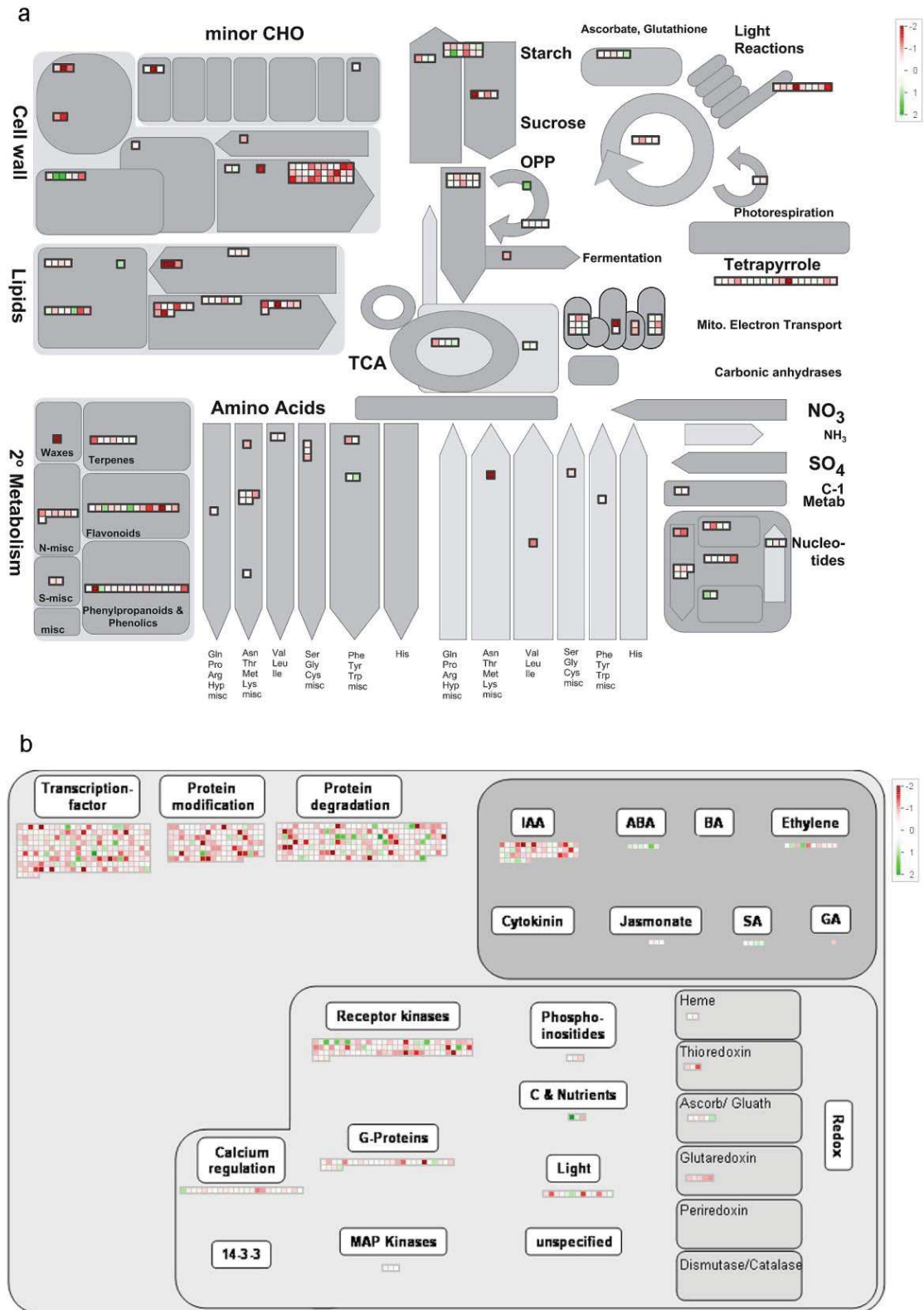


Figure 3.11 Representation of differentially expressed genes between *raptor3g raptor5g* mutants and wt plants. Differentially expressed genes with with $p \leq 0.01$ in (a) metabolism and (b) regulation.

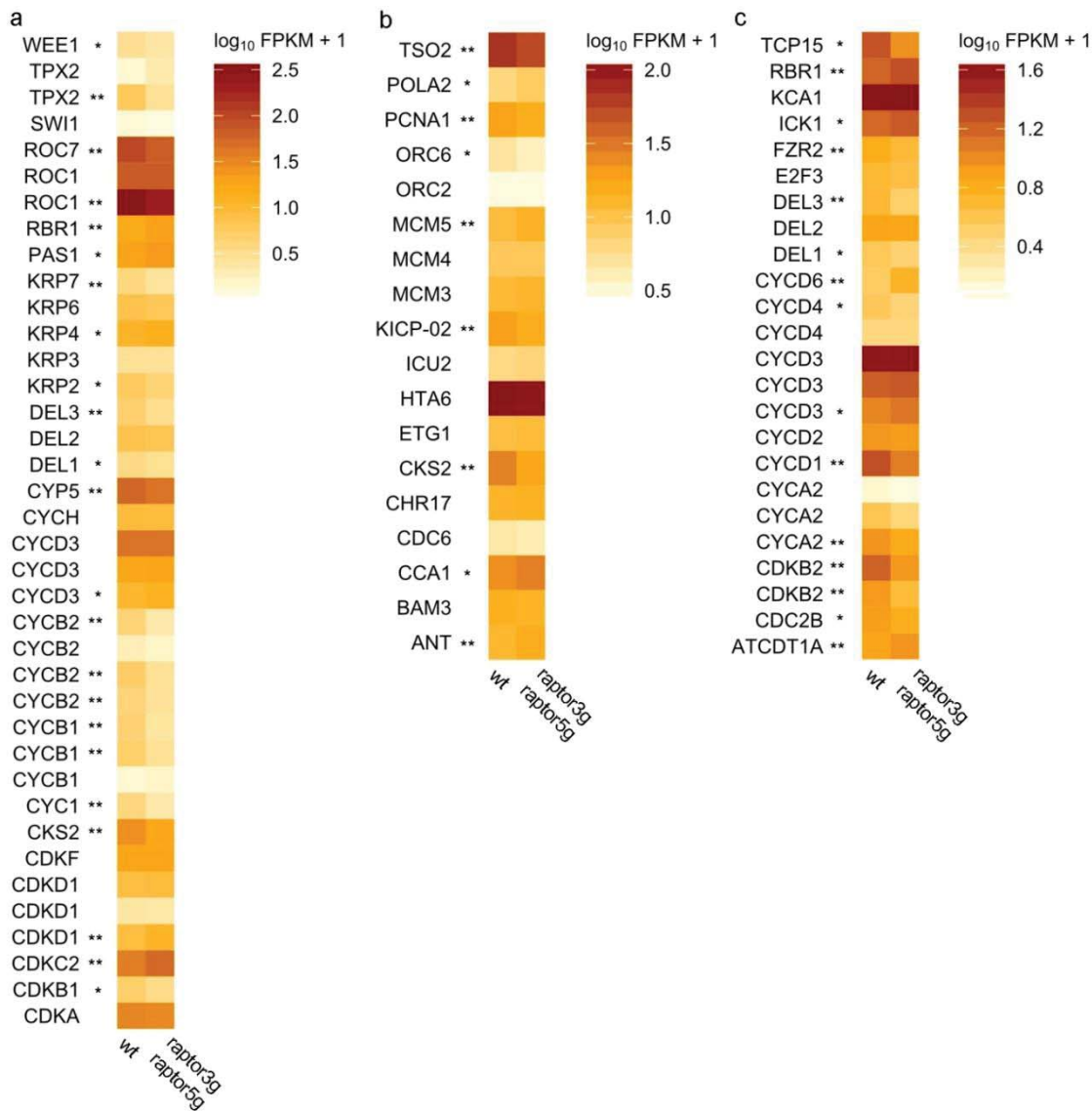


Figure 3.12 Expression profile of cell cycle-related genes in wt and *raptor3g raptor5g* mutants. (a) Genes related to cell cycle regulation, (b) E2Fa target genes and (c) genes linked to endoreduplication in wt and *raptor3g raptor5g* mutants. Figure includes only marker genes for which significant transcription data was detected in wt and *raptor3g raptor5g* mutants. The significance of the differential expression is indicated next to the gene name by asterisks (*: P value \leq 0.05; **: P value \leq 0.01).

The transcriptomic profile reflected the severe growth reduction of *raptor3g raptor5g* mutants. A wide range of cellular functions and anabolic processes, including cell cycle, energy storage and protein synthesis were reduced. This was accompanied with changes in the expression of regulatory genes involved in redox homeostasis and auxin signalling.

3.6 Root hairs of *raptor3g raptor5g* mutants show altered development and ROS accumulation

The transcriptomic analysis described in the previous section indicates changes in ROS accumulation and redox homeostasis, which were shown to play a role in various stages of plant development which includes the facilitation of tip growth in root hairs and pollen tubes (Foreman et al., 2003; Potocky et al., 2007).

To investigate changes in root development, wt and *raptor* mutants were grown vertically on MS medium. While single *raptor* mutants did not show differences in root hair development compared to the wild type, root hair extension was strongly reduced in *raptor3g raptor5g* mutants (Figure 3.13; Figure 3.14). I tested the accumulation of ROS in these plants to investigate the underlying mechanism for this phenotype. To visualize the ROS accumulation specifically in root hairs, I applied H₂DCF-DA, which reacts with ROS to form the highly fluorescent dichlorofluorescein. Confocal microscopic analysis revealed a strong staining in the root hairs of wt plants. In contrast, root hairs of *raptor3g raptor5g* mutants displayed no detectable staining, indicating a reduced ROS accumulation (Figure 3.15). To strengthen these observations, I conducted quantitative measurements of H₂O₂ concentration of shoot and root extracts. Therefore, plants were grown under short day conditions to the same developmental stage of eight to ten leaves on MS medium. Root and shoot tissue were sampled separately and three replicas per genotype were used for the analysis. The data confirmed a significantly lower H₂O₂ accumulation in *raptor3g raptor5g* mutants compared to wt plants (Figure 3.16).

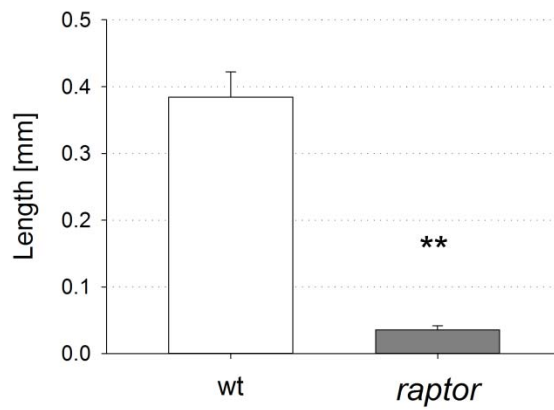


Figure 3.13 Length of root hairs in wt and *raptor3g raptor5g* mutants. Wt and *raptor3g raptor5g* plants were grown on MS media for four weeks under short day conditions; n=50. The calculated student's t-test was significant (indicated by asterisks; P value \leq 0.01).

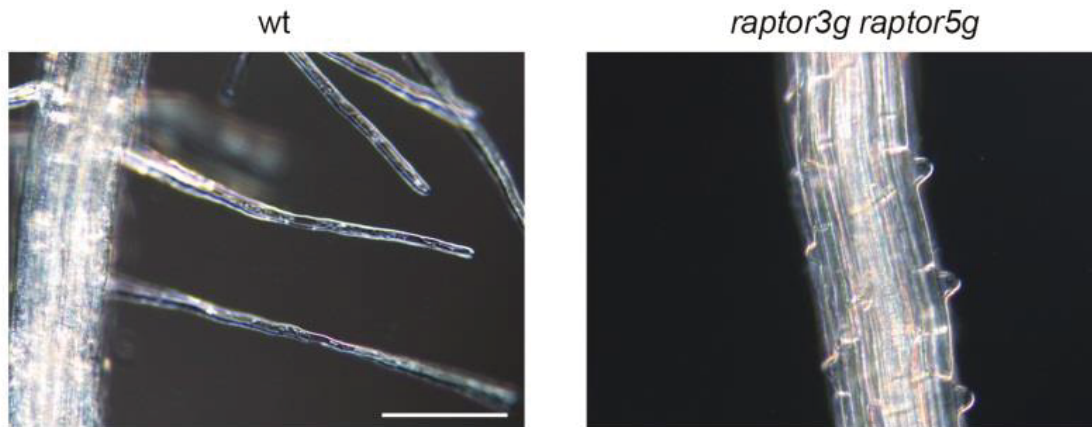


Figure 3.14 Root hairs of mature primary roots. Wt and *raptor3g raptor5g* mutants were grown vertically on MS media for two weeks under long day conditions. Scale bar = 200 μ m.

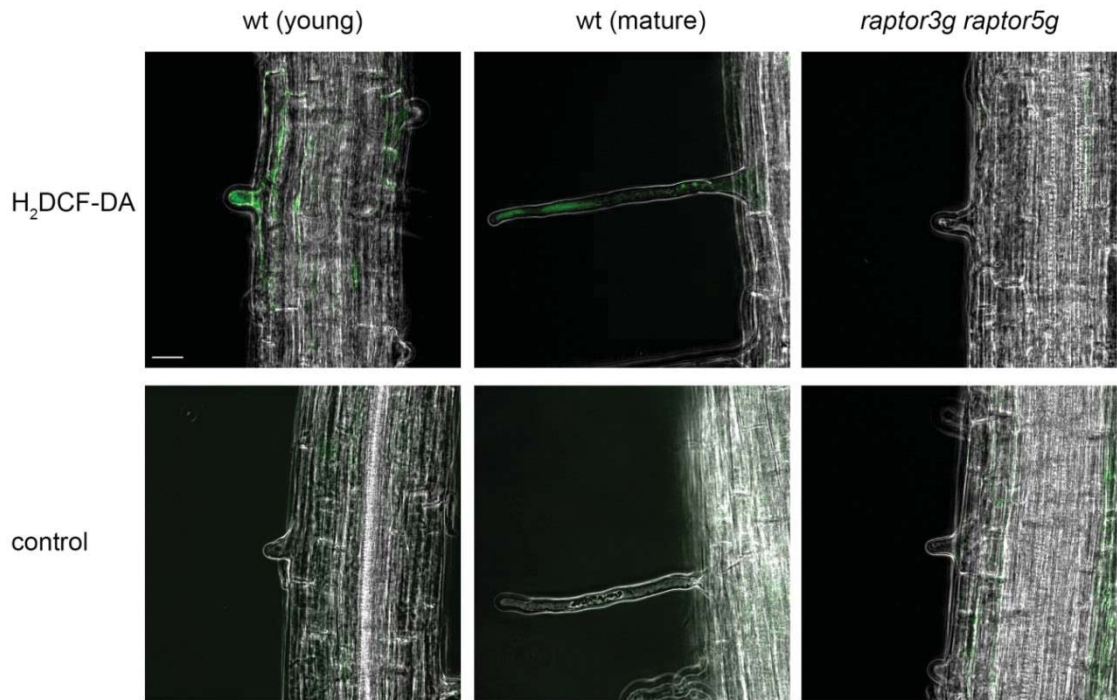


Figure 3.15 ROS accumulation in root hairs. Roots of wt (at age of two weeks) and *raptor3g raptor5g* mutants (at age of four weeks) were stained with H₂DCF-DA. Control shows roots treated in phosphate buffer without H₂DCF-DA. Scale bar = 20 μm .

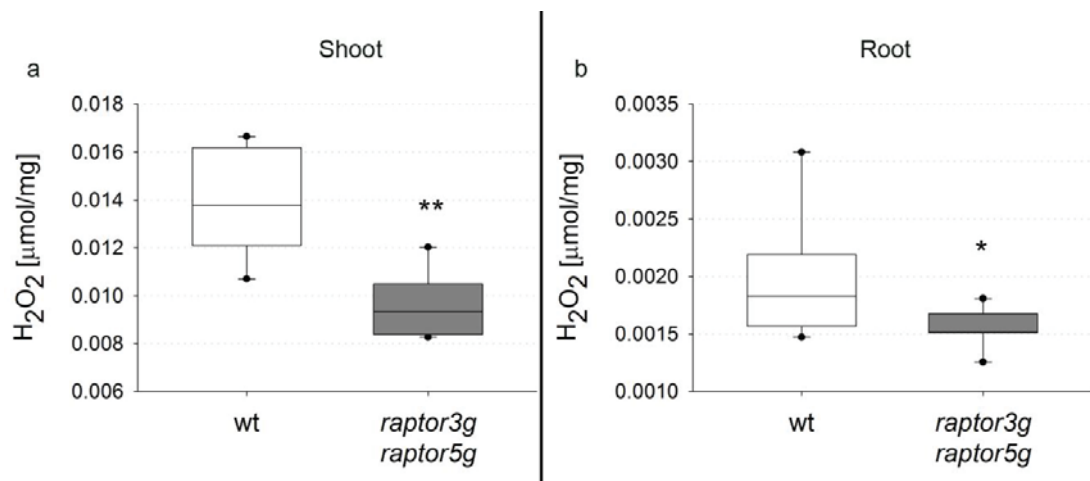


Figure 3.16 Quantitative measurements of H₂O₂ levels. Wt and *raptor3g raptor5g* mutants were grown under short day conditions to the same developmental stage. (a) Shoot tissue and (b) root tissue were sampled and analysed separately. Levels of significance are indicated by asterisks (*: P value \leq 0.05; **: P value \leq 0.01). The lower border of the box indicates the 25th percentile, the line within the box shows the median, and the upper border of the box represents the 75th percentile. The whiskers above and below the box indicate the 90th and the 10th percentile, respectively.

Raptor3g raptor5g mutants displayed a severe reduction in the polar extension of root hairs. The transcriptomic profile of these mutants, which was presented in the previous section, indicated alterations in the ROS and redox homeostasis. The quantitative and microscopic analysis of ROS accumulation and peroxidase activity in *raptor3g raptor5g* mutants and wt support a potential link between the loss of RAPTOR function, ROS homeostasis and the defects in root hair development.

3.7 RAPTOR is involved in regulating growth and development through controlling meristem size

Plant growth is maintained through a cell flux from meristematic regions, primarily in the apical regions of shoot and root. Other aspects of growth include regulation of individual cell size and cell expansion. To investigate which of these aspects are affected in *raptor* mutants, I looked at the organization of the root apical meristem (RAM).

Plants were grown on media containing EdU for 30min. EdU is a modified thymidine analogue, which is incorporated into the DNA during synthesis and replication. An azide modified fluorescent dye was subsequently added to the media, which formed a covalent bond with EdU and thus allowed a fluorescent labelling of replicating cells. In comparison to wt roots, the EdU-marked cells were limited to a smaller area of the RAM in *raptor3g raptor5g* mutants (Figure 3.17). Additionally, the number of stained cells within the meristem seemed to be reduced in *raptor3g raptor5g* mutants. This implied a lower activity of the meristem in which fewer cells were replicating during the reaction time of 30min when compared to the RAM of wt plants (Figure 3.17).

To identify if cell sizes were affected in *raptor* mutants, the lengths of the first ten cortex cells were measured along the longitudinal axis. To limit any potential bias of the comparison through the different developmental stages of wt and mutant plants, young wt seedlings with the same root length, as well as plants of the same age, were

included. However, the comparison of cortex cells from *raptor3g raptor5g* mutants and wt plants showed no significant difference in length (Figure 3.18).

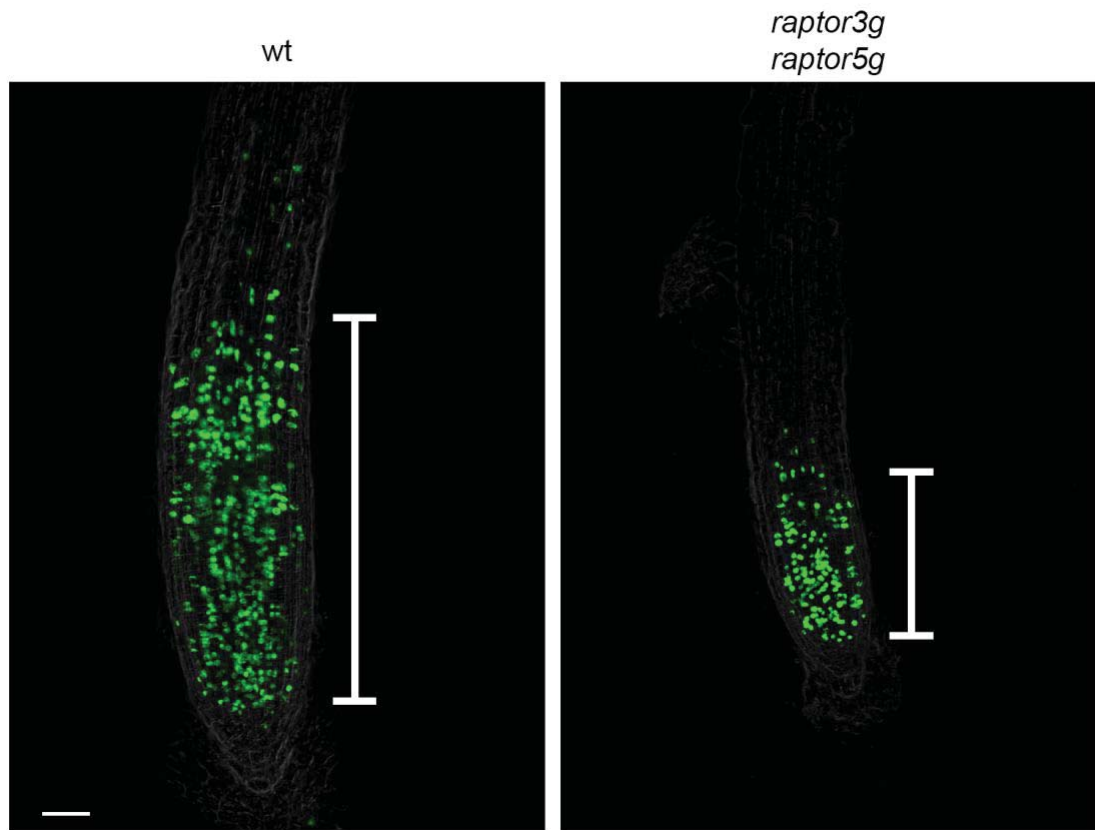


Figure 3.17 S-phase staining of cell with EdU. *Wt* and *raptor3g raptor5g* seedlings were grown in long day conditions for 10 days. Lengths of the RAMs are indicated in brackets. Scale bar = 50 μ m.

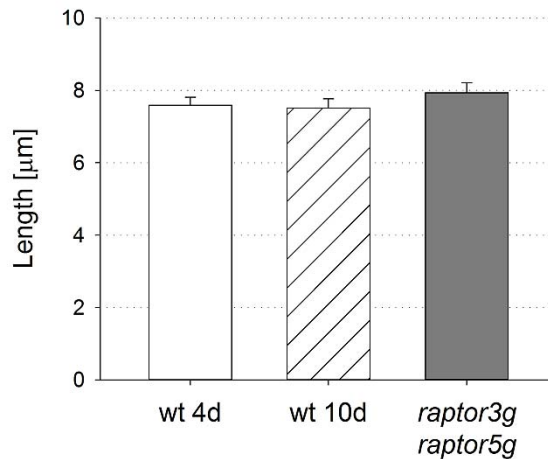


Figure 3.18 Longitudinal length of cortex cells in wt and *raptor3g raptor5g* mutants. Seedlings were grown vertically under long day conditions for 4 or 10 days. First ten cortex cells within the RAM were measured, $n \geq 5$. The calculated student's t-tests were not significant (P value ≥ 0.05).

The comparison of root meristems indicated a reduction in size and activity in *raptor3g raptor5g* mutants. This implied a limitation of the cell flux leaving the meristem and therefore limiting the growth of these mutants. However, the measurements of cell sizes within the meristem displayed no significant differences compared to the wild type, indicating that *raptor3g raptor5g* mutants were not affected in their cell size control.

3.8 *Raptor* mutants show reduced endoreduplication accompanied with altered trichome development and reduced organ size

As described above, restricted root growth in *raptor* mutants was based on changes in meristematic activity. In this section, I describe how deletion of RAPTOR function affects the shoot tissue.

When grown to the same age, *raptor3g raptor5g* mutants produced fewer leaves of smaller individual surface area (Figure 3.19). To understand the underlying mechanism of the difference in leaf size, *raptor3g raptor5g* mutants and wt plants were grown

under identical conditions and leaves of the first pair were analysed to ensure matured development and thereby limit any bias through different developmental rates at the time of comparison. Images of the abaxial leaf surface were taken with SEM (Figure 3.20). Using the SEM image, outlines of pavement cells were measured to calculate the cell surface area. The comparison of the cell surface area did not indicate any significant differences between pavement cells of wt plants and *raptor3g raptor5g* mutants in these leaves (Figure 3.21).

Further examination revealed that the leaves of *raptor3g raptor5g* displayed an obvious defect in the development of trichomes (Figure 3.22). Quantitative evaluation confirmed these observations (Table 3.1). These indicated that wt plants predominately develop trifurcated trichomes, which are created by two subsequent branching events (Hulskamp et al., 1994). In contrast, trichomes of *raptor3g raptor5g* mutants were less branched and contained predominately bifurcated trichomes (Table 3.1).

As it has been shown that trichome branching is closely related to endoreduplication, I conducted flow cytometry to identify the DNA content of nuclei extracted from leaf tissue (Melaragno et al., 1993). To reduce any potential bias caused by differences in the development of mutant and wt plants, I analysed pooled samples of cotyledons and the first leaf pair. As shown in Figure 3.23, the cell population of wt leaves consists of a variety of different degrees of ploidy, in which 2C, 4C, and 8C are the most represented types. The endoreduplication index (EI), which represents the average number of endocycles per nuclei, was calculated based on the histogram data shown in Figure 3.23. This resulted in an EI of 1.17 and 1.28 for wt plants grown under short and long day conditions, respectively. This profile correlated well with data from comparable tissue type, age and growth conditions described in the literature (Lin et al., 2007; Skiryicz et al., 2011). Compared to wt plants *raptor3g raptor5g* mutants showed a lower EI of 0.64 and 0.84 under short and long day conditions, respectively. The relative population of cells with higher DNA content was largely reduced in these mutants

(Figure 3.23). Under short day conditions, 0.7% of the total cell population within the leaf contained a DNA content of 16C, while in wt plants the relative population with DNA content of 16C was 9.2% (Figure 3.23). When grown under long day conditions, the 16C population increased to 4.5% in *raptor3g raptor5g* mutants, compared to 9.8% in wt plants. Cells with 8C showed a similar trend, which demonstrates that endoreduplication was limited in *raptor3g raptor5g* mutants.



Figure 3.19: Leaf development of wt and *raptor3g raptor5g* mutants. Dissected leaves of wt (at flower initiation, stage 5) and *raptor3g raptor5g* (at age of eight weeks). Scale bar = 1cm.

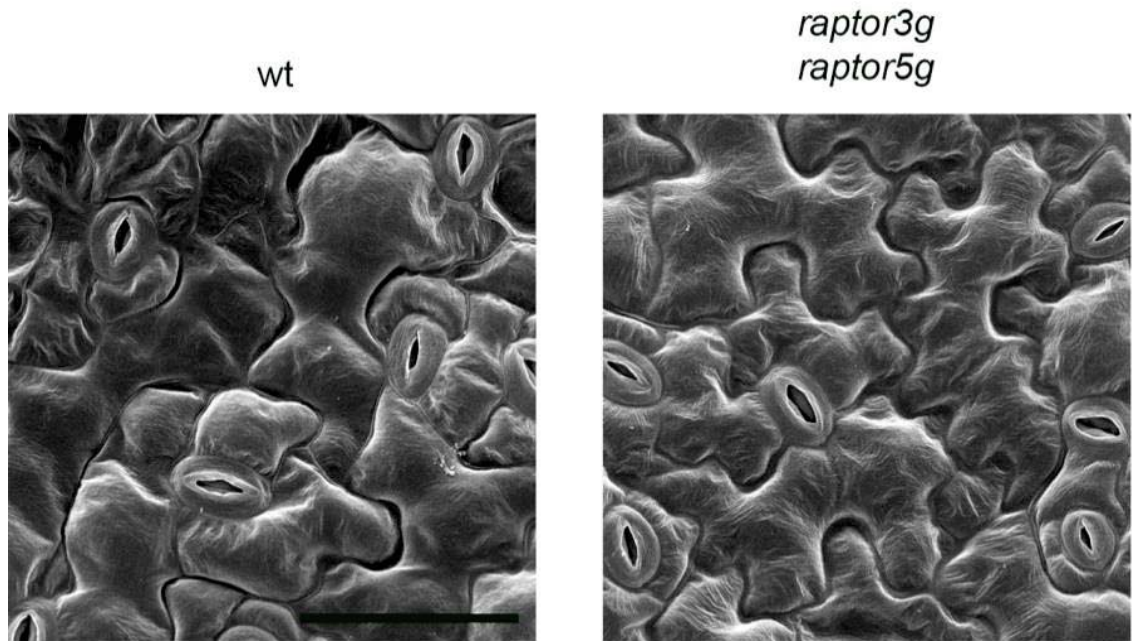


Figure 3.20 Leaf epidermis of wt and *raptor3g raptor5g* mutants. SEM images of the abaxial surface from leaves of the first leaf pair. Plants were grown under long day conditions for six weeks. Scale bar = 50 μ m.

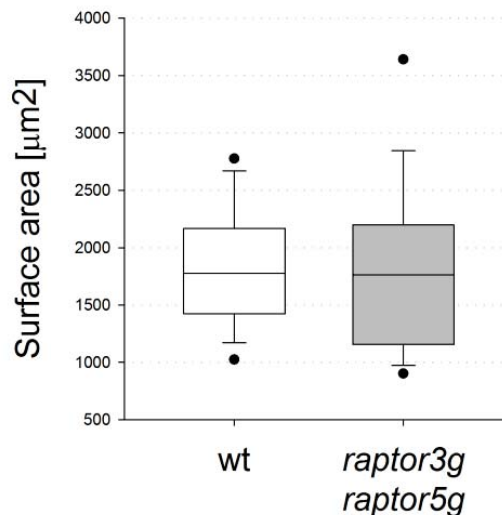


Figure 3.21 Quantitative measurements of the surface area of pavement cells. Wt and *raptor3g raptor5g* mutants were grown on MS media for six weeks under short day conditions. SEM images were taken of the abaxial surface of leaves from the first leaf pair. Per genotype, images of four replicas were analysed and the surface area of 20 cells per image was measured. The calculated student's t-test was not significant (P value=0.837). The lower border of the box indicates the 25th percentile, the line within the box shows the median, and the upper

border of the box represents the 75th percentile. The whiskers above and below the box indicate the 90th and the 10th percentile, respectively.

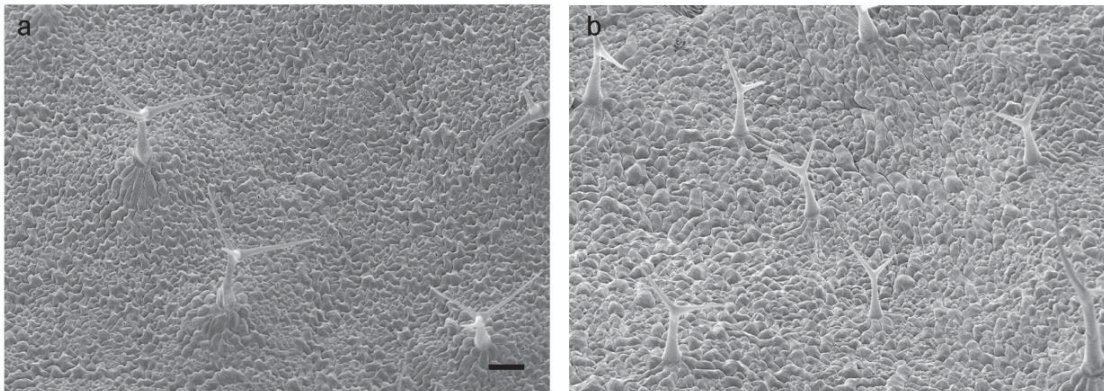


Figure 3.22 Trichomes of wt and *raptor3g raptor5g* mutants. SEM images from the adaxial leaf surface of (a) wt and (b) *raptor3g raptor5g* mutants. Plants were grown on MS media under long day conditions. Scale bar=100µm

Table 3.1 Relative representation of trichome phenotypes of wt and *raptor3g raptor5g* mutants. Plants were grown on MS media under long day conditions. Trichomes of wt were analysed after three weeks (n=220), and *raptor3g raptor5g* mutants after six weeks (n=280).

Branching type	wt	<i>raptor3g raptor5g</i>
Unbranched	-	13%
Bifurcated	1%	86%
Trifurcated	94%	1%
Quadfurcated	5%	-

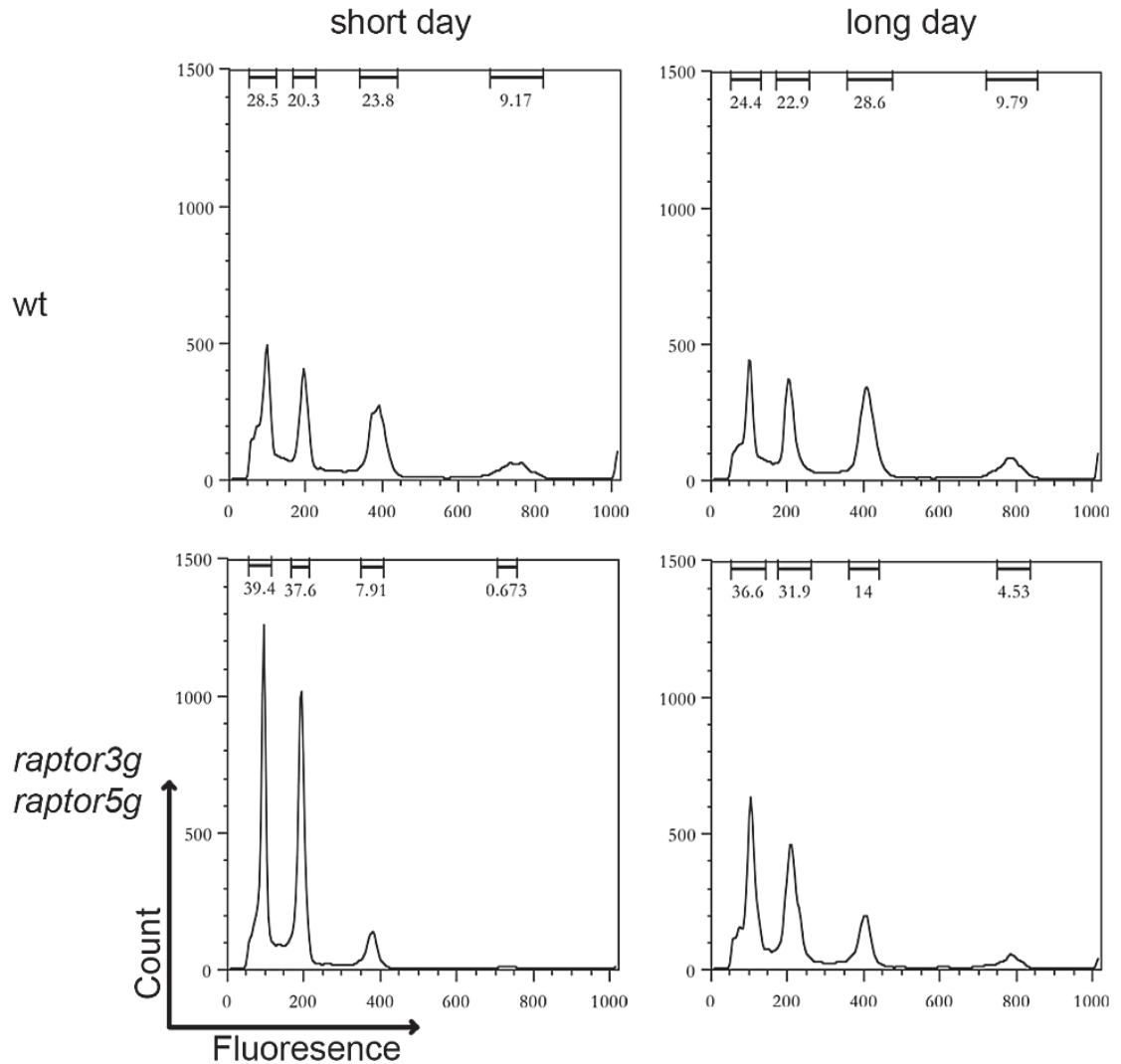


Figure 3.23 DNA content analysis using flow cytometry. Nuclei were isolated from cotyledons and the first leaf pair of wt and *raptor3g raptor5g* mutants grown under short day conditions (left panel) and under long day conditions (right panel). Extracted nuclei were stained with propidium iodide and analysed with flow cytometer. Images show the fluorescence frequency histograms of nuclei. Selection bars indicate the percentage of nuclei within the region of a major peak.

Taken together, *raptor3g raptor 5g* mutants develop smaller leaves while the individual cells size is not significantly different compared to wt plants. The development of leaves was also altered, which results in reduced trichome branching and endoreduplication.

Discussion

The findings of this study present novel aspects of TOR function and new angles on how TOR signalling is implemented in plants. The deletion of the *RAPTOR3G* led to plants with reduced growth rate and delayed development and therefore support the observations described by Anderson et al. (2005) as opposed to those by Deprost et al. (2005), who found this deletion to be lethal. In consensus with both previous studies, the deletion of *RAPTOR5G* alone did not cause any obvious phenotypic changes compared to the wild type. However, the combined deletion of both *RAPTOR* genes in *raptor3g raptor5g* deletions led to a dramatic intensification of the *raptor3g* phenotype, with further reduction of growth and development (Figure 3.4). This implies that the *RAPTOR5G* gene is indeed functional and contributes to TOR function in a redundant manner with *RAPTOR3G*. However, any visible phenotype of its sole deletion is obscured by *RAPTOR3G* in *raptor5g* mutants, which prevents any noticeable phenotypic difference compared to wt plants. This is further supported by the expression profile received from the GUS assay. There, *RAPTOR3G* was found to be highly expressed while *RAPTOR5G* expression was only detectable in very specific tissues during gametophyte and embryo development (Figure 3.8). This generally is conform with microarray data of previous publications (Anderson et al., 2005). The intensification of the phenotype between single *raptor3g* and *raptor3g raptor5g* mutants also suggests a dose-dependent function of RAPTOR. This might further imply that phenotypical differences of *raptor3g* and *raptor5g* mutants could be based on the differences in expression levels of the genes rather than their functional divergence.

The deletion of *TOR* led to an early embryonic arrest in fungi and animals (Kunz and Hall, 1993; Long et al., 2002). A similar arrest was also described for the deletion of *RAPTOR*, due to its essential contribution to TOR function (Hara et al., 2002; Loewith et al., 2002). The presented finding of viable *raptor* mutants in *A. thaliana* stands in great contrast to these observations. The experiments with the TOR inhibitor AZD0855

indicated that TOR maintained some activity in *raptor3g raptor5g* mutants (Figure 3.6). This residual TOR activity may explain the vegetative growth and the comparatively mild developmental defects of these plants. Yet, the growth rate was severely limited and some aspects of plant development were affected, which ultimately caused sterility in *raptor3g raptor5g* mutants (0). This suggests that RAPTOR is required for full TOR activity and to maintain specific functions but is not essential for TOR activity *per se* like in fungi and animals, which hints a fundamental difference to TOR function in plants.

The finding that *raptor3g raptor5g* mutants survived embryonic development represents a novel discovery. In contrast to observations made by Anderson et al., these mutants overcame the embryonic stage and were capable of vegetative growth and even flower initiation (Anderson et al., 2005). The growth of shoot and root seen in these plants was very limited, showing a reduced growth rate of about 30% compared to wt plants (Figure 3.5). This reduction of growth resulted from a decrease in meristematic activity, at least in the root. The same observations of reduced RAM size were made in TOR-inhibited *A. thaliana* by Sheen et al., which confirms that RAPTOR is involved in this branch of TOR function (Xiong and Sheen, 2014).

Raptor3g raptor5g showed also a delayed development, resulting in late germination, delay of flower initiation and senescence. Following flower initiation, shoot growth appeared more branched, which was also described for *raptor3g* mutants previously (Anderson et al., 2005). The transcriptomic analysis revealed significant expression changes of genes involved in auxin synthesis and distribution (Figure 3.11). Among these were several PIN-FORMED (PIN) genes, including PIN1, PIN3, PIN6 and PIN7 (Appendix 15 and Appendix 16), which encode auxin carriers that regulate auxin cell-to-cell transduction in meristems and therefore are important factors regulating organ growth (reviewed by Křeček, 2009). Further, the AGC kinases PINOID, WAG1 and WAG2 were significantly down-regulated (Appendix 16). These genes are contribute to auxin signalling by directing the subcellular distribution of PIN proteins (Friml et al.,

2004; Santner and Watson, 2006). These findings suggest that disturbed auxin signalling is likely to cause the loss of apical dominance seen in *raptor3g raptor5g* mutants.

The transcriptomic profile of *raptor3g raptor5g* further indicated a decrease in the expression of oxidoreductases of the mitochondrial electron chain (Figure 3.11), which represent major sources of ROS (Brand et al., 2004). Furthermore, ROS scavengers including thioredoxin, glutaredoxin and glutathione were down-regulated (Figure 3.11). Quantitative measurements proved that the accumulation of ROS in *raptor3g raptor5g* was significantly reduced compared to wt plants (Figure 3.16). This further supports the conclusion that ROS homeostasis is out of balance in *raptor3g raptor5g* mutants. Alterations in ROS accumulation was linked to various developmental processes including senescence and root hair growth (reviewed by Petrov and Van Breusegem, 2012). For root hair growth, ROS accumulation was shown to be essential to promote a calcium gradient in the root hair tip, which is required for the polar extension of root hairs (Wymer et al., 1997; Foreman et al., 2003). This stands in agreement with the observations of stunted root hairs in *raptor3g raptor5g* mutants (Figure 3.13). Similar observations were previously made in seedlings treated with rapamycin, which suggests an essential role of TOR in polar tip growth of root hairs (Ren et al., 2012; Xiong et al., 2013). The visualization of reduced ROS accumulation in root hairs of *raptor3g raptor5g* mutants further strengthened the interpretation that limitations in ROS production are the underlying mechanism behind the stunted root hair phenotype of these mutants (Figure 3.15).

Another distinct developmental aspect of *raptor3g raptor5g* mutants was the limited branching of trichomes (Table 3.1). The event of branching was tightly linked to endoreduplication in trichome initial cells, which were shown to contain a DNA content of up to 32C (Hulskamp et al., 1994). The flow cytometry data of *raptor3g raptor5g* mutants indicated an inhibition of endoreduplication compared to wt plants, which was

likely to contribute to the reduced trichome branching in these mutants. The development of trichomes is a complex process, which was linked to the function of the transcription factors GLABRA1 (GL1) and GLABRA3 (GL3) (Oppenheimer et al., 1991; Payne et al., 2000). Both were shown to control the expression level of the transcription factor RBR1, a central regulator of cell cycle progression, whose activity inhibits the transition from G₁ to S phase through interaction with E2F family transcription factors (Morohashi and Grotewold, 2009). Consistent with this, inactivation of RBR1 led to an increase of trichome branching (Desvoyes et al., 2006). Interestingly, the role of TOR activity on RBR1-E2F signalling has been intensively discussed in the literature based on two seemingly contradictory findings: The TOR substrate S6K1 was shown to associate with the RBR1-E2F complex and contributed to RBR1 activity by supporting its nuclear localization, which subsequently resulted in a suppression of the cell cycle. Therefore, plants with reduced S6K1 expression showed an amplified cell cycle progression, which resulted in increased trichome ploidy and branching (Henriques et al., 2010). Opposing this negative role in cell cycle regulation, Xiong et al. (2013) demonstrated a direct phosphorylation of E2Fa *in vitro* and confirmed a down-regulation of E2Fa target genes in seedlings upon treatment with rapamycin (Xiong et al., 2013). This is supported by the transcriptomic analysis of *raptor3g raptor5g*, which revealed a down-regulation of several E2Fa target genes (Figure 3.12). Yet, this trend was not consistently significant in all tested genes. However, this might be a consequence of the RNA sampling from whole seedlings opposed to the specific RNA extraction from root meristems as done in the study by Xiong et al. (2013). It remains yet to be elucidated how the seemingly contradictory function of TOR and S6K are to be explained. An ambiguous role of TOR in cell cycle regulation was further supported by the finding that PP2A directly inhibits S6K activity in mammals (Peterson et al., 1999; Westphal et al., 1999). Although unconfirmed in plants yet, a positive impact of TOR activity on cell cycle progression through inhibiting PP2A would align well with the described trichome phenotype of *raptor3g raptor5g* mutants. However, the

increase in trichome ploidy and branching in *s6k* knock-down plants reported by Henriques et al. (2010) contradicts findings of this study. The different strategy by applying RNAi knock-down against *S6K* might offer an explanation for the contradictory results. Also, compensatory mitigation through feedback responses within the pathway (i.e. through *S6K*) and TOR-independent regulation of *S6K* further hinders any correlation with *raptor* mutants (reviewed by Magnuson et al., 2012). Nevertheless, because of the conflicting observations, it would be important to determine how *S6K* phosphorylation is affected in *raptor3g raptor5g* mutants.

Alongside altered trichome development, *raptor3g raptor5g* mutants displayed stunted root hairs (Figure 3.13). The coincidence of these phenotypes might be related to their similar regulation, which is comprised of the GL3-EGL3-MYC1 complex (reviewed by Bruex et al., 2012). A hint on how TOR activity might influence root hair formation was found through a suppressor screen of *leucine-rich repeat/extensin 1 (lrx1)* mutants (Leiber et al., 2010). *LRX1* regulates cell wall synthesis in root hairs, and mutants showed a branched and swollen root hair phenotype (Baumberger et al., 2001; Baumberger et al., 2003). *LRX1* was negatively regulated by REPRESSOR OF *LRX1* (*ROL5*), which homolog in yeast, *Ncs6p*, was found affected by TOR signalling (Chan et al., 2000). This was supported by experiments in *A. thaliana*, in which the treatment with rapamycin led to the restoration of wild type root hair growth in *lrx1* mutants (Chan et al., 2000; Leiber et al., 2010). This indicated a positive regulation of root hair growth by TOR through activating *LRX1*.

The regulation of endoreduplication represents another function of *RAPTOR*-dependent TOR activity, which was identified in this study. Besides its role in trichome branching, increase in DNA content was closely linked to cell and organ size in plants (reviewed by Sablowski and Carnier Dornelas, 2014). Although the mechanisms by which ploidy affects these remain to be elucidated. According to the “karyoplasmic ratio” theory, an increase of DNA content may be required to maintain higher growth

rates and larger volumes of cytoplasm (Kondorosi et al., 2000; Jorgensen and Tyers, 2004). TOR was described determining cell size by previous studies in *A. thaliana*, in which plants with inhibited TOR activity and S6K expression caused a decrease in cell size in various leaf cell types (Henriques et al., 2010; Ren et al., 2012). Similar links between TOR function and cell size control were also made in fungi and animals (Edgar, 2006; Laplante and Sabatini, 2012). These findings suggest that TOR could act as a key element in the coupling of cell cycle and cell growth. However, *raptor3g raptor5g* did not indicate any sign of altered cell size before or after post-mitotic expansion (Figure 3.21). This finding seems contradictory since endoreduplication and organ size were found reduced in these mutants. However, endoreduplication was found to be reduced rather than completely blocked. This might explain why defects were only seen in trichomes, which requires repeated endocycles during its development, while other tissues remained unaffected. According to Melaragno et al. (1993), the majority of cells undergo only one to two cycles of endoreduplication during leaf expansion. As populations with 4C and 8C DNA contents were detected in *raptor3g raptor5g* mutants, the change in endoreduplication might be too minor to affect cell expansion. Further, the role of endoreduplication on cell expansion is still controversial, since several studies provided examples of *A. thaliana* mutants, in which alterations of ploidy did not proportionally result in changes of cell size (John and Qi, 2008; Massonnet et al., 2011; Tsukaya, 2013). In a recent study on various *A. thaliana* mutants, which were characterized by abnormal cell size, no correlation between cell volume and ploidy level was found (Tsukaya, 2013). Rather than through changes in cell size, limited growth in *raptor3g raptor5g* mutants seemed to follow a reduced meristematic activity (Figure 3.17). In previous studies, which used transgenic lines expressing the yeast FKBP12 protein, treatment with rapamycin led to a significant reduction of the RAM size (Ren et al., 2012). The same phenomenon was reported by Xiong and Sheen (2014), who showed a reduction of RAM size following the knock-down of TOR, and Montane and Menand (2013), who applied TOR inhibitors to reduce

TOR activity. Despite the differentiation of meristematic cells, the general *bauplan* of the meristem was found not to be affected in these studies. This stands in agreement with the observations in *raptor3g raptor5g* mutants, which further implies that the regulation of meristem size is a RAPTOR-dependent function of TOR. The staining of S-phase cells in root meristems indicated that the location of cell division and its rate was limited in *raptor3g raptor5g* mutants (Figure 3.17). Subsequently, the flow of cells leaving the meristem was drastically reduced, which caused the reduction seen in root and overall size. Therefore, a reduction of meristem size and activity rather than a reduction of individual cell size might be the underlying cause of small organ size, although this needs to be verified in other organs i.e. for leaf and flower. The change of meristem size is likely to involve action of phytohormones, particularly auxin and cytokinin (Dello Iorio et al., 2007; Dello Iorio et al., 2008). This is also supported by the changes in the transcription of genes involved in auxin synthesis and distribution found in *raptor3g raptor5g* mutants (Figure 3.11). A recent study found RBR1 activity to be regulated by cytokinin, which raised the possibility that this regulation could be channelled through TOR (Perilli et al., 2013). Interestingly, the same study found the size of the RAM to be limited in *A. thaliana* overexpressing *RBR1*, which matches the observations in *raptor3g raptor5g* mutants (Figure 3.17). Although the details of the molecular interactions remain to be identified, the here presented findings indicate that the interplay between altered hormone signalling and reduced TOR activity accounts for the reduced meristem size in *raptor3g raptor5g* mutants.

To summarize this chapter, this study presents the first report of *raptor* null mutants to overcome the embryonic stage of development. The creation and analysis of the *raptor3g raptor5g* mutant in *A. thaliana* revealed *RAPTOR*-independent TOR activity, which conceded minimal vegetative growth. This growth allowed a phenotypic analysis of this mutant that exposed several *RAPTOR*-related functions in plants, including the regulation of ROS homeostasis, endoreduplication, and meristem size.

Chapter 4

Flower development and transmission of *raptor* mutants

Introduction

The role of TOR activity on vegetative growth was addressed by several studies, but very little is known yet about the impact of TOR on the development and growth during the reproductive phase. Of the two previous studies on RAPTOR function in *A. thaliana*, flower development was addressed only by Anderson et al. (2005), who described the *raptor3g* mutant as late flowering and sterile. Further insights might be provided by studies on VPS34 and PTEN function in *A. thaliana*, as homologs of these proteins are linked to the regulation of TOR signalling in other species (reviewed in Chapter 1.7). Studies on these factors described a role in pollen development by regulating autophagy and nuclear division (Gupta, 2002; Lee et al., 2008b; Jaber et al., 2012). Although the link between VPS34, PTEN and TOR signalling remains to be confirmed in plants, these findings offered a first indication of a potential function of TOR in the development of gametophytes. To further expand the understanding of TOR function in the growth and development during this stage, I examined the phenotypes of *raptor* mutants in *A. thaliana*. Also, the discovery of relatively healthy *raptor3g raptor5g* as described in the 0 enabled the first in-depth RAPTOR loss-of-function analysis in flower development.

Results

4.1 Flower development of *A. thaliana raptor* mutants

For the phenotypic analysis, plants were grown on soil or MS medium under long day conditions to promote flowering. At the time of flowering initiation, *raptor3g raptor5g* mutants were about twice the age and had twice the number of rosette leaves compared

to wt plants (Figure 4.1). Phenotypes of flowering wt and *raptor3g raptor5g* plants are shown in Figure 4.2, which demonstrates the reduced growth and increased branching of *raptor3g raptor5g* mutants. Microscopic studies showed that the individual disruption of *raptor3g* and *raptor5g* has only a minor impact on the development of inflorescences (Figure 4.3). When compared to flowers of wt plants, inflorescences of *raptor3g* mutants were reduced in overall size, while *raptor5g* showed no readily discernible differences (Figure 4.3). The combined disruption of both *RAPTOR* genes in *raptor3g raptor5g* mutants led to further reduction of overall size compared to *raptor3g* mutants. Moreover, the outgrowth of petals and extension of filaments in stamen was limited (Figure 4.3). Ultimately, flowers failed to produce viable seeds, which demonstrated the severe developmental defects of these mutants.

To elucidate fertility of gametophytes in *raptor* mutants, I crossed single and double *raptor* mutants with wt plants. While crosses with single *raptor* mutants did not indicate any alterations in the transmission of the mutant allele, attempts to pollinate *raptor3g raptor5g* with pollen of wt, and *vice versa* did not yield any seeds, which indicated defects in female and male gametophytes of *raptor3g raptor5g* mutants (data not shown). This demonstrated that the deletion of individual *RAPTOR* genes did not significantly affect the development of floral organs. However, disruption of both genes resulted in smaller and sterile flowers.

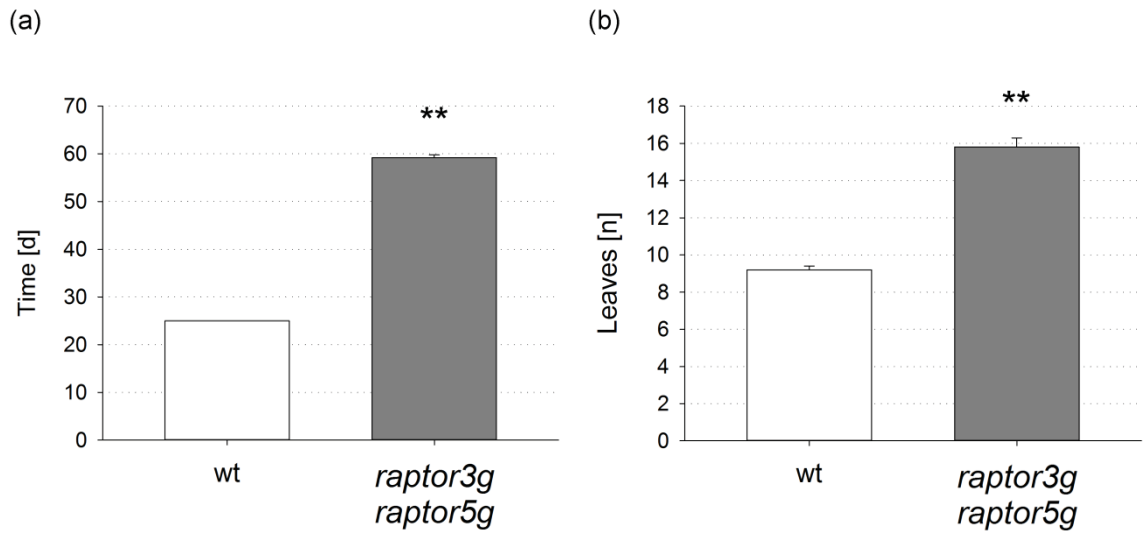


Figure 4.1 Flower initiation of wt and *raptor3g raptor5g* mutants. Plants were grown soil under long day conditions (n=5 per genotype). (a) Time and (b) number of rosette leaves at time of flower initiation. Student t-test was significant (indicated by two asterisks; P value \leq 0.01).

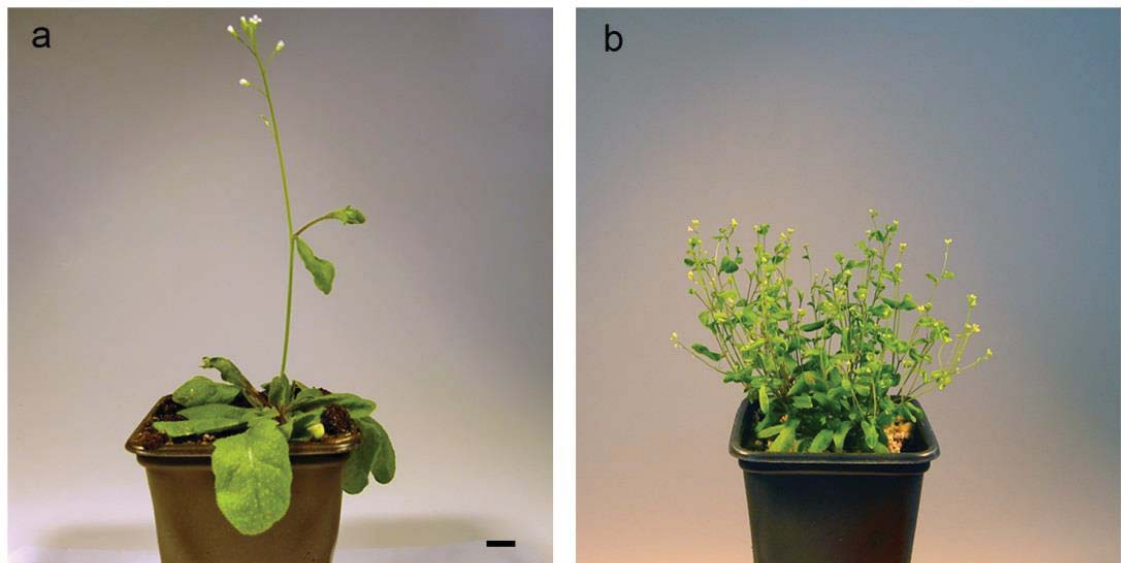


Figure 4.2 Phenotypes of wt and *raptor3g raptor5g* mutants at time of flowering. Plants were grown on soil under long day conditions. (a) Wt plant at age of four weeks; (b) *raptor3g raptor5g* mutant at age of 16 weeks. Scale bar = 1cm.

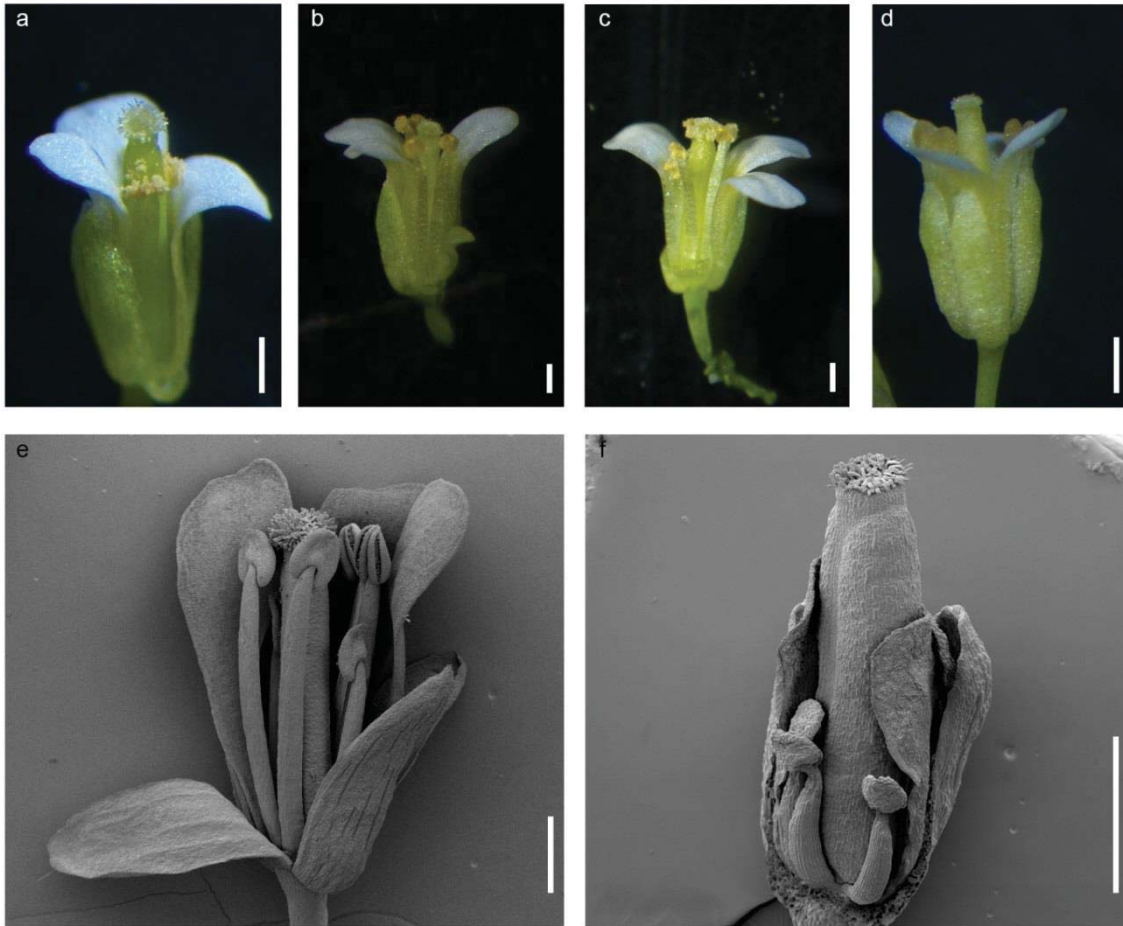


Figure 4.3 Inflorescences of *A. thaliana* *raptor* mutants. Dissecting microscope images of (a) wt, (b) *raptor3g*, (c) *raptor5g*, (d) *raptor3g raptor5g* mutants. SEM images of (e) partially dissected mature inflorescences from wt and (f) late inflorescence/early silique staged inflorescence from *raptor3g raptor5g*. Sepals and petals facing the front were removed for better viewing. Scale bar = 0.5mm.

4.2 Arrest of female gametophyte in *raptor3g raptor5g* mutants causes sterility

I analysed the pistil development of *raptor3g raptor5g* mutants more closely to address the sterility of their flowers. Plants were grown under long day conditions to promote flower initiation. Pistils of wt plants and *raptor3g raptor5g* mutants were sampled and examined under light and confocal microscope. The analysis revealed a defect in embryo sac formation of embryos of *raptor3g raptor5g*, which suggested an arrest at or prior to the gametophyte developmental stage FG3 following the classification developed by Pagnussat et al. (2009) (Figure 4.4). The missing cellular structures

within the embryo pointed towards an even earlier arrest point (Figure 4.4f). This confirmed that female gametophytes of *raptor3g raptor5g* mutants arrest at an early developmental stage.

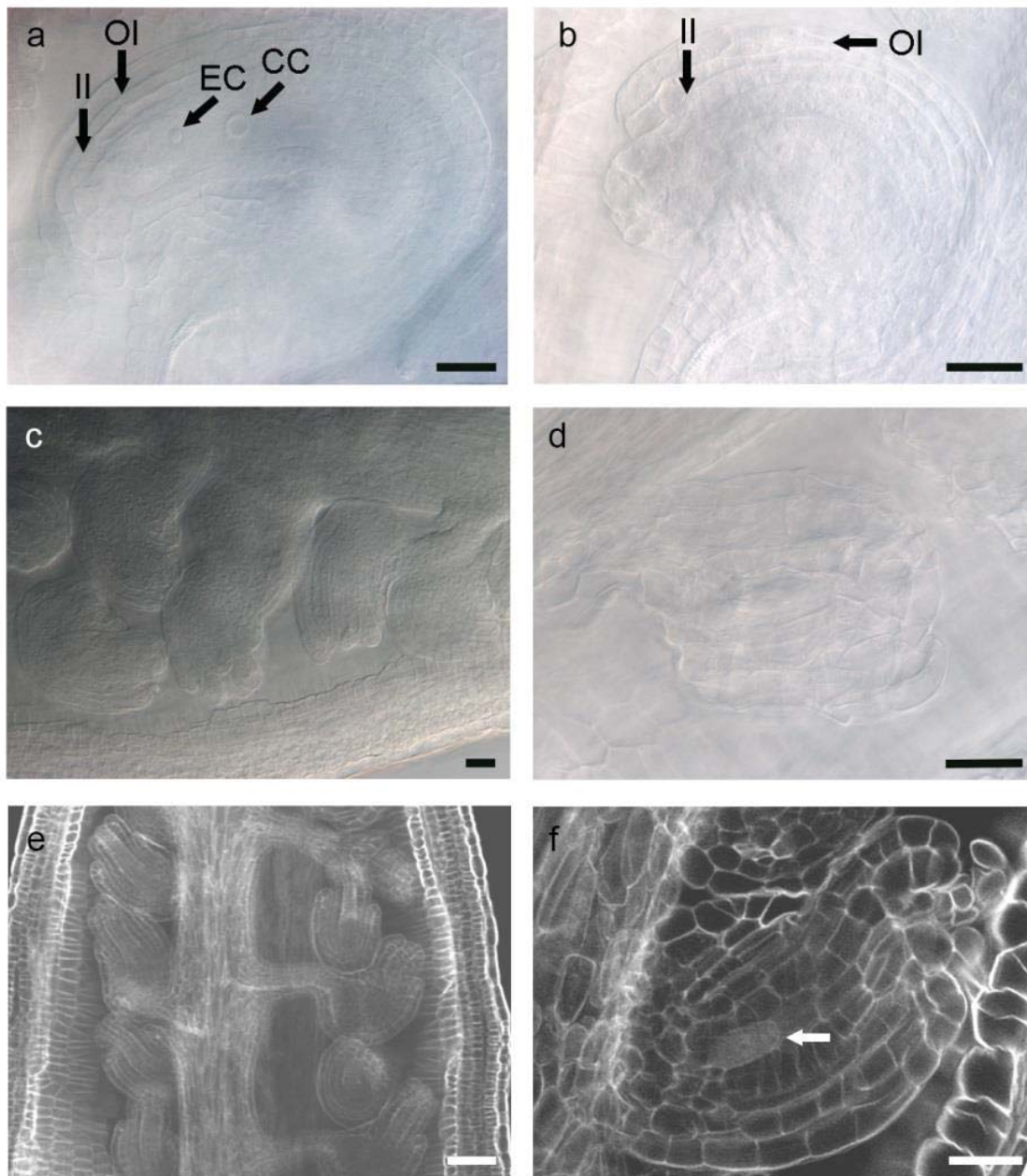


Figure 4.4 Female gametophytes of wt and *raptor3g raptor5g* mutants. Plants were grown on soil under long day conditions. (a) Nomarsky microscopy images of megagametophytes from wt plants. (b) Arrested gametophyte at FG stage 5, (c) arrested ovules within mature carpel (c) and distorted ovule of late pistil developmental stage (d) of *raptor3g raptor5g* mutants. Outer (OI) and inner integument (II), central cell (CC) and egg cell (EC) are indicated. (e) Confocal images of mature pistil and (f) arrested embryo (indicated by arrow) of *raptor3g raptor5g* mutants. Scale bar = 20 μ m.

4.3 RAPTOR is involved in pollen maturation and pollen tube growth

As described in Chapter 4.1, attempts to pollinate wt plants with the pollen of *raptor3g raptor5g* did not succeed. Here, I explored potential causes for this defect.

For the analysis of pollen, mature anthers from mutants and wt plants were studied under the light microscope. Anthers were stained with Alexander staining to elucidate the viability of pollen. Pollen grains from *raptor3g raptor5g* mutants showed a blue coloration, which illustrated that these were not binding the red-coloured fuchsin, a component of the Alexander's staining solution (Figure 4.5). As fuchsin stains the protoplast of mature pollen, this indicated a pre-mature arrest (Barrow, 1982). Additionally, *raptor3g raptor5g* mutants failed in anther dehiscence and subsequently to release pollen. In contrast, the magenta coloration through incorporation of fuchsin in wt and single *raptor* mutants indicated viable pollen (Figure 4.5).

The reciprocal crossing of single *raptor* mutants and wt plants did not show any significant difference in the transmission of the mutant allele as described above. In order to investigate the function of *RAPTOR3G* and *RAPTOR5G* individually, I generated plants that were homozygous for *RAPTOR3G* and heterozygous for *RAPTOR5g*, and *vice versa*. Plants of these lines were grown in the glasshouse under long day conditions and crossed with wt. The transmission of the heterozygous gene was then identified by genotyping the progeny. The crosses between wt and heterozygous *raptor5g* mutants in a homozygous *raptor3g* background (*raptor3g^{-/-} raptor5g^{+/-}*) did not indicate any significant deviation from the expected ratio of genotypes in the progeny (Table 4.1). However, the crosses between wt pistils with pollen of heterozygous *raptor3g* mutants in a homozygous *raptor5g* background (*raptor3g^{+/-} raptor5g^{-/-}*) revealed a reduced transmission of the *raptor3g* gene through male gametophytes (Table 4.1). To identify a potential cause of the loss of transmission through the pollen of *raptor3g^{+/-} raptor5g^{-/-}* mutants, I monitored the growth of pollen tubes. Pollen were taken from freshly dehisced anthers of wt and *raptor* mutant plants, which were grown under identical conditions, and transferred to emasculated inflorescences of wt plants. These were sampled after 3h and stained with aniline blue (Figure 4.6). The data showed that the growth of *raptor3g* pollen tube

was reduced by ~25% compared to wt. This limited growth of *raptor3g* pollen indicated a reduced competitiveness, and therefore promoted the transmission in favour of the *RAPTOR3G* allele.

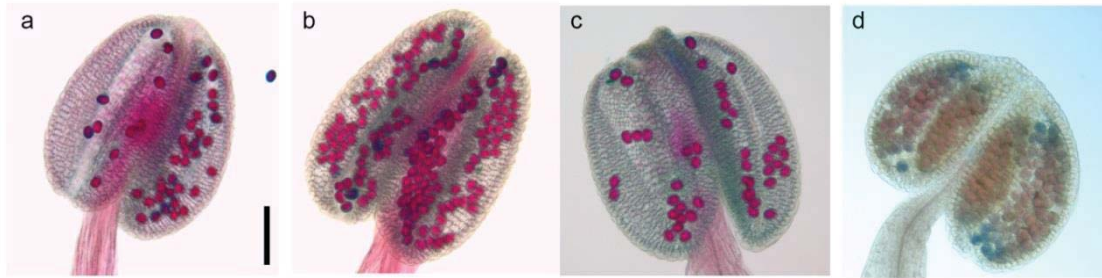


Figure 4.5 Pollen viability test using Alexander staining. Nomarsky images of (a) wt, (b) *raptor3g*, (c) *raptor5g*, (d) *raptor3g raptor5g* anthers. Scale bar = 100µm.

Table 4.1 Transmission ratio of *raptor* alleles through the male and female gametophyte. Plants were grown on soil under long day conditions. Flowers were emasculated prior the pollination with an excess of pollen. Three siliques were sampled per cross. Seeds were germinated on MS media and genotyped by PCR.

Female	male	n	did not germinate	expected	observed	SD	X ² (1:1 ratio)	Probability
Wt	<i>raptor3g</i> ^{+/-} <i>raptor5g</i> ^{-/-}	198	1	0.5	0.233	0.060	46.545	8.952E-12
Wt	<i>raptor3g</i> ^{-/-} <i>raptor5g</i> ^{+/-}	162	4	0.5	0.455	0.068	2.000	0.157
<i>raptor3g</i> ^{+/-} <i>raptor5g</i> ^{-/-}	wt	145		0.5	0.511	0.062	0.559	0.455
<i>raptor3g</i> ^{-/-} <i>raptor5g</i> ^{+/-}	wt	59	3	0.5	0.375	0.042	1.373	0.241

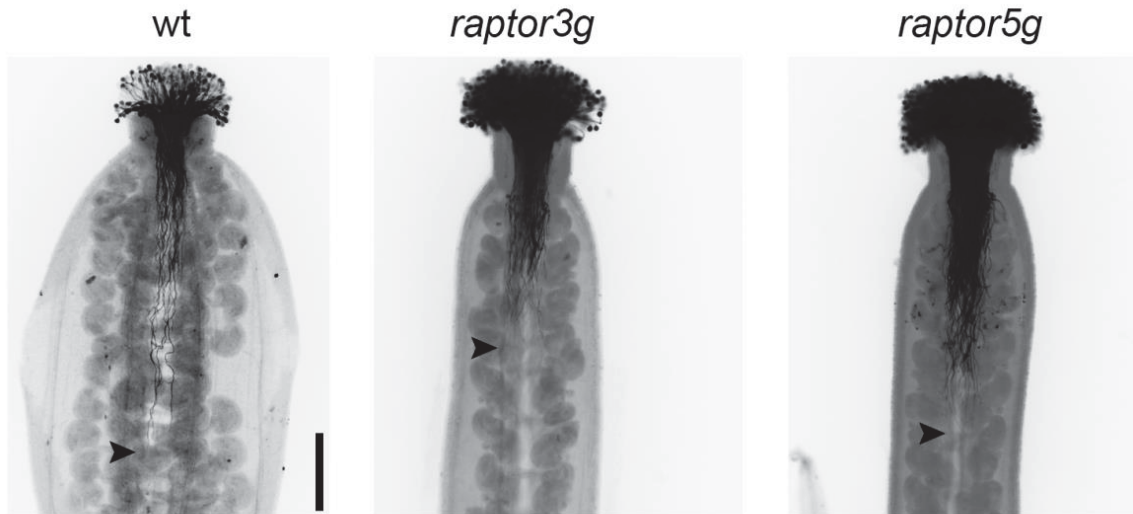


Figure 4.6 Measurement of pollen tube growth. Pistils of wt plants were emasculated 24h before pollination with an excess of pollen from wt, *raptor3g* or *raptor5g* plants. Figure shows aniline blue staining of pollen tubes 3h after pollination. Images were taken with a microscope using UV light. Displayed images are shown in false colours. Arrows indicate point of furthest polar extension. Scale bar = 200 μ m.

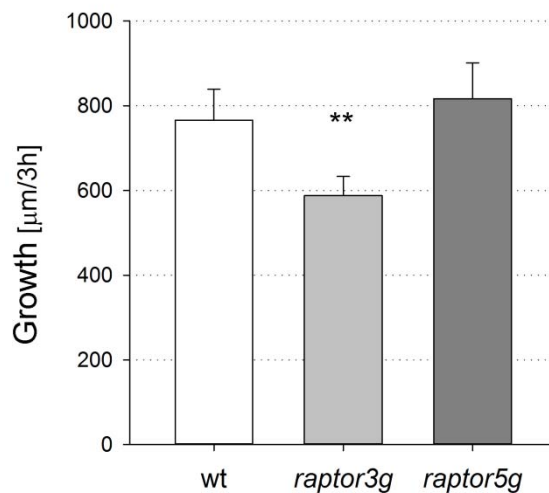


Figure 4.7 Quantitative measurement of pollen tube growth. Quantitative measurement of the extension of pollen tubes from wt, *raptor3g* and *raptor5g* as shown and described in Figure 4.6. Pollen of wt (n=5), *raptor3g* (n=19), and *raptor5g* (n=14) was applied to wt pistils and sampled after 3h. Pollen tubes were stained with aniline blue and images were taken with a microscope using UV light. Images were used to measure pollen tubes with imaging software. Student t-test of *raptor3g* was significant (indicated by asterisks; P value \leq 0.01). Student t-test of *raptor5g* was not significant (P value \geq 0.05).

This analysis showed that single *raptor* mutants were fertile, although the reduced transmission of pollen from *raptor3g^{+/-} raptor5g^{+/-}* mutants indicated a function of *RAPTOR* in pollen development. This was further supported by the finding that pollen from *raptor3g* mutants showed a reduced pollen tube length.

Discussion

While Anderson et al. (2005) described *raptor3g raptor5g* mutants to arrest at an early seedling stage, the data presented here showed that these mutants were capable to reach maturity and develop reproductive organs (Figure 4.2). Flower initiation, however, was drastically delayed, which led to a lengthening of the life cycle (Figure 4.1). A similar effect was described for *A. thaliana* treated with rapamycin (Ren et al., 2012). The author of this study argued that the prolonged life cycle seen in *A. thaliana* followed similar mechanisms that led to an expansion of life spans in nematodes and mice with inhibited TOR activity (Harrison et al., 2009; Ren et al., 2012; Robida-Stubbs et al., 2012). These studies identified reduced metabolic activity along with limited accumulation of ROS as potential causes of longevity. Transcriptomic data from *raptor3g raptor5g* mutants, which indicated changes in genes related to ROS production and scavenging, alongside with the detection of reduced ROS accumulation imply a similar state in *raptor* mutants (Figure 3.11; Figure 3.16). However, a general comparison of alterations in the lifespan between kingdoms is difficult due to the fundamental differences in the basics that relate to aging in animals and the onset of senescence in plants (Thomas, 2002). Nevertheless, some cellular processes that lead to the accumulation of ROS and activation of autophagy as a response to stress have been linked to lifespan extension and might be conserved among eukaryotes. Recent studies in *A. thaliana* provided first evidences of a relation between ATG gene activity and longevity, as well as a function of ROS as part of the ethylene response pathway, which induces floral transition in response to environmental cues (Chen et al., 2012b; Chen et al., 2012a; Minina et al., 2013). Hence, the described role of TOR

activity in regulating autophagy and ROS production alleges an at least indirect impact on initiation of senescence and subsequently on the lifespan of plants.

An additional cause for the delay of flower initiation in plants with inhibited TOR activity was identified by the characterization of *lst8.1* mutants, which revealed a strong repression of the transcription of *FLOWERING LOCUS T (FT)*, a well-described regulator of flowering time that impinges signals from photoperiod and temperature (Kardailsky et al., 1999; Moreau et al., 2012). As described later in 0, a similar repression of *FT* was also found in *raptor3g raptor5g* mutants (Table 6.2), which strengthens the conclusion that the limited TOR signalling affects flower development *via* down-regulation of *FT*.

After the initiation of bolting, *raptor3g raptor5g* mutants displayed an increased axillary branching of the shoot compared to wt plants. These characteristics were also found in *raptor3g* mutants to a lesser degree and were previously described by Anderson et al. (2005). The increase in axillary branching is likely linked to a reduced biosynthesis of auxin (reviewed by Ward and Leyser, 2004). A direct application of auxin to *raptor3g* seedlings did not result in a significant effect in earlier studies (Anderson et al., 2005). However, the differential regulation of several auxin-related genes as indicated by the transcriptomic analysis (Chapter 3.5) further support a disturbance of auxin signalling in *raptor3g raptor5g* mutants. Contributing to this, disturbances in the ROS homeostasis, which were described above, are likely connected to auxin signalling (Krishnamurthy and Rathinasabapathi, 2013). Although the details are yet poorly understood, few studies have provided evidence for an interaction of both signalling pathways. For instance, ROS was found to be involved in the redistribution of auxin within the root of *Zea mays* and disturbances of the redox homeostasis caused perturbations in auxin transport and metabolism in *A. thaliana* (Joo et al., 2001; Bashandy et al., 2010). *Vice versa*, exogenous application of auxin was found to increase H₂O₂ levels (Peer et al., 2013). These findings suggest that the limited accumulation of ROS as described in

Chapter 3.6 or a more direct alteration of auxin signalling could result in the loss of apical dominance in *raptor3g raptor5g* mutants.

The reduced size of petals and overall size in *raptor3g* and *raptor3g raptor5g* mutants corresponded to the growth phenotype of these mutants and might relate to mechanisms that led to limited meristematic activity as found in the root (Chapter 3.2). Optical sections of pistils and siliques from *raptor3g raptor5g* mutants revealed infertile female gametophytes that arrested uniformly at an early developmental stage (Figure 4.4). The arrest occurred prior to enlargement of the central vacuole, which indicated a failure during the two-nucleate stage. The cause of this arrest might be related to a failure in the control of cell division facilitated by the anaphase promoting complex/cyclosome (APC/C). Components of this complex were identified in a screen of mutants with defects in the embryo sac development and activators of the APC/C were demonstrated to be regulated *via* the RBR1-E2F complex (Pagnussat et al., 2005; Magyar et al., 2012). Further, mutants of *RBR1*, which is potentially regulated by TOR via S6K, have also been reported to develop an early female gametophytic arrest (Ebel et al., 2004; Henriques et al., 2010). The arrest in these mutants was caused by a dysfunctional regulation of the cell cycle that gives rise to excessive nuclear proliferation in the embryo sac. Although no evidence of super-numerous nuclei could be identified in the embryo sac of *raptor3g raptor5g* mutants, these findings might provide a potential example how the reduced TOR signalling of *raptor3g raptor5g* might relate to the observed defects in female gametophyte development.

The development of male organs was also impaired in *raptor3g raptor5g* mutants. Flowers of these mutants consisted of shortened petals and stamen, which failed to produce fertile pollen (Figure 4.3; Figure 4.5). A similar phenotype was also described for *A. thaliana* mutant overexpressing S6K, which was shown to be activated by TOR (Mahfouz et al., 2006; Tzeng et al., 2009). In this study, S6K was found to regulate the

translation of several flower development genes. Therefore, it is likely that defects seen in *raptor3g raptor5g* mutants are caused by a similar misregulation of S6K.

As shown in Chapter 3.4, *RAPTOR3G* was strongly expressed in pollen grains. Although *raptor3g* mutants produce viable flowers, the segregation ratios indicated a reduced transmission through male gametes, which was likely a result of restricted polar extension in pollen tubes (Table 4.1; Figure 4.7). These observations demonstrated that *RAPTOR* is essential for gametophyte development. Similar defects in pollen tube growth were also described for heterozygous mutants of *vps34* (Lee et al., 2008b). Pollen development was also affected in mutants of *AtPTEN1* and phospholipid kinases, which emphasised an essential role of phospholipid signalling in pollen development through yet unknown functions (Gupta, 2002; Lee et al., 2008b; Gao and Zhang, 2012). The resemblance to the phenotypes of these mutants suggests a related defect of phospholipid signalling in *raptor3g raptor5g* mutants. Although the connection between phospholipid signalling and TOR activity *via* the PI3K-PTEN-PDK cascade is well understood in animals, a direct link has yet to be confirmed in plants (Chapter 1.7 and 1.11). However, the here presented data further support a close relation of both signalling pathways also in plants.

The underlying mechanism leading to the growth limitation of pollen tubes might also relate to the short root hair phenotype of plants with inhibited TOR activity due to the high similarity in the regulation of polar tip growth of pollen tubes and root hairs (reviewed by Cárdenas, 2009). As discussed in Chapter 3, this could relate to a limited ROS production in *raptor3g raptor5g*, which is required together with Ca^{2+} to initiate cell wall loosening during polar extension of root hairs and pollen tubes (Foreman et al., 2003; Liskay et al., 2004; Kaya et al., 2014).

Taken together, the presented data further characterized the function of *RAPTOR* in flower initiation and gametophyte development in *A. thaliana*. It further presented the

discovery of a novel RAPTOR function in the transmission through the male gametophyte, which was linked to limited extension of pollen tubes.

Chapter 5

Analysis of mosaic *raptor* knock-outs

Introduction

The use of T-DNA knock-out lines is a widely used method for loss-of-function studies in *A. thaliana*. However, this technique bears some disadvantages for the analysis of essential genes, in which a disruption causes a lethal phenotype that prevents any analysis (Radhamony, 2005). The use of RNAi silencing represents an alternative approach, in which the gene function is reduced rather than completely eliminated and by that prevents an otherwise lethal phenotype. In a preliminary approach, this method was applied to create tissue-specific knock-downs of *TOR* (unpublished dataset, B. Veit). In this study, the most prominent reduction of growth was achieved when an amiRNA against TOR was driven by the promoter of *LIPID TRANSFER PROTEIN 1* (*LTP1*). Since *LTP1* is specifically expressed in the epidermis, this hinted to a tissue-specific function of TOR (Sharon et al., 1994). However, the use of RNAi holds some difficulties in respect to the evaluation of its efficiency in limiting the expression of the target gene. This is particularly true for tissue-specific knock-downs, as an evaluation requires a RNA extraction specifically from selected tissues. Further, this method encompasses some potential bias caused by unspecific off-target effects in which the small RNA utilized in this method is also hybridizing with genes other than the target gene (reviewed by Jackson et al., 2003; Sledz and Williams, 2005). In order to study the potential tissue-specific aspects of TOR function and circumvent the poor growth phenotype of *raptor3g raptor5g* mutants, I implemented a method to induce genetic mosaic *raptor* knock-out sectors in *A. thaliana*.

Genetic mosaics have been used for the analysis of development and cell biology for over hundred years and empowered research to study cell-autonomy and intracellular signal transduction (Morgan, 1914; Morgan, 1920; Sturtevant, 1920).

The discovery and further development of advanced methods like the Cre//lox system and similar techniques have added the ability to induce specific mutations, which provided a useful tool for the loss-of-function study of essential genes. The CRE recombinase was initially discovered in the bacteriophage P1 and was subsequently adapted for the use in other species (Sternberg and Hamilton, 1981; Hoess et al., 1982; McLeod et al., 1986). The method requires the target gene to be flanked by specific 34bp-long sequences, so called *lox* sites. When activated through the use of a tissue-specific or inducible promoter, CRE is able to recognize and bind to these *lox*-sites within the genome. There, CRE introduces double-strand breaks, which result in an excision of the gene-coding DNA sequence located between the *lox* sites. Lastly, the DNA repair machinery fixes the open-ended DNA strands resulting in a deletion of the gene from the genome. Since this deletion represents a stable mutation, it will be passed on to daughter cells in following cell divisions and thereby create a cell lineage of clonal null mutants. Since the initial studies in *D. melanogaster* in the 1980s, this method has been used successfully in many species including plants (Dale and Ow, 1990; Odell et al., 1990; Bayley et al., 1992). Excellent examples for the application of this method are the studies on *SCARECROW* and *RBR1* function in the root meristem of *A. thaliana* (Heidstra et al., 2004; Wachsman et al., 2011). I adapted the CRE//lox system, which was developed in these studies to knock-out *RAPTOR* function and overcome the limitations of previous knock-down and constitutive knock-out studies described above (Heidstra et al., 2004). The creation of sectorial knock-outs in various regions within the plant allowed me to address the potential tissue-specific function of RAPTOR-dependent TOR activity in *A. thaliana*. Further, this allowed insights to the requirement of *RAPTOR* function in different developmental stages of tissues and cell

lineages. Through the comparison of deletion sectors and neighbouring cells, the CRE/lox analysis also enabled an investigation of potential cell-autonomous and non-cell-autonomous functions of RAPTOR.

Results

5.1 Generation of *A. thaliana* lines with lox-flanked RAPTOR

For the creation of mosaic *raptor* knock-outs, I adapted a CRE/lox system that was previously developed by Heidstra et al. (2004). This system utilizes two separate binary vector constructs, which are individually transformed into *A. thaliana*. The first vector, pCBI (Appendix 2), is used for the introduction of a lox-flanked gene of interest (GOI^{lox}), which corresponds to $RAPTOR3G^{lox}$ in this study. It also contains the *GREEN FLUORESCENCE PROTEIN (GFP)* gene, which is controlled by a promoter system that is activated in response to the CRE-mediated excision event (Figure 5.1). This way, the onset of GFP fluorescence specifically marks deletion sectors within plant tissues. The GFP fluorescence is then used as a criterion to identify deletion sectors with a fluorescence microscope. Additionally, the pCBI vector contains the *BAR* gene, which provides resistance to the herbicide phosphinothricin to allow a positive selection of transformants *in planta* (Block et al., 1987). Here, I outline the adaptation of the pCBI vector construct and its integration into *raptor* T-DNA lines for the clonal analysis of *RAPTOR* gene function.

Since CRE targets lox sites and not the gene sequence directly, an additional lox-flanked *RAPTOR* transgene had to be introduced into the genome. In order to create a *raptor* null mutation through the CRE-mediated excision of this lox-flanked *RAPTOR*, the two endogenous *RAPTOR* genes in *A. thaliana* were required to be dysfunctional. For this purpose I have utilized T-DNA lines, which were combined to create the *raptor3g raptor5g* mutants as described in 0. In this, the T-DNA lines SALK_078159 and SALK_043920 were used to eliminate the gene function of *RAPTOR3G* and

RAPTOR5G gene function (Figure 3.1). As highlighted in 0, *RAPTOR* function in *A. thaliana* is predominately maintained by *RAPTOR3G*. Therefore, I selected this gene for the generation of a *lox*-flanked *RAPTOR* to complement for the loss-of-function in the *raptor3g raptor5g* mutants. For this purpose, the entire gene sequence of *RAPTOR3G*, which included a 1.5kb promoter and a 0.2kb terminator region, was cloned in between the *lox* sequences of the pCBI vector (pCBI-*RAPTOR3G*^{lox}; Appendix 5). This construct was then transformed into the *A. thaliana raptor3g raptor5g* mutants. In order to circumvent the slow growth and sterility of these mutants and to allow a transformation of these plants, the pCBI-*RAPTOR3G*^{lox} construct was transformed into the wt-like *raptor3g*^{+/-} *raptor5g* mutants, which were heterozygous for the *raptor3g* and homozygous for the *raptor5g* disruption. Subsequently, seeds were germinated on soil and screened for the resistance to phosphinothricin to identify transformed plants. Transformants were then crossed to *raptor3g*^{+/-} *raptor5g* mutants to recover the *raptor3g raptor5g RAPTOR3G*^{lox} genotype in the following generation.

Since *A. tumefaciens*-mediated transformation of *A. thaliana* often integrates multiple copies of the T-DNA into the genome, the crossing to *raptor3g*^{+/-} *raptor5g* mutants was also required to receive plants with a single integration of *RAPTOR*^{lox} (Tzfira et al., 2003; Windels et al., 2003). This is crucial for the later application of the CRE/*lox* system, as the marking of deletion events by GFP fluorescence does not allow a differentiation between one or more events within one sector.

To ensure the function of the integrated *RAPTOR3G*^{lox} in transformed lines, only *raptor3g raptor5g RAPTOR3G*^{lox} plants were selected for further progression, which showed a phenotype indistinguishable to those of wt plants. This indicated a full complementation of the disrupted endogenous genes. For simplicity, plants with the *raptor3g raptor5g RAPTOR3G*^{lox} genotype are from here on referred to as *RAPTOR3G*^{lox}. The created *RAPTOR3G*^{lox} lines were then further characterized by TAIL-PCR to localize the T-DNA insertion of *RAPTOR3G*^{lox} within the genome. This

subsequently allowed the identification of the allelic configuration of individual *RAPTOR3G^{lox}* plants. The generated *RAPTOR3G^{lox}* lines, of which the T-DNA insertions were localized and used in the analysis, are listed in Table 5.1. The primers used for the identification of these lines by genotyping PCR are given in Appendix 13. From the initial transformation with *pCBI-RAPTOR3G^{lox}*, ten positive transformants were selected. Of these, four independent lines showed a full complementation for the disruption of *RAPTOR* in *raptor3g raptor5g* mutants and were successfully characterized by TAIL-PCR (Table 5.1).

To conclude, I have successfully created several *RAPTOR3G^{lox}* lines, in which a *lox*-flanked *RAPTOR3G* transgene complemented for the disruption of both endogenous *RAPTOR* genes. These lines were subsequently crossed with lines carrying the *CRE* recombinase gene as described in the sections below.

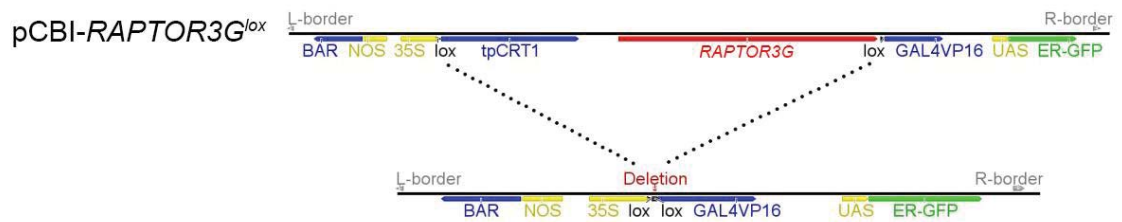


Figure 5.1 T-DNA sequence of *pCBI-RAPTOR3G^{lox}* vector. The figure represents a model of the T-DNA as introduced into the genome of *A. thaliana* by the transformation with the *pCBI-RAPTOR3G^{lox}* vector. The sequence includes the *RAPTOR3G* gene and promoter sequence flanked by *lox* sites, which separates 35S and GAL4VP16/UAS promoter sequences to block expression of the *GFP* gene. A *BAR* gene driven by a NOS promoter gene and a norflurazon resistance gene (tpCRT1) enables the selection *in planta*. The mutated sequence following a CRE-mediated excision is indicated below. The dotted lines indicate the introduced deletion, which results in the approximation of 35S and GAL4VP16/UAS promoter sequences and facilitate the transcription of *ER-GFP*.

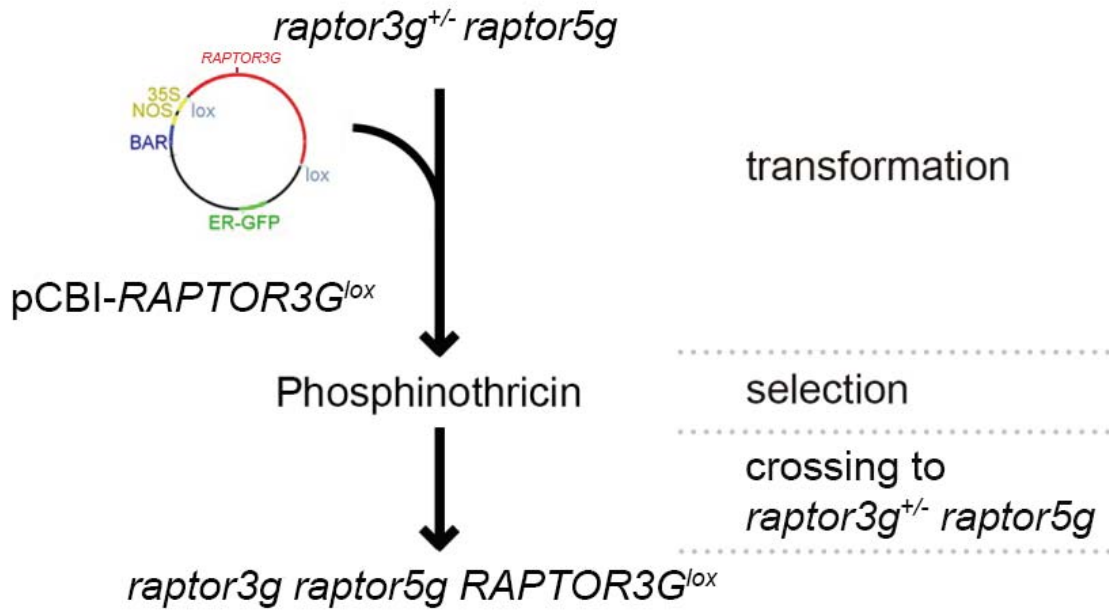


Figure 5.2 Scheme for the creation of *RAPTOR3G*^{lox} lines. *Raptor3g*^{+/-} *raptor5g* mutants were transformed with the pCBI-*RAPTOR3G*^{lox} construct. Transformants were selected with phosphinothricin and subsequently crossed with *raptor3g*^{+/-} *raptor5g* mutants. In the progeny, plants with the genotype *raptor3g raptor5g RAPTOR3G*^{lox} were identified by genotyping.

Table 5.1 List of *RAPTOR3G*^{lox} lines. Name, genotype and location of the *RAPTOR*^{lox} transgene integration within the genome of *A. thaliana*.

Name	Genotype	Genomic location of <i>RAPTOR3G</i> ^{lox}
<i>RAPTOR3G</i> ^{lox} 3	<i>raptor3g raptor5g RAPTOR3G</i> ^{lox}	Chromosome 2: ~19,487,533
<i>RAPTOR3G</i> ^{lox} 5	<i>raptor3g raptor5g RAPTOR3G</i> ^{lox}	Chromosome 1: ~28,219,435
<i>RAPTOR3G</i> ^{lox} 7	<i>raptor3g raptor5g RAPTOR3G</i> ^{lox}	Chromosome 4: ~18,100,285
<i>RAPTOR3G</i> ^{lox} 8	<i>raptor3g raptor5g RAPTOR3G</i> ^{lox}	Chromosome 3: ~6,671,432

5.2 Introduction of an inducible CRE recombinase to *A. thaliana*

The excision of the *RAPTOR*^{lox} gene in *A. thaliana* was facilitated by an inducible CRE recombinase. The *CRE* gene including an inducible promoter were transformed into the plant genome with the use of a binary vectors, which were designed and provided by

Heidstra et al. (2004). Two different variants of the *CRE* carrying vector were used in this study, pHS::*CRE* and pWOXp::*CRE:GR* (Appendix 3 and Appendix 4). The pHSp::*CRE* construct contains a T-DNA encoding a heat shock inducible promoter (HSp) coupled with the *CRE* gene (Figure 5.3). The pWOXp::*CRE:GR* included a T-DNA with the promoter of *WUSCHEL-RELATED HOMEODOMAIN 5* (*WOX5p*), which is expressed in the quiescent centre of the root meristem (Haecker et al., 2004). The *WOX5p* controls the expression of a chimeric *CRE* recombinase, which is fused to the ligand binding domain of the glucocorticoid receptor (GR)(Brocard et al., 1998). Since the *WOX5p* is a tissue-specific promoter that defines the spatiotemporal expression of *CRE*, the fusion of the GR domain *CRE* added the ability to fine-tune the timing of the *CRE* activation. Only when the GR domain is bound to its ligand dexamethasone (DEX) is the *CRE:GR* fusion protein able to enter the nucleus and target the *lox*-sites within the DNA. Therefore, this fusion allows to control the recombinase activity of *CRE:GR* through the addition of DEX to the media.

The pHSp::*CRE* and pWOX5p::*CRE:GR* vectors were also transformed into *raptor3g^{+/-} raptor5g^{-/-}* mutants of *A. thaliana* (Figure 5.4). The T-DNA of both vectors contained a hygromycin resistance gene, which allowed a positive selection *in planta* (Figure 5.3). For the selection of transformants, seeds of transformed plants were germinated on MS media containing hygromycin. Resistant seedlings were subsequently transferred to soil and crossed to *raptor3g^{+/-} raptor5g* mutants to generate plants with the genotype *raptor3g^{+/-} raptor5g WOX5p::CRE:GR* and *raptor3g^{+/-} raptor5g HSp::CRE* in the progeny (Figure 5.4). To avoid potential artefacts caused by the T-DNA integration, only plants that showed no visible phenotypical abnormalities compared to wt plants were progressed further. The integration of the T-DNA was localized in *raptor3g^{+/-} raptor5g WOX5p::CRE:GR* and *raptor3g^{+/-} raptor5g HSp::CRE* lines by TAIL PCR, to allow genotyping of the allele in individual plants. Through self-pollination of these plants, *raptor3g^{+/-} raptor5g* mutants with homozygous *CRE* alleles were generated and

identified by genotyping PCR. This maximised the transmission rate of *CRE* in further crosses as described in the next section.

For each construct, two independent lines of *raptor3g^{+/-} raptor5g HSp::CRE* and *raptor3g^{+/-} raptor5g WOXp::CRE:GR* were identified, which met the requirement of a wt-like phenotype (Table 5.2 and Appendix 13).



Figure 5.3 T-DNA sequences of pCRE vectors. The figure represents a model of the T-DNA as introduced into the genome of *A. thaliana* by the transformation with the pCRE vectors pHSp::CRE and pWOX5p::CRE:GR. Both T-DNAs contain a hygromycin resistance gene (HygromycinR) for the selection *in planta*. Border sequences (blue), promoter sequences (yellow), gene sequences (grey), and terminator sequences (orange) are indicated.

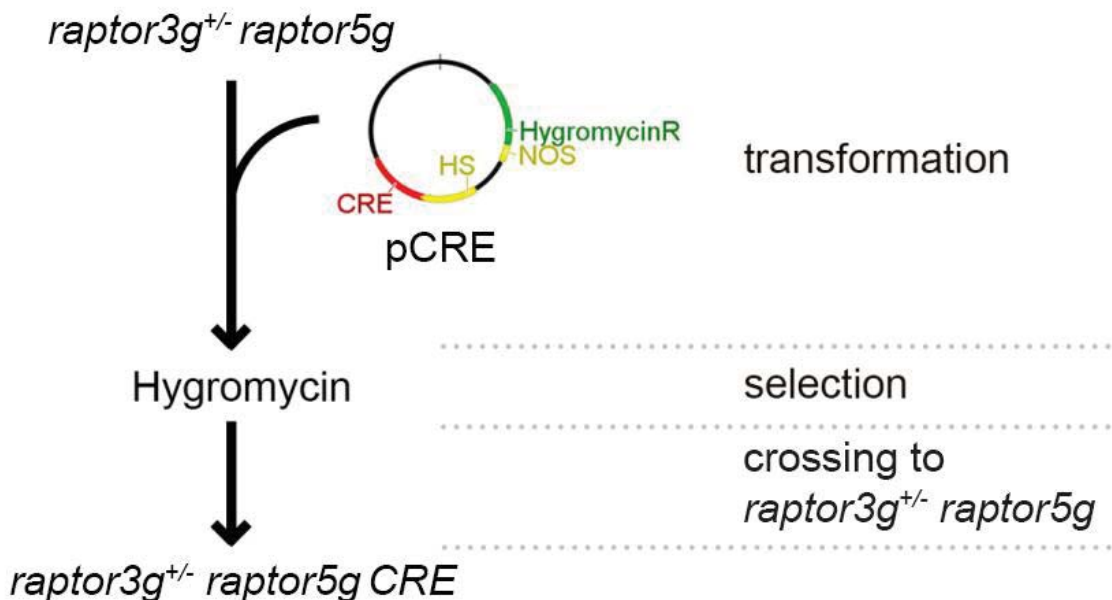


Figure 5.4 Scheme for the creation of *A. thaliana* CRE lines. *Raptor3g^{+/-} raptor5g* mutants were transformed with a CRE carrying vector construct (pCRE). Transformants were selected with hygromycin and subsequently crossed with *raptor3g^{+/-} raptor5g* mutants. In the progeny, plants with the genotype *raptor3g^{+/-} raptor5g CRE* were identified by genotyping.

Table 5.2 List of CRE lines. Name, genotype and location of the *RAPTOR^{lox}* transgene integration within the genome of *A. thaliana*.

Name	Genotype	Genomic location of <i>CRE^x</i>
HSp::CRE A	<i>raptor3g^{+/-} raptor5g HSp::CRE</i>	Chromosome 5: ~2,180,783
HSp::CRE C	<i>raptor3g^{+/-} raptor5g HSp::CRE</i>	Chromosome 2: ~18,626,712
WOXp::CRE:GR A	<i>raptor3g^{+/-} raptor5g WOXp::CRE:GR</i>	Not localized
WOXp::CRE:GR B	<i>raptor3g^{+/-} raptor5g WOXp::CRE:GR</i>	Chromosome 1: ~26,517,556

5.3 Generation of the *CRE/RAPTOR3G^{lox}* system in *A. thaliana*

In the final step to create the *CRE/lox* system in *A. thaliana*, the *CRE* recombinase and the *lox*-flanked *RAPTOR3G* construct were combined. This process was analogous for creation of lines with *HSp::CRE* and *WOXp::CRE:GR*. Therefore, I refer to both of them as *CRE* from here on if not specifically stated. A summary of the process is given in Figure 5.5. Therefore plants of *RAPTOR3G^{lox}* lines, which were heterozygous for the *RAPTOR3G^{lox}* insertion (*RAPTOR3G^{lox/Δ}*), and *raptor3g^{+/-} raptor5g CRE* plants, which were homozygous for *CRE* (*CRE^{CRE/CRE}*) were crossed. Therefore, all four *RAPTOR^{lox}* lines (Table 5.1) were individually crossed to one line of each *CRE* construct, HSp::CRE line A and WOX5p::CRE:GR line B.

Through genotyping PCR, individuals with the genotype of *raptor3g raptor5g CRE^{CRE/Δ} RAPTOR3G^{lox/Δ}* were identified in the progeny and subsequently allowed to self-pollinate to yield plants with homozygous *CRE* in the progeny. Plants with the genotype *raptor3g raptor5g RAPTOR3G^{lox/Δ} CRE^{CRE/CRE}* were again allowed to self-pollinate. This generated the final generation yielding the genotypes *raptor3g raptor5g HSp::CRE^{CRE/CRE} RAPTOR3G^{lox/Δ}* and *raptor3g raptor5g WOX5p::CRE:GR^{CRE/CRE} RAPTOR3G^{lox/Δ}*, which were used for the analysis.

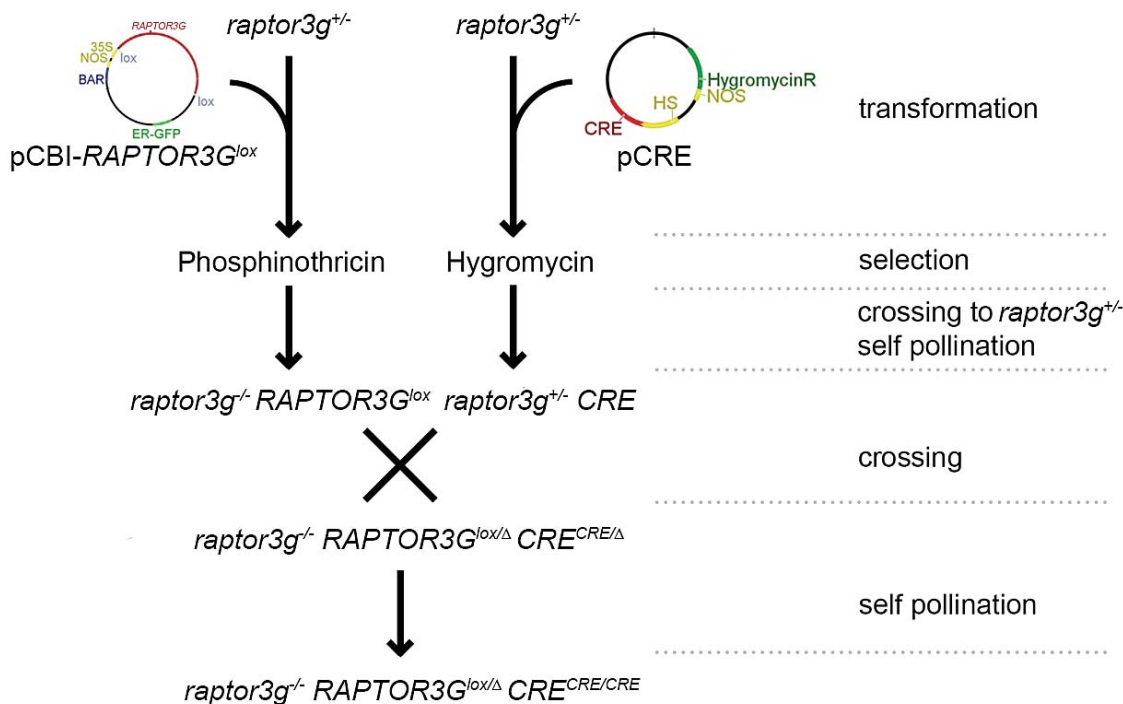


Figure 5.5 Overview of the generation of *RAPTOR3G^{lox} CRE* lines. All shown genotypes contain the *raptor5g* mutation, which is excluded from annotations in the figure. A. *thaliana raptor3g^{+/-} raptor5g* mutants were transformed with *pCBI-RAPTOR3G^{lox}* and *pCRE* constructs. Transformants were selected and crossed to *raptor3g^{+/-} raptor5g* mutants. Crosses between *RAPTOR3G^{lox}* and *CRE* lines yielded plants with the *raptor3g raptor5g RAPTOR3G^{lox/Δ} CRE^{CRE/Δ}* genotype. Self-pollination of these plants allowed the recovery of the *raptor3g raptor5g RAPTOR3G^{lox/Δ} CRE^{CRE/CRE}* genotype, of which seeds were used for the analysis.

5.4 Functional testing of the *CRE//lox* system through the induction of *HSp::CRE RAPTOR3G^{lox}* and control lines

The generated *raptor3g raptor5g HSp::CRE^{CRE/CRE} RAPTOR3G^{lox/Δ}* and *raptor3g raptor5g WOX5p::CRE:GR^{CRE/CRE}* were tested to ensure a correct function of the system. Experiments were designed to confirm the correct function of the transgenes, responsiveness of promoter, GFP fluorescence, and general confirmation of the CRE-mediated gene excision.

For these experiments, I focussed on *RAPTOR3G^{lox}* lines with the *HSp::CRE* construct, as it was expected to allow the induction of large sectors in root and shoot tissues. This

would enable a comparative analysis of the phenotypic change in whole seedlings between induced and uninduced samples. Plants of *raptor3g raptor5g HSp::CRE^{CRE/CRE} RAPTOR3G^{lox/Δ}* were grown alongside several control lines, which included a *raptor* mutant line with only the *CRE* transgene (*raptor3g raptor5g HSp::CRE*). Further, plants with the genotype *raptor3g^{+/-} raptor5g HSp::CRE^{CRE/CRE} RAPTOR3G^{lox/Δ}*, which contained a functional copy of the endogenous *RAPTOR* gene, and wt control were included. Seeds were germinated on MS medium and grown in short day conditions. One week after germination, seedlings were incubated at 37°C for 4h to induce the heat shock promoter. The heat shock treatment was repeated three times on a weekly basis before plants were analysed and genotyped.

The analysis of control lines and plants with *HSp::CRE* (line A) and *RAPTOR^{lox}* (line 5) is shown in Figure 5.6. Herein, the phenotypes of wt plants with or without treatment did not display any noticeable differences, which indicated that applied heat shock treatment did not interfere with growth or development of these plants (Figure 5.6). Further, the induced and uninduced *raptor3g raptor5g HSp::CRE* mutants developed identical phenotypes, which showed that the insertion of the *CRE* transgene and the expression of *CRE* did not interfere with the growth of these plants (Figure 5.6). In lines that contained *RAPTOR3G^{lox}* and *HSp::CRE*, the heat shock-treatment resulted in a GFP fluorescence that was detectable throughout the tissue, which indicated a successful induction of *CRE* expression and subsequent *RAPTOR3G^{lox}* excision (Figure 5.6). Noteworthy, a minor GFP activity was also visible in the uninduced lines containing *HSp::CRE* and *RAPTOR3G^{lox}*, which hinted to an activity of the HSp without prior heat treatment (Figure 5.6).

The comparison of induced and uninduced *raptor3g raptor5g HSp::CRE RAPTOR3G^{lox/Δ}* demonstrated the phenotypic changes through the excision of *RAPTOR^{lox}*. Further, I included a line in the comparison that contained a functional endogenous copy of *RAPTOR* (*raptor3g^{+/-} raptor5g HSp::CRE RAPTOR3G^{lox/Δ}*). This

allowed the differentiation of potential phenotypic changes that resulted from the induction of the CRE/lox system but were not linked to the loss of *RAPTOR* function, i.e. artefacts caused by non-specific CRE activity. The uninduced *raptor3g raptor5g HSp::CRE RAPTOR3G^{lox/Δ}* plants showed a similar growth compared to wt plants (Figure 5.6). This indicated that the introduced *RAPTOR3G^{lox}* complemented fully for the loss of *RAPTOR* function. In contrast, the induced plants of this line displayed a visually noticeable reduction of growth (Figure 5.6). This effect was abolished in the line that retained a functional endogenous *RAPTOR* copy. This showed that the reduction of growth was directly linked to the loss of *RAPTOR* function and not caused by potential artefacts related to the system itself.

However, the growth of induced *raptor3g raptor5g HSp::CRE RAPTOR^{lox/Δ}* was not as limited as that of the constitutive knockout *raptor3g raptor5g* plants (Figure 5.6). Although the GFP fluorescence indicated an efficient induction of CRE in this line, the excision of *RAPTOR^{lox}* resulted in minimal reduction of growth compared to wt and controls. The difference in development was more pronounced, as induced *raptor3g raptor5g HSp::CRE RAPTOR^{lox/Δ}* formed seven rosette leaves, while wt and control plants developed ten to eleven leafs (Appendix 17).

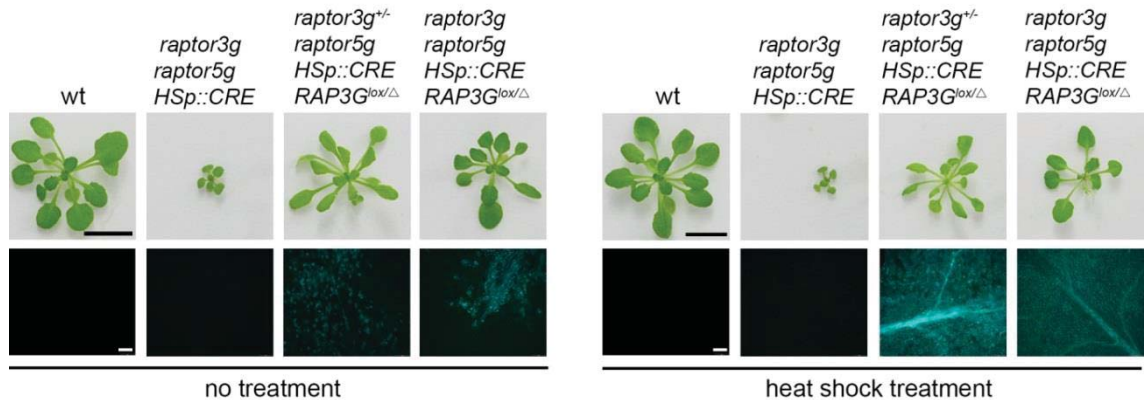


Figure 5.6 Induction of HSP::CRE RAPTOR3G^{lox} and control lines. Plants of wt, *raptor3g raptor5g HSp::CRE* and *HSp::CRE RAPTOR3G^{lox}* (*RAP3G*) line 5 were grown under short day conditions for four weeks on MS media. Treated plants were induced weakly with heat shock for 4h starting at age of one week. Representative plants are shown in upper row. Fluorescence microscope images taken under UV light of a leaf of the first leaf pair from the corresponding plant are given underneath. Scale bars = 1cm (upper row); 200μm (lower row).

The experiments showed that the introduced *RAPTOR3G^{lox}* transgene was fully functional and complemented the disrupted endogenous copies of *RAPTOR* in *raptor3g raptor5g RAPTOR3G^{lox} HSp::CRE* plants. Further, the inducible promoter was activated successfully by a heat shock treatment, which was indicated by the detected GFP fluorescence following the excision of *RAPTOR^{lox}*. Further, the heat shock treatment itself did not interfere with the general growth and development of *A. thaliana*. Most importantly, the induction of the CRE//lox system led to phenotypic changes in *raptor3g raptor5g HSp::CRE RAPTOR3G^{lox/Δ}* plants, which were specific to the loss of *RAPTOR3G^{lox}*. Generally, the presented data demonstrated that the CRE//lox system operated as predicted.

5.5 *RAPTOR* is not required to maintain growth and development in small *RAPTOR^{lox}* deletion sectors within the root meristem

As described in the introduction, previous findings indicated a tissue-specific function of TOR. To address this, I generated and analysed *RAPTOR^{lox}* deletion sectors in the root of *A. thaliana*. With its well-defined stereotypical organization, the RAM offered ideal

conditions to identify any potential phenotypic changes of induced *raptor* deletion sectors compared to unaffected neighbouring tissues.

For the experiments, seeds of *raptor3g raptor5g WOX5p::CRE:GR^{CRE/CRE} RAPTOR3G^{lox/Δ}* and *raptor3g raptor5g HSp::CRE RAPTOR3G^{lox/Δ}* were grown vertically on MS plates and induced 3 days after germination. For the induction of the lines with *HSp::CRE*, seedlings were incubated for 37°C for five to 30 min. Lines containing the *WOX5::CRE:GR* construct were induced by transferring seedling to MS media containing 20μM DEX for six to 24h. Afterwards, seedlings were returned to MS plates and placed vertically as described before. For the analysis, cell walls within the root were stained with propidium iodide and subsequently analysed with a confocal microscope.

In these root meristems, deletion sectors were generated within cells of the quiescent centre and the initials. The continuous divisions of induced cells in these meristematic regions resulted in *raptor* cell lineages in the columella (Figure 5.7b), epidermis (Figure 5.7c), cortex (Figure 5.7d), and vasculature (Figure 5.7e). Induced sectors were easily differentiated from the uninduced neighbouring tissues by the GFP fluorescence, which resulted from the CRE-mediated *RAPTOR^{lox}* excision. However, no distinguishable phenotypic change of these sectors in cell size or shape could be identified when compared to the surrounding unaffected tissues (Figure 5.7). The stereotypical patterning of the root meristem was not disturbed through the deletion of *RAPTOR^{lox}*, which indicated a normal rate of cell divisions (Figure 5.7a-e). Also, as represented in Figure 5.7f, sectors within the transition zone between the core meristem and the elongation zone did not show any indication of an altered cell elongation. This indicated that *RAPTOR* was not required for the development of cells within the RAM.

To conclude, the *Cre/lox* was used to induce traceable *raptor* cell lineages within various tissues of the root meristem. The observation of these deletion sectors did not indicate any tissue-specific function of *RAPTOR* within the RAM of *A. thaliana*. Also,

RAPTOR deletion within individual cell lineages with the root indicated that *RAPTOR* is not required to maintain cellular growth and development in the RAM.

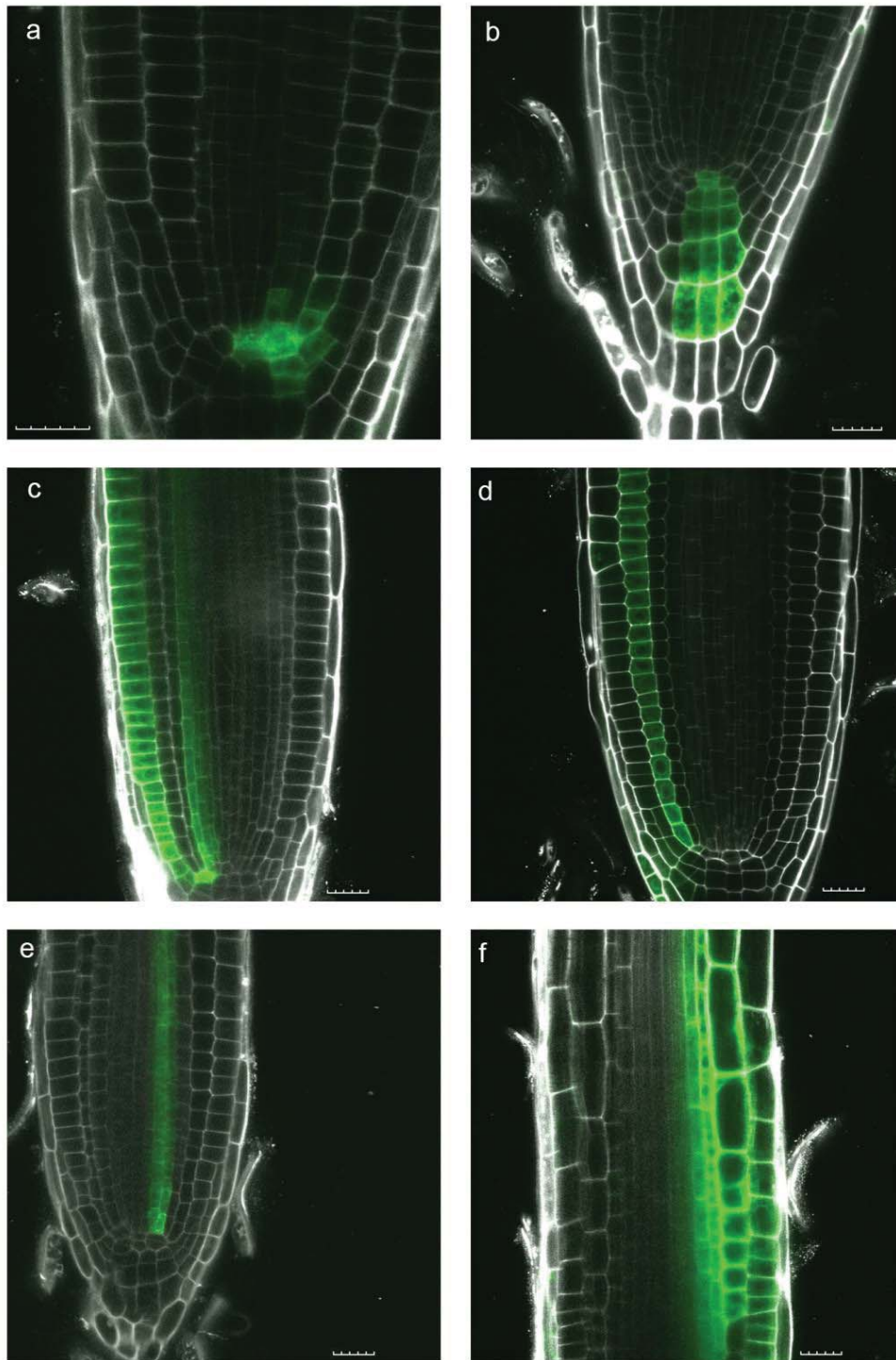


Figure 5.7 Induction of *raptor* deletion sectors in various tissue of the RAM. Roots of *raptor3g raptor5g* $RAPTOR3G^{lox/\Delta}$ $WOX::CRE:GR$ B (a-c) and *raptor3g raptor5g* $RAPTOR3G^{lox/\Delta}$ $HS::CRE$ A (d-f) were analysed. Plants were germinated on MS media and grown vertically. Seedlings were induced three DAG. Images represent optical sections stained with propidium iodide (white). Induced *raptor* deletion sectors are indicated by GFP expression (green). (a) Quiescent centre and initials five DAI in $RAPTOR^{lox}$ line 8; (b) columella five DAI in $RAPTOR^{lox}$ line 8, (c) epidermis and pericycle five DAI in $RAPTOR^{lox}$ line 8, (d) cortex seven DAI in $RAPTOR^{lox}$ line 5, (e) vasculature 14 DAI $RAPTOR^{lox}$ line 3, and (f) epidermis with pericycle 14 DAI in $RAPTOR^{lox}$ line 8. Scales = 20 μ m.

5.6 *Raptor* deletion sectors in the root show reduced meristem size

Previous studies presented evidence that TOR signalling is linked to the regulation of meristematic activity in the RAM (Xiong et al., 2013). Similar observations were made in *raptor3g raptor5g* mutants, which were presented in 0 (Figure 3.17). To verify this function, I used CRE/lox system to induced large *raptor* deletion sectors in the RAM. Further, by comparing the induced deletions in RAPTOR^{lox} lines to the constitutive *raptor* knock-out in *raptor3g raptor5g* T-DNA lines, I was able to highlight phenotypes that were linked to loss of *RAPTOR*.

Therefore, seeds of RAPTOR3G^{lox} with *HSp::CRE* and *WOX5p::CRE:GR* were germinated and grown vertically on MS media. Three days after germination (DAG), large sectors in seedlings were induced through the incubation at 37°C for 4h for RAPTOR3g^{lox} lines with the *HSp::CRE* construct. Lines containing *WOX5p::CRE:GR* were induced by transferring seedlings onto MS media with 20µM DEX for 24h. Roots of seedlings were then analysed after two weeks following the induction. Therefore, roots were stained with propidium iodide and analysed with a confocal microscope.

The induction of large *raptor* deletion sectors, which covered the entire root, resulted in a reduction of the RAM length compared to uninduced roots (Figure 5.8). This was observed in different RAPTOR^{lox} lines and with both CRE promoter constructs and replicated observations in *raptor3g raptor5g* mutants (Figure 5.8; Figure 3.17). The reduced RAM length in RAPTOR^{lox} lines asserted a role of *RAPTOR* in the regulation of meristematic activity.

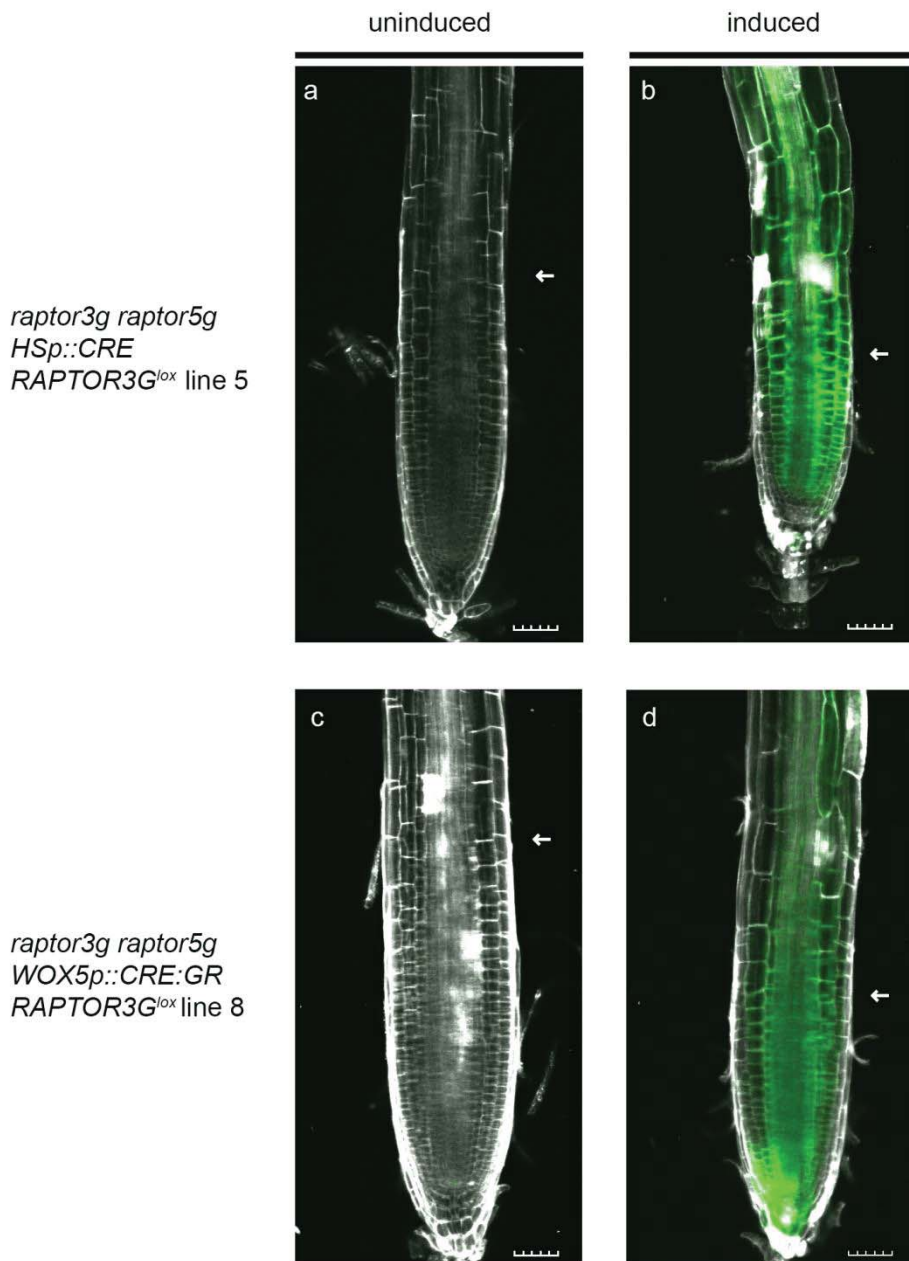


Figure 5.8 Induction of large *raptor* deletion sectors in the root Plants of *RAPTOR3G^{lox}* *HSp::CRE* (a-b, line 5) and *RAPTOR3G^{lox}* *WOX5p::CRE* (c-d, line 8) were grown vertically on MS media under short day conditions. Seedlings were induced three DAG with heat shock for 4h or 20 μ M DEX for 24h. At 14 DAI, roots were stained with propidium iodide (white) and analysed with confocal microscope. Images represent optical sections of the root and induced *raptor* deletion sectors are indicated by GFP fluorescence (green). Images show representative roots of (a, c) uninduced and (b, d) induced plants at same age. Boundaries between core meristem and elongation zone are indicated by arrows. Scale bars = 50 μ m.

Discussion

The presented data showed that I successfully adapted the CRE//lox system developed by Heidstra et al. (2004) for the analysis of sectorial *raptor* knock-outs. Several lines that were independently transformed with the $RAPTOR^{lox}$ construct were created to validate observations and to identify potential line-dependent artefacts caused by the transgenes. Also, generated lines were outcrossed multiple times to limit the possibility of multiple integrations of the $RAPTOR^{lox}$ transgene. Experiments were designed to test the correct operation of the CRE//lox system in generated lines. These demonstrated a successful activation of the system, which was indirectly verified through the detection of GFP fluorescence (Figure 5.6; Appendix 17; Appendix 18). Further, experiments confirmed that phenotypic changes, which resulted from the induction of the CRE//lox system, were specifically linked to the loss of RAPTOR function in these sectors (Figure 5.6).

The induction of large *raptor* deletion sectors, which were generated by long and repeated heat shock treatments, resulted in the characteristic growth reduction, which was described in *raptor3g raptor5g* mutants (Chapter 3.2). This effect was confirmed in several $RAPTOR3G^{lox}$ lines (Figure 5.6; Appendix 17). Yet, the growth reduction of induced $RAPTOR3G^{lox}$ line 3 plants was accompanied by a decolouration of rosette leaves (Appendix 17). Since this was also observed in a control line, which carried only the empty pCBI vector and *HSp::CRE*, this phenotype is unlikely linked to any *RAPTOR*-related function (Appendix 17). However, it is possible that this artefact is caused by the CRE//lox system or by the integration of the $RAPTOR3G^{lox}$ T-DNA into the genome. Kang et al. (1999) pointed out that high activation of the UAS-VP16 promoter system, which was utilized in the pCBI vector to activate *GFP* expression, could cause toxicity in plants. This was based on previous reports on studies in yeast, which showed an interference of Gal4-VP16 with general transcription factors (Berger et al., 1992; Kang et al., 1999). However, as the decolouration was only observed in

RAPTOR3G^{lox} sectors after a repeated induction for several hours, this side effect of GAL4-VP16 could be limited to very large sectors in leaf tissues. Also, since decolouration was not detected throughout all generated *RAPTOR3G^{lox}* lines, this phenotype could represent a line-specific artefact, which did not interfere with the analysis in other lines and tissues.

In the root, large deletion sectors caused a decreased length of the root meristem (Figure 5.8). However, this effect could not be seen in smaller sectors limited to few cells or individual tissues (Figure 5.7). A compensatory effect by the surrounding unaffected cells, which retained *RAPTOR* function, could provide a potential explanation for this observation. This would imply a non-cell-autonomous regulation of RAPTOR-dependent TOR activity. Similar observations were made in studies using inducible knockouts of *raptor* in *D. melanogaster*, which found indications for a non-cell-autonomous function in regulating cell size (Polak et al., 2008). However, other studies in *D. melanogaster* and human cell lines identified strictly cell-autonomous functions of TOR (Bohni et al., 1999; Oldham et al., 2000; Zhang et al., 2000; Laplante et al., 2012; Gancz and Gilboa, 2013). These studies were based on the inhibition of TOR activity through induced knock-outs or limiting insulin signalling in individual cells. As TOR retains a partial activity in *raptor3g raptor5g* T-DNA lines, which were used for the disruption of the endogenous copies of *RAPTOR* in *RAPTOR3G^{lox}* lines (Chapter 5.1), a potential cell-autonomous function might be obscured in *raptor* mosaic sectors. This infers further that RAPTOR is not required to maintain a potential cell-autonomous function of TOR in *A. thaliana*.

The primary aim of the CRE//lox study was to investigate any potential tissue-specific functions of *RAPTOR*. According to the tensile string theory, the epidermis is thought to direct growth of underlying tissues (reviewed by Javelle et al., 2011). Studies on epidermis-specific brassinosteroid signalling supported this theory in recent years through the discovery of brassinosteroid-dependent regulation of meristem size and

shoot growth (Savaldi-Goldstein et al., 2007; Hacham et al., 2011). This was linked to TOR function through results of preliminary studies using tissue-specific RNAi targeted against TOR. These resulted in an exaggerated growth arrest when expressed in the epidermis compared to expression in other tissues (unpublished dataset, B. Veit). However, the presented data did not support any differences between root tissues types and developmental stages in response to induced deletion of *RAPTOR3G^{lox}* (Figure 5.7). Again, the remaining TOR activity in *raptor* mutants could prevent the exposure of a potential function. In this case, this would imply that a potential epidermis-specific function of TOR as indicated by the results of the RNAi knock-down lines is RAPTOR-independent.

The residual TOR activity in *raptor* mutants of *A. thaliana* limit the potential and credibility of the data acquired by the CRE//lox knockout system presented here. Nevertheless, they provide the first evidence of non-cell-autonomous function of *RAPTOR* in plants.

Chapter 6

Comparison of *raptor* and *Ist8* knock-out mutants in *A. thaliana* and its implications on the presence of a TORC2 in plants

Introduction

The characterization of the two TOR genes in yeast has led to the discovery of two distinct TOR complexes (Loewith et al., 2002). Later, these were found functionally conserved in animal systems, which generally retain only a single TOR gene (Chapter 1.4). Thus, TOR complexes were entirely defined by the associated interaction partners in animals (Sarbasov et al., 2004; Lee and Chung, 2007; Jones et al., 2009). Intensive research in the medical field has led to the discovery of further distinct components of the two TOR complexes in mammals, like DEPTOR and PRAS 40 (Sancak, 2007; Peterson et al., 2009). Even so, the molecular details of the regulation and function of the TORC2 in particular are yet poorly understood (reviewed by Huang and Fingar, 2014).

Relative to yeast and animal systems, the knowledge of TOR complexes and their function in plants is even more limited. Besides RAPTOR, the only associated factor identified in plants at this time is LST8 (Deprost et al., 2005; Moreau et al., 2012). Like *RAPTOR*, *A. thaliana* contains two genes of *LST8*, *LST8.1* (*AT3G18140*) and *LST8.2* (*AT2G22040*) but only one of them, *LST8.1*, was found to be expressed (Moreau et al., 2012). Moreau et al. (2012) reported that *Ist8.1* knock-outs in *A. thaliana* were viable. Although these were severely limited in growth, plants survived the embryonic phase and were capable of producing fertile seeds (Moreau et al., 2012). This finding represents the first indication of a divergent function of TOR within plants compared to other systems. In budding yeast and mammals, disruption of *LST8* was reported to cause an early embryonic arrest, which occurred at the same developmental stage as

riCTOR mutants (Roberg et al., 1997; Kim et al., 2003; Guertin et al., 2006). This indicated an essential function of LST8 in maintaining TORC2 activity, yet LST8 was also found incorporated within the TORC1 (Yip et al., 2010; Yang et al., 2013). Therefore it is thought that LST8 is bound to TOR within both TOR complexes, although details of its contribution to the activity of these are yet poorly understood (Chapter 1.4.3). In plants, LST8 represents the only interaction partner of TOR within the TORC2, since there are no indications that RICTOR, which is a distinct component of the TORC2 in other systems, is represented here (van Dam et al., 2011). With the absence of *RICTOR* and given the differences of *lst8* knockout phenotypes to observations in fungi and animals, it is questionable whether a TORC2 is generally represented in plants. Also, the most prominent specific target of TORC2, PKB/Akt, has no obvious homologue in plants (Treins et al., 2010). Hence there are no indications of a functional TORC2 in plants to this day.

To explore the establishment of different TOR complexes in plants, I compared the phenotypes of *RAPTOR* and *LST8* mutants in *A. thaliana*. In this comparison, the disruption of TORC1 was represented by the *RAPTOR* mutant, while both TOR complexes were assumed to be dysfunctional in the *LST8* mutant. Thus, the search for distinct functions in these mutants provided a first investigation into the presence of independent TOR complexes in plants.

Results

6.1 Generation of *A. thaliana* lines with *lox*-flanked *LST8*

To identify a potential tissue-specific function of LST8, sectorial deletion sectors were generated in the root of *A. thaliana*. Therefore, the *CRE/lox* system developed by Heidstra et al. (2004) was adapted in a similar manner as described for *RAPTOR* (Chapter 5.1). Since the second *LST8* gene in *A. thaliana*, *LST8.2*, is likely to represent a pseudogene (Moreau et al., 2012), I focused entirely on *LST8.1* for this

study. Therefore, the T-DNA line SALK_002459 (received from ABRC) was used to disrupt the endogenous *LST8.1* gene. The complete *LST8.1* gene sequence, which included a 1.2kb promoter and 100bp terminator region, was cloned in between *lox* sequences of the pCBI vector (Appendix 11; Appendix 6). The construct was subsequently transformed into heterozygous plants of the SALK_002459 T-DNA line (*lst8.1^{+/-}*) to circumvent the slow growth of the homozygous plants. Subsequently, seeds were germinated on soil and screened for the resistance to phosphinothricin to identify transformed plants with the *LST8.1^{lox}* transgene. Transformants were then crossed to *lst8.1^{+/-}* mutants to recover the *lst8.1 LST8.1^{lox}* genotype in the following generation. Several independently transformed plants were selected based on the ability to complement for the disruption of the endogenous *LST8.1* gene (Table 6.1), which ensured that the *LST8.1^{lox}* transgene was fully functional. These lines were then further characterized by TAIL-PCR to localize the T-DNA insertion of *LST8.1^{lox}* within the genome. This allowed the identification of the allelic configuration of the *LST8.1^{lox}* transgene. Subsequently, plants with the genotype *lst8.1 LST8.1^{lox/Δ}* were identified, which are from here on referred to as *LST8.1^{lox}*. From the initial transformation with pCBI-*LST8.1^{lox}*, nine positive transformants were selected. Of these, four independent lines showed a full complementation for the disruption of *LST8.1* in *lst8.1* mutants and were successfully characterized by TAIL-PCR (Table 6.1). The selected *LST8.1^{lox}* lines, of which the T-DNA insertions were localized and that were used for the analysis, are listed in Table 6.1. The primers used for the identification of these lines by genotyping PCR are given in Appendix 13. These lines were subsequently crossed with lines carrying the *CRE* recombinase gene as described in the sections below.

Table 6.1 List of LST8.1^{lox} lines. Name, genotype and location of the *LST8.1^{lox}* transgene integration within the genome of *A. thaliana*

Name	Genotype	Genomic location of <i>RAPTOR3G^{lox}</i>
LST8.1 ^{lox} 3	<i>Ist8.1 LST8.1^{lox}</i>	Chromosome 1: ~ 2,067,175
LST8.1 ^{lox} 5	<i>Ist8.1 LST8.1^{lox}</i>	Chromosome 1: ~ 17,908,396
LST8.1 ^{lox} 6	<i>Ist8.1 LST8.1^{lox}</i>	Chromosome 2: ~ 7,081,730
LST8.1 ^{lox} 7	<i>Ist8.1 LST8.1^{lox}</i>	Chromosome 1: ~ 6,376,318

6.2 Generation of the CRE/LST8.1^{lox} system in *A. thaliana*

A. thaliana lines carrying the *CRE* recombinase were crossed to *Ist8.1^{+/-}* mutants repeatedly to create plants with the genotype *Ist8.1^{+/-} HSp::CRE* and *Ist8.1^{+/-} WOX5p::CRE:GR*. Therefore, I used the *HSp::CRE* line C and *WOX5p::CRE:GR* line B (Table 5.2). Plants, which were homozygous for the *CRE* transgene (*CRE^{CRE/CRE}*), were selected by genotyping PCR using the primers listed in Appendix 13. Subsequently, *Ist8.1^{+/-} HSp::CRE^{CRE/CRE}* and *Ist8.1^{+/-} WOX5p::CRE:GR^{CRE/CRE}* were crossed to each of the LST8.1^{lox} lines (Table 6.1). The process was analogous to that described for *RAPTOR^{lox}* in Chapter 5.3. After the first cross between LST8.1^{lox} and *CRE*-carrying lines, individual plants with the genotype of *Ist8.1^{+/-} HSp::CRE^{CRE/Δ} LST8.1^{lox/Δ}* and *Ist8.1^{+/-} WOX5p::CRE:GR^{CRE/Δ} LST8.1^{lox/Δ}* were identified through genotyping PCR in the progeny. Subsequently, these were allowed to self-pollinate to produce plants with homozygous *CRE* in the progeny. The seeds of these plants then yielded individuals with the target genotype *Ist8.1^{-/-} HSp::CRE^{CRE/CRE} LST8.1^{lox/Δ}* and *Ist8.1^{-/-} WOX5p::CRE:GR^{CRE/CRE} LST8.1^{lox/Δ}*, which were used for the analysis.

6.3 Functional testing of the CRE//ox system in HSp::CRE LST8.1^{lox} and control lines

The general function of the CRE//ox system was tested through the comparison of induced and uninduced *Ist8.1*^{+/-} HSp::CRE^{CRE/CRE} LST8.1^{lox/Δ} plants and control lines. The controls included a *Ist8.1* mutant line with only the CRE transgene (*Ist8.1* HSp::CRE) and a wt control. Identical to the test of RAPTOR^{lox} lines, seeds were germinated on MS medium and grown under short day conditions. One week after germination, seedlings were incubated at 37°C for 4h to induce the heat shock promoter. The heat shock treatment was repeated three times on a weekly basis before plants were analysed and genotyped.

The examination after three weeks confirmed a strong reduction of growth compared to uninduced plants (Figure 6.1). These observations were confirmed in several lines (Appendix 19; Appendix 20). Although GFP fluorescence was also detected in uninduced plants, this did not result in any change of the phenotype when compared to wt plants (Figure 6.1 ;Appendix 20). Similar to the observations in *Ist8.1* T-DNA lines reported by Moreau et al. (2012), the deletion of *Ist8.1* in large sectors led to a severe growth reduction. This indicated that the CRE//ox system operated as intended.

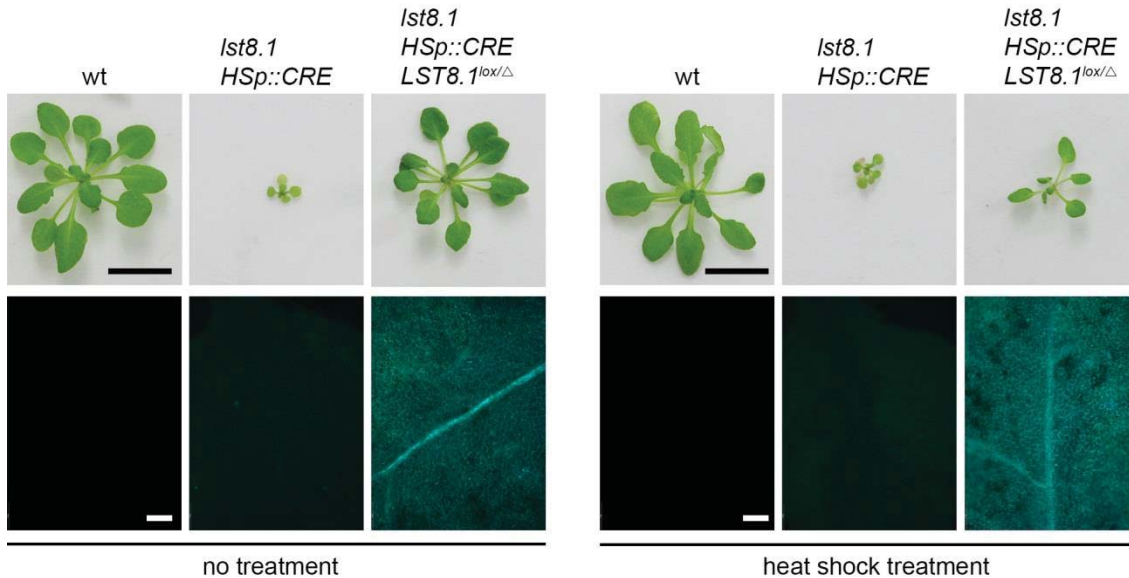


Figure 6.1 Control series of HSp::CRE LST8.1^{lox} and control lines. Plants of wt, *Ist8.1 HSp::CRE* and *HSp::CRE LST8.1^{lox/Δ}* line 6 were grown under short day conditions for four weeks on MS media. Treated plants were induced weakly with heat shock for 4h starting at age of one week. Representative plants are shown in upper row. Fluorescence microscope images taken under UV light of a leaf of the first leaf pair from the corresponding plant are given underneath. Scale bars = 1cm (upper row); 200 μ m (lower row).

6.4 Deletion of LST8 mimics the phenotype of *raptor* null sectors

To investigate the function of LST8.1 in the root meristem and to compare it to the observations made in *raptor* deletion sectors (Chapter 5.6), large *Ist8.1* deletion sectors were induced using the adapted CRE//lox system. For this, lines containing the *WOX5::CRE:GR* construct were used. Seeds of LST8.1^{lox} *WOX5::CRE:GR* were germinated and induced three DAG by transferring seedling to MS media containing 20 μ M DEX for 24h. Afterwards, seedlings were returned to MS plates and placed vertically. For the analysis, cell walls within the root were stained with propidium iodide and subsequently analysed with a confocal microscope. The *Ist8.1* deletion sectors resulted in the shortening of the core meristem (Figure 6.2).

To address the potential tissue-specific function, which was hinted by the preliminary results using amiRNA against TOR, *Ist8.1* deletion sectors covering a small number of cells were induced within the RAM. For the induction of the lines with *HSp::CRE*,

seedlings were incubated for 37°C for five to 30 min. Lines containing the *WOX5::CRE:GR* construct were induced by transferring seedling to MS media containing 20µM DEX for six to 24h. Afterwards, seedlings were returned to MS plates and placed vertically as described above. For the analysis, cell walls within the root were stained with propidium iodide and subsequently analysed with a confocal microscope. The results showed that the excision of *LST8.1* in cells within the epidermis showed no distinguishable difference in cell shape or size to neighbouring uninduced cells (Figure 6.3a). Also, the deletion of *LST8.1* did not affect the development of cells within the meristem. Neither the deletion of *LST8.1* in cells situated within the core meristem nor within the elongation zone did result in visible alterations of the phenotype compared to unaffected cells (Figure 6.3b and Figure 6.3c).

The presented data showed that the *CRE/lox* system was successfully adapted for the creation of *lst8.1* sectorial deletions. The induction of large *lst8.1* deletion sectors covering the entire root resulted in a reduction of the RAM size. However, the excision of *lst8.1* in sectors limited to a small number of cells resulted in no distinguishable phenotypic changes compared to unaffected neighbouring cells.

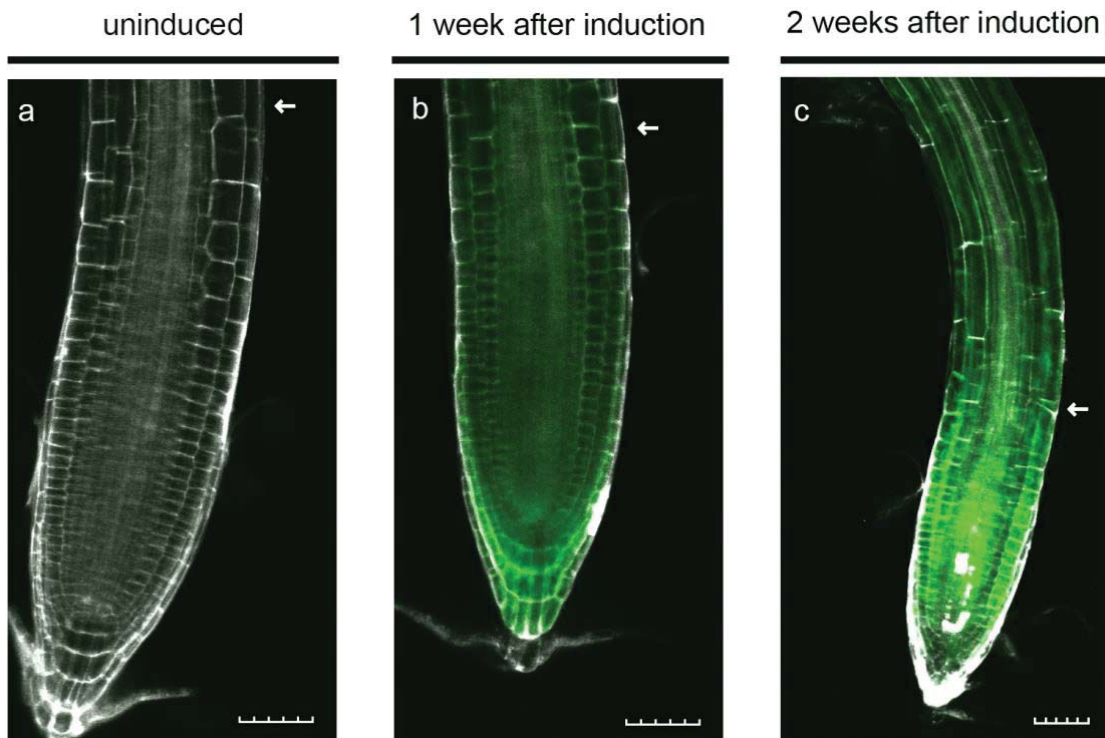


Figure 6.2 Induction of large *Ist8.1* deletion sectors in the root. Plants of $LST8.1^{lox}$ with *WOX5p::CRE* were grown vertically on MS media under short day conditions. Seedlings were induced three DAG with 20 μ M DEX for 24h. Roots were stained with propidium iodide (white) and analysed with confocal microscope. Images represent optical sections of the root and induced *Ist8.1* deletion sectors are indicated by GFP fluorescence (green). Roots of $LST8.1^{lox}$ line 6 at same age with (a) no DEX treatment and (b) one week after treatment. (c) Roots of $LST8.1^{lox}$ line 6 at two weeks after induction. Boundaries between core meristem and elongation zone are indicated by arrows. Scale bars = 50 μ m.

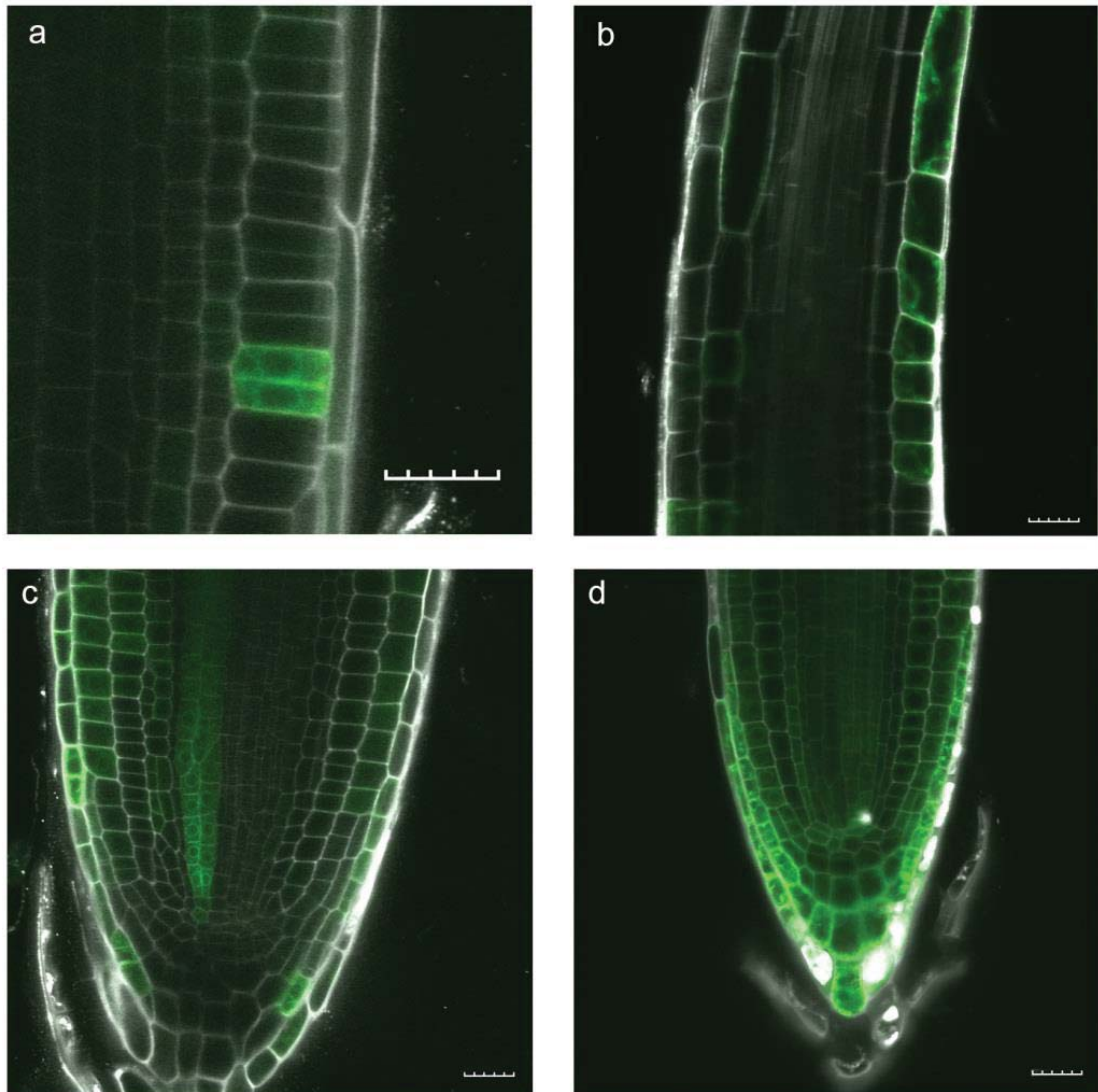


Figure 6.3 Induction of *Ist8.1* deletion sectors in various tissue of the RAM. Roots of *Ist8.1* LST8.1^{lox/Δ} with HS::CRE C (a-c) and WOX::CRE:GR B (d) were analysed. Plants were germinated on MS media and grown vertically. Seedlings were induced three DAG. Images represent optical sections stained with propidium iodide (white). *Ist8.1* deletion sectors are indicated by GFP expression (green). (a) Small *Ist8.1* sector in the epidermis one DAI (LST8.1^{lox} line 7); (b) *Ist8.1* sector in epidermis seven days after induction (LST8.1^{lox} line 7); (c) *Ist8.1* sector in vasculature seven days after induction (LST8.1^{lox} line 6); (d) sector covering entire root meristem seven days after induction (LST8.1^{lox} line 6). Scale bars = 20μm.

6.5 *Raptor3g raptor5g* and *Ist8.1* mutants show differences in the response to changes of the light period

To identify potential functional differences of *RAPTOR* and *LST8* in *A. thaliana*, I compared the phenotypes of knock-out lines. Therefore, I utilized the same T-DNA lines described in Chapter 3.1 for the disruption of *RAPTOR3G* and *RAPTOR5G*. To

eliminate *LST8.1* gene function, I utilized the T-DNA line SALK_002459, which was previously characterized in the first study of LST8 function in plants by Moreau et al. (2012). In this study, *lst8.1* mutants were described to show an irregular response to long day conditions. Compared to the growth under short day conditions, *lst8.1* mutants were more stunted and slower in their development as when grown under long day conditions. This opposed observations of wt plants that showed an increase of growth and accelerated development under a long day period (Moreau et al., 2012). I compared *raptor3g raptor5g* and *lst8.1* mutants to identify potential differences in the response to changes in the light period. Therefore, *raptor3g raptor5g* and *lst8.1* T-DNA lines were grown on MS plates under short day conditions for two weeks. Subsequently, plants were moved to long day conditions to grow for a further two weeks, while a control remained under short day conditions. The analysis after four weeks showed an increase of growth in wt plants after the shift to long day conditions (Figure 6.4). Similarly, *raptor3g raptor5g* mutants responded to longer light periods with an increase in growth. In contrast, the growth of *lst8.1* mutants did not accelerate with the increase of light period (Figure 6.4).

The results showed that the severe growth limitation of *raptor3g raptor5g* mutants could be partially lifted by increasing the length of the light period. The relative increase of vegetative growth following an extension of the light period was comparable with that in wt plants. However, *lst8.1* mutants failed to adapt to changes of the light period and were not capable to utilize the longer light periods.

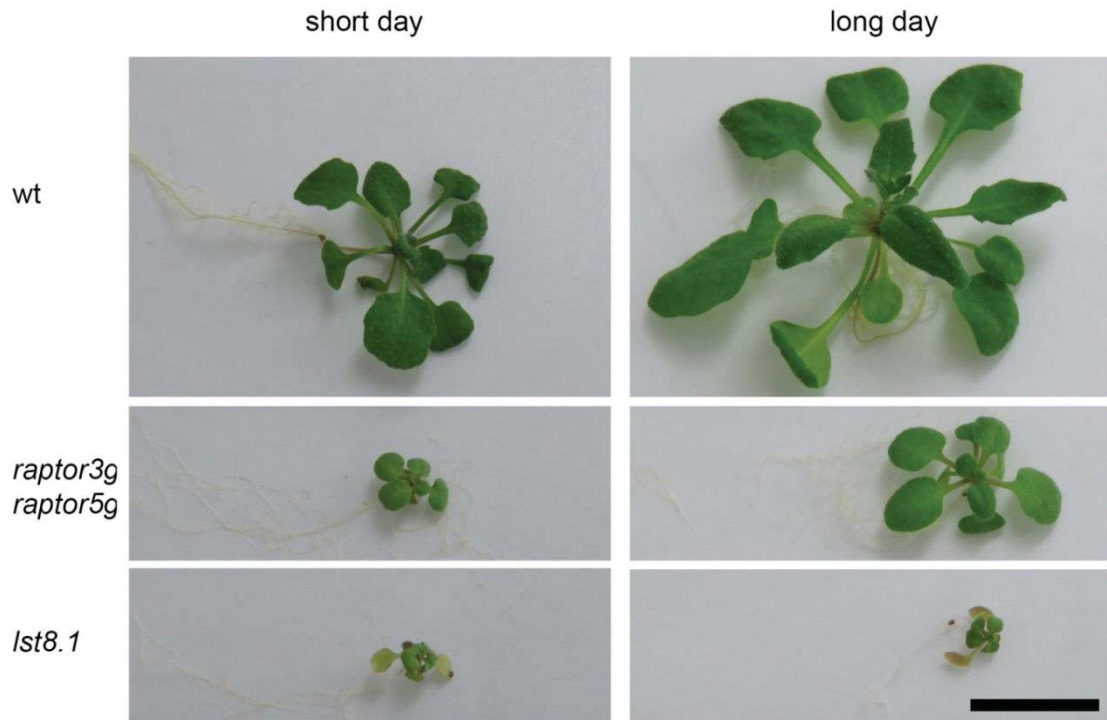


Figure 6.4 Phenotypes of wt, *raptor3g raptor5g* and *lst8.1* mutants in response to light period changes. Plants were germinated on MS media and grown for two weeks under short day conditions, followed by two weeks under long day conditions. Control was grown continuously under short day conditions for four weeks. Images show representative plants. Scale bar = 1cm.

6.6 *Raptor3g raptor5g* and *lst8.1* mutants show differences in DNA content under long day condition.

Raptor3g raptor5g mutants showed a characteristic decrease in endoreduplication (Chapter 3.8). To identify potential similarities or differences with *lst8.1* mutants, I compared the DNA content of both mutants. For the analysis of ploidy, plants were grown continuously under short or long day conditions for four weeks before cotyledons and the first leaf pair were sampled and analysed. Histograms of the DNA content are shown in Figure 6.5. As already described in Chapter 3.8, the data revealed that wt plants showed a higher DNA content in long day conditions, which was represented by a EI of 1.17 under short day conditions, and 1.28 under long day conditions. The difference of DNA content between light periods was more prominent in

raptor3g raptor5g, indicated an EI of 0.64 under short day conditions and 0.84 under long day conditions. Similarly, endoreduplication was reduced in *Ist8.1* mutants (Figure 6.5). However, the DNA content of *Ist8.1* mutants was lower under long day conditions, which was indicated by an EI of 0.57 under short day conditions compared to 0.47 in long day conditions.

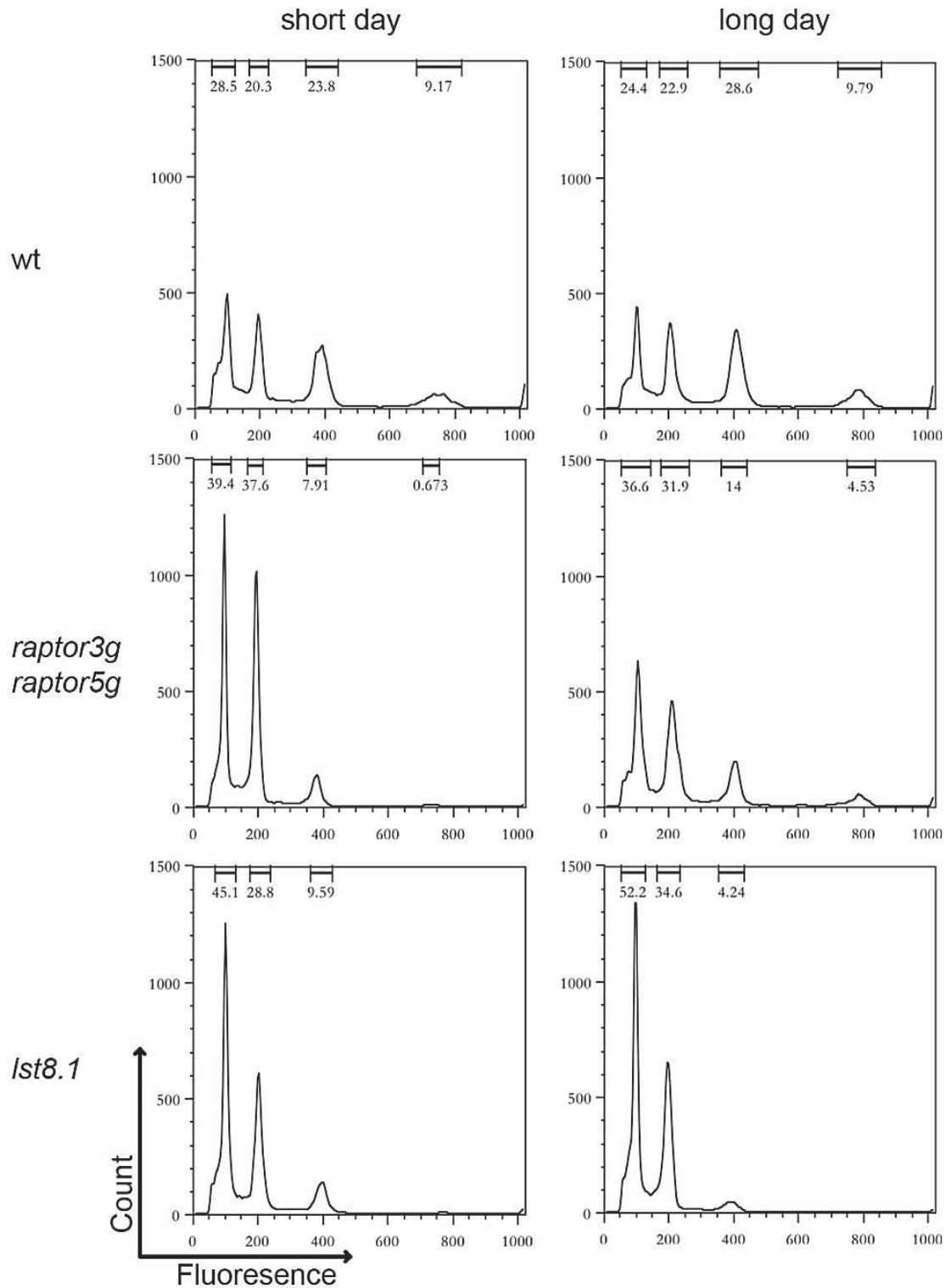


Figure 6.5 DNA content analysis of *raptor3g raptor5g* and *Ist8.1* mutants using flow cytometry. Nuclei were isolated from cotyledons and the first leaf pair of plants grown under short day conditions (left panel) and long day conditions (right panel). Extracted nuclei were stained with propidium iodide and analysed with flow cytometer. Images show the fluorescence frequency histograms of nuclei. Selection bars indicate the percentage of nuclei within the region of a major peak.

The analysis of DNA contents in *raptor3g raptor5g* and *Ist8.1* mutants confirmed a similar reduction of endoreduplication in these mutants when compared to wt plants. However, in contrast to wt and *raptor3g raptor5g* mutants, an extension of the light period resulted in a decrease of DNA content in *Ist8.1* mutants.

6.7 *Raptor3g raptor5g* and *Ist8.1* mutants show a similar but not identical transcriptomic profile

The failure of *Ist8.1* mutants to adapt to changes in the light period was already described by Moreau et al. (2012). In contrast, *raptor3g raptor5g* mutants displayed a similar response to day length changes as seen in wt plants, which was described in Chapter 6.6. To examine these differences at the transcriptomic level, I compared the transcriptomic data published by Moreau et al. (2012) with transcriptomic data of *raptor3g raptor5g* mutants as described in Chapter 3.5. The published data set included relative expression levels of several specific genes involved in cell wall synthesis, metabolism and regulation. The transcription levels of these genes in *raptor3g raptor5g* mutants were correlated to those of wt plants and compared to the relative expression levels of genes in *Ist8.1* mutants (Moreau et al., 2012).

The comparison of expression levels in *raptor3g raptor5g* and *Ist8.1* mutants indicated a broadly similar expression profile of the selected genes (Table 6.2). Several cell wall synthesis related genes like expansins were similarly down regulated. The same was observed in genes involved in metabolism like *GALACTINOL SYNTHASE* and *MIPS1*. In contrast, differences were detected in the expression of *SEC14*, encoding a phosphatidylinositol transfer protein, which is involved in vesicle trafficking. While no differential regulation was detected for *NR* and *NIR*, the nitrate transporter *NRT1* was repressed in *Ist8.1* and upregulated in *raptor3g raptor5g* mutants (Table 6.2). Contrarily, the flowering time regulator *FLC* was down-regulated in *raptor3g raptor5g* and up-regulated in *Ist8.1*. Further differential regulation was found in the *ADENOSINE*

5'-PHOSPHOSULFATE REDUCTASE 2 (*APR2*), *METHIONE SYNTHASE*, and the sugar transporters *AT5G17630* and *SFP1*, which were less expressed compared to *lst8.1* mutants.

Table 6.2 Transcriptomic comparison of *raptor3g raptor5g* and *lst8.1* mutants.

Relative expression of selected genes in *lst8.1* mutants published by Moreau et al. (2012) was compared with relative expression in *raptor3g raptor5g* mutants. In the study of Moreau et al. (2012), RNA was extracted from leaf (grown under SD) sampled at developmental growth stage 3.1 (Boyes et al., 2001). In this study, RNA was sampled from shoot tissues (grown under SD) when plants developed 10-12 rosette leaves. Expression levels were correlated to those of wt plants. Levels of significance are indicated by asterisks (*: $p \leq 0.05$; **: $p \leq 0.01$).

Function	Gene name	Gene ID	Wt / <i>raptor3g raptor5g</i> log2		wt / <i>lst8.1</i> log2
Cell Wall	<i>EXPANSIN B1</i>	AT2G20750	-1.186	**	-1.5
	<i>EXPANSIN B3</i>	At4G28250	-1.885	**	-3
	<i>EXPANSIN A6</i>	AT2G28950	-0.175		-0.8
	<i>EXPANSIN A8</i>	AT2G40610	-1.881	**	-1.5
	<i>PECTATE LYASE</i>	AT3G53190	-1.198	**	-1.5
	<i>PECTATE LYASE</i>	AT5G63180	-1.516	**	-0.8
	<i>ARABINO GALACTAN 7</i>	AT5G65390	0.111		1
	<i>ARABINO GALACTAN 12</i>	AT3G13520	0.208		1
	<i>ARABINO GALACTAN 15</i>	AT5G11740	0.579	**	3
	<i>ARABINO GALACTAN 21</i>	AT1G55330	-0.013		3
Regulation	<i>PIF 4</i>	At2G43010	0.038		-1.5
	<i>PIN4</i>	AT2G01420	-0.295	**	-1.5
	<i>GASA 4</i>	AT5G15230	-0.535	**	-0.8
	<i>FT</i>	AT1G65480	-2.442		-1.5
	<i>HAT 2</i>	AT5G47370	-0.543	**	-0.8
	<i>PLDε</i>	AT1G55180	-0.317		-0.8
	<i>XLARGE G PROTEIN 3</i>	AT1G31930	-0.010		-3
	<i>60S L37 PROTEIN</i>	AT1G15250	0.740	**	1
	<i>40S S9P PROTEIN</i>	AT5G39850	1.674	**	1
	<i>SAUR-like</i>	AT2G21210	0.426	**	3
	<i>SEC 14</i>	AT1G22530	-0.798	*	1
	<i>NITRILASE 1</i>	AT3G44310	-0.117		1
	<i>GASA 1</i>	AT1G75750	-0.087		3
	<i>BTB TAZ 2</i>	AT3G48360	1.477	**	3
	<i>BTB TAZ 4</i>	AT5G67480	0.133		1
	<i>FLC</i>	AT5G10140	-2.742	**	1
	<i>MYB 11</i>	AT3G46130	0.451	**	1
	<i>ATG8G</i>	AT3G60640	0.549	**	1

Table 6.2 continued.

Function	Gene name	Gene ID	Wt / <i>raptor3g</i> / <i>raptor5g</i> log2		wt / <i>lst8.1</i> log2
Metabolism	<i>IRT 3</i>	AT1G60960	-0.910	**	-1.5
	<i>NODULIN MtN21</i>	AT3G28070	-0.724	**	-0.8
	<i>TGG2</i>	At5G25980	-1.873	**	-1.5
	<i>LUPEOL SYNTHASE G3</i>	At1G78970	-1.464	**	-1.5
	<i>CELLULASE SYNTHASE G3</i>	AT4G23990	-0.216		-1.5
	<i>PHOSPHOGLUCOMUTASE</i>	AT5G51820	-0.513	**	-0.8
	<i>NRT1.1</i>	AT1G12110	0.764	**	-0.8
	<i>PLASTOCYANIN</i>	AT4G12880	-1.114	**	-0.8
	<i>SULTR3;1</i>	AT3G51895	0.221		-0.8
	<i>PSAD-2</i>	AT1G03130	-0.342	*	-0.8
	<i>LHCB2;2</i>	AT2G05070	-0.125		-0.8
	<i>MANNITOL DEHYDROGENASE</i>	AT4G39330	-0.132		-0.8
	<i>MIPS 1</i>	AT4G39800	-1.797	**	-1.5
	<i>MIPS 2</i>	AT2G22240	-1.561	**	-1.5
	<i>P5CS 1</i>	AT2G39800	-0.858	**	-1.5
	<i>GALACTINOL SYNTHASE 1</i>	AT2G47180	0.401		-3
	<i>GALACTINOL SYNTHASE 2</i>	At1G56600	-3.067	**	-1.5
	<i>GALACTINOL SYNTHASE 3</i>	At1G09350	-1.543	**	-0.8
	<i>NR 1</i>	AT1G77760	2.023	**	3
	<i>NR 2</i>	AT1G37130	1.581	**	3
	<i>NIR 1</i>	AT2G15620	1.268	**	3
	<i>LOB 39</i>	AT4G37540	1.180	**	1
	<i>GOGAT 1</i>	AT5G53460	-0.207		1
	<i>ASN 2</i>	AT5G65010	0.297	**	3
	<i>UPM1</i>	AT5G40850	1.524	**	3
	<i>CATION EXCHANGE 1</i>	AT2G38170	-0.107		3
	<i>Apr-02</i>	AT1G62180	-0.454	**	1
	<i>METHIONE SYNTHASE</i>	AT3G03780	-0.384	**	1
	<i>SAM DECARBOXYLASE</i>	AT3G02470	-0.138		1
	<i>FERREDOXIN 3</i>	AT2G27510	1.170	**	1
	<i>ACETOLACTATE SYNTHASE</i>	AT2G31810	0.777	**	1
	<i>P5CS 2</i>	AT3G55610	0.390	**	1
	<i>PEPC 2</i>	AT2G42600	0.424	**	3
	<i>GLC6P TRANSPORTER</i>	AT5G17630	-0.368	**	1
	<i>PHLOEM PROTEIN 2-A</i>	AT1G63090	0.461	**	1
	<i>SFP1</i>	AT5G27350	-0.680	**	1
	<i>APS KINASE</i>	AT2G14750	0.194		1
	<i>NICOTINAMINE SYNTHASE</i>	AT5G04950	0.446	**	3
	<i>PRO TRANSPORTER 3</i>	AT2G36590	0.289		1
	<i>NADP IDH</i>	AT1G65930	0.195		1
	<i>FLAVONOL SYNTHASE</i>	AT5G08640	0.578	**	1

Comparison of expression levels of specific genes between *raptor3g raptor5g* and *lst8.1* mutants presented a widely identical transcription profile. However, the comparison also revealed differences in the expression of specific genes involved in

flower initiation, membrane composition, sulphur and nitrate assimilation, and sugar transport.

6.8 *RAPTOR* and *LST8* are not essential for TOR activity in plants

T-DNA knockout lines of *raptor3g raptor5g* and *lst8.1* mutants displayed a severe reduction of growth (Chapter 3.2; Moreau et al. (2012)). As described in Chapter 3.2, residual TOR activity was detected in *raptor3g raptor5g* mutants. To investigate whether *lst8.1* mutants retained TOR activity, I combined T-DNA knockout lines of *raptor3g raptor5g* and *lst8.1* with those of *tor*. For the disruption of the *TOR* gene, the T-DNA line SALK_036379 (received from ABRC) was used in a heterozygous state ($TOR^{+/-}$) since homozygous were shown to arrest during embryo development (Ren et al., 2011). $TOR^{+/-}$ plants were grown in the glasshouse and crossed with previously described heterozygous T-DNA lines of *raptor* and *lst8*, $raptor3g^{+/-} raptor5g$ and $lst8.1^{+/-}$ (Chapter 3.1 and 6.5). The progeny was then grown on MS plates and plants with the genotype $raptor3g raptor5g TOR^{+/-}$, $raptor3g raptor5g tor^{+/+}$, $lst8.1 TOR^{+/-}$, and $lst8.1 TOR^{+/+}$ were identified by genotyping PCR (Chapter 2.3.3). After six weeks of growth under short day conditions the phenotypes were compared. Despite the already weak growth phenotype of *raptor3g raptor5g* mutants, the additional disruption of a single *TOR* allele in $raptor3g raptor5g TOR^{+/-}$ plants led to a further reduction of growth (Figure 6.6). A similar effect was displayed by $lst8.1 TOR^{+/-}$ mutants.



Figure 6.6 Phenotypes of *raptor3g raptor5g* and *Ist8.1* with reduced TOR gene dosage. Plants were crossed with *TOR*^{+/-} T-DNA line. *Raptor3g raptor5g* and *Ist8.1* mutants with two (left panel; *TOR*^{+/+}) and a single *TOR* allele(s) (right panel; *TOR*^{+/-}). Plants were grown under short day conditions for 6 weeks. Scale bars = 1cm.

Raptor3g raptor5g and *Ist8.1* mutants showed a significant decrease of growth with the additional disruption of a single *TOR* allele. This indicated a residual TOR activity in these mutants, which implied further that RAPTOR and LST8 are not essential to maintain TOR function in *A. thaliana*.

Discussion

The presented data indicated prevailing similarities in the phenotypes of *raptor3g raptor5g* and *Ist8.1* mutants in *A. thaliana*. Both mutants completed embryonic development and were capable of vegetative growth (Figure 6.4; Moreau et al. (2012)). This opposed observations in fungi and animals, in which *raptor* and *Ist8* mutants arrested early during the embryonic phase (Loewith et al., 2002; Kim et al., 2003; Guertin et al., 2006). Further investigation indicated that residual TOR activity could

account for the continued growth in *raptor3g raptor5g* and *lst8.1* mutants (Figure 6.6). By using TOR inhibitors and through limiting the gene dosage of *TOR* by disrupting one *TOR* allele, experiments indicated that TOR retained activity in these mutants (Figure 6.6; Chapter 3.3). This offers an explanation for the relatively normal growth of these plants compared to knock-out mutants in other species. The finding of RAPTOR and LST8-independent activity of TOR in plants further commends that the function of these components within the TOR complex could be differentially adapted to those of their homologues in fungi and animals. This might reflect changes that evolved during the separate evolution of plants, in which this pathway was accustomed to the requirements of growth regulation in plants.

Despite the remaining TOR activity in these mutant lines, growth was severely limited in both mutants, which resulted from limited meristem size and activity (Figure 6.2; Chapter 3.7). The induced excision of *RAPTOR3G* or *LST8.1* through the use of a *CRE/lox* system indicated similar non-cell-autonomous function of *lst8.1* as described for *RAPTOR* deletions in Chapter 5.5 (Figure 6.2).

Endoreduplication, which was discovered to be limited in *raptor3g raptor5g* mutants, was equally reduced in *lst8.1* mutants (Figure 6.5). This suggests that the ability of TOR to activate cell cycle genes either directly or via S6K is similarly affected by the deletion of *LST8* and *RAPTOR* genes (Chapter 3.8).

Differences between *raptor3g raptor5g* and *lst8.1* mutants became evident, when plants were grown in long day conditions. Under extended light periods, *raptor3g raptor5g* mutants showed an accelerated growth rate and increase of DNA content compared to growth under short day conditions. In contrast, *lst8.1* mutants did not indicate any phenotypic changes after the shift from short to long day conditions (Figure 6.4). The ploidy measurements suggested a decrease of endoreduplication under long day conditions, which is opposed to effects seen in wt and *raptor3g raptor5g* mutants (Figure 6.5). This indicated that *lst8.1* mutants failed to

adapt and utilize a longer light period, which was previously reported by Moreau et al. (2012). In this study, the response to various light periods was correlated with transcriptomic data obtained from *lst8.1* mutants grown under various light conditions. Alterations in expression levels of *GALACTINOL SYNTHASE* and *MYO-INOSITOL-1 PHOSPHATE SYNTHASE 1 (MIPS1)* hinted to perturbations of phospholipid signalling, which were associated with reduced growth (Moreau et al., 2012). Further, comparison with wt plants indicated irregular changes of the nitrogen metabolism, including the genes *NITROGEN REDUCTASE (NR)* and *NITRITE REDUCTASE (NiR)*. The expression of these genes was reported to be reduced in response to a shift to long day conditions in wt plants (Corbesier, 1998; Corbesier et al., 2002). In *lst8.1* mutants, the expression of these genes was elevated, which might relate to the poor adaption to long light periods (Moreau et al., 2012). However, the comparison of transcriptomic data from *lst8.1* and *raptor3g raptor5g* mutants revealed a similar pattern in the expression of genes representing the nitrogen metabolism in both mutants (Table 6.2). This asserted a role of TOR function in the regulation of nitrogen metabolism. However, the overall similarity between *raptor3g raptor5g* and *lst8.1* in the expression of these genes indicated that changes in the nitrogen assimilation are unlikely to account for the different phenotypes of both mutants in response to longer light periods.

Lst8.1 and *raptor3g raptor5g* mutants indicated also differences in flower development. Flowering initiation was delayed in *raptor3g raptor5g* mutants when compared to the wt (Figure 3.4). In contrast, I did not observe any flower development in *lst8.1* mutants. This stands in conflict with data published by Moreau et al., who reported flower initiation of *lst8.1* mutants under long day conditions (Moreau et al., 2012). This might reflect slight differences in growth conditions between the studies, such as light quality. As a potential cause for the delay in flower initiation of *lst8.1* mutants, Moreau et al. identified a strong repression of the transcription of *FT*, which was also found in *raptor3g raptor5g* mutants (Chapter 4.1). This supports the conclusion that the limited

TOR signalling in *raptor3g raptor5g* and *lst8.1* mutants affect flower development via down-regulation of *FT*. Interestingly, transcription of *FLOWERING LOCUS C (FLC)*, a repressor of flowering, was found repressed in *raptor3g raptor5g* mutants and up-regulated *lst8.1* mutants, as shown in Table 6.2 (Michaels and Amasino, 1999; Moreau et al., 2012). The expression of *FLC* was shown to be regulated by vernalisation and the autonomous pathway, which negatively affect the transcription of *FLC* and subsequently enable the initiation of flowering (Sheldon et al., 1999; Amasino, 2010). Hereby, the repression of *FLC* was shown to be mediated by chromatin-modification via the Polycomb Repressive Complex 2 (PRC2) (Gendall et al., 2001; Bastow et al., 2004; Sung, 2004). PRC2 is conserved among eukaryotes and PRC2-mediated histone methylation was shown to be rapamycin-sensitive in mice (Shaver et al., 2010; Blättler et al., 2012). These relations suggest that a differential regulation of *FLC* expression might explain the disparity in flower initiation of *raptor* and *lst8* mutants. The differences in *FLC* regulation could further imply distinct roles of RAPTOR and LST8 in the activation of PRC2 by TOR. Yet further evidence is required to clarify how TOR signalling affects PRC2 activity in plants.

To conclude, *raptor3g raptor5g* and *lst8.1* mutants displayed only minor phenotypic differences. This provides little support for a differential TOR function in these mutants. As described in the introduction, disruptions of *raptor* and *lst8* were lethal in fungi and animals (see above). Therefore, the major novel finding presented in this study is that TOR remains active in both mutants in *A. thaliana*. As a result of this residual activity, distinct functional differences of RAPTOR and LST8, or TORC1 and TORC2 respectively, were potentially obscured. It remains to be identified how the functions of RAPTOR and LST8 relate to the differences observed in day length response and flower initiation. These could mark distinct functions of RAPTOR and LST8 to facilitate the binding of TOR to specific substrates, or else reflect changes in the activities of TOR complexes. Overall, the minor differences between the phenotypes of *raptor* and

Ist8 mutants in *A. thaliana* favour the conclusion that TORC2 is not represented in plants, although further investigation is required to confirm this hypothesis.

Chapter 7

Final discussion, outlook and concluding remarks

The diversity of morphologies and life strategies that has evolved during the evolution of eukaryotes is enormous. Despite this, the TOR kinase has remained conserved among the vast majority of eukaryotes, signifying it as a fundamental regulator of growth (van Dam et al., 2011). Yet very limited knowledge has been established to this day on how the TOR signalling pathway has been adapted during evolution to suit the requirements of the sessile and photoautotroph lifestyle of plants. This thesis addresses this deficit by presenting novel TOR functions, which contribute to development and growth in plants. Foremost, the finding that homologues of RAPTOR and LST8, two essential TOR components in animals and yeast, are not required to maintain TOR activity in *A. thaliana* represents the most compelling discovery of this thesis. As a result, mutants of *raptor3g raptor5g* and *lst8.1* showed a relatively normal phenotype despite the reduction in growth. This is in line with a previous study, which described *lst8.1* mutants to be capable of vegetative growth (Moreau et al., 2012). A very similar phenotype was also observed in *raptor3g raptor5g* mutants. Due to the early arrests of *raptor* and *lst8* mutants in fungi and animals, very little is known about the requirement for RAPTOR and LST8 at later stages of development in these systems. This prevents a comparison with my observations in *A. thaliana*. Yet reports from tissue-specific deletion of RAPTOR in mice and knock-down experiments in nematodes suggested an essential contribution to TOR activity (Hara et al., 2002; Bentzinger et al., 2008). Still controversial is the requirement for LST8 function as *lst8* knock-out mutants caused embryonic arrest in mice, while *lst8.1* mutants in insects were viable (Guertin et al., 2006; Wang et al., 2012). Interestingly, studies in these systems showed that *LST8* was not required to maintain the function of TORC1. Therefore, the variation of phenotypes of *lst8* mutants between *taxa* might reflect the

specific requirement for TORC2 functions. However, it is uncertain at this time if a TORC2 is represented in plants, since *RICTOR* is not conserved here (van Dam et al., 2011). The comparison of *lst8.1* and *raptor3g raptor5g* mutants in this study revealed that phenotypes of both mutants displayed only minor differences. Also, a correlation of transcription levels of selected genes involved in metabolism, regulation and cell wall synthesis revealed highly similar profiles for both mutants. These findings further support the hypothesis that a TORC2 is not implemented in plants. Together with the viability and the residual TOR activity found in *raptor3g raptor5g* and *lst8.1* mutants, the findings of this thesis indicate compelling differences in the operation of TOR in plants compared to fungi and animals.

TOR has been proposed to play a key role in the interplay between cell cycle and cell size (Davie and Petersen, 2012; Sablowski and Carnier Dornelas, 2014; Xiong and Sheen, 2014). Knowledge of the link between cell cycle progression and cell size is most advanced in unicellular yeast. Here, cell cycle progression from G1 to S phase depends on the cell size to surpass a certain threshold (reviewed by Jorgensen and Tyers, 2004; Di Talia et al., 2007). *Vice versa*, TOR-mediated cell cycle regulation via S6K was shown to determine cell size in *S. pombe* (Davie and Petersen, 2012). Due to the increased complexity in multicellular organisms through the impact of developmental cues and neighbouring cells, the analysis of this connection is more difficult. Yet several studies have highlighted a function of TOR in the regulation of cell cycle and cell size in plants. By influencing the transcription of cell cycle genes through phosphorylation of RBR1 and E2F proteins, TOR was shown to influence cell cycle regulation (Henriques et al., 2010; Xiong et al., 2013). Furthermore, *A. thaliana* mutants with inhibited TOR activity were also found to form smaller cells (Henriques et al., 2010; Ren et al., 2012). The transcriptomic profile of *raptor3g raptor5g* presented in this thesis further supports this connection as the expression of several cell cycle-related genes including E2F target genes was significantly down-regulated. This is

likely to have contributed to the reduced rate of endoreduplication detected in these mutants. However, despite the decrease in DNA content, *raptor3g raptor5g* mutants did not indicate any alterations in cell size. This contradiction to previous studies might correspond to the remaining TOR activity in *raptor3g raptor5g* mutants.

Rather than through differences in cell size, the reduced growth of *raptor3g raptor5g* mutants could be caused by a reduced meristematic activity, since the size of the root meristem was severely limited in these mutants. Similar observations were also made in roots of induced *Ist8.1* knock-out mutants. These findings are in line with previous reports, which describe a reduced meristem size in roots of TOR inhibited seedlings of *A. thaliana* (Xiong et al., 2013). The changes in meristem size and activity were found to be closely associated with the action and crosstalk of the phytohormones auxin, cytokinin, brassinosteroids and gibberellic acid (reviewed by Müller and Sheen, 2008; Hacham et al., 2011; Petricka et al., 2012). The antagonistic functions of auxin and cytokinin in controlling cell division and differentiation within the root meristem have been particularly well-characterized (Dello Iorio et al., 2007; Dello Iorio et al., 2008). Therefore, it seems plausible that the limited meristem size found in roots of *raptor3g raptor5g* mutants is caused by imbalanced hormone signalling, which is supported by the transcriptomic changes of auxin-related genes in these mutants. Also, the non-cell-autonomous phenotype of induced *raptor* and *Ist8* deletions in sectors of the apical root meristem endorses a link to hormonal regulation. *Vice versa*, auxin was also found to promote TOR functions, which presents the prospect of an interdependent crosstalk between hormonal and TOR signalling (Schepetilnikov et al., 2013).

A few studies have hinted that the hormone signalling in plants could be relayed to TOR through phospholipid signalling by PI or PA in a similar manner to the insulin signal transduction in mammals *via* the PI3K-PTEN-PDK cascade (Pribat et al., 2012; Bögre et al., 2013). The findings of this thesis further promote a potential link between phospholipid signalling and TOR activity in plants. As previously described by Moreau

et al. (2012) for mutants of *lst8.1*, the data presented here revealed a reduced expression of *MIPS1* and *GALACTINOL SYNTHASE* in *raptor3g raptor5g* mutants, which indicated a limited synthesis of the second messenger PI and its derivatives (Loewus and Murthy, 2000). This might imply an explanation for the defects in auxin signalling indicated by the reduced meristem size and apical dominance in *raptor3g raptor5g* mutants, as limited MIPS1 activity was demonstrated to alter the expression of *PIN* genes and the subcellular localization of their proteins (Chen and Xiong, 2010; Luo et al., 2011). Although not confirmed yet, this was likely caused by subsequently reduced phospholipid signalling to PDK1, which was shown to regulate PIN localization via phosphorylation of PINOID (Zegzouti et al., 2006; reviewed by Scherer et al., 2012). However, experiments have yet to confirm if TOR activity also affects this pathway directly. The AGC kinase PINOID represents a potential target of TOR phosphorylation, since several members of this family are known to be phosphorylated by TOR, for example S6K, PKB and PKC (reviewed by Su and Jacinto, 2011). Also, the involvement of VPS34 and PTEN in signal transduction between phospholipids and TOR activity is unclear to date. However phenotypic similarities in defects of the polar tip extension of root hairs and pollen tubes of *raptor3g raptor5g* mutants and mutants with altered phospholipid signalling through reduced *vps34* activity and overexpression of *AtPTEN1* hint at a potential link to TOR activity (Gupta, 2002; Monteiro et al., 2005; Lee et al., 2008a; Lee et al., 2008b). Again, further investigation is required to address this potential connection between VPS34, PTEN, and PDK1 signalling and its significance for TOR signalling in plants.

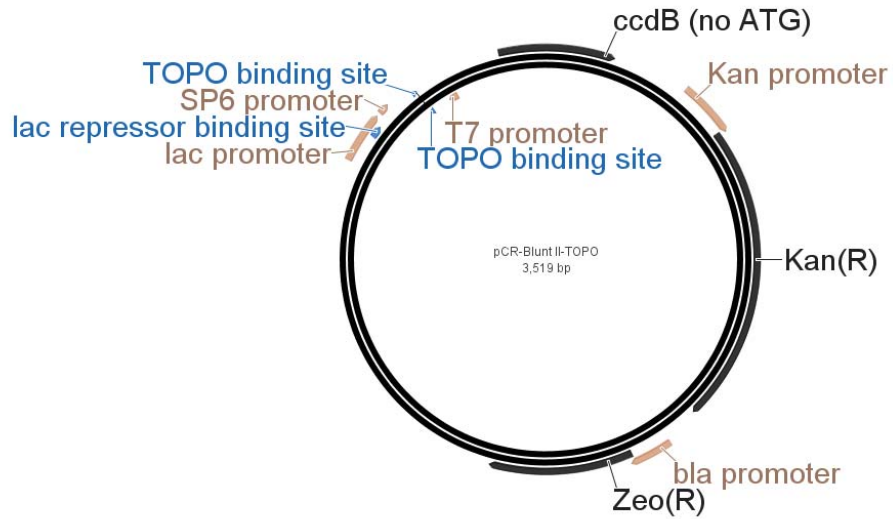
In conclusion, the difference in the requirement of RAPTOR and LST8 for TOR function discovered in this study indicates a divergent function of TOR complexes compared to other systems. Future research needs to address the molecular basis of this by unravelling the molecular details of the TOR complex composition in plants. Identification of novel interaction partners remains a crucial task in order to identify the

links between TOR and the specific functions highlighted in this thesis, such as polar tip extension of root hairs and pollen tubes, gametophyte development and day length response. Further identification and characterization of interaction partners of TOR would be equally important to elucidate novel members of a signalling cascade that regulates TOR activity. This would aid in the search for the as yet undiscovered link to other signalling pathways, such as auxin and phospholipids, which are suspected to impinge on TOR activity.

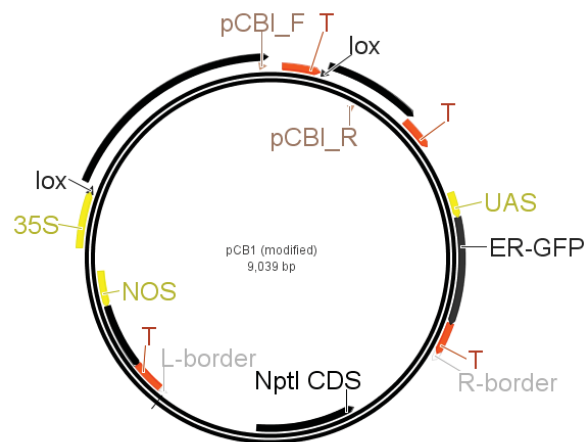
This thesis also strengthened the hypothesis of a connection between hormone, phospholipid signalling and TOR function. The analysis of the CRE//ox system showed no obvious phenotypic changes following the sectorial deletion of *RAPTOR* and *LST8* in small sectors within the root meristem, which also hinted at a non-cell-autonomous character of TOR function. Further investigation is required to confirm these findings given the residual activity of TOR in *raptor3g raptor5g* and *lst8.1* mutants. The most direct approach to address this would be to adapt the CRE//ox system for the induction of sectorial deletion of *TOR* itself. Furthermore, to improve this system for the analysis of cell-autonomy it would also be beneficial to add a translational fusion of a fluorescent protein to the gene of interest. This would allow positive marking of the protein within sectors and would address the uncertainty of potential residual mRNA and protein within sectors of the current system.

To conclude, this data presents further evidence of the altered requirement of *RAPTOR* and *LST8* function for TOR signalling in plants compared to observations in fungi and animals. It further indicates a non-cell-autonomous function of TOR affecting meristem size and draws attention to the connection with other signalling pathways. The analysis of *raptor* mutants revealed how TOR function impinges on developmental processes such as flower initiation and gametophyte development and cellular functions such as ROS homeostasis and endoreduplication.

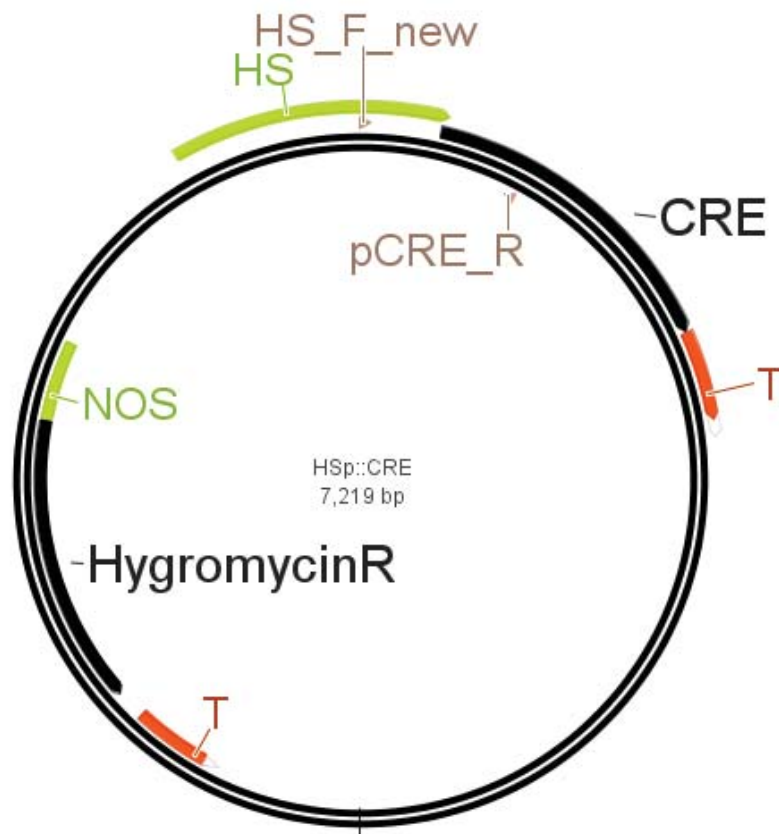
Appendices



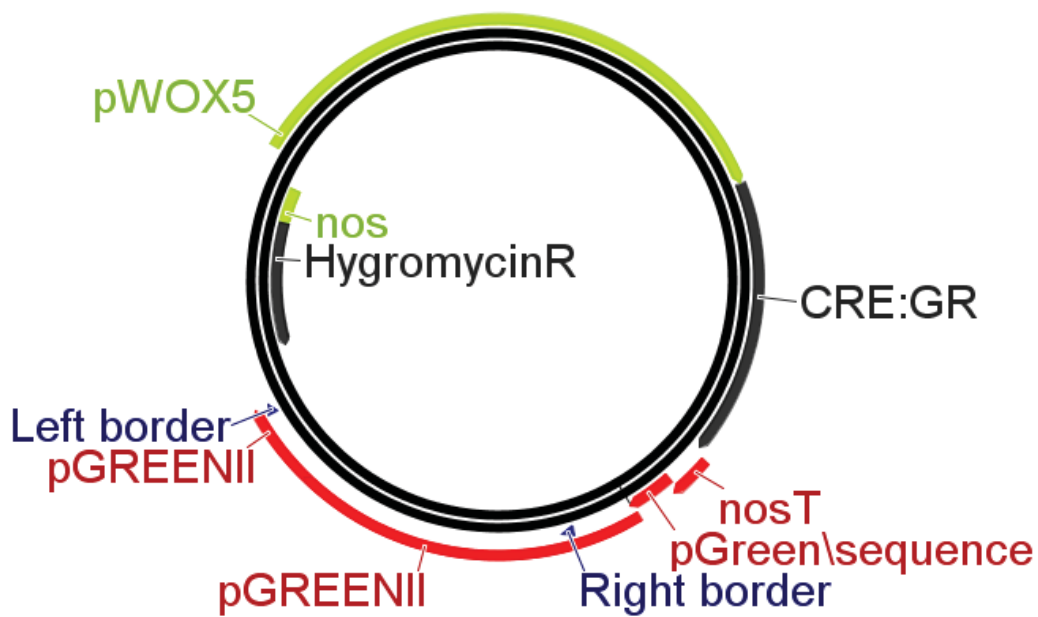
Appendix 1 Genetic map of pCR4[®] cloning vector.



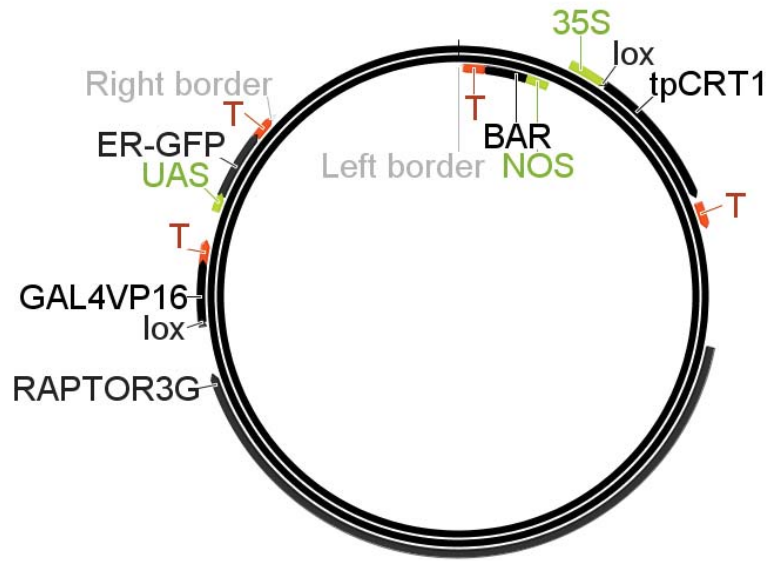
Appendix 2 Genetic map of pCBI vector.



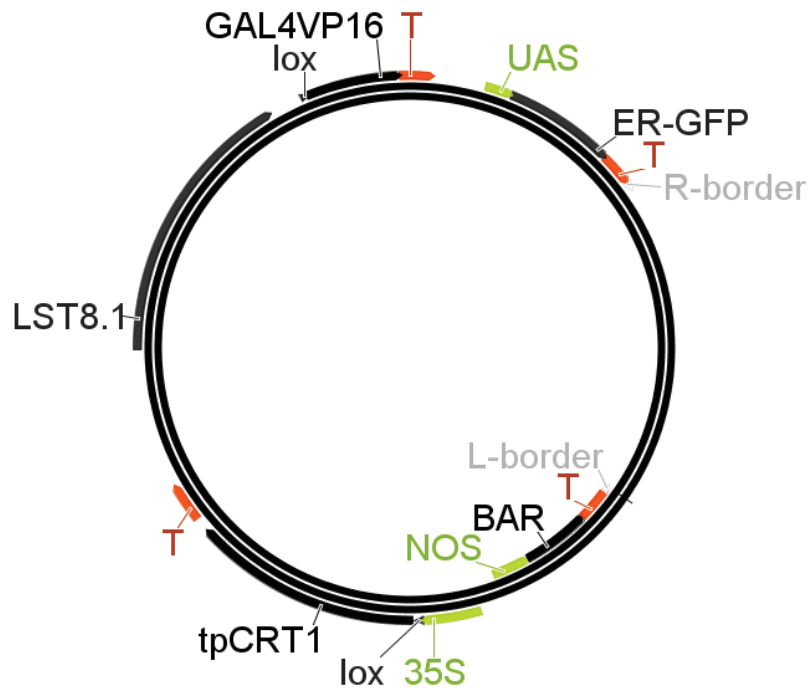
Appendix 3 Genetic map of pHSp::CRE vector.



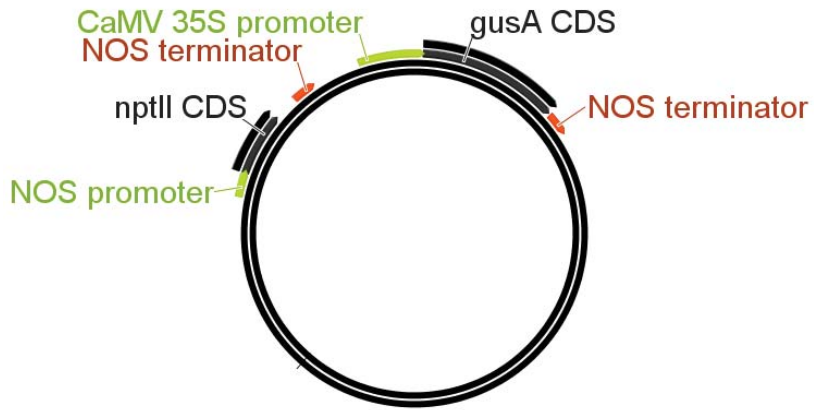
Appendix 4 Genetic map of pWOX5p::CRE vector.



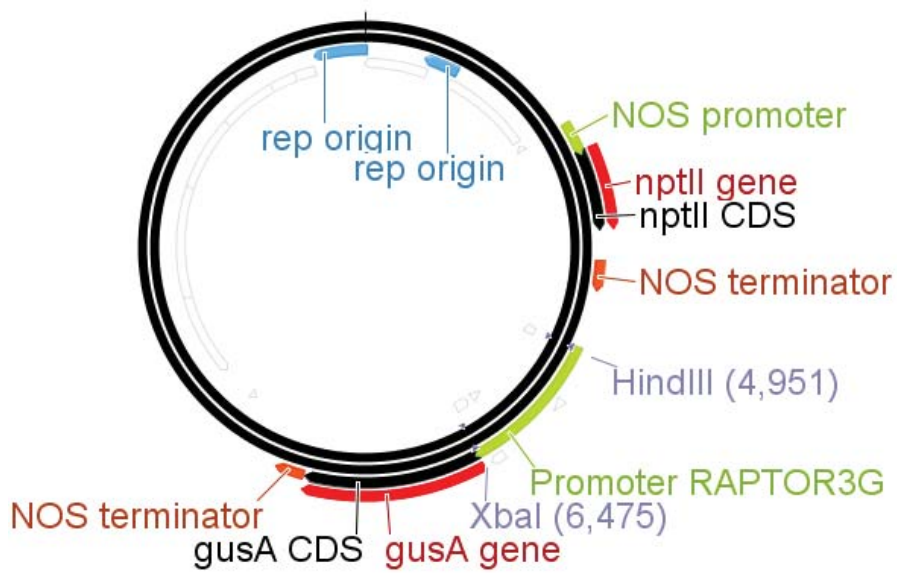
Appendix 5 Genetic map of pCBI-RAPTOR3G vector.



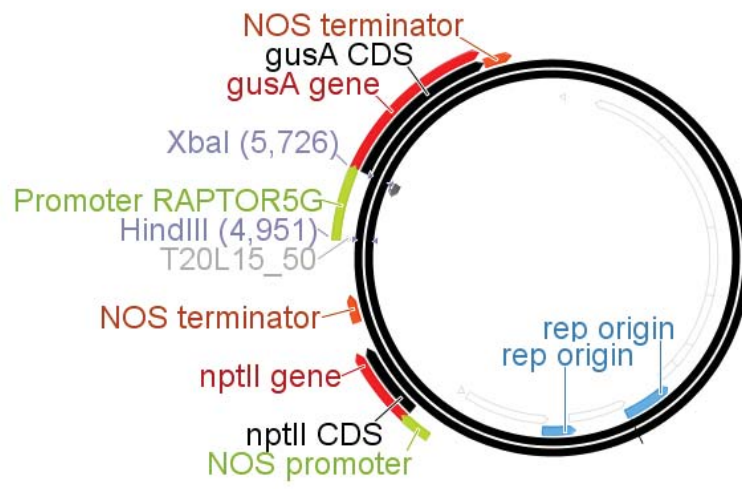
Appendix 6 Genetic map of pCBI-LST8.1 vector.



Appendix 7 Genetic map of pB121 vector.



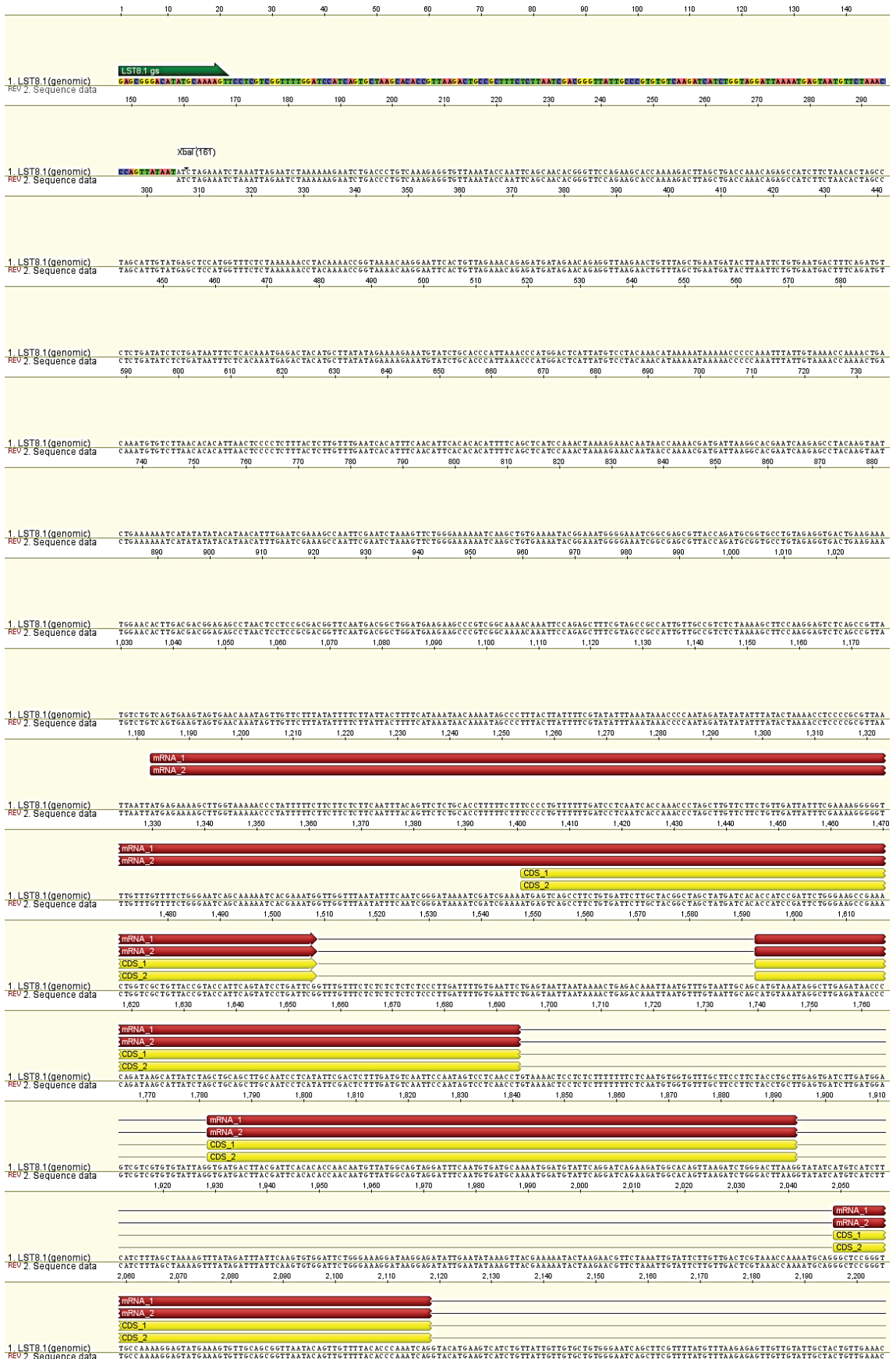
Appendix 8 Genetic map of pB121-ProRAPTOR3G::GUS.

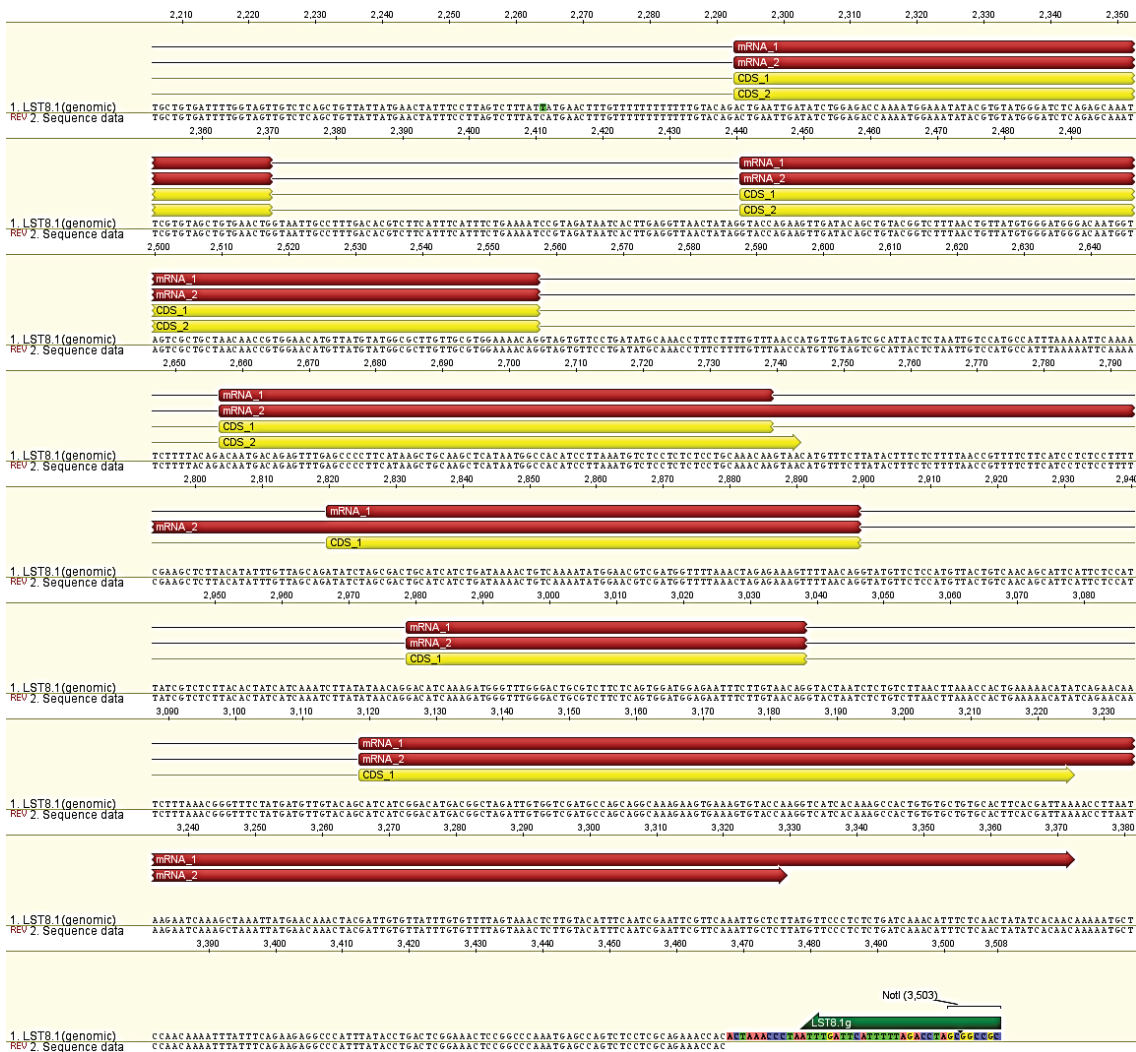


Appendix 9 Genetic map of pB121-ProRAPTOR5G::GUS

Appendix 10 Buffers and solutions.

Lysogeny broth (LB) medium:	ddH ₂ O 1 % (w/v) Tryptone 0.5 % (w/v) Yeast extract 1 % (w/v) Sodium chloride adjusted to pH 7 using NaOH
Murashige and Skoog (MS) medium:	ddH ₂ O 0.433 % (w/v) MS medium adjusted to pH 5.7 using KOH
Plant DNA extraction buffer	200 mM TrisCl 250 mM NaCl 25 mM EDTA 0.5 % SDS
SEM buffer:	PIPES 10 mM MnCl ₂ 55 mM CaCl ₂ 15 mM KCL250 mM
SOC medium	ddH ₂ O 4 % (w/v) Tryptone 1% (w/v) Yeast extract 1% (w/v) Sodium chloride 2.5 mM Potassium chloride
STET buffer:	8 % (w/v) sucrose 0.5 % (v/v) Triton X-100 50 mM EDTA 10 mM Tris-Cl (pH 8.0)
TE buffer	0.01M Tris-HCl 0.001M EDTA pH 8.0
YEBS liquid media	0.1 % (w/v) yeast extract 0.5 % (w/v) beef extract 5 % (w/v) sucrose, 0.5 % (w/v) bacto-peptone, 0.05 % (w/v) magnesium sulfate; adjusted pH 7 using NaOH





Appendix 11 LST8.1 sequence data. Theoretical PCR product with flanking primers (green) on LST8.1 genomic sequence (lane 1; AT2G22040, received from NCBI database) assembled with consensus sequence data of pCBI-LST8.1 (lane 2). Sequence differences highlighted; mRNA (red) and CDS (yellow) are indicated.

Appendix 12 List of *A. thaliana* T-DNA lines. Name, gene location and genotyping primers of all T-DNA insertion lines.

T-DNA line	Gene name	Gene ID	Primer set
SALK_078159	RAPTOR3G	AT3G08850	Rap3gMLTF1, Rap3gMLTR1, pROK-737
SAIL_400_D05	RAPTOR3G	AT3G08850	SAIL_400_D05_LP, SAIL_400_RP2, LB1
SALK_043920	RAPTOR5G	AT5G01770	SALK_043920LP.1, SALK_043920RP.1, LBb1.3
SAIL_558_H11	RAPTOR5G	AT5G01770	SAIL_400LP, SAIL_400RP2, LB1
SALK_002459	LST8.1	AT3G18140	SALK_002459_LP, SALK_002459_RP, pROK-737
SALK_036379	TOR	AT1G50030	tor-3LP, tor-3LP, LBb1.3

Appendix 13 List of *A. thaliana* T-DNA lines created for the CRE/lox system.
Name and genotyping primers are given for each line.

Line	T-DNA	Primer set
HSp::CRE A	HS::CRE	20836HS_F2, 20836HS_R, HS-LB3
HSp::CRE C	HS::CRE	HSc_L, HSc_R, HS-LB3
WOXp::CRE:GR A	WOX::CRE:GR	
WOXp::CRE:GR B	WOX::CRE:GR	WOXb_L, WOXb_L, pWOX::CRE-RB3
pCBI	pCBI	pCBI For, pCBI Rev
RAPTOR3G ^{lox} 3	RAPTOR3G ^{lox}	20839pRAP_L2, 20839pRAP_R2, pCBI_LB2
RAPTOR3G ^{lox} 5	RAPTOR3G ^{lox}	pRAP-5_F, pRAP-5_F, pCBI_LB3
RAPTOR3G ^{lox} 7	RAPTOR3G ^{lox}	pRAP-7_L, pRAP-7_R, pCBI_LB2
RAPTOR3G ^{lox} 8	RAPTOR3G ^{lox}	pRAP-8_L3, pRAP-8_R3, pCBI_LB2
LST8.1 ^{lox} 3	LST8.1 ^{lox}	pL8-3_L, pL8-3_R, pCBI_LB2
LST8.1 ^{lox} 5	LST8.1 ^{lox}	pL8-5_L, pL8-5_R, pCBI_LB2
LST8.1 ^{lox} 6	LST8.1 ^{lox}	pL8-6_L, pL8-6_R, pCBI_LB2
LST8.1 ^{lox} 7	LST8.1 ^{lox}	pL8-7_L, pL8-7_R, pCBI_LB2

Appendix 14 List of DNA primers.

Name	DNA sequence
20836HS_F2	AGTTTCTAGCTCGGCCACCG
20836HS_R	ACGGCTACGTATTTGCATCGCCT
20839pRAP_L2	TGGGCCACATTGGATACTCCG
20839pRAP_R2	TGAAGTCAACGCAACGACCG
AC1	ACGATGGACTCCAGAG
AP1	GTAATTCGCATCACTATAGCTC
AP2	ACTATAGCTCACCGCTGGT
DEX_Seq	ATT TGG AGA GGA CAC GCT
HS_F	GGATTGCATTTCCGGTCTTGT
HSc_L	AGGAGCGAGTCACCAGAAAGCA
HSc_R	ACAAGTGGGTTTTACGGCAGG
HS-LB1	ATGCCGACCGAACAAGAGCTGATTTGAGAACGCC
HS-LB2	CAAGGCAAATGCGAGAGAACGGCCTTACGCTTGGT
HS-LB3	CGCGCGCGGTGTCATCTATGT
LAD1	ACGATGGACTCCAGAGCGGCCGC(G/C/A)N(G/C/A)NNNGGAA
LAD2	ACGATGGACTCCAGAGCGGCCGC(G/C/T)N(G/C/T)NNNGGTT
LAD3	ACGATGGACTCCAGAGCGGCCGC(G/C/A)(G/C/A)N(G/C/A)N (G/C/A)NNNCCAA
LAD4	ACGATGGACTCCAGAGCGGCCGC(G/C/T)(G/A/T)N(G/C/T)NNNC GCT
LB1	GCCTTTTCAGAAATGGATAAATAGCCTTGCTTCC
LBb1.3	ATTTTGCCGATTTCCGGAAC
LST8.1 g as +not1	GCGGCCGCTAGGTCTAAAAATGAATCAAAT
LST8.1 g s	GAGCGGGACATATGCAAAAAGT
Lst8.1g_1129_R	TGGGATGGGACAATGGTAGT
Lst8.1g_1289_F	TTCCATTTTGGTCTCCAGAT
Lst8.1g_1667_R	GTGTGGATTCTGGGAAAGGA
Lst8.1g_175_R	CCAAATGAGCCAGTCTCCTC
Lst8.1g_1793_F	TGCCATAACATTGTTGGTGTG
Lst8.1g_2136_R	CGCTGTTACCGTACCATTCA
Lst8.1g_2281_F	ACAAACAAACCCCTTTTCG
Lst8.1g_2620_R	TGCCGTCTCTAAAAGCTTCC
Lst8.1g_2779_F	TCCCCATTTCCGTATTTTCA
Lst8.1g_3115_R	ATGTATCTGCACCCATTAACC
Lst8.1g_3296_F	CCATGGAGCTCATACAATGC
Lst8.1g_3584_R	TCGGTTTTGGATCCATCAGT
Lst8.1g_619_R	GTTTGGGACTGCGTCTTCTC
Lst8.1g_770_F	TCAGATGATGCAGTCGCTAGA
M13 Forward	GTAAAACGACGGCCAGT
M13 Reverse	GGAAACAGCTATGACCATG
pCBI For	AAAGCGACAGCAGGTTTGAT
pCBI Rev	CTGGAGGGAGTCCATTTTCA
pCBI_LB1	GCTCCACGCTCTACACCCACCTGCTGAAGT
pCBI_LB2	ACGGGAACTGGCATGACGTGGGTTTCTGGC
pCBI_LB3	CGTCCGGTCTGCCCCGTCACCGAGATCTGA

pCBI-LB1a	AGGCACAGGGCTTCAAGAGCGTGGTCGCTGTCAT
pCBI-RB1	AGCCAACCTTCAAGACCCGCCACA
pCBI-RB1a	GGCATCAAAGCCAACTTCAAGACCCGCC
pCBI-RB2	AGCTGCTGGGATTACACATGGC
pCBI-RB2a	AGCTGCTGGGATTACACATGGCATGGATGAACT
pCBI-RB3	TCGGTACGCTGAAATCACCAGTC
pCRE_R	GCATGTTTAGCTGGCCCAA
pHS::CRE-RB1	GAGATACCTGGCCTGGTCTGGA
pHS::CRE-RB2	GCCTGCTGGAAGATGGCGATTA
pHS::CRE-RB3	TTCTGTCAGCCCCTCGAATTTCCC
pL8-3_L	AGCCGCTTTTGCTCCTTCTCCG
pL8-3_R	CAGTTGCCACCTGCTTCCCA
pL8-5_L	TCACAGACAGGGTCTCGCGT
pL8-5_R	ACGCCCAACTGTCCTGGCTT
pL8-6_L	TGGTTAACCGAGCTCGCAGG
pL8-6_R	GAACAATCCTGATGATCGGCGT
pL8-7_L	TTCTGCGGTTGCTGTGCTC
pL8-7_R	AAGGTCGACGCTCCGGTTGA
pRAP-5_F	CGGGTCGTGGTTAGGTGGTG
pRAP-5_R	ATGAGTTCGCACGTGAAGGC
pRAP-7_L	ACACCTACTCATCCACGCCCA
pRAP-7_R	AGGCAGCAATCCCCACGGTT
pRAP-8_L3	AGCAACGCAGCCACACCATA
pRAP-8_R3	CGTGCAACCAAACATCGCCA
pRAP8-8_L2	CCTCGTGGCCCTGATGATCCAA
pROK-737	GGGAATTCAGTGGCCGTCGTTTTACAA
Prom3g_Seq4	GCT GAC ACT TTG TTA CGT GAG T
Prom3g_Seq5	GCG TGT GCA ATG ATG ATC CC
Prom3g_Seq6	GGT GGC GGC AGA AGA GAA AA
pWOX::CRE-RB1	GTTACTAGATCGGGAATTCTCCAG
pWOX::CRE-RB2	CCTCGCTCACTGACTACAACCTTA
pWOX::CRE-RB3	GAACATGAAGGCCTTGACAGGA
Rap_Flank_F	GATACACCTGTGGGGCAAAC
RAP_Flank_F2	CAAAGACGAGGAAGTGGTAGAAATGGCG
Rap_Flank_R	CTTTGCTTTGCACGTGTCAGTA
RAP_Flank_R2	CCTTCTCCTATGCCGCTAGTCATCGAAA
RAP3g gen as	GCGGCCGCTTATTAACCAAATGATAAAG
RAP3g gen s	CCTAGGCTTCAAGTATGCATAGTGTCTTTC
Rap3gMLTF1	GGGGGCATACATACTTCATA
Rap3gMLTR1	TCCTCAATCCACTCAGGTAG
Raptor_Seq10-4215	AAGGGTAAATCTTCTTCAAGTTG
Raptor_Seq11-4616	TATACGACGGCGCTTGT
Raptor_Seq12-5017	GTGCTCTTGTACTTCTTGGAAAG
Raptor_Seq13-5418	GAGTGTGGACCTTGATGGAA
Raptor_Seq14-5819	CCAAGTGATCCACAACCAG
Raptor_Seq15-6220	AGCAGAGGTTGCCGTAGGTA

Raptor_Seq1-606	TTTCATTTTTTTACCAACTACAAT
Raptor_Seq16-6621	CCCCTAGTCGCTCTGTTGTT
Raptor_Seq17-7022	AGTGCGTCCGAGCTATGTT
Raptor_Seq18-7423	CATTAGAGTTCAGGCCTCATCT
Raptor_Seq19-7824	CACCCATTCTCTCCTATTGTAG
Raptor_Seq20-8225	ACTCTCTGCTACTTGTTGCATC
Raptor_Seq2-1007	TAATTAAACTAGACTGAT
Raptor_Seq21-8626	CACTTTGGGACCTGGAGAA
Raptor_Seq22-9027	CTTTAACAGAACTCCTCA
Raptor_Seq23-9428	AGGGACACATACCTGACGA
Raptor_Seq24-9829	TTCGTTAGCCTCCGTCCAA
Raptor_Seq3-1408	CCAATTTTCGCATCCTCAC
Raptor_Seq4-1809	GGTTCTCGCAATCTTCTGTT
Raptor_Seq5-2210	TGCTATTGTTGCTACTATGTTAG
Raptor_Seq6-2611	CCTTTTTTTTTGTCGCCACAG
Raptor_Seq7-3012	CTCTACCATGTTCTTGTTCC
Raptor_Seq8-3413	CGTTGAGTTTCCAGCTGATGTT
Raptor_Seq9-3814	CTTTCTGTCTGGCTAAGTATT
SAIL_400LP	TTAATGGTGTCTCGGTTCTCG
SAIL_400RP2	CCCCAATCATGAAGCTGGCG
SALK_002459_LP	AGCTTCGAAAAGGAGAGGATG
SALK_002459_RP	ATCTAGCTGCAGCTTGCAATC
SALK_043920LP.1	GCCAGAAGCTTAGCTAACTTATA
SALK_043920RP.1	CACTAGAGATCATATAATACGA
tor-3LP	TGTCCCTGTAGATTGCTCCAC
tor-3RP	GGCAGTCAAACCTATCAGCCTG
WOX_F	TTTTACATCTTGCAGTCATC
WOXb_L	TGGGTACGTCATCAATCACAGGGA
WOXb_R	ACGAGTGACCACAAACAAAGCCA
WOX-LB1	GAGCTGATTTTCGAGAACGCCTCAGCCAGCAACTCG
WOX-LB2	TTACGCTTGGTGGCACAGTTCTCGTCCACAGTTCCG
WOX-LB3	ATCGCGCGCGGTGTCATCTA

Appendix 15 Significantly differentially expressed genes related to auxin signalling in *raptor3g raptor5g* mutants. Differential gene expression data received from the comparison of transcriptomes from wt and *raptor3g raptor5g* mutants was analysed with MAPMAN. Table shows differentially expressed genes (P value ≤ 0.01) within the functional cluster of auxin-related genes. The relative change of expression in *raptor3g raptor5g* mutants compared to wt plants is given in log2 scale.

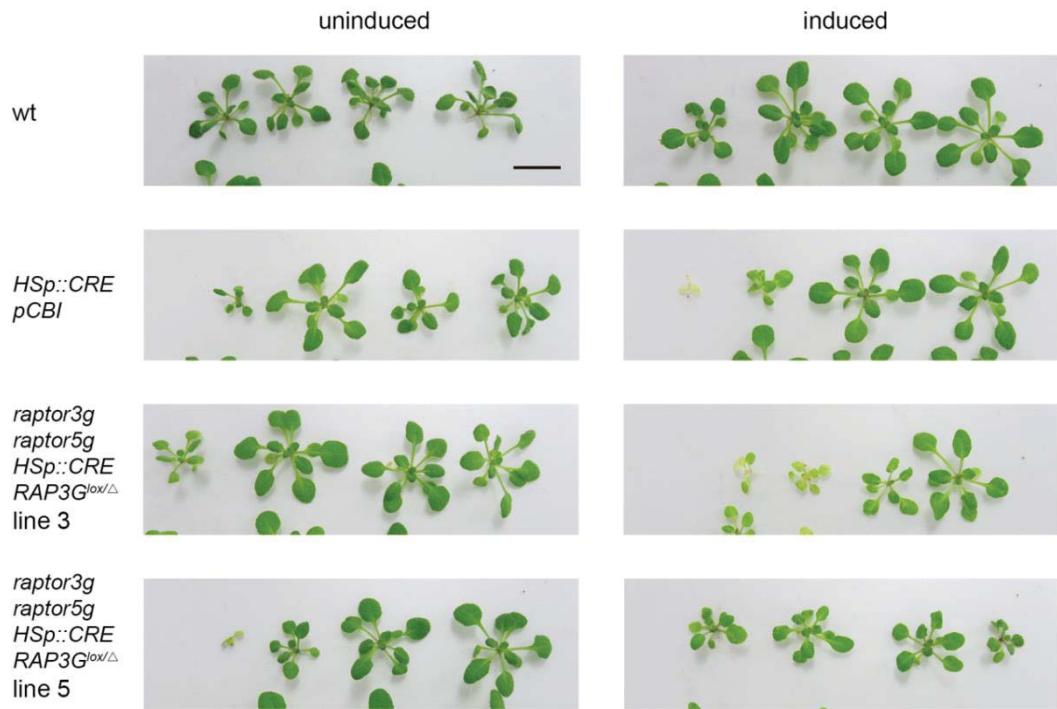
Gene ID	Gene name and description	log2
at1g05560	Symbols: UGT1, UGT75B1 UGT75B1 (UDP-GLUCOSYLTRANSFERASE 75B1); UDP-glucose:4-aminobenzoate acylglucosyltransferase/ UDP-glucosyltransferase/ UDP-glycosyltransferase/ abscisic acid glucosyltransferase/ transferase, transferring glycosyl groups chr1:1645498-1647147 REVERSE	-0.224
at1g12820	Symbols: AFB3 AFB3 (AUXIN SIGNALING F-BOX 3); auxin binding / ubiquitin-protein ligase chr1:4368760-4371293 REVERSE	0.407
at1g14970	unknown protein chr1:5161949-5164917 REVERSE	-0.44
at1g16510	auxin-responsive family protein chr1:5644572-5645443 REVERSE	1.72
at1g20470	auxin-responsive family protein chr1:7094260-7094869 FORWARD	-0.524
at1g23080	Symbols: PIN7, ATPIN7 PIN7 (PIN-FORMED 7); auxin efflux transmembrane transporter/ auxin:hydrogen symporter/ transporter chr1:8180577-8183570 REVERSE	-0.813
at1g28130	Symbols: GH3.17 GH3.17; indole-3-acetic acid amido synthetase chr1:9825286- 9828067 FORWARD	0.653
at1g29430	auxin-responsive family protein chr1:10302650-10303335 REVERSE	-0.751
at1g29450	auxin-responsive protein, putative chr1:10305951-10306499 REVERSE	-0.691
at1g29460	auxin-responsive protein, putative chr1:10307507-10308143 REVERSE	-0.69
at1g29500	auxin-responsive protein, putative chr1:10321210-10321864 FORWARD	-0.622
at1g51760	Symbols: IAR3, JR3 IAR3 (IAA-ALANINE RESISTANT 3); IAA-Ala conjugate hydrolase/ metalloproteinase chr1:19199419-19201642 FORWARD	0.273
at1g53700	Symbols: WAG1, PK3AT WAG1 (WAG 1); kinase/ protein serine/threonine kinase chr1:20048586-20050115 FORWARD	-0.896
at1g56150	auxin-responsive family protein chr1:21017385-21017939 FORWARD	1.172
at1g60680	aldo/keto reductase family protein chr1:22347622-22349297 REVERSE	1.092
at1g60690	aldo/keto reductase family protein chr1:22349892-22351668 REVERSE	-0.74
at1g60730	aldo/keto reductase family protein chr1:22358035-22360158 REVERSE	1.184
at1g68370	Symbols: ARG1 ARG1 (ALTERED RESPONSE TO GRAVITY 1); cytoskeletal protein binding chr1:25631745-25634738 REVERSE	0.246
at1g70940	Symbols: PIN3, ATPIN3 PIN3 (PIN-FORMED 3); auxin:hydrogen symporter/ transporter chr1:26743054-26746395 FORWARD	-0.33
at1g72430	auxin-responsive protein-related chr1:27264911-27265630 REVERSE	-1.069
at1g73590	Symbols: PIN1, ATPIN1 PIN1 (PIN-FORMED 1); transporter chr1:27659673- 27663178 FORWARD	-1.037
at1g76190	auxin-responsive family protein chr1:28592225-28592596 FORWARD	0.912
at1g76270	unknown protein chr1:28613207-28616739 REVERSE	-0.528
at1g77110	Symbols: PIN6 PIN6 (PIN-FORMED 6); auxin:hydrogen symporter/ transporter chr1:28970802-28974603 FORWARD	-0.568
at2g01420	Symbols: PIN4 PIN4 (PIN-FORMED 4); auxin:hydrogen symporter/ transporter chr2:180105-183328 REVERSE	-0.261
at2g04850	auxin-responsive protein-related chr2:1704283-1705778 FORWARD	-0.72
at2g07677	auxin-responsive factor (ARF) -related, low similarity to auxin response factor 10 (<i>Arabidopsis thaliana</i>) GI:6165644; blastp match of 82% identity and 6.9e-77 P-value to GP 3717296 emb CAA03738.1 A63701 unnamed protein product chr2:3278376- 3280384 FORWARD	-2.757

at2g21210	auxin-responsive protein, putative chr2:9085210-9085909 REVERSE	0.494
at2g23170	Symbols: GH3.3 GH3.3; indole-3-acetic acid amido synthetase chr2:9863855-9866562 REVERSE	-0.711
at2g33830	dormancy/auxin associated family protein chr2:14309484-14310351 REVERSE	0.639
at2g34680	Symbols: AIR9 AIR9; protein binding chr2:14616622-14629129 REVERSE	-0.555
at2g46690	auxin-responsive family protein chr2:19180730-19181467 FORWARD	0.373
at2g47750	Symbols: GH3.9 GH3.9 (PUTATIVE INDOLE-3-ACETIC ACID-AMIDO SYNTHETASE GH3.9) chr2:19560127-19563191 REVERSE	-0.497
at3g02250	unknown protein chr3:423801-427061 REVERSE	-0.342
at3g03810	Symbols: EDA30 EDA30 (embryo sac development arrest 30) chr3:971672-976367 REVERSE	-0.345
at3g03820	auxin-responsive protein, putative chr3:976933-977223 REVERSE	-1.489
at3g03830	auxin-responsive protein, putative chr3:979984-980488 REVERSE	-1.457
at3g03840	auxin-responsive protein, putative chr3:981072-981798 FORWARD	-1.827
at3g03850	auxin-responsive protein, putative chr3:983121-983751 FORWARD	-1.907
at3g07390	Symbols: AIR12 AIR12; extracellular matrix structural constituent chr3:2365301-2366496 FORWARD	-0.581
at3g10870	Symbols: MES17, ATMES17 MES17 (METHYL ESTERASE 17); hydrolase/ hydrolase, acting on ester bonds / methyl indole-3-acetate esterase chr3:3401078-3402672 REVERSE	-0.374
at3g12830	auxin-responsive family protein chr3:4078651-4079608 REVERSE	0.907
at3g15450	unknown protein chr3:5212984-5214121 FORWARD	1.999
at3g26370	unknown protein chr3:9656744-9659935 FORWARD	-0.31
at3g30300	FUNCTIONS IN: molecular_function unknown; INVOLVED IN: biological_process unknown; LOCATED IN: endomembrane system; EXPRESSED IN: 22 plant structures; EXPRESSED DURING: 13 growth stages; CONTAINS InterPro DOMAIN/s: Protein of unknown function DUF246, plant (InterPro:IPR004348); BEST Arabidopsis thaliana protein match is: EDA30 (embryo sac development arrest 30) (TAIR:AT3G03810.1); Has 512 Blast hits to 417 proteins in 20 species: Archae - 0; Bacteria - 0; Metazoa - 0; Fungi - 0; Plants - 512; Viruses - 0; Other Eukaryotes - 0 (source: NCBI BLink). chr3:11921198-11924414 REVERSE	-0.251
at3g44300	Symbols: NIT2 NIT2 (nitrilase 2); indole-3-acetonitrile nitrilase/ indole-3-acetonitrile nitrile hydratase/ nitrilase chr3:15983311-15985535 FORWARD	1.817
at3g47620	Symbols: AtTCP14 AtTCP14 (TEOSINTE BRANCHED1, CYCLOIDEA and PCF (TCP) 14); transcription factor chr3:17558849-17560767 FORWARD	-0.302
at3g54100	unknown protein chr3:20034071-20037953 REVERSE	0.358
at3g60690	auxin-responsive family protein chr3:22435121-22435949 FORWARD	1.061
at3g62980	Symbols: TIR1 TIR1 (TRANSPORT INHIBITOR RESPONSE 1); auxin binding / protein binding / ubiquitin-protein ligase chr3:23273116-23276375 REVERSE	-0.334
at4g00880	auxin-responsive family protein chr4:366373-367274 REVERSE	-0.402
at4g02980	Symbols: ABP1, ABP ABP1 (ENDOPLASMIC RETICULUM AUXIN BINDING PROTEIN 1); auxin binding chr4:1319656-1321477 REVERSE	-0.284
at4g12980	auxin-responsive protein, putative chr4:7589395-7591102 REVERSE	-1.252
at4g27260	Symbols: GH3.5, WES1 WES1; indole-3-acetic acid amido synthetase chr4:13653609-13656204 FORWARD	1.177
at4g27450	unknown protein chr4:13727484-13728886 REVERSE	0.397
at4g34750	auxin-responsive protein, putative / small auxin up RNA (SAUR_E) chr4:16577482-16578452 FORWARD	0.621
at4g34790	auxin-responsive family protein chr4:16594469-16595153 FORWARD	1.408
at4g34800	auxin-responsive family protein chr4:16596860-16597144 FORWARD	1.364

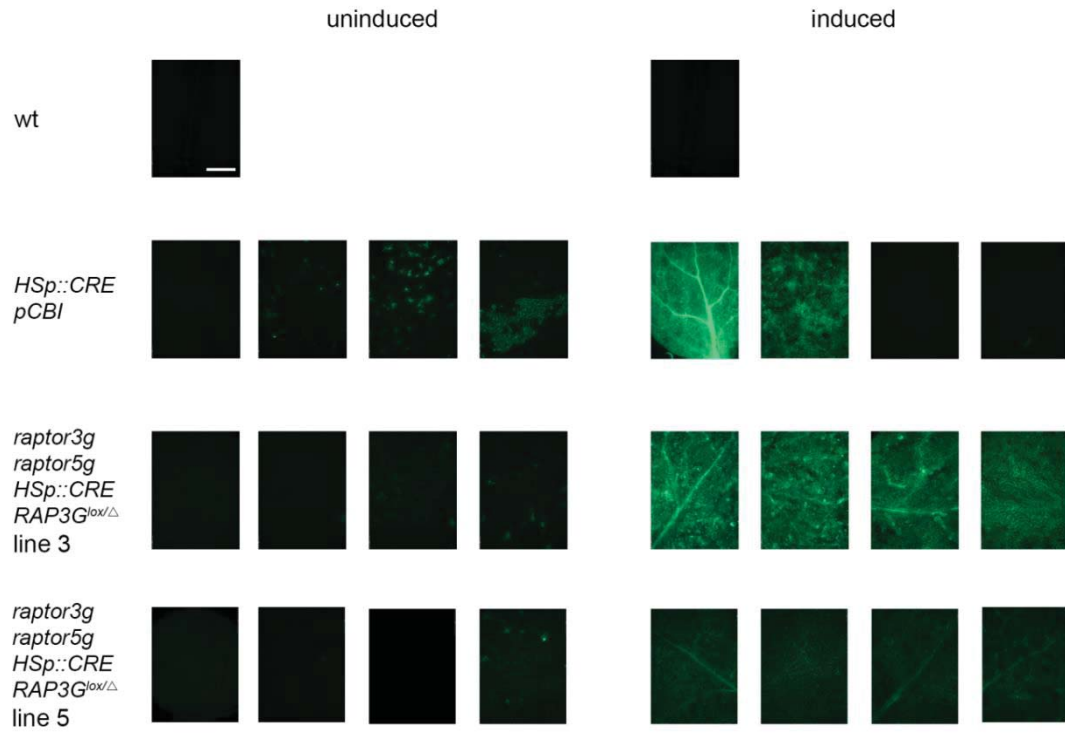
at4g38850	Symbols: SAUR_AC1, ATSAUR15, SAUR15, SAUR-AC1 SAUR15 (SMALL AUXIN UPREGULATED 15) chr4:18126171-18126680 FORWARD	-0.529
at5g10990	auxin-responsive family protein chr5:3476839-3477704 FORWARD	-2.641
at5g13360	auxin-responsive GH3 family protein chr5:4283466-4286295 FORWARD	0.316
at5g13370	auxin-responsive GH3 family protein chr5:4286819-4289554 FORWARD	0.801
at5g16530	Symbols: PIN5 PIN5 (PIN-FORMED 5); auxin:hydrogen symporter/ transporter chr5:5400735-5402626 FORWARD	-1.188
at5g18010	auxin-responsive protein, putative chr5:5962897-5963405 REVERSE	-1.587
at5g18020	auxin-responsive protein, putative chr5:5966183-5966677 REVERSE	-1.676
at5g18030	auxin-responsive protein, putative chr5:5968435-5968938 FORWARD	-1.497
at5g18050	auxin-responsive protein, putative chr5:5974567-5975054 REVERSE	-1.836
at5g18060	auxin-responsive protein, putative chr5:5975954-5976496 FORWARD	-1.043
at5g18080	auxin-responsive protein, putative chr5:5983840-5984112 FORWARD	-0.948
at5g20820	auxin-responsive protein-related chr5:7046751-7047396 REVERSE	-1.643
at5g25980	Symbols: TGG2, BGLU37 TGG2 (GLUCOSIDE GLUCOHYDROLASE 2); hydrolase, hydrolyzing O-glycosyl compounds / thioglucosidase chr5:9072727-9075690 FORWARD	-1.87
at5g35735	auxin-responsive family protein chr5:13900752-13902997 REVERSE	0.386
at5g43830	unknown protein chr5:17622336-17624329 REVERSE	-0.612
at5g50760	auxin-responsive family protein chr5:20644661-20645469 FORWARD	1.94
at5g51470	auxin-responsive GH3 family protein chr5:20907287-20909340 FORWARD	-1.207
at5g54510	Symbols: GH3.6, DFL1 DFL1 (DWARF IN LIGHT 1); indole-3-acetic acid amido synthetase chr5:22131093-22133678 REVERSE	0.42
at5g56660	Symbols: ILL2 ILL2; IAA-Ala conjugate hydrolase/ IAA-amino acid conjugate hydrolase/ metalloproteinase chr5:22933267-22935316 FORWARD	0.411
at5g57090	Symbols: EIR1, WAV6, ATPIN2, PIN2, AGR, AGR1 EIR1 (ETHYLENE INSENSITIVE ROOT 1); auxin efflux transmembrane transporter/ auxin:hydrogen symporter/ transporter chr5:23100693-23104735 FORWARD	1.487
at5g65470	unknown protein chr5:26172131-26175033 FORWARD	-0.507

Appendix 16 Relative expression of auxin-transport and auxin-response marker genes in *raptor3g raptor5g* mutants. Differential gene expression data was received from the comparison of transcriptomes from wt and *raptor3g raptor5g* mutants (Chapter 2.4). Selection of auxin-response marker genes was based on Paponov et al. (2008). Only significantly differentially expressed genes are shown (P value ≤ 0.01). The relative change of expression in *raptor3g raptor5g* mutants compared to wt plants is given in log2 scale.

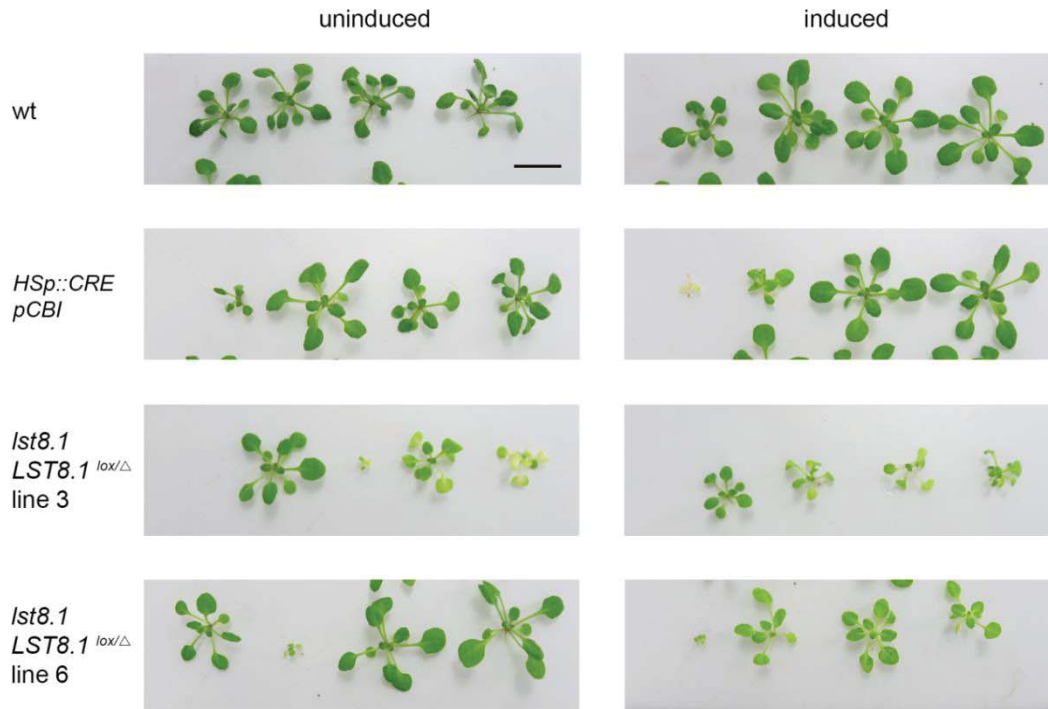
Gene ID	Gene name	log2
AT2G34650	PID	-0.912
AT1G73590	PIN1	-1.046
AT1G70940	PIN3	-0.339
AT2G01420	PIN4	-0.294
AT5G16530	PIN5	-1.21
AT1G77110	PIN6	-0.573
AT1G23080	PIN7	-0.851
AT1G53700	WAG1	-0.896
AT3G14370	WAG2	-1.446
AT1G15580	IAA5	-3.726
AT2G33310	IAA13	-0.289
AT3G15540	IAA19	-1.769
AT4G32280	IAA29	-2.051
AT4G17350	AT4G17350	-0.774
AT5G19530	ACL5	-0.664
AT5G06860	PGIP1	0.771
AT4G37770	ACS8	1.024



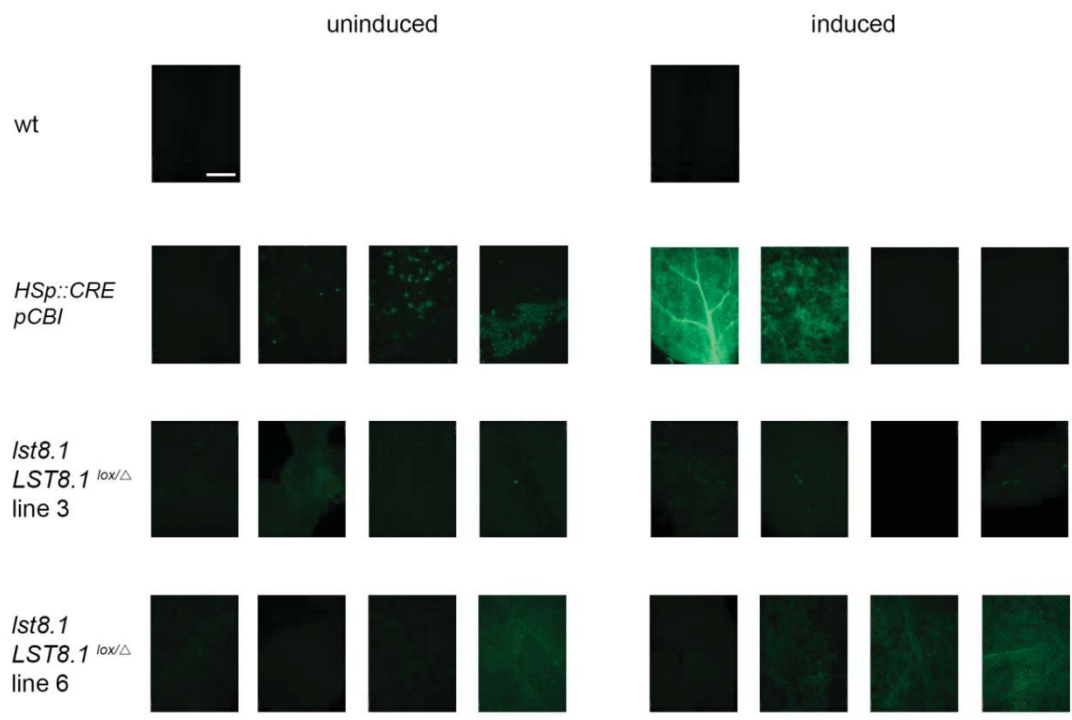
Appendix 17 Induction of *HSp::CRE RAPTOR3G^{lox}* and control lines Wt plants, the empty vector control *HS::CRE pCBI*, and the *RAPTOR3G^{lox}* lines 3 and 5 were grown under short day conditions for three weeks. Treated plants were induced weekly for 4h starting at the age of one week. Fluorescence images of corresponding plants are shown in Appendix 18. Sale bar = 1cm.



Appendix 18 Fluorescence images corresponding to plants shown in Appendix 17. Fluorescence images were taken under UV light of a leaf of the first leaf pair. Scale bar = 200μm.



Appendix 19 Induction of *LST8.1* deletions in *LST8.1^{lox}* lines 3 and 6. Wt plants, the empty vector control *HS::CRE pCBI*, and *LST8.1^{lox}* lines were grown under short day conditions for three weeks. Treated plants were induced weekly for 4h starting at the age of one week. Fluorescence images of corresponding plants are shown in Appendix 20. Sale bar = 1cm.



Appendix 20 Fluorescence images corresponding to plants shown in Appendix 19. Fluorescence images were taken under UV light of a leaf of the first leaf pair. Scale bar = 200µm.

Bibliography

- Adami, A., Garcia-Alvarez, B., Arias-Palomo, E., Barford, D., and Llorca, O.** (2007). Structure of TOR and its complex with KOG1. *Mol Cell* **27**, 509-516.
- Ahn, C.S., Ahn, H.-K., and Pai, H.-S.** (2014). Overexpression of the PP2A regulatory subunit Tap46 leads to enhanced plant growth through stimulation of the TOR signalling pathway. *Journal of Experimental Botany*.
- Ahn, C.S., Han, J.A., Lee, H.S., Lee, S., and Pai, H.S.** (2011). The PP2A Regulatory Subunit Tap46, a Component of the TOR Signaling Pathway, Modulates Growth and Metabolism in Plants. *The Plant Cell* **23**, 185-209.
- Alarcon, C.M., Heitman, J., and Cardenas, M.E.** (1999). Protein kinase activity and identification of a toxic effector domain of the target of rapamycin TOR proteins in yeast. *Mol Biol Cell* **10**, 2531-2546.
- Alexander, M.P.** (1969). Differential Staining of Aborted and Nonaborted Pollen. *Stain Technology* **44**, 117.
- Amasino, R.** (2010). Seasonal and developmental timing of flowering. *The Plant Journal* **61**, 1001-1013.
- Anderson, G.H., and Hanson, M.R.** (2005). The Arabidopsis Mei2 homologue AML1 binds AtRaptor1B, the plant homologue of a major regulator of eukaryotic cell growth. *BMC Plant Biol* **5**, 2.
- Anderson, G.H., Veit, B., and Hanson, M.R.** (2005). The Arabidopsis AtRaptor genes are essential for post-embryonic plant growth. *BMC Biol* **3**, 12.
- Andrade, M.A., and Bork, P.** (1995). HEAT repeats in the Huntington's disease protein. *Nat Genet* **11**, 115-116.
- Audhya, A., Loewith, R., Parsons, A.B., Gao, L., Tabuchi, M., Zhou, H., Boone, C., Hall, M.N., and Emr, S.D.** (2004). Genome-wide lethality screen identifies new PI4,5P(2) effectors that regulate the actin cytoskeleton. *The EMBO Journal* **23**, 3747-3757.
- Barrow, J.R.** (1982). Comparisons among pollen viability measurement methods in cotton *Gossypium hirsutum*. *Crop Science (USA)*.
- Bashandy, T., Guillemint, J., Vernoux, T., Caparros-Ruiz, D., Ljung, K., Meyer, Y., and Reichheld, J.P.** (2010). Interplay between the NADP-linked thioredoxin and glutathione systems in Arabidopsis auxin signaling. *Plant Cell* **22**, 376-391.
- Bastow, R., Mylne, J.S., Lister, C., Lippman, Z., Martienssen, R.A., and Dean, C.** (2004). Vernalization requires epigenetic silencing of FLC by histone methylation. *Nature* **427**, 164-167.
- Baumberger, N., Ringli, C., and Keller, B.** (2001). The chimeric leucine-rich repeat/extensin cell wall protein LRX1 is required for root hair morphogenesis in Arabidopsis thaliana. *Genes Dev* **15**, 1128-1139.
- Baumberger, N., Steiner, M., Ryser, U., Keller, B., and Ringli, C.** (2003). Synergistic interaction of the two paralogous Arabidopsis genes LRX1 and LRX2 in cell wall formation during root hair development. *Plant J* **35**, 71-81.

- Bayley, C.C., Morgan, M., Dale, E.C., and Ow, D.W.** (1992). Exchange of gene activity in transgenic plants catalyzed by the Cre-lox site-specific recombination system. *Plant Mol Biol* **18**, 353-361.
- Bentzinger, C.F., Romanino, K., Cloëtta, D., Lin, S., Mascarenhas, J.B., Oliveri, F., Xia, J., Casanova, E., Costa, C.F., Brink, M., Zorzato, F., Hall, M.N., and Rüegg, M.A.** (2008). Skeletal Muscle-Specific Ablation of raptor, but Not of rictor, Causes Metabolic Changes and Results in Muscle Dystrophy. *Cell Metabolism* **8**, 411-424.
- Berchtold, D., Piccolis, M., Chiaruttini, N., Riezman, I., Riezman, H., Roux, A., Walther, T.C., and Loewith, R.** (2012). Plasma membrane stress induces relocalization of Slm proteins and activation of TORC2 to promote sphingolipid synthesis. *Nat Cell Biol* **14**, 542-547.
- Beretta, L., Gingras, A.C., Svitkin, Y.V., Hall, M.N., and Sonenberg, N.** (1996). Rapamycin blocks the phosphorylation of 4E-BP1 and inhibits cap-dependent initiation of translation. *EMBO J* **15**, 658-664.
- Berger, S.L., Pina, B., Silverman, N., Marcus, G.A., Agapite, J., Regier, J.L., Triezenberg, S.J., and Guarente, L.** (1992). Genetic isolation of ADA2: a potential transcriptional adaptor required for function of certain acidic activation domains. *Cell* **70**, 251-265.
- Berset, C., Trachsel, H., and Altmann, M.** (1998). The TOR (target of rapamycin) signal transduction pathway regulates the stability of translation initiation factor eIF4G in the yeast *Saccharomyces cerevisiae*. *Proc Natl Acad Sci U S A* **95**, 4264-4269.
- Bhalerao, R.P., Salchert, K., Bako, L., Okresz, L., Szabados, L., Muranaka, T., Machida, Y., Schell, J., and Koncz, C.** (1999). Regulatory interaction of PRL1 WD protein with Arabidopsis SNF1-like protein kinases. *Proc Natl Acad Sci U S A* **96**, 5322-5327.
- Bickle, M., Delley, P.A., Schmidt, A., and Hall, M.N.** (1998). Cell wall integrity modulates RHO1 activity via the exchange factor ROM2. *The EMBO Journal* **17**, 2235-2245.
- Biondi, R.M., Kieloch, A., Currie, R.A., Deak, M., and Alessi, D.R.** (2001). The PIF-binding pocket in PDK1 is essential for activation of S6K and SGK, but not PKB. *EMBO J* **20**, 4380-4390.
- Bjedov, I., Toivonen, J.M., Kerr, F., Slack, C., Jacobson, J., Foley, A., and Partridge, L.** (2010). Mechanisms of Life Span Extension by Rapamycin in the Fruit Fly *Drosophila melanogaster*. *Cell Metabolism* **11**, 35-46.
- Blanc, G., Barakat, A., Guyot, R., Cooke, R., and Delseny, M.** (2000). Extensive Duplication and Reshuffling in the Arabidopsis Genome (*American Society of Plant Physiologists*), pp. 1093.
- Blättler, S.M., Cunningham, J.T., Verdeguer, F., Chim, H., Haas, W., Liu, H., Romanino, K., Rüegg, M.A., Gygi, S.P., Shi, Y., and Puigserver, P.** (2012). Yin Yang 1 deficiency in skeletal muscle protects against rapamycin-induced diabetic-like symptoms through activation of insulin/IGF signaling. *Cell Metabolism* **15**, 505-517.
- Block, M.D., Botterman, J., Vandewiele, M., Dockx, J., Thoen, C., Gossele, V., Movva, N.R., Thompson, C., Montagu, M.V., and Leemans, J.** (1987). Engineering herbicide resistance in plants by expression of a detoxifying enzyme. *EMBO J* **6**, 2513-2518.
- Bögre, L., Henriques, R., and Magyar, Z.** (2013). TOR tour to auxin. *The EMBO Journal* **32**, 1069-1071.
- Bohni, R., Riesgo-Escovar, J., Oldham, S., Brogiolo, W., Stocker, H., Andrus, B.F., Beckingham, K., and Hafen, E.** (1999). Autonomous control of cell and organ size by CHICO, a *Drosophila* homolog of vertebrate IRS1-4. *Cell* **97**, 865-875.

- Boulbes, D., Chen, C.-H., Shaikenov, T., Agarwal, N.K., Peterson, T.R., Addona, T.A., Keshishian, H., Carr, S.A., Magnuson, M.A., Sabatini, D.M., and Sarbassov, D.D.** (2010). Rictor Phosphorylation on the Thr-1135 Site Does Not Require Mammalian Target of Rapamycin Complex 2. *Molecular Cancer Research* **8**, 896-906.
- Bourdon, M., Coriton, O., Pirrello, J., Cheniclet, C., Brown, S.C., Poujol, C., Chevalier, C., Renaudin, J.P., and Frangne, N.** (2011). In planta quantification of endoreduplication using fluorescent in situ hybridization (FISH). *Plant J* **66**, 1089-1099.
- Boyes, D.C., Zayed, A.M., Ascenzi, R., McCaskill, A.J., Hoffman, N.E., Davis, K.R., and Görlach, J.** (2001). Growth Stage –Based Phenotypic Analysis of Arabidopsis: A Model for High Throughput Functional Genomics in Plants. *The Plant Cell* **13**, 1499-1510.
- Brand, M.D., Affourtit, C., Esteves, T.C., Green, K., Lambert, A.J., Miwa, S., Pakay, J.L., and Parker, N.** (2004). Mitochondrial superoxide: production, biological effects, and activation of uncoupling proteins. *Free radical biology & medicine* **37**, 755-767.
- Brocard, J., Feil, R., Chambon, P., and Metzger, D.** (1998). A chimeric Cre recombinase inducible by synthetic, but not by natural ligands of the glucocorticoid receptor. *Nucleic Acids Res* **26**, 4086-4090.
- Brogliolo, W., Stocker, H., Ikeya, T., Rintelen, F., Fernandez, R., and Hafen, E.** (2001). An evolutionarily conserved function of the Drosophila insulin receptor and insulin-like peptides in growth control. *Current Biology* **11**, 213-221.
- Brown, E.J.A., M. W.; Shin, T. T.; Ichikawa, T.; Keith, C. T.; Lane, W. S.; Schreiber, S. L.** (1994). A mammalian protein targeted by G1-arresting rapamycin-receptor complex. *Nature* **369**, 756-758.
- Bruex, A., Kainkaryam, R.M., Wieckowski, Y., Kang, Y.H., Bernhardt, C., Xia, Y., Zheng, X., Wang, J.Y., Lee, M.M., Benfey, P., Woolf, P.J., and Schiefelbein, J.** (2012). A gene regulatory network for root epidermis cell differentiation in Arabidopsis. *PLoS Genet* **8**, e1002446.
- Brugarolas, J., Lei, K., Hurley, R.L., Manning, B.D., Reiling, J.H., Hafen, E., Witters, L.A., Ellisen, L.W., and Kaelin, W.G., Jr.** (2004). Regulation of mTOR function in response to hypoxia by REDD1 and the TSC1/TSC2 tumor suppressor complex. *Genes Dev* **18**, 2893-2904.
- Brunn, G.J., Hudson, C.C., Sekulic, A., Williams, J.M., Hosoi, H., Houghton, P.J., Lawrence, J.C., Jr., and Abraham, R.T.** (1997). Phosphorylation of the translational repressor PHAS-I by the mammalian target of rapamycin. *Science* **277**, 99-101.
- Burnett, P.E., Barrow, R.K., Cohen, N.A., Snyder, S.H., and Sabatini, D.M.** (1998). RAFT1 phosphorylation of the translational regulators p70 S6 kinase and 4E-BP1. *Proc Natl Acad Sci U S A* **95**, 1432-1437.
- Byfield, M.P., Murray, J.T., and Backer, J.M.** (2005). hVps34 Is a Nutrient-regulated Lipid Kinase Required for Activation of p70 S6 Kinase. *Journal of Biological Chemistry* **280**, 33076-33082.
- Cafferkey, R., Young, P.R., McLaughlin, M.M., Bergsma, D.J., Koltin, Y., Sathe, G.M., Faucette, L., Eng, W.K., Johnson, R.K., and Livi, G.P.** (1993). Dominant missense mutations in a novel yeast protein related to mammalian phosphatidylinositol 3-kinase and VPS34 abrogate rapamycin cytotoxicity. *Mol Cell Biol* **13**, 6012-6023.
- Caldana, C., Li, Y., Leisse, A., Zhang, Y., Bartholomaeus, L., Fernie, A.R., Willmitzer, L., and Giavalisco, P.** (2013). Systemic analysis of inducible target of rapamycin mutants reveal a general metabolic switch controlling growth in Arabidopsis thaliana. *The Plant Journal* **73**, 897-909.

- Cárdenas, L.** (2009). New findings in the mechanisms regulating polar growth in root hair cells. *Plant Signaling & Behavior* **4**, 4-8.
- Chan, T.F., Carvalho, J., Riles, L., and Zheng, X.F.** (2000). A chemical genomics approach toward understanding the global functions of the target of rapamycin protein (TOR). *Proc Natl Acad Sci U S A* **97**, 13227-13232.
- Chauvin, C., Koka, V., Nouschi, A., Mieulet, V., Hoareau-Aveilla, C., Dreazen, A., Cagnard, N., Carpentier, W., Kiss, T., Meyuhas, O., and Pende, M.** (2014). Ribosomal protein S6 kinase activity controls the ribosome biogenesis transcriptional program. *Oncogene* **33**, 474-483.
- Chen, E.J.** (2003). LST8 negatively regulates amino acid biosynthesis as a component of the TOR pathway. *The Journal of Cell Biology* **161**, 333-347.
- Chen, G.H., Liu, C.P., Chen, S.C., and Wang, L.C.** (2012a). Role of ARABIDOPSIS A-FIFTEEN in regulating leaf senescence involves response to reactive oxygen species and is dependent on ETHYLENE INSENSITIVE2. *J Exp Bot* **63**, 275-292.
- Chen, G.H., Chan, Y.L., Liu, C.P., and Wang, L.C.** (2012b). Ethylene response pathway is essential for ARABIDOPSIS A-FIFTEEN function in floral induction and leaf senescence. *Plant Signal Behav* **7**, 457-460.
- Chen, H., and Xiong, L.** (2010). myo-Inositol-1-phosphate synthase is required for polar auxin transport and organ development. *J Biol Chem* **285**, 24238-24247.
- Chen, Y., Chen, H., Rhoad, A.E., Warner, L., Caggiano, T.J., Failli, A., Zhang, H., Hsiao, C.L., Nakanishi, K., and Molnar-Kimber, K.L.** (1994). A putative sirolimus (rapamycin) effector protein. *Biochem Biophys Res Commun* **203**, 1-7.
- Cherkasova, V.A., and Hinnebusch, A.G.** (2003). Translational control by TOR and TAP42 through dephosphorylation of eIF2alpha kinase GCN2. *Genes Dev* **17**, 859-872.
- Choi, J., Chen, J., Schreiber, S.L., and Clardy, J.** (1996). Structure of the FKBP12-rapamycin complex interacting with the binding domain of human FRAP. *Science* **273**, 239-242.
- Cook, M., and Tyers, M.** (2007). Size control goes global. *Current Opinion in Biotechnology* **18**, 341-350.
- Corbesier, L., Bernier, G., and Perilleux, C.** (2002). C : N ratio increases in the phloem sap during floral transition of the long-day plants *Sinapis alba* and *Arabidopsis thaliana*. *Plant & cell physiology* **43**, 684-688.
- Corbesier, L., ; Lejeune, p.; Bernier, G.** (1998). The role of carbohydrates in the induction of flowering in *Arabidopsis thaliana*: comparison between the wild type and a starchless mutant. *Planta* **206**, 131-137.
- Cosentino, G.P., Schmelzle, T., Haghghat, A., Helliwell, S.B., Hall, M.N., and Sonenberg, N.** (2000). Eap1p, a novel eukaryotic translation initiation factor 4E-associated protein in *Saccharomyces cerevisiae*. *Mol Cell Biol* **20**, 4604-4613.
- Cunningham, J.T., Rodgers, J.T., Arlow, D.H., Vazquez, F., Mootha, V.K., and Puigserver, P.** (2007). mTOR controls mitochondrial oxidative function through a YY1-PGC-1 transcriptional complex. *Nature* **450**, 736-740.
- Cybulski, N., Polak, P., Auwerx, J., Ruegg, M.A., and Hall, M.N.** (2009). mTOR complex 2 in adipose tissue negatively controls whole-body growth. *Proceedings of the National Academy of Sciences* **106**, 9902-9907.

- Dale, E.C., and Ow, D.W.** (1990). Intra- and intermolecular site-specific recombination in plant cells mediated by bacteriophage P1 recombinase. *Gene* **91**, 79-85.
- Dames, S.A.** (2010). Structural basis for the association of the redox-sensitive target of rapamycin FATC domain with membrane-mimetic micelles. *J Biol Chem* **285**, 7766-7775.
- Davie, E., and Petersen, J.** (2012). Environmental control of cell size at division. *Curr Opin Cell Biol* **24**, 838-844.
- De Smet, I., Voss, U., Jurgens, G., and Beeckman, T.** (2009). Receptor-like kinases shape the plant. *Nat Cell Biol* **11**, 1166-1173.
- De Virgilio, C., and Loewith, R.** (2006). The TOR signalling network from yeast to man. *The International Journal of Biochemistry & Cell Biology* **38**, 1476-1481.
- Deak, M., Casamayor, A., Currie, R.A., Downes, C.P., and Alessi, D.R.** (1999). Characterisation of a plant 3-phosphoinositide-dependent protein kinase-1 homologue which contains a pleckstrin homology domain. *FEBS Lett* **451**, 220-226.
- Dello Ioio, R., Linhares, F.S., Scacchi, E., Casamitjana-Martinez, E., Heidstra, R., Costantino, P., and Sabatini, S.** (2007). Cytokinins determine Arabidopsis root-meristem size by controlling cell differentiation. *Current biology : CB* **17**, 678-682.
- Dello Ioio, R., Nakamura, K., Moubayidin, L., Perilli, S., Taniguchi, M., Morita, M.T., Aoyama, T., Costantino, P., and Sabatini, S.** (2008). A genetic framework for the control of cell division and differentiation in the root meristem. *Science* **322**, 1380-1384.
- Deprost, D., Truong, H.N., Robaglia, C., and Meyer, C.** (2005). An Arabidopsis homolog of RAPTOR/KOG1 is essential for early embryo development. *Biochem Biophys Res Commun* **326**, 844-850.
- Deprost, D., Yao, L., Sormani, R., Moreau, M., Leterreux, G., Nicolai, M., Bedu, M., Robaglia, C., and Meyer, C.** (2007). The Arabidopsis TOR kinase links plant growth, yield, stress resistance and mRNA translation. *EMBO Rep* **8**, 864-870.
- Desvoyes, B., Ramirez-Parra, E., Xie, Q., Chua, N.H., and Gutierrez, C.** (2006). Cell type-specific role of the retinoblastoma/E2F pathway during Arabidopsis leaf development. *Plant Physiol* **140**, 67-80.
- DeYoung, M.P., Horak, P., Sofer, A., Sgroi, D., and Ellisen, L.W.** (2008). Hypoxia regulates TSC1/2-mTOR signaling and tumor suppression through REDD1-mediated 14-3-3 shuttling. *Genes Dev* **22**, 239-251.
- Di Como, C.J., and Arndt, K.T.** (1996). Nutrients, via the Tor proteins, stimulate the association of Tap42 with type 2A phosphatases. *Genes Dev* **10**, 1904-1916.
- Di Talia, S., Skotheim, J.M., Bean, J.M., Siggia, E.D., and Cross, F.R.** (2007). The effects of molecular noise and size control on variability in the budding yeast cell cycle. *Nature* **448**, 947-951.
- Diaz-Troya, S., Florencio, F.J., and Crespo, J.L.** (2008). Target of rapamycin and LST8 proteins associate with membranes from the endoplasmic reticulum in the unicellular green alga *Chlamydomonas reinhardtii*. *Eukaryot Cell* **7**, 212-222.
- Dibble, C.C., Asara, J.M., and Manning, B.D.** (2009). Characterization of Rictor phosphorylation sites reveals direct regulation of mTOR complex 2 by S6K1. *Mol Cell Biol* **29**, 5657-5670.

- Dunlop, Elaine A., and Tee, Andrew R.** (2013). The kinase triad, AMPK, mTORC1 and ULK1, maintains energy and nutrient homeostasis. *Biochemical Society Transactions* **41**, 939-943.
- Dunlop, E.A., Dodd, K.M., Seymour, L.A., and Tee, A.R.** (2009). Mammalian target of rapamycin complex 1-mediated phosphorylation of eukaryotic initiation factor 4E-binding protein 1 requires multiple protein-protein interactions for substrate recognition. *Cell Signal* **21**, 1073-1084.
- Dunlop, E.A., Hunt, D.K., Acosta-Jaquez, H.A., Fingar, D.C., and Tee, A.R.** (2011). ULK1 inhibits mTORC1 signaling, promotes multisite Raptor phosphorylation and hinders substrate binding. *Autophagy* **7**, 737-747.
- Ebel, C., Mariconti, L., and Gruissem, W.** (2004). Plant retinoblastoma homologues control nuclear proliferation in the female gametophyte. *Nature* **429**, 776-780.
- Edgar, B.A.** (2006). How flies get their size: genetics meets physiology. *Nature Reviews Genetics*, 907.
- Ellisen, L.W., Ramsayer, K.D., Johannessen, C.M., Yang, A., Beppu, H., Minda, K., Oliner, J.D., McKeon, F., and Haber, D.A.** (2002). REDD1, a developmentally regulated transcriptional target of p63 and p53, links p63 to regulation of reactive oxygen species. *Mol Cell* **10**, 995-1005.
- Fadri, M., Daquinag, A., Wang, S., Xue, T., and Kunz, J.** (2005). The Pleckstrin Homology Domain Proteins Slm1 and Slm2 Are Required for Actin Cytoskeleton Organization in Yeast and Bind Phosphatidylinositol-4,5-Bisphosphate and TORC2. *Molecular Biology of the Cell* **16**, 1883-1900.
- Fang, Y., Vilella-Bach, M., Bachmann, R., Flanigan, A., and Chen, J.** (2001). Phosphatidic Acid-Mediated Mitogenic Activation of mTOR Signaling (American Society for the Advancement of Science), pp. 1942.
- Feng, Z., Zhang, H., Levine, A.J., and Jin, S.** (2005). The coordinate regulation of the p53 and mTOR pathways in cells. *Proceedings of the National Academy of Sciences of the United States of America* **102**, 8204-8209.
- Foreman, J., Demidchik, V., Bothwell, J.H., Mylona, P., Miedema, H., Torres, M.A., Linstead, P., Costa, S., Brownlee, C., Jones, J.D., Davies, J.M., and Dolan, L.** (2003). Reactive oxygen species produced by NADPH oxidase regulate plant cell growth. *Nature* **422**, 442-446.
- Freire, M.A., Tourneur, C., Granier, F., Camonis, J., El Amrani, A., Browning, K.S., and Robaglia, C.** (2000). Plant lipoxygenase 2 is a translation initiation factor-4E-binding protein. *Plant Mol Biol* **44**, 129-140.
- Frias, M.A., Thoreen, C.C., Jaffe, J.D., Schroder, W., Sculley, T., Carr, S.A., and Sabatini, D.M.** (2006). mSin1 is necessary for Akt/PKB phosphorylation, and its isoforms define three distinct mTORC2s. *Current biology : CB* **16**, 1865-1870.
- Friml, J.Y., X.; Michniewicz, M.; Weijers, D.; Quint, A.T., O.; Benjamins, R., Ouwkerk, P.L., K.; Sandberg, G., and Hooykaas, P.P., K.; Offringa, R.** (2004). A PINOID-Dependent Binary Switch in Apical-Basal PIN Polar Targeting Directs Auxin Efflux.
- Galloni, M., and Edgar, B.A.** (1999). Cell-autonomous and non-autonomous growth-defective mutants of *Drosophila melanogaster*. *Development (Cambridge, England)* **126**, 2365-2375.

- Gancz, D., and Gilboa, L.** (2013). Insulin and Target of rapamycin signaling orchestrate the development of ovarian niche-stem cell units in *Drosophila*. *Development* **140**, 4145-4154.
- Gangloff, Y.G., Mueller, M., Dann, S.G., Svoboda, P., Sticker, M., Spetz, J.F., Um, S.H., Brown, E.J., Cereghini, S., Thomas, G., and Kozma, S.C.** (2004). Disruption of the Mouse mTOR Gene Leads to Early Postimplantation Lethality and Prohibits Embryonic Stem Cell Development. *Molecular and Cellular Biology* **24**, 9508-9516.
- Ganley, I.G., Lam du, H., Wang, J., Ding, X., Chen, S., and Jiang, X.** (2009). ULK1.ATG13.FIP200 complex mediates mTOR signaling and is essential for autophagy. *J Biol Chem* **284**, 12297-12305.
- Gao, X.Q., and Zhang, X.S.** (2012). Metabolism and roles of phosphatidylinositol 3-phosphate in pollen development and pollen tube growth in *Arabidopsis*. *Plant Signal Behav* **7**, 165-169.
- Garrocho-Villegas, V., and de Jimenez, E.S.** (2012). TOR pathway activation in *Zea mays* L. tissues: conserved function between animal and plant kingdoms. *Plant Signal Behav* **7**, 675-677.
- Gendall, A.R., Levy, Y.Y., Wilson, A., and Dean, C.** (2001). The VERNALIZATION 2 Gene Mediates the Epigenetic Regulation of Vernalization in *Arabidopsis*. *Cell* **107**, 525-535.
- Giardine, B., Hardison, R.C., Elnitski, L., Albert, I., Kent, W.J., Riemer, C., Burhans, R., Shah, P., Yi, Z., Blakenberg, D., Taylor, J., Nekrutenko, A., and Miller, W.** (2005). Galaxy: A platform for interactive large-scale genome analysis (Cold Spring Harbor Laboratory Press), pp. 1451.
- Gingras, A.C.** (2001). Regulation of translation initiation by FRAP/mTOR. *Genes & Development* **15**, 807-826.
- Goff, L.T., C. and Kelley, D.** (2013). cummeRbund: Analysis, exploration, manipulation, and visualization of Cufflinks high-throughput sequencing data. R package version 2.8.2.
- Grandison, R.C., Piper, M.D.W., and Partridge, L.** (2009). Amino acid imbalance explains extension of lifespan by dietary restriction in *Drosophila*. *Nature* **462**, 1061-1064.
- Groves, M.R., and Barford, D.** (1999). Topological characteristics of helical repeat proteins. *Curr Opin Struct Biol* **9**, 383-389.
- Guertin, D.A., Stevens, D.M., Thoreen, C.C., Burds, A.A., Kalaany, N.Y., Moffat, J., Brown, M., Fitzgerald, K.J., and Sabatini, D.M.** (2006). Ablation in mice of the mTORC components raptor, rictor, or mLST8 reveals that mTORC2 is required for signaling to Akt-FOXO and PKCalpha, but not S6K1. *Developmental cell* **11**, 859-871.
- Gupta, R.** (2002). A Tumor Suppressor Homolog, AtPTEN1, Is Essential for Pollen Development in *Arabidopsis*. *The Plant Cell Online* **14**, 2495-2507.
- Gwinn, D.M., Shackelford, D.B., Egan, D.F., Mihaylova, M.M., Mery, A., Vasquez, D.S., Turk, B.E., and Shaw, R.J.** (2008). AMPK phosphorylation of raptor mediates a metabolic checkpoint. *Mol Cell* **30**, 214-226.
- Hacham, Y., Holland, N., Butterfield, C., Ubeda-Tomas, S., Bennett, M.J., Chory, J., and Savaldi-Goldstein, S.** (2011). Brassinosteroid perception in the epidermis controls root meristem size. *Development* **138**, 839-848.
- Haecker, A., Gross-Hardt, R., Geiges, B., Sarkar, A., Breuninger, H., Herrmann, M., and Laux, T.** (2004). Expression dynamics of WOX genes mark cell fate decisions during early embryonic patterning in *Arabidopsis thaliana*. *Development* **131**, 657-668.

- Hara, K., Maruki, Y., Long, X., Yoshino, K., Oshiro, N., Hidayat, S., Tokunaga, C., Avruch, J., and Yonezawa, K.** (2002). Raptor, a binding partner of target of rapamycin (TOR), mediates TOR action. *Cell* **110**, 177-189.
- Hardie, D.G., Carling, D., and Carlson, M.** (1998). The AMP-activated/SNF1 protein kinase subfamily: metabolic sensors of the eukaryotic cell? *Annu Rev Biochem* **67**, 821-855.
- Hardt, M., Chantaravisoot, N., and Tamanoi, F.** (2011). Activating mutations of TOR (target of rapamycin). *Genes Cells* **16**, 141-151.
- Harrison, D.E., Strong, R., Sharp, Z.D., Nelson, J.F., Astle, C.M., Flurkey, K., Nadon, N.L., Wilkinson, J.E., Frenkel, K., Carter, C.S., Pahor, M., Javors, M.A., Fernandez, E., and Miller, R.A.** (2009). Rapamycin fed late in life extends lifespan in genetically heterogeneous mice. *Nature* **460**, 392-395.
- Hartwell, L.H., Mortimer, R.K., Culotti, J., and Culotti, M.** (1973). Genetic Control of the Cell Division Cycle in Yeast: V. Genetic Analysis of *cdc* Mutants. *Genetics* **74**, 267-286.
- He, J.X., Gendron, J.M., Yang, Y., Li, J., and Wang, Z.Y.** (2002). The GSK3-like kinase BIN2 phosphorylates and destabilizes BZR1, a positive regulator of the brassinosteroid signaling pathway in Arabidopsis. *Proc Natl Acad Sci U S A* **99**, 10185-10190.
- He, X., Anderson, J.C., del Pozo, O., Gu, Y.Q., Tang, X., and Martin, G.B.** (2004). Silencing of subfamily I of protein phosphatase 2A catalytic subunits results in activation of plant defense responses and localized cell death. *Plant J* **38**, 563-577.
- Heidstra, R., Welch, D., and Scheres, B.** (2004). Mosaic analyses using marked activation and deletion clones dissect Arabidopsis SCARECROW action in asymmetric cell division. *Genes Dev* **18**, 1964-1969.
- Heitman, J., Movva, N.R., and Hall, M.N.** (1991). Targets for cell cycle arrest by the immunosuppressant rapamycin in yeast. *Science* **253**, 905-909.
- Helliwell, S.B., Wagner, P., Kunz, J., Deuter-Reinhard, M., Henriquez, R., and Hall, M.N.** (1994). TOR1 and TOR2 are structurally and functionally similar but not identical phosphatidylinositol kinase homologues in yeast. *Mol Biol Cell* **5**, 105-118.
- Henriques, R., Magyar, Z., Monardes, A., Khan, S., Zalejski, C., Orellana, J., Szabados, L., de la Torre, C., Koncz, C., and Bögre, L.** (2010). Arabidopsis S6 kinase mutants display chromosome instability and altered RBR1-E2F pathway activity. *The EMBO Journal* **29**, 2979-2993.
- Hirayama, T., Ishida, C., Kuromori, T., Obata, S., Shimoda, C., Yamamoto, M., Shinozaki, K., and Ohto, C.** (1997). Functional cloning of a cDNA encoding Mei2-like protein from Arabidopsis thaliana using a fission yeast pheromone receptor deficient mutant. *FEBS Letters* **413**, 16-20.
- Hoess, R.H., Ziese, M., and Sternberg, N.** (1982). P1 site-specific recombination: nucleotide sequence of the recombining sites. *Proc Natl Acad Sci U S A* **79**, 3398-3402.
- Hong, Y., Pan, X., Welti, R., and Wang, X.** (2008). Phospholipase D α 3 is involved in the hyperosmotic response in Arabidopsis. *Plant Cell* **20**, 803-816.
- Hosokawa, N., Hara, T., Kaizuka, T., Kishi, C., Takamura, A., Miura, Y., Iemura, S., Natsume, T., Takehana, K., Yamada, N., Guan, J.L., Oshiro, N., and Mizushima, N.** (2009). Nutrient-dependent mTORC1 association with the ULK1-Atg13-FIP200 complex required for autophagy. *Mol Biol Cell* **20**, 1981-1991.
- Huang da, W., Sherman, B.T., and Lempicki, R.A.** (2009a). Systematic and integrative analysis of large gene lists using DAVID bioinformatics resources. *Nat Protoc* **4**, 44-57.

- Huang da, W., Sherman, B.T., and Lempicki, R.A.** (2009b). Bioinformatics enrichment tools: paths toward the comprehensive functional analysis of large gene lists. *Nucleic Acids Res* **37**, 1-13.
- Huang, J., and Manning, B.D.** (2008). The TSC1-TSC2 complex: a molecular switchboard controlling cell growth. *Biochem J* **412**, 179-190.
- Huang, J., and Manning, B.D.** (2009). A complex interplay between Akt, TSC2 and the two mTOR complexes. *Biochem Soc Trans* **37**, 217-222.
- Huang, J., Dibble, C.C., Matsuzaki, M., and Manning, B.D.** (2008). The TSC1-TSC2 complex is required for proper activation of mTOR complex 2. *Mol Cell Biol* **28**, 4104-4115.
- Huang, K., and Fingar, D.C.** (2014). Growing knowledge of the mTOR signaling network. *Seminars in cell & developmental biology*.
- Huber, A., French, S.L., Tekotte, H., Yerlikaya, S., Stahl, M., Perepelkina, M.P., Tyers, M., Rougemont, J., Beyer, A.L., and Loewith, R.** (2011). Sch9 regulates ribosome biogenesis via Stb3, Dot6 and Tod6 and the histone deacetylase complex RPD3L. *EMBO J* **30**, 3052-3064.
- Hulskamp, M., Misra, S., and Jurgens, G.** (1994). Genetic dissection of trichome cell development in Arabidopsis. *Cell* **76**, 555-566.
- Ikenoue, T., Inoki, K., Yang, Q., Zhou, X., and Guan, K.L.** (2008). Essential function of TORC2 in PKC and Akt turn motif phosphorylation, maturation and signalling. *EMBO J* **27**, 1919-1931.
- Inoki, K., Li, Y., Xu, T., and Guan, K.L.** (2003). Rheb GTPase is a direct target of TSC2 GAP activity and regulates mTOR signaling. *Genes Dev* **17**, 1829-1834.
- Inoki, K., Li, Y., Zhu, T., Wu, J., and Guan, K.-L.** (2002). TSC2 is phosphorylated and inhibited by Akt and suppresses mTOR signalling. *Nat Cell Biol* **4**, 648-657.
- Inoki, K., Ouyang, H., Zhu, T., Lindvall, C., Wang, Y., Zhang, X., Yang, Q., Bennett, C., Harada, Y., Stankunas, K., Wang, C.Y., He, X., MacDougald, O.A., You, M., Williams, B.O., and Guan, K.L.** (2006). TSC2 integrates Wnt and energy signals via a coordinated phosphorylation by AMPK and GSK3 to regulate cell growth. *Cell* **126**, 955-968.
- Inoue, H., Nojima, H., and Okayama, H.** (1990). High efficiency transformation of Escherichia coli with plasmids. *Gene* **96**, 23-28.
- Jaber, N., Dou, Z., Chen, J.-S., Catanzaro, J., Jiang, Y.-P., Ballou, L.M., Selinger, E., Ouyang, X., Lin, R.Z., Zhang, J., and Zong, W.-X.** (2012). Class III PI3K Vps34 plays an essential role in autophagy and in heart and liver function. *Proceedings of the National Academy of Sciences* **109**, 2003-2008.
- Jacinto, E., Facchinetti, V., Liu, D., Soto, N., Wei, S., Jung, S.Y., Huang, Q., Qin, J., and Su, B.** (2006). SIN1/MIP1 Maintains rictor-mTOR Complex Integrity and Regulates Akt Phosphorylation and Substrate Specificity. *Cell* **127**, 125-137.
- Jackson, A.L., Bartz, S.R., Schelter, J., Kobayashi, S.V., Burchard, J., Mao, M., Li, B., Cavet, G., and Linsley, P.S.** (2003). Expression profiling reveals off-target gene regulation by RNAi. *Nature biotechnology* **21**, 635-637.
- Javelle, M., Vernoud, V., Rogowsky, P.M., and Ingram, G.C.** (2011). Epidermis: the formation and functions of a fundamental plant tissue. *New Phytologist* **189**, 17-39.
- Jefferson, R.** (1987). Assaying chimeric genes in plants: The GUS gene fusion system. *Plant Molecular Biology Reporter* **5**, 387.

- Jia, K., Chen, D., and Riddle, D.L.** (2004). The TOR pathway interacts with the insulin signaling pathway to regulate *C. elegans* larval development, metabolism and life span. *Development* **131**, 3897-3906.
- Jing, Y., Cui, D., Bao, F., Hu, Z., Qin, Z., and Hu, Y.** (2009). Tryptophan deficiency affects organ growth by retarding cell expansion in *Arabidopsis*. *The Plant Journal* **57**, 511-521.
- John, P.C., and Qi, R.** (2008). Cell division and endoreduplication: doubtful engines of vegetative growth. *Trends Plant Sci* **13**, 121-127.
- Jones, K.T., Greer, E.R., Pearce, D., and Ashrafi, K.** (2009). Rictor/TORC2 regulates *Caenorhabditis elegans* fat storage, body size, and development through *sgk-1*. *PLoS Biol* **7**, e60.
- Joo, J.H., Bae, Y.S., and Lee, J.S.** (2001). Role of Auxin-Induced Reactive Oxygen Species in Root Gravitropism. *Plant Physiology* **126**, 1055-1060.
- Jorgensen, P., and Tyers, M.** (2004). How cells coordinate growth and division. *Current biology* : CB **14**, R1014-1027.
- Jorgensen, P., Rupes, I., Sharom, J.R., Schneper, L., Broach, J.R., and Tyers, M.** (2004). A dynamic transcriptional network communicates growth potential to ribosome synthesis and critical cell size. *Genes Dev* **18**, 2491-2505.
- Jossier, M., Bouly, J.P., Meimoun, P., Arjmand, A., Lessard, P., Hawley, S., Grahame Hardie, D., and Thomas, M.** (2009). SnRK1 (SNF1-related kinase 1) has a central role in sugar and ABA signalling in *Arabidopsis thaliana*. *Plant J* **59**, 316-328.
- Julien, L.A., Carriere, A., Moreau, J., and Roux, P.P.** (2010). mTORC1-activated S6K1 phosphorylates Rictor on threonine 1135 and regulates mTORC2 signaling. *Mol Cell Biol* **30**, 908-921.
- Jung, C.H., Seo, M., Otto, N.M., and Kim, D.-H.** (2011). ULK1 inhibits the kinase activity of mTORC1 and cell proliferation. *Autophagy* **7**, 1212-1221.
- Jung, C.H., Jun, C.B., Ro, S.H., Kim, Y.M., Otto, N.M., Cao, J., Kundu, M., and Kim, D.H.** (2009). ULK-Atg13-FIP200 complexes mediate mTOR signaling to the autophagy machinery. *Mol Biol Cell* **20**, 1992-2003.
- Kamada, Y., Yoshino, K.-i., Kondo, C., Kawamata, T., Oshiro, N., Yonezawa, K., and Ohsumi, Y.** (2010). Tor Directly Controls the Atg1 Kinase Complex To Regulate Autophagy. *Molecular and Cellular Biology* **30**, 1049-1058.
- Kang, H.G., Fang, Y., and Singh, K.B.** (1999). A glucocorticoid-inducible transcription system causes severe growth defects in *Arabidopsis* and induces defense-related genes. *Plant J* **20**, 127-133.
- Kapahi, P., Zid, B.M., Harper, T., Koslover, D., Sapin, V., and Benzer, S.** (2004). Regulation of Lifespan in *Drosophila* by Modulation of Genes in the TOR Signaling Pathway. *Current biology* : CB **14**, 885-890.
- Kardailsky, I., Shukla, V.K., Ahn, J.H., Dagenais, N., Christensen, S.K., Nguyen, J.T., Chory, J., Harrison, M.J., and Weigel, D.** (1999). Activation Tagging of the Floral Inducer FT (*American Society for the Advancement of Science*), pp. 1962.
- Kaur, J., Sebastian, J., and Siddiqi, I.** (2006). The *Arabidopsis*-*mei2*-like genes play a role in meiosis and vegetative growth in *Arabidopsis*. *Plant Cell* **18**, 545-559.

- Kawai, M.N., A.; Ueno, M.; Ushimaru, T.; Aiba, K.; Doi, H.; Uritani, M.** (2001). Fission yeast Tor1 functions in response to various stresses including nitrogen starvation, high osmolarity, and high temperature. *Curr Genet* **39**, 166-174.
- Kaya, H., Nakajima, R., Iwano, M., Kanaoka, M.M., Kimura, S., Takeda, S., Kawarazaki, T., Senzaki, E., Hamamura, Y., Higashiyama, T., Takayama, S., Abe, M., and Kuchitsu, K.** (2014). Ca²⁺-activated reactive oxygen species production by Arabidopsis RbohH and RbohJ is essential for proper pollen tube tip growth. *The Plant Cell* **26**, 1069-1080.
- Kemp, J.T.B., M.K.; Gould, K.L.** (1997). A *wat1* mutant of fission yeast is defective in cell morphology. *Mol Gen Genet.* **254**, 127-138.
- Kim, D.H., Sarbassov, D.D., Ali, S.M., King, J.E., Latek, R.R., Erdjument-Bromage, H., Tempst, P., and Sabatini, D.M.** (2002). mTOR interacts with raptor to form a nutrient-sensitive complex that signals to the cell growth machinery. *Cell* **110**, 163-175.
- Kim, D.H., Sarbassov, D.D., Ali, S.M., Latek, R.R., Guntur, K.V., Erdjument-Bromage, H., Tempst, P., and Sabatini, D.M.** (2003). GbetaL, a positive regulator of the rapamycin-sensitive pathway required for the nutrient-sensitive interaction between raptor and mTOR. *Mol Cell* **11**, 895-904.
- Kim, E., Goraksha-Hicks, P., Li, L., Neufeld, T.P., and Guan, K.-L.** (2008). Regulation of TORC1 by Rag GTPases in nutrient response. *Nature Cell Biology* **10**, 935-945.
- Kim, J., Kundu, M., Viollet, B., and Guan, K.-L.** (2011). AMPK and mTOR regulate autophagy through direct phosphorylation of Ulk1. *Nat Cell Biol* **13**, 132-141.
- Kim, S.H.Z., K.; Novak, R. F.** (2009). Rapamycin Effects on mTOR Signaling in Benign, Premalignant and Malignant Human Breast Epithelial Cells. *Anticancer Research* **29**, 1143-1150.
- Knutson, B.A.** (2010). Insights into the domain and repeat architecture of target of rapamycin. *J Struct Biol* **170**, 354-363.
- Koltin, Y., Faucette, L., Bergsma, D.J., Levy, M.A., Cafferkey, R., Koser, P.L., Johnson, R.K., and Livi, G.P.** (1991). Rapamycin sensitivity in *Saccharomyces cerevisiae* is mediated by a peptidyl-prolyl cis-trans isomerase related to human FK506-binding protein. *Mol Cell Biol* **11**, 1718-1723.
- Komeili, A., Wedaman, K.P., O'Shea, E.K., and Powers, T.** (2000). Mechanism of metabolic control. Target of rapamycin signaling links nitrogen quality to the activity of the Rtg1 and Rtg3 transcription factors. *J Cell Biol* **151**, 863-878.
- Koncz, C., and Schell, J.** (1986). The promoter of TL-DNA gene 5 controls the tissue-specific expression of chimaeric genes carried by a novel type of *Agrobacterium* binary vector. *Molec Gen Genet* **204**, 383-396.
- Kondorosi, E., Roudier, F., and Gendreau, E.** (2000). Plant cell-size control: growing by ploidy? *Current Opinion in Plant Biology* **3**, 488-492.
- Kotogány, E., Dudits, D., Horváth, G.V., and Ayaydin, F.** (2010). A rapid and robust assay for detection of S-phase cell cycle progression in plant cells and tissues by using ethynyl deoxyuridine. *Plant Methods* **6**, 5.
- Koyanagi, M., Asahara, S.-i., Matsuda, T., Hashimoto, N., Shigeyama, Y., Shibutani, Y., Kanno, A., Fuchita, M., Mikami, T., Hosooka, T., Inoue, H., Matsumoto, M., Koike, M., Uchiyama, Y., Noda, T., Seino, S., Kasuga, M., and Kido, Y.** (2011). Ablation of TSC2 Enhances Insulin Secretion by Increasing the Number of Mitochondria through Activation of mTORC1. *PLoS ONE* **6**, e23238.

- Křeček, P.S., P.; Libus, J.; Naramoto, S.; Tejos, R.; Friml, J.; Eva Zažímalová, E.** (2009). The PIN-FORMED (PIN) protein family of auxin transporters.
- Krishnamurthy, A., and Rathinasabapathi, B.** (2013). Oxidative stress tolerance in plants: Novel interplay between auxin and reactive oxygen species signaling. *Plant Signaling & Behavior* **8**, e25761.
- Kumar, A., Harris, T.E., Keller, S.R., Choi, K.M., Magnuson, M.A., and Lawrence, J.C.** (2008). Muscle-Specific Deletion of Rictor Impairs Insulin-Stimulated Glucose Transport and Enhances Basal Glycogen Synthase Activity. *Molecular and Cellular Biology* **28**, 61-70.
- Kunz, J., and Hall, M.N.** (1993). Cyclosporin A, FK506 and rapamycin: more than just immunosuppression. *Trends Biochem Sci* **18**, 334-338.
- Kunz, J., Schneider, U., Howald, I., Schmidt, A., and Hall, M.N.** (2000). HEAT repeats mediate plasma membrane localization of Tor2p in yeast. *J Biol Chem* **275**, 37011-37020.
- Kunz, J., Henriquez, R., Schneider, U., Deuter-Reinhard, M., Movva, N.R., and Hall, M.N.** (1993). Target of rapamycin in yeast, TOR2, is an essential phosphatidylinositol kinase homolog required for G1 progression. *Cell* **73**, 585-596.
- Kuru, J., Schneider, I.U., Henriquez, R., Deuter-Reinhard, M., Movva, N.R., and Hall, M.N.** (1993). Target of Rapamycin in Yeast, TOR2, is an Essential Phosphatidylinositol Kinase Homolog Required for G1 Progression. *Cell* **73**, 585-596.
- Kwak, J.M., Moon, J.H., Murata, Y., Kuchitsu, K., Leonhardt, N., DeLong, A., and Schroeder, J.I.** (2002). Disruption of a guard cell-expressed protein phosphatase 2A regulatory subunit, RCN1, confers abscisic acid insensitivity in Arabidopsis. *Plant Cell* **14**, 2849-2861.
- Laplante, M., and Sabatini, David M.** (2012). mTOR Signaling in Growth Control and Disease. *Cell* **149**, 274-293.
- Laplante, M., Horvat, S., Festuccia, W.T., Birsoy, K., Prevorsek, Z., Efeyan, A., and Sabatini, D.M.** (2012). DEPTOR cell-autonomously promotes adipogenesis, and its expression is associated with obesity. *Cell Metab* **16**, 202-212.
- Lazo, G.R., Stein, P.A., and Ludwig, R.A.** (1991). A DNA transformation-competent Arabidopsis genomic library in Agrobacterium. *Biotechnology (N Y)* **9**, 963-967.
- Lee, D.Y.** (2013). Metabolomic Response of *Chlamydomonas reinhardtii* to the Inhibition of Target of Rapamycin (TOR) by Rapamycin. *Journal of Microbiology and Biotechnology* **23**, 923-931.
- Lee, G., and Chung, J.** (2007). Discrete functions of rictor and raptor in cell growth regulation in *Drosophila*. *Biochem Biophys Res Commun* **357**, 1154-1159.
- Lee, S.B., Kim, S., Lee, J., Park, J., Lee, G., Kim, Y., Kim, J.M., and Chung, J.** (2007). ATG1, an autophagy regulator, inhibits cell growth by negatively regulating S6 kinase. *EMBO reports* **8**, 360-365.
- Lee, Y., Bak, G., Choi, Y., Chuang, W.I., and Cho, H.T.** (2008a). Roles of Phosphatidylinositol 3-Kinase in Root Hair Growth. *Plant Physiology* **147**, 624-635.
- Lee, Y., Kim, E.S., Choi, Y., Hwang, I., Staiger, C.J., Chung, Y.Y., and Lee, Y.** (2008b). The Arabidopsis phosphatidylinositol 3-kinase is important for pollen development. *Plant Physiol* **147**, 1886-1897.
- Leiber, R.M., John, F., Verhertbruggen, Y., Diet, A., Knox, J.P., and Ringli, C.** (2010). The TOR pathway modulates the structure of cell walls in Arabidopsis. *Plant Cell* **22**, 1898-1908.

- Lempiäinen, H., Uotila, A., Urban, J., Dohnal, I., Ammerer, G., Loewith, R., and Shore, D.** (2009). Sfp1 Interaction with TORC1 and Mrs6 Reveals Feedback Regulation on TOR Signaling. *Molecular Cell* **33**, 704-716.
- Li, F., and Vierstra, R.D.** (2012). Regulator and substrate: dual roles for the ATG1-ATG13 kinase complex during autophagic recycling in Arabidopsis. *Autophagy* **8**, 982-984.
- Li, G., and Xue, H.W.** (2007). Arabidopsis PLDzeta2 regulates vesicle trafficking and is required for auxin response. *Plant Cell* **19**, 281-295.
- Liko, D., Conway, M.K., Grunwald, D.S., and Heideman, W.** (2010). Stb3 plays a role in the glucose-induced transition from quiescence to growth in *Saccharomyces cerevisiae*. *Genetics* **185**, 797-810.
- Lin, J., Handschin, C., and Spiegelman, B.M.** (2005). Metabolic control through the PGC-1 family of transcription coactivators. *Cell Metabolism* **1**, 361-370.
- Lin, Z., Yin, K., Zhu, D., Chen, Z., Gu, H., and Qu, L.-J.** (2007). AtCDC5 regulates the G2 to M transition of the cell cycle and is critical for the function of Arabidopsis shoot apical meristem. *Cell research* **17**, 815-828.
- Lippman, S.I., and Broach, J.R.** (2009). Protein kinase A and TORC1 activate genes for ribosomal biogenesis by inactivating repressors encoded by Dot6 and its homolog Tod6. *Proc Natl Acad Sci U S A* **106**, 19928-19933.
- Liszskay, A., Zalm, E.v.d., and Schopfer, P.** (2004). Production of reactive oxygen intermediates (O₂[•], H₂O₂, and ÔH) by maize roots and their role in wall loosening and elongation growth. *Plant physiology*.
- Liu, Y.-G., and Chen, Y.** (2007). High-efficiency thermal asymmetric interlaced PCR for amplification of unknown flanking sequences. *BioTechniques* **43**, 649-656.
- Liu, Y., and Bassham, D.C.** (2010). TOR is a negative regulator of autophagy in Arabidopsis thaliana. *PLoS One* **5**, e11883.
- Loewith, R.** (2011). A brief history of TOR. *Biochemical Society Transactions* **39**, 437-442.
- Loewith, R., Jacinto, E., Wullschleger, S., Lorberg, A., Crespo, J.L., Bonenfant, D., Oppliger, W., Jenoe, P., and Hall, M.N.** (2002). Two TOR complexes, only one of which is rapamycin sensitive, have distinct roles in cell growth control. *Mol Cell* **10**, 457-468.
- Loewus, F.A., and Murthy, P.P.N.** (2000). myo-Inositol metabolism in plants. *Plant Science* **150**, 1-19.
- Long, X., Muller, F., and Avruch, J.** (2004). TOR action in mammalian cells and in *Caenorhabditis elegans*. *Curr Top Microbiol Immunol* **279**, 115-138.
- Long, X., Spycher, C., Han, Z.S., Rose, A.M., Müller, F., and Avruch, J.** (2002). TOR Deficiency in *C. elegans* Causes Developmental Arrest and Intestinal Atrophy by Inhibition of mRNA Translation. *Current Biology* **12**, 1448-1461.
- Luo, Y., Qin, G., Zhang, J., Liang, Y., Song, Y., Zhao, M., Tsuge, T., Aoyama, T., Liu, J., Gu, H., and Qu, L.J.** (2011). D-myo-Inositol-3-Phosphate Affects Phosphatidylinositol-Mediated Endomembrane Function in Arabidopsis and Is Essential for Auxin-Regulated Embryogenesis. *The Plant Cell* **23**, 1352-1372.
- Magnuson, B., Ekim, B., and Fingar, D.C.** (2012). Regulation and function of ribosomal protein S6 kinase (S6K) within mTOR signalling networks. *Biochem J* **441**, 1-21.
- Magyar, Z., Horváth, B., Khan, S., Mohammed, B., Henriques, R., De Veylder, L., Bakó, L., Scheres, B., and Bögre, L.** (2012). Arabidopsis E2FA stimulates proliferation and

endocycle separately through RBR-bound and RBR-free complexes. *The EMBO Journal* **31**, 1480-1493.

- Mahfouz, M.M., Kim, S., Delauney, A.J., and Verma, D.P.S.** (2006). Arabidopsis TARGET OF RAPAMYCIN interacts with RAPTOR, which regulates the activity of S6 kinase in response to osmotic stress signals. *The Plant Cell* **18**, 477-490.
- Maniatis, T., Fritsch, E.F., and Sambrook, J.** (1982). *Molecular cloning : a laboratory manual*. (Cold Spring Harbor, N.Y. : Cold Spring Harbor Laboratory, 1982).
- Manning, B.D., Tee, A.R., Logsdon, M.N., Blenis, J., and Cantley, L.C.** (2002). Identification of the tuberous sclerosis complex-2 tumor suppressor gene product tuberlin as a target of the phosphoinositide 3-kinase/akt pathway. *Mol Cell* **10**, 151-162.
- Massonnet, C., Tisne, S., Radziejwoski, A., Vile, D., De Veylder, L., Dauzat, M., and Granier, C.** (2011). New Insights into the Control of Endoreduplication: Endoreduplication Could Be Driven by Organ Growth in Arabidopsis Leaves. *Plant Physiology* **157**, 2044-2055.
- McLeod, M., Craft, S., and Broach, J.R.** (1986). Identification of the crossover site during FLP-mediated recombination in the *Saccharomyces cerevisiae* plasmid 2 microns circle. *Mol Cell Biol* **6**, 3357-3367.
- McLoughlin, F., Arisz, S.A., Dekker, H.L., Kramer, G., de Koster, C.G., Haring, M.A., Munnik, T., and Testerink, C.** (2013). Identification of novel candidate phosphatidic acid-binding proteins involved in the salt-stress response of Arabidopsis thaliana roots. *Biochem J* **450**, 573-581.
- Melaragno, J.E., Mehrotra, B., and Coleman, A.W.** (1993). Relationship between Endopolyploidy and Cell Size in Epidermal Tissue of Arabidopsis (*American Society of Plant Physiologists*), pp. 1661.
- Menand, B., Desnos, T., Nussaume, L., Berger, F., Bouchez, D., Meyer, C., and Robaglia, C.** (2002). Expression and disruption of the Arabidopsis TOR (target of rapamycin) gene. *Proceedings of the National Academy of Sciences* **99**, 6422-6427.
- Michaels, S.D., and Amasino, R.M.** (1999). FLOWERING LOCUS C encodes a novel MADS domain protein that acts as a repressor of flowering. *Plant Cell* **11**, 949-956.
- Michels, A.A.** (2011). MAF1: a new target of mTORC1. *Biochem Soc Trans* **39**, 487-491.
- Miller, R.A., Harrison, D.E., Astle, C.M., Fernandez, E., Flurkey, K., Han, M., Javors, M.A., Li, X., Nadon, N.L., Nelson, J.F., Pletcher, S., Salmon, A.B., Sharp, Z.D., Van Roekel, S., Winkleman, L., and Strong, R.** (2014). Rapamycin-mediated lifespan increase in mice is dose and sex dependent and metabolically distinct from dietary restriction. *Aging Cell* **13**, 468-477.
- Minina, E.A., Sanchez-Vera, V., Moschou, P.N., Suarez, M.F., Sundberg, E., Weih, M., and Bozhkov, P.V.** (2013). Autophagy mediates caloric restriction-induced lifespan extension in Arabidopsis. *Aging Cell* **12**, 327-329.
- Miron, M., Lasko, P., and Sonenberg, N.** (2003). Signaling from Akt to FRAP/TOR Targets both 4E-BP and S6K in *Drosophila melanogaster*. *Molecular and Cellular Biology* **23**, 9117-9126.
- Mizoguchi, T., Hayashida, N., Yamaguchi-Shinozaki, K., Kamada, H., and Shinozaki, K.** (1995). Two genes that encode ribosomal-protein S6 kinase homologs are induced by cold or salinity stress in Arabidopsis thaliana. *FEBS Lett* **358**, 199-204.

- Montane, M.H., and Menand, B.** (2013). ATP-competitive mTOR kinase inhibitors delay plant growth by triggering early differentiation of meristematic cells but no developmental patterning change. *Journal of Experimental Botany* **64**, 4361-4374.
- Monteiro, D., Liu, Q., Lisboa, S., Scherer, G.E.F., Quader, H., and Malhó, R.** (2005). Phosphoinositides and phosphatidic acid regulate pollen tube growth and reorientation through modulation of $[Ca^{2+}]_c$ and membrane secretion. *Journal of Experimental Botany* **56**, 1665-1674.
- Moreau, M., Azzopardi, M., Clement, G., Dobrenel, T., Marchive, C., Renne, C., Martin-Magniette, M.L., Tacconnat, L., Renou, J.P., Robaglia, C., and Meyer, C.** (2012). Mutations in the Arabidopsis homolog of LST8/GbetaL, a partner of the target of Rapamycin kinase, impair plant growth, flowering, and metabolic adaptation to long days. *Plant Cell* **24**, 463-481.
- Morgan, T.H.** (1914). Mosaics and gynandromorphs in *Drosophila*. *Proc. Soc. Exp. Biol. Med* **11**, 171-172.
- Morgan, T.H.a.B., C. B.** (1920). The origin of gynandromorphs. *Carn. Inst. Wash. Publ.*, 1-22.
- Mori, T., Kuroiwa, H., Higashiyama, T., and Kuroiwa, T.** (2006). GENERATIVE CELL SPECIFIC 1 is essential for angiosperm fertilization. *Nature Cell Biology*, 64.
- Morimoto, T., Suzuki, Y., and Yamaguchi, I.** (2002). Effects of partial suppression of ribosomal protein S6 on organ formation in *Arabidopsis thaliana*. *Biosci Biotechnol Biochem* **66**, 2437-2443.
- Morohashi, K., and Grotewold, E.** (2009). A systems approach reveals regulatory circuitry for *Arabidopsis* trichome initiation by the GL3 and GL1 selectors. *PLoS Genet* **5**, e1000396.
- Müller, B., and Sheen, J.** (2008). Cytokinin and auxin interplay in root stem-cell specification during early embryogenesis. *Nature* **453**, 1094-1097.
- Munnik, T., and Vermeer, J.E.M.** (2010). Osmotic stress-induced phosphoinositide and inositol phosphate signalling in plants. *Plant, Cell & Environment* **33**, 655-669.
- Nakashima, A., Maruki, Y., Imamura, Y., Kondo, C., Kawamata, T., Kawanishi, I., Takata, H., Matsuura, A., Lee, K.S., Kikkawa, U., Ohsumi, Y., Yonezawa, K., and Kamada, Y.** (2008). The Yeast Tor Signaling Pathway Is Involved in G2/M Transition via Polo-Kinase. *PLoS ONE* **3**, e2223.
- Nash, P., Tang, X., Orlicky, S., Chen, Q., Gertler, F.B., Mendenhall, M.D., Sicheri, F., Pawson, T., and Tyers, M.** (2001). Multisite phosphorylation of a CDK inhibitor sets a threshold for the onset of DNA replication. *Nature* **414**, 514-521.
- Nobukuni, T., Joaquin, M., Roccio, M., Dann, S.G., Kim, S.Y., Gulati, P., Byfield, M.P., Backer, J.M., Natt, F., Bos, J.L., Zwartkruis, F.J.T., and Thomas, G.** (2005). Amino acids mediate mTOR/raptor signaling through activation of class 3 phosphatidylinositol 3OH-kinase. *Proceedings of the National Academy of Sciences* **102**, 14238-14243.
- Nojima, H., Tokunaga, C., Eguchi, S., Oshiro, N., Hidayat, S., Yoshino, K., Hara, K., Tanaka, N., Avruch, J., and Yonezawa, K.** (2003). The mammalian target of rapamycin (mTOR) partner, raptor, binds the mTOR substrates p70 S6 kinase and 4E-BP1 through their TOR signaling (TOS) motif. *J Biol Chem* **278**, 15461-15464.
- Nurse, P.** (1975). Genetic control of cell size at cell division in yeast. *Nature* **256**, 547-551.
- Odell, J., Caimi, P., Sauer, B., and Russell, S.** (1990). Site-directed recombination in the genome of transgenic tobacco. *Molecular & general genetics : MGG* **223**, 369-378.

- Oldham, S., Montagne, J., Radimerski, T., Thomas, G., and Hafen, E.** (2000). Genetic and biochemical characterization of dTOR, the Drosophila homolog of the target of rapamycin. *Genes Dev* **14**, 2689-2694.
- Oppenheimer, D.G., Herman, P.L., Sivakumaran, S., Esch, J., and Marks, M.D.** (1991). A myb gene required for leaf trichome differentiation in Arabidopsis is expressed in stipules. *Cell* **67**, 483-493.
- Oshiro, N., Takahashi, R., Yoshino, K., Tanimura, K., Nakashima, A., Eguchi, S., Miyamoto, T., Hara, K., Takehana, K., Avruch, J., Kikkawa, U., and Yonezawa, K.** (2007). The proline-rich Akt substrate of 40 kDa (PRAS40) is a physiological substrate of mammalian target of rapamycin complex 1. *J Biol Chem* **282**, 20329-20339.
- Pagnussat, G.C., Alandete-Saez, M., Bowman, J.L., and Sundaresan, V.** (2009). Auxin-Dependent Patterning and Gamete Specification in the Arabidopsis Female Gametophyte. *Science* **324**, 1684-1689.
- Pagnussat, G.C., Yu, H.-J., Ngo, Q.A., Rajani, S., Mayalagu, S., Johnson, C.S., Capron, A., Xie, L.-F., Ye, D., and Sundaresan, V.** (2005). Genetic and molecular identification of genes required for female gametophyte development and function in Arabidopsis. *Development* **132**, 603-614.
- Paponov, I.A., Paponov, M., Teale, W., Menges, M., Chakrabortee, S., Murray, J.A.H., and Palme, K.** (2008). Comprehensive Transcriptome Analysis of Auxin Responses in Arabidopsis. *Molecular Plant* **1**, 321-337.
- Payne, C.T., Zhang, F., and Lloyd, A.M.** (2000). GL3 encodes a bHLH protein that regulates trichome development in arabidopsis through interaction with GL1 and TTG1. *Genetics* **156**, 1349-1362.
- Pearce, L.R., Komander, D., and Alessi, D.R.** (2010). The nuts and bolts of AGC protein kinases. *Nature reviews. Molecular cell biology* **11**, 9-22.
- Peer, W.A., Cheng, Y., and Murphy, A.S.** (2013). Evidence of oxidative attenuation of auxin signalling. *J Exp Bot* **64**, 2629-2639.
- Perez-Perez, M.E., and Crespo, J.L.** (2010). Autophagy in the model alga Chlamydomonas reinhardtii. *Autophagy* **6**, 562-563.
- Perilli, S., Perez-Perez, J.M., Di Mambro, R., Peris, C.L., Diaz-Trivino, S., Del Bianco, M., Pierdonati, E., Moubayidin, L., Cruz-Ramirez, A., Costantino, P., Scheres, B., and Sabatini, S.** (2013). RETINOBLASTOMA-RELATED protein stimulates cell differentiation in the Arabidopsis root meristem by interacting with cytokinin signaling. *Plant Cell* **25**, 4469-4478.
- Peterson, R.T., Desai, B.N., Hardwick, J.S., and Schreiber, S.L.** (1999). Protein phosphatase 2A interacts with the 70-kDa S6 kinase and is activated by inhibition of FKBP12-rapamycin-associated protein. *Proc Natl Acad Sci U S A* **96**, 4438-4442.
- Peterson, T.R., Laplante, M., Thoreen, C.C., Sancak, Y., Kang, S.A., Kuehl, W.M., Gray, N.S., and Sabatini, D.M.** (2009). DEPTOR Is an mTOR Inhibitor Frequently Overexpressed in Multiple Myeloma Cells and Required for Their Survival. *Cell* **137**, 873-886.
- Petricka, J.J., Winter, C.M., and Benfey, P.N.** (2012). Control of Arabidopsis Root Development. *Annual Review of Plant Biology* **63**, 563-590.
- Petrov, V.D., and Van Breusegem, F.** (2012). Hydrogen peroxide-a central hub for information flow in plant cells. *AoB plants* **2012**, pls014.

- Platt, A.R., Woodhall, R.W., and George, A.L., Jr.** (2007). Improved DNA sequencing quality and efficiency using an optimized fast cycle sequencing protocol. *Biotechniques* **43**, 58, 60, 62.
- Polak, P., Cybulski, N., Feige, J.N., Auwerx, J., Rüegg, M.A., and Hall, M.N.** (2008). Adipose-Specific Knockout of raptor Results in Lean Mice with Enhanced Mitochondrial Respiration. *Cell Metabolism* **8**, 399-410.
- Poli, A., Mongiorgi, S., Cocco, L., and Follo, M.Y.** (2014). Protein kinase C involvement in cell cycle modulation. *Biochemical Society Transactions* **42**, 1471-1476.
- Potocky, M., Jones, M.A., Bezvoda, R., Smirnoff, N., and Zarsky, V.** (2007). Reactive oxygen species produced by NADPH oxidase are involved in pollen tube growth. *The New phytologist* **174**, 742-751.
- Potter, C.J., Pedraza, L.G., and Xu, T.** (2002). Akt regulates growth by directly phosphorylating Tsc2. *Nat Cell Biol* **4**, 658-665.
- Pribat, A., Sormani, R., Rousseau-Gueutin, M., Julkowska, Magdalena M., Testerink, C., Joubès, J., Castroviejo, M., Laguerre, M., Meyer, C., Germain, V., and Rothan, C.** (2012). A novel class of PTEN protein in Arabidopsis displays unusual phosphoinositide phosphatase activity and efficiently binds phosphatidic acid. *Biochemical Journal* **441**, 161-171.
- Pullen, N., Dennis, P.B., Andjelkovic, M., Dufner, A., Kozma, S.C., Hemmings, B.A., and Thomas, G.** (1998). Phosphorylation and activation of p70s6k by PDK1. *Science* **279**, 707-710.
- Radhamony, R.N.** (2005). T-DNA insertional mutagenesis in Arabidopsis: a tool for functional genomics.
- Raught, B., Peiretti, F., Gingras, A.C., Livingstone, M., Shahbazian, D., Mayeur, G.L., Polakiewicz, R.D., Sonenberg, N., and Hershey, J.W.** (2004). Phosphorylation of eucaryotic translation initiation factor 4B Ser422 is modulated by S6 kinases. *EMBO J* **23**, 1761-1769.
- Reiling, J.H., and Hafen, E.** (2004). The hypoxia-induced paralogs Scylla and Charybdis inhibit growth by down-regulating S6K activity upstream of TSC in Drosophila. *Genes Dev* **18**, 2879-2892.
- Reinke, A.** (2004). TOR Complex 1 Includes a Novel Component, Tco89p (YPL180w), and Cooperates with Ssd1p to Maintain Cellular Integrity in *Saccharomyces cerevisiae*. *Journal of Biological Chemistry* **279**, 14752-14762.
- Ren, M., Qiu, S., Venglat, P., Xiang, D., Feng, L., Selvaraj, G., and Datla, R.** (2011). Target of Rapamycin Regulates Development and Ribosomal RNA Expression through Kinase Domain in Arabidopsis. *Plant Physiology* **155**, 1367-1382.
- Ren, M., Venglat, P., Qiu, S., Feng, L., Cao, Y., Wang, E., Xiang, D., Wang, J., Alexander, D., Chalivendra, S., Logan, D., Mattoo, A., Selvaraj, G., and Datla, R.** (2012). Target of Rapamycin Signaling Regulates Metabolism, Growth, and Life Span in Arabidopsis. *The Plant Cell* **24**, 4850-4874.
- Roberg, K.J., Bickel, S., Rowley, N., and Kaiser, C.A.** (1997). Control of amino acid permease sorting in the late secretory pathway of *Saccharomyces cerevisiae* by SEC13, LST4, LST7 and LST8. *Genetics* **147**, 1569-1584.
- Robida-Stubbs, S., Glover-Cutter, K., Lamming, D.W., Mizunuma, M., Narasimhan, S.D., Neumann-Haefelin, E., Sabatini, D.M., and Blackwell, T.K.** (2012). TOR signaling and

rapamycin influence longevity by regulating SKN-1/Nrf and DAF-16/FoxO. *Cell Metab* **15**, 713-724.

- Rodgers, B.D., Levine, M.A., Bernier, M., and Montrose-Rafizadeh, C.** (2001). Insulin regulation of a novel WD-40 repeat protein in adipocytes. *The Journal of endocrinology* **168**, 325-332.
- Roy, B., Vaughn, J.N., Kim, B.H., Zhou, F., Gilchrist, M.A., and Von Arnim, A.G.** (2010). The h subunit of eIF3 promotes reinitiation competence during translation of mRNAs harboring upstream open reading frames. *RNA (New York, N.Y.)* **16**, 748-761.
- RStudio.** (2012). RStudio: Integrated development environment for R
- Sablowski, R., and Carnier Dornelas, M.** (2014). Interplay between cell growth and cell cycle in plants. *J Exp Bot* **65**, 2703-2714.
- Sancak, Y., Bar-Peled, L., Zoncu, R., Markhard, A.L., Nada, S., and Sabatini, D.M.** (2010). Ragulator-Rag complex targets mTORC1 to the lysosomal surface and is necessary for its activation by amino acids. *Cell* **141**, 290-303.
- Sancak, Y., Peterson, T.R., Shaul, Y.D., Lindquist, R.A., Thoreen, C.C., Bar-Peled, L., and Sabatini, D.M.** (2008). The Rag GTPases bind raptor and mediate amino acid signaling to mTORC1. *Science* **320**, 1496-1501.
- Sancak, Y.T., C.C.; Peterson, T.R.; Lindquist, R.A.; Kang, S.A.; Spooner, E.; Carr, S.A.; Sabatini, D.M.** (2007). PRAS40 is an insulin-regulated inhibitor of the mTORC1 protein kinase. *Mol Cell.* **25**, 903-915.
- Santner, A.A., and Watson, J.C.** (2006). The WAG1 and WAG2 protein kinases negatively regulate root waving in Arabidopsis. *Plant J* **45**, 752-764.
- Sarbassov, D.D., Guertin, D.A., Ali, S.M., and Sabatini, D.M.** (2005). Phosphorylation and regulation of Akt/PKB by the rictor-mTOR complex. *Science* **307**, 1098-1101.
- Sarbassov, D.D., Ali, S.M., Kim, D.H., Guertin, D.A., Latek, R.R., Erdjument-Bromage, H., Tempst, P., and Sabatini, D.M.** (2004). Rictor, a novel binding partner of mTOR, defines a rapamycin-insensitive and raptor-independent pathway that regulates the cytoskeleton. *Curr Biol* **14**, 1296-1302.
- Savaldi-Goldstein, S., Peto, C., and Chory, J.** (2007). The epidermis both drives and restricts plant shoot growth. *Nature* **446**, 199-202.
- Schalm, S.S., Fingar, D.C., Sabatini, D.M., and Blenis, J.** (2003). TOS motif-mediated raptor binding regulates 4E-BP1 multisite phosphorylation and function. *Current biology : CB* **13**, 797-806.
- Schepetilnikov, M., Dimitrova, M., Mancera-Martínez, E., Geldreich, A., Keller, M., and Ryabova, L.A.** (2013). TOR and S6K1 promote translation reinitiation of uORF-containing mRNAs via phosphorylation of eIF3h. *The EMBO Journal* **32**, 1087-1102.
- Scherer, G.F.E., Labusch, C., and Effendi, Y.** (2012). Phospholipases and the network of auxin signal transduction with ABP1 and TIR1 as two receptors: a comprehensive and provocative model. *Frontiers in Plant Science* **3**.
- Schmidt, A., Kunz, J., and Hall, M.N.** (1996). TOR2 is required for organization of the actin cytoskeleton in yeast. *Proceedings of the National Academy of Sciences of the United States of America* **93**, 13780-13785.

- Schmidt, A., Bickle, M., Beck, T., and Hall, M.N.** (1997). The Yeast Phosphatidylinositol Kinase Homolog TOR2 Activates RHO1 and RHO2 via the Exchange Factor ROM2. *Cell* **88**, 531-542.
- Schneider, C.A., Rasband, W.S., and Eliceiri, K.W.** (2012). NIH Image to ImageJ: 25 years of image analysis. *Nature methods* **9**, 671-675.
- Schulman, E.** (1958). Bristlecone pine, oldest known living thing. *National Geographic* **113**, 355-372.
- Scott, R.C., Juhász, G., and Neufeld, T.P.** (2007). Direct Induction of Autophagy by Atg1 Inhibits Cell Growth and Induces Apoptotic Cell Death. *Current Biology* **17**, 1-11.
- Selvy, P.E., Lavieri, R.R., Lindsley, C.W., and Brown, H.A.** (2011). Phospholipase D: enzymology, functionality, and chemical modulation. *Chemical reviews* **111**, 6064-6119.
- Shahbazian, D., Roux, P.P., Mieulet, V., Cohen, M.S., Raught, B., Taunton, J., Hershey, J.W., Blenis, J., Pende, M., and Sonenberg, N.** (2006). The mTOR/PI3K and MAPK pathways converge on eIF4B to control its phosphorylation and activity. *EMBO J* **25**, 2781-2791.
- Shamji, A.F., Kuruvilla, F.G., and Schreiber, S.L.** (2000). Partitioning the transcriptional program induced by rapamycin among the effectors of the Tor proteins. *Current Biology* **10**, 1574-1581.
- Shang, L., Chen, S., Du, F., Li, S., Zhao, L., and Wang, X.** (2011). Nutrient starvation elicits an acute autophagic response mediated by Ulk1 dephosphorylation and its subsequent dissociation from AMPK. *Proceedings of the National Academy of Sciences* **108**, 4788-4793.
- Sharon, T., Ursula, H., Arina, K., Jose, B., Sacco De, V., and Somerville, C.** (1994). Tissue-Specific Expression of a Gene Encoding a Cell Wall-Localized Lipid Transfer Protein from Arabidopsis (*American Society of Plant Physiologists*), pp. 35.
- Shaver, S., Casas-Mollano, J.A., Cerny, R.L., and Cerutti, H.** (2010). Origin of the polycomb repressive complex 2 and gene silencing by an E(z) homolog in the unicellular alga *Chlamydomonas*. *Epigenetics : official journal of the DNA Methylation Society* **5**, 301-312.
- Sheen, J.** (2014). Master Regulators in Plant Glucose Signaling Networks. *Journal of Plant Biology* **57**, 67-79.
- Sheldon, C.C., Burn, J.E., Perez, P.P., Metzger, J., Edwards, J.A., Peacock, W.J., and Dennis, E.S.** (1999). The FLF MADS Box Gene: A Repressor of Flowering in Arabidopsis Regulated by Vernalization and Methylation (*American Society of Plant Physiologists*), pp. 445.
- Shinozaki-Yabana, S., Watanabe, Y., and Yamamoto, M.** (2000). Novel WD-repeat protein Mip1p facilitates function of the meiotic regulator Mei2p in fission yeast. *Mol Cell Biol* **20**, 1234-1242.
- Shiota, C., Woo, J.-T., Lindner, J., Shelton, K.D., and Magnuson, M.A.** (2006). Multiallelic Disruption of the rictor Gene in Mice Reveals that mTOR Complex 2 Is Essential for Fetal Growth and Viability. *Developmental cell* **11**, 583-589.
- Skirycz, A., Claeys, H., De Bodt, S., Oikawa, A., Shinoda, S., Andriankaja, M., Maleux, K., Eloy, N.B., Coppens, F., Yoo, S.D., Saito, K., and Inze, D.** (2011). Pause-and-stop: the effects of osmotic stress on cell proliferation during early leaf development in Arabidopsis and a role for ethylene signaling in cell cycle arrest. *Plant Cell* **23**, 1876-1888.

- Sledz, C.A., and Williams, B.R.** (2005). RNA interference in biology and disease. *Blood* **106**, 787-794.
- Smeekens, S., Ma, J., Hanson, J., and Rolland, F.** (2010). Sugar signals and molecular networks controlling plant growth. *Current Opinion in Plant Biology* **13**, 273-278.
- Smith, T.F., Gaitatzes, C., Saxena, K., and Neer, E.J.** (1999). The WD repeat: a common architecture for diverse functions. *Trends in biochemical sciences* **24**, 181-185.
- Smyth, D.R., Bowman, J.L., and Meyerowitz, E.M.** (1990). *Early Flower Development in Arabidopsis* (American Society of Plant Physiologists), pp. 755.
- Sormani, R., Yao, L., Menand, B., Ennar, N., Lecampion, C., Meyer, C., and Robaglia, C.** (2007). *Saccharomyces cerevisiae* FKBP12 binds *Arabidopsis thaliana* TOR and its expression in plants leads to rapamycin susceptibility. *BMC Plant Biol* **7**, 26.
- Soulard, A., Cremonesi, A., Moes, S., Schutz, F., Jenö, P., and Hall, M.N.** (2010). The rapamycin-sensitive phosphoproteome reveals that TOR controls protein kinase A toward some but not all substrates. *Mol Biol Cell* **21**, 3475-3486.
- Stambolic, V., MacPherson, D., Sas, D., Lin, Y., Snow, B., Jang, Y., Benchimol, S., and Mak, T.W.** (2001). Regulation of PTEN transcription by p53. *Mol Cell* **8**, 317-325.
- Stan, R., McLaughlin, M.M., Cafferkey, R., Johnson, R.K., Rosenberg, M., and Livi, G.P.** (1994). Interaction between FKBP12-rapamycin and TOR involves a conserved serine residue. *J Biol Chem* **269**, 32027-32030.
- Sternberg, N., and Hamilton, D.** (1981). Bacteriophage P1 site-specific recombination. I. Recombination between loxP sites. *J Mol Biol* **150**, 467-486.
- Stirnimann, C.U., Petsalaki, E., Russell, R.B., and Müller, C.W.** (2010). WD40 proteins propel cellular networks. *Trends in biochemical sciences* **35**, 565-574.
- Stocker, H.R., T.; Schindelholz, B.; Wittwer, F.; Belawat P.; Daram, P.; Breuer, S.; Thomas, G.; Hafen, E.** (2003). Rheb is an essential regulator of S6K in controlling cell growth in *Drosophila*. *Nat Cell Biol.* 2003 Jun;5(6):559-65. **5**, 559-565.
- Sturtevant, A.H.** (1920). The vermilion gene and gynandromorphism. *Proc. Soc. Exp. Biol. Med.* **17**.
- Su, B., and Jacinto, E.** (2011). Mammalian TOR signaling to the AGC kinases. *Critical Reviews in Biochemistry and Molecular Biology*, 1-21.
- Sun, Y., Fang, Y., Yoon, M.S., Zhang, C., Rocco, M., Zwartkuis, F.J., Armstrong, M., Brown, H.A., and Chen, J.** (2008). Phospholipase D1 is an effector of Rheb in the mTOR pathway. *Proceedings of the National Academy of Sciences* **105**, 8286-8291.
- Sung, S.R.M.** (2004). Vernalization in *Arabidopsis thaliana* is mediated by the PHD finger protein VIN3. *Nature* **427**, 159-164.
- Takahashi, T., Hara, K., Inoue, H., Kawa, Y., Tokunaga, C., Hidayat, S., Yoshino, K., Kuroda, Y., and Yonezawa, K.** (2000). Carboxyl-terminal region conserved among phosphoinositide-kinase-related kinases is indispensable for mTOR function in vivo and in vitro. *Genes Cells* **5**, 765-775.
- Team, R.D.C.** (2008). R: A language and environment for statistical computing.
- Thedieck, K.P., P.; Kim, M.L.; Molle, K.D.; Cohen, A.; Jenö, P.; Arriemerlou, C.; Hall, M.N.** (2007). PRAS40 and PRR5-Like Protein Are New mTOR Interactors that Regulate Apoptosis. *PLoS ONE* **2**.

- Thimm, O., Blasing, O., Gibon, Y., Nagel, A., Meyer, S., Kruger, P., Selbig, J., Muller, L.A., Rhee, S.Y., and Stitt, M.** (2004). MAPMAN: a user-driven tool to display genomics data sets onto diagrams of metabolic pathways and other biological processes. *Plant J* **37**, 914-939.
- Thomas, H.** (2002). Ageing in plants. *Mechanisms of ageing and development* **123**, 747-753.
- Toker, A., and Marmiroli, S.** (2014). Signaling specificity in the Akt pathway in biology and disease. *Advances in biological regulation* **55**, 28-38.
- Toschi, A., Lee, E., Xu, L., Garcia, A., Gadir, N., and Foster, D.A.** (2009). Regulation of mTORC1 and mTORC2 complex assembly by phosphatidic acid: competition with rapamycin. *Mol Cell Biol* **29**, 1411-1420.
- Trapnell, C., Roberts, A., Goff, L., Pertea, G., Kim, D., Kelley, D.R., Pimentel, H., Salzberg, S.L., Rinn, J.L., and Pachter, L.** (2014). Differential gene and transcript expression analysis of RNA-seq experiments with TopHat and Cufflinks. *Nature Protocols*, 2513.
- Treins, C., Warne, P.H., Magnuson, M.A., Pende, M., and Downward, J.** (2010). Rictor is a novel target of p70 S6 kinase-1. *Oncogene* **29**, 1003-1016.
- Tsukaya, H.** (2013). Does Ploidy Level Directly Control Cell Size? Counterevidence from Arabidopsis Genetics. *PLoS ONE Volume 8*.
- Turck, F., Kozma, S.C., Thomas, G., and Nagy, F.** (1998). A heat-sensitive Arabidopsis thaliana kinase substitutes for human p70s6k function in vivo. *Mol Cell Biol* **18**, 2038-2044.
- Tyburski, J., Dunajska-Ordak, K., Skorupa, M., and Tretyn, A.** (2012). Role of Ascorbate in the Regulation of the Arabidopsis thaliana Root Growth by Phosphate Availability. *Journal of Botany*, 1-11.
- Tzeng, T.Y., Kong, L.R., Chen, C.H., Shaw, C.C., and Yang, C.H.** (2009). Overexpression of the lily p70(s6k) gene in Arabidopsis affects elongation of flower organs and indicates TOR-dependent regulation of AP3, PI and SUP translation. *Plant & cell physiology* **50**, 1695-1709.
- Tzfira, T., Frankman, L.R., Vaidya, M., and Citovsky, V.** (2003). Site-specific integration of Agrobacterium tumefaciens T-DNA via double-stranded intermediates. *Plant Physiol* **133**, 1011-1023.
- Urban, J., Soulard, A., Huber, A., Lippman, S., Mukhopadhyay, D., Deloche, O., Wanke, V., Anrather, D., Ammerer, G., Riezman, H., Broach, J.R., De Virgilio, C., Hall, M.N., and Loewith, R.** (2007). Sch9 is a major target of TORC1 in Saccharomyces cerevisiae. *Mol Cell* **26**, 663-674.
- van Dam, T.J., Zwartkruis, F.J., Bos, J.L., and Snel, B.** (2011). Evolution of the TOR pathway. *J Mol Evol* **73**, 209-220.
- Vander Haar, E., Lee, S.I., Bandhakavi, S., Griffin, T.J., and Kim, D.H.** (2007). Insulin signalling to mTOR mediated by the Akt/PKB substrate PRAS40. *Nat Cell Biol* **9**, 316-323.
- Vellai, T., Takacs-Vellai, K., Zhang, Y., Kovacs, A.L., Orosz, L., and Muller, F.** (2003). Genetics: Influence of TOR kinase on lifespan in C. elegans. *Nature* **426**, 620-620.
- Vezina, C., Kudelski, A., and Sehgal, S.N.** (1975). Rapamycin (AY-22,989), a new antifungal antibiotic. I. Taxonomy of the producing streptomycete and isolation of the active principle. *J Antibiot (Tokyo)* **28**, 721-726.

- von Arnim, A.G., Jia, Q., and Vaughn, J.N.** (2014). Regulation of plant translation by upstream open reading frames. *Plant science : an international journal of experimental plant biology* **214**, 1-12.
- Wachsman, G., Heidstra, R., and Scheres, B.** (2011). Distinct Cell-Autonomous Functions of RETINOBLASTOMA-RELATED in Arabidopsis Stem Cells Revealed by the Brother of Brainbow Clonal Analysis System. *The Plant Cell* **23**, 2581-2591.
- Wang, T., Blumhagen, R., Lao, U., Kuo, Y., and Edgar, B.A.** (2012). LST8 regulates cell growth via target-of-rapamycin complex 2 (TORC2). *Mol Cell Biol* **32**, 2203-2213.
- Wanke, V., Cameroni, E., Uotila, A., Piccolis, M., Urban, J., Loewith, R., and De Virgilio, C.** (2008). Caffeine extends yeast lifespan by targeting TORC1. *Molecular Microbiology* **69**, 277-285.
- Ward, S.P., and Leyser, O.** (2004). Shoot branching. *Curr Opin Plant Biol* **7**, 73-78.
- Webster, C.M., Wu, L., Douglas, D., and Soukas, A.A.** (2013). A non-canonical role for the *C. elegans* dosage compensation complex in growth and metabolic regulation downstream of TOR complex 2. *Development* **140**, 3601-3612.
- Wei, Y., Tsang, C.K., and Zheng, X.F.** (2009). Mechanisms of regulation of RNA polymerase III-dependent transcription by TORC1. *EMBO J* **28**, 2220-2230.
- Wei, Y., Zhang, Y.J., Cai, Y., and Xu, M.H.** (2014). The role of mitochondria in mTOR-regulated longevity. *Biological reviews of the Cambridge Philosophical Society*.
- Weigel, D., and Glazebrook, J.** (2002). *Arabidopsis: A Laboratory Manual*. (Cold Spring Harbor Laboratory Press).
- Weisman, R., and Choder, M.** (2001). The Fission Yeast TOR Homolog, tor1+, Is Required for the Response to Starvation and Other Stresses via a Conserved Serine. *Journal of Biological Chemistry* **276**, 7027-7032.
- Welters, P., Takegawa, K., Emr, S.D., and Chrispeels, M.J.** (1994). AtVPS34, a phosphatidylinositol 3-kinase of Arabidopsis thaliana, is an essential protein with homology to a calcium-dependent lipid binding domain. *Proc Natl Acad Sci U S A* **91**, 11398-11402.
- Westphal, R.S., Coffee, R.L., Jr., Marotta, A., Pelech, S.L., and Wadzinski, B.E.** (1999). Identification of kinase-phosphatase signaling modules composed of p70 S6 kinase-protein phosphatase 2A (PP2A) and p21-activated kinase-PP2A. *J Biol Chem* **274**, 687-692.
- Windels, P., De Buck, S., Van Bockstaele, E., De Loose, M., and Depicker, A.** (2003). T-DNA integration in Arabidopsis chromosomes. Presence and origin of filler DNA sequences. *Plant Physiol* **133**, 2061-2068.
- Wullschleger, S., Loewith, R., and Hall, M.N.** (2006). TOR Signaling in Growth and Metabolism. *Cell* **124**, 471-484.
- Wullschleger, S., Loewith, R., Oppliger, W., and Hall, M.N.** (2005). Molecular organization of target of rapamycin complex 2. *J Biol Chem* **280**, 30697-30704.
- Wymer, C.L., Bibikova, T.N., and Gilroy, S.** (1997). Cytoplasmic free calcium distributions during the development of root hairs of Arabidopsis thaliana. *Plant J* **12**, 427-439.
- Xiao, W., Sheen, J., and Jang, J.C.** (2000). The role of hexokinase in plant sugar signal transduction and growth and development. *Plant Mol Biol* **44**, 451-461.

- Xiong, Y., and Sheen, J.** (2012). Rapamycin and glucose-target of rapamycin (TOR) protein signaling in plants. *J Biol Chem* **287**, 2836-2842.
- Xiong, Y., and Sheen, J.** (2014). The Role of Target of Rapamycin Signaling Networks in Plant Growth and Metabolism. *Plant Physiology* **164**, 499-512.
- Xiong, Y., McCormack, M., Li, L., Hall, Q., Xiang, C., and Sheen, J.** (2013). Glucose-TOR signalling reprograms the transcriptome and activates meristems. *Nature* **496**, 181-186.
- Xu, C., Jing, R., Mao, X., Jia, X., and Chang, X.** (2007). A wheat (*Triticum aestivum*) protein phosphatase 2A catalytic subunit gene provides enhanced drought tolerance in tobacco. *Ann Bot* **99**, 439-450.
- Xu, J., Ji, J., and Yan, X.-H.** (2011). Cross-Talk between AMPK and mTOR in Regulating Energy Balance. *Critical Reviews in Food Science and Nutrition* **52**, 373-381.
- Yaffe, M.B., and Elia, A.E.** (2001). Phosphoserine/threonine-binding domains. *Curr Opin Cell Biol* **13**, 131-138.
- Yang, H., Rudge, D.G., Koos, J.D., Vaidialingam, B., Yang, H.J., and Pavletich, N.P.** (2013). mTOR kinase structure, mechanism and regulation. *Nature* **497**, 217-223.
- Yang, Q., Inoki, K., Ikenoue, T., and Guan, K.-L.** (2006). Identification of Sin1 as an essential TORC2 component required for complex formation and kinase activity. *Genes & Development* **20**, 2820-2832.
- Yip, C.K., Murata, K., Walz, T., Sabatini, D.M., and Kang, S.A.** (2010). Structure of the Human mTOR Complex I and Its Implications for Rapamycin Inhibition. *Molecular Cell* **38**, 768-774.
- Yokogami, K., Wakisaka, S., Avruch, J., and Reeves, S.A.** (2000). Serine phosphorylation and maximal activation of STAT3 during CNTF signaling is mediated by the rapamycin target mTOR. *Current Biology* **10**, 47-50.
- Yoon, M.S., Du, G., Backer, J.M., Frohman, M.A., and Chen, J.** (2011). Class III PI-3-kinase activates phospholipase D in an amino acid-sensing mTORC1 pathway. *J Cell Biol* **195**, 435-447.
- Yorimitsu, T., He, C., Wang, K., and Klionsky, D.J.** (2009). Tap42-associated protein phosphatase type 2A negatively regulates induction of autophagy. *Autophagy* **5**, 616-624.
- Zegzouti, H., Anthony, R.G., Jahchan, N., Bogre, L., and Christensen, S.K.** (2006). Phosphorylation and activation of PINOID by the phospholipid signaling kinase 3-phosphoinositide-dependent protein kinase 1 (PDK1) in Arabidopsis. *Proc Natl Acad Sci U S A* **103**, 6404-6409.
- Zhang, H., Stallock, J.P., Ng, J.C., Reinhard, C., and Neufeld, T.P.** (2000). Regulation of cellular growth by the *Drosophila* target of rapamycin dTOR. *Genes & Development*, 2712.
- Zhang, S.H., Lawton, M.A., Hunter, T., and Lamb, C.J.** (1994). atpk1, a novel ribosomal protein kinase gene from Arabidopsis. I. Isolation, characterization, and expression. *J Biol Chem* **269**, 17586-17592.
- Zheng, X.F., Florentino, D., Chen, J., Crabtree, G.R., and Schreiber, S.L.** (1995). TOR kinase domains are required for two distinct functions, only one of which is inhibited by rapamycin. *Cell* **82**, 121-130.

Zinzalla, V., Stracka, D., Oppliger, W., and Hall, M.N. (2011). Activation of mTORC2 by association with the ribosome. *Cell* **144**, 757-768.